BIOMIMETIC STUDIES RELATED TO LIGNIN DEGRADATION

by

FUTONG CUI

B. Sc., Nankai University, P.R. China, 1984

A THESIS SUBMITTED IN PARTIAL FULFILMENT OF

THE REQUIREMENTS FOR THE DEGREE OF

DOCTOR OF PHILOSOPHY

IN

THE FACULTY OF GRADUATE STUDIES

DEPARTMENT OF CHEMISTRY

WE ACCEPT THIS THESIS AS CONFORMING

TO THE REQUIRED STANDARD

THE UNIVERSITY OF BRITISH COLUMBIA
AUGUST, 1990

In presenting this thesis in partial fulfilment of the requirements for an advanced degree at the University of British Columbia, I agree that the Library shall make it freely available for reference and study. I further agree that permission for extensive copying of this thesis for scholarly purposes may be granted by the head of my department or by his or her representatives. It is understood that copying or publication of this thesis for financial gain shall not be allowed without my written permission.

Department of Chemistry

The University of British Columbia
Vancouver, Canada

Date NOV. 14, 1990

DE-6 (2/88)

Abstract

Lignin is the second most abundant biopolymer on Earth. It is an amorphous, cross-linked, aromatic polymer composed of phenylpropanoid units. There has been an ever growing interest in the biodegradation of this complex polymer for the last 30 years. White-rot fungi have been found to be an important lignin degraders in the natural environment. With the discovery of two groups of hemoprotein enzymes, lignin peroxidases and manganese(II)-dependent peroxidases, from the lignin degrading culture of a white-rot fungus, *Phanerochaete chrysosporium*, rapid progress has been made in understanding the mechanism of lignin biodegradation.

Synthetic metalloporphyrins, the iron(III) and manganese(III) complexes of *meso*-tetra(2,6-dichloro-3-sulfonatophenyl)porphyrin (TDCSPPFeCl and TDCSPPMnCl) and *meso*-tetra(2,6-dichloro-3-sulfonatophenyl)-ß-octachloroporphyrin (Cl_{16}TSPPFeCl and Cl_{16}TSPPMnCl), were used in this study to mimic the functions of the "lignin degrading" enzymes. Factors affecting the catalytic activities of these biomimetic catalysts were studied. TDCSPPFeCl could closely mimic lignin peroxidase in the degradation of a number of lignin model compounds, including veratryl alcohol, ß-1, ß-O-4, ß-5, 5-5′ biphenyl, phenylpropane, and phenylpropene model compounds. The reactions catalyzed by TDCSPPFeCl include benzyl alcohol oxidation, C_α-C_β side chain cleavage, demethoxylation, aromatic ring cleavage, benzylic methylene hydroxylation, and C_α-C_β double bond hydroxylation (glycol formation). Novel solvent incorporated compounds isolated from the oxidation of veratryl alcohol give insights about the site of attack of substrate cation radical by solvent molecules. The isolation of a solvent incorporated product from the oxidation of a phenylpropene model compound suggests a cation radical mechanism for the oxidation of this lignin substructure. The formation of

a number of direct aromatic ring cleavage products during the oxidation of some model compounds supports the previously proposed mechanism of aromatic ring cleavage. TDCSPPFeCl was also able to catalyze the oxidation of environmental pollutants such as pyrene and 2,4,6-trichlorophenol.

Veratryl alcohol and manganese(II)-complexes have been suggested to function as redox mediators for lignin biodegradation. Evidence has been provided to demonstrate their mediating power during electrochemical and biomimetic degradation of lignin model compounds.

In addition to the mechanistic information obtained, the successful oxidation of the model compounds suggests that metalloporphyrins can be important catalysts for the pulp and paper industry and for pollution control.

Table of Contents

Abstract	ii
Table of Contents	iv
List of Tables	x
List of Figures	xi
List of Schemes	xx
List of Abbreviations	xxi
List of identification of compounds and structures	xxiii
Acknowledgements	xxviii

Chapter 1 Introduction 1

1.1 Structure of lignin 1

1.2 The importance of lignin biodegradation studies 4

1.3 Lignin degrading microorganisms 7

1.3.1 Bacteria 7

1.3.2 Fungi 7

1.4 Lignin degrading enzymes 9

1.5 Reactions catalyzed by lignin peroxidase (LiP1) 14

1.5.1 The mechanism of lignin model compound degradation by LiP1 15

1.5.2 Reactions catalyzed by lignin peroxidase 16

A C_α-C_β cleavage 16

B ß-O-4 bond cleavage and dealkoxylation reactions 19
C Aromatic ring cleavage reactions 19
D Benzylic alcohol oxidations 22
E Glycol formation from C_α-C_β double bonds 25
F. Hydroxylation of benzylic methylene groups 26
G. Degradation (oxidation) of lignin polymers 28
1.6 Biomimetic approaches in lignin biodegradation 29
1.6.1 Degradation of lignin model compounds by iron porphyrins 30
1.6.2 Oxidation of lignin model compounds by inorganic one-electron oxidants 32
1.6.3 Electrochemical oxidation of lignin model compounds 33
1.7 The purpose of this study 34
References for chapter 1 37

Chapter 2 Metalloporphyrins as lignin peroxidase models 45

2.1 Results and discussion 45
2.1.1 Stability of the metalloporphyrins towards excess oxidants 45
2.1.2 Oxidized intermediates of the metalloporphyrins 53
2.1.2.1 Oxidized intermediates of TDCSPPMnCl 55

A Oxidation of TDCSPPMnCl by sodium hypochlorite 55
B Oxidation of TDCSPPMnCl by H_2O_2, t-BuOOH, and *m*CPBA 58
2.1.2.2 Oxidized intermediates of Cl_{16}TSPPMnCl 61
A Oxidation of Cl_{16}TSPPMnCl by NaClO 61
B Oxidation of Cl_{16}TSPPMnCl by *m*CPBA 73
2.1.2.3 Oxidized intermediates of TDCSPPFeCl 75
2.1.2.4 Oxidized intermediates of Cl_{16}TSPPFeCl 75
2.1.3 Factors affecting the catalytic activity of the metalloporphyrins 81
2.1.3.1 pH of the solvent 82
A TDCSPPFeCl as catalyst 82
B Cl_{16}TSPPFeCl as catalyst 92
C TDCSPPMnCl as catalyst 98
D Cl_{16}TSPPMnCl as catalyst 98
2.1.3.2 Oxidant 109
2.1.3.3 The effect of manganese complexes 111
2.1.3.4 The effect of imidazole 116
2.2 Conclusions 120

2.3 Experimental 121

2.3.1 General 121

2.3.2 The stability of the metalloporphyrins towards excess oxidants 124

2.3.3 The oxidized intermediates of the metalloporphyrins 125

2.3.4 Factors affecting the catalytic activity of the metalloporphyrins 126

References for chapter 2 128

Chapter 3 Oxidation of lignin model compounds catalyzed by *meso*-tetra(2,6-dichloro-3-sulfonatophenyl)porphyrin iron chloride (TDCSPPFeCl) 131

3.1 Results and discussion 131

3.1.1 Oxidation of veratryl alcohol and veratryl acetate 132

3.1.2 Oxidation of phenylpropane model compounds 141

3.1.3 Oxidation of phenylpropene model compounds 145

3.1.4 Oxidation of diarylpropane model compounds 147

3.1.5 Oxidation of arylglycerol-ß-aryl ether (ß-O-4) model compounds 150

3.1.6 Oxidation of phenylcoumaran (ß-5) model compounds 151

3.1.7 Oxidation of 5-5′ biphenyl model compounds 154

3.1.8 Oxidation of pyrene 157

3.1.9 Oxidation of 2,4,6-trichlorophenol 158

3.2 Conclusions 159

3.3 Experimental 160

3.3.1 General 160

3.3.2 Syntheses of lignin model compounds 161

3.3.3 The oxidation of the lignin model and related compounds 163

3.3.4 Characterization of compounds 167

References for chapter 3 189

Chapter 4 Redox mediation in lignin biodegradation 194

4.1 Manganese complexes as mediators in lignin biodegradation 195

4.1.1 Results 196

4.1.1.1 Cyclic voltammetry (CV) of manganese complexes 196

4.1.1.2 Manganese mediated decolorization of Poly B-411 199

4.1.2 Discussion 208

4.2 Veratryl alcohol as a possible mediator in lignin biodegradation 210

4.2.1 Results and discussion 211

4.3 Experimental 217

References for chapter 4 221

Chapter 5 Summary 224

Appendices 234

Appendix 1 The oxidation of Lignin Indulin AT 234

Introduction 234

Results and discussion 235

Experimental 240

Appendix 2 Metallophthalocyanines as possible lignin peroxidase models 242

Introduction 242

Results and discussion 243

Conclusions 248

Experimental 270

References for appendices 273

List of Tables

Table		
2.1	Optimum pH for the oxidation of veratryl alcohol by various metalloporphyrin/oxidant	107
4.1	Cyclic voltammetry of manganese sulfate (10 mM solution, pH 4.5) in the presence of various ligands	197
4.2	Comparison of the optimum concentrations of carboxylic acids in the electrochemical decolorization of Poly B-411 and those in the MnP enzyme system	199
4.3	The oxidation of veratryl alcohol by TDCSPPFeCl and *m*CPBA at various pH values (yield based on substrate)	216
A-1	Yield for the oxidation of veratryl alcohol by TSPCMnCl and TSPCFeCl under various conditions	235
A-2	The effect of imidazole on the oxidation of veratryl alcohol by TSPCMnCl and H_2O_2 at pH 7	234

List of Figures

Figure		
1.1	The structure of conifer lignin proposed by Adler	3
1.2	The structure of hardwood (beech) lignin proposed by Nimz	4
1.3	The main substructures of spruce lignin	5
1.4	Proposed catalytic cycle of lignin peroxidase	12
1.5	Proposed catalytic cycle of manganese-dependent peroxidase	13
1.6	The mechanism of C_α-C_β cleavage of ß-1 model compounds	17
1.7	The mechanism of C_α-C_β cleavage of ß-O-4 model compounds	18
1.8	The mechanism of ß-O-4 cleavage of ß-O-4 model compounds	20
1.9	Possible mechanism of demethoxylation of lignin model compounds	21
1.10	Proposed mechanism of aromatic ring cleavage of veratryl alcohol	23
1.11	Possible mechanism of C_α-oxidation of lignin model compounds	24
1.12	Possible mechanism of C_α-hydroxylation of lignin model compounds	27
1.13	The structure of some metalloporphyrins	31
2.1	The relative stability of metalloporphyrins (7.5×10^{-6} M) towards 100 fold excess of hydrogen peroxide (7.5×10^{-4} M) at pH 3 (0.1 M phosphate buffer) in the presence of veratryl alcohol (2.5×10^{-3} M) at room temperature	47
2.2	The relative stability of metalloporphyrins (7.5×10^{-6} M) towards 100 fold excess of hydrogen peroxide (7.5×10^{-4} M) at pH 10 (0.1 M phosphate buffer) in the presence of veratryl	

	alcohol (2.5×10^{-3} M) at room temperature	49
2.3	The stability of TDCSPPFeCl (1×10^{-5} M) towards *m*CPBA (1×10^{-4} M) in 0.1 M phosphate buffer at room temperature in the absence of veratryl alcohol	50
2.4	The stability of TDCSPPFeCl (1×10^{-5} M) towards hydrogen peroxide (1×10^{-4} M) in 0.1 M phosphate buffer at room temperature in the absence of veratryl alcohol	51
2.5	The stability of Cl_{16}TSPPFeCl towards t-BuOOH and H_2O_2 at pH 3 in the presence of veratryl alcohol at room temperature	52
2.6	UV-vis spectral changes when veratryl alcohol was added to the oxidized intermediate **16** (TDCSPPMn^{IV}=O, λ_{max} 432 nm)	56
2.7	The decay of the oxidized intermediate **17** (TDCSPPMn^{V}=O, λ_{max} 446 nm) to give intermediate **16** (λ_{max} 432 nm) and the manganese(III) porphyrin (λ_{max} 472 nm)	59
2.8	The UV-vis spectra of TDCSPPMnCl (λ_{max} 472 nm), TDCSPPMn^{IV}=O (**16**, λ_{max} 432 nm), and TDCSPPMn^{V}=O (**17**, λ_{max} 446 nm)	60
2.9	The conversion of Cl_{16}TSPPMnCl (λ_{max} 482 nm) to the intermediate **18** (Cl_{16}TSPPMn^{II}, λ_{max} 452 nm) after veratryl alcohol oxidation stopped	63
2.10	The conversion of the oxidized intermediate **19** (λ_{max} 428 nm) to intermediate **20** (λ_{max} 452 nm) upon addition of veratryl alcohol	64
2.11	The reduction of intermediate **20** (λ_{max} 452 nm) to Cl_{16}TSPPMnCl (λ_{max} 482 nm) by veratryl alcohol	65
2.12	The reduction of intermediate **20** (λ_{max} 452 nm) to Cl_{16}TSPPMnCl (λ_{max} 482 nm) by veratryl alcohol at pH 10	66

2.13 The UV-vis spectra of intermediate **18** (dash-dotted line) and **20** (continuous line) 68

2.14 The UV-vis spectra of $Cl_{16}TSPPMnCl$ (λ_{max} 482 nm), $Cl_{16}TSPPMn^{V}=O$ (**19**, λ_{max} 428 nm), and $Cl_{16}TSPPMn^{IV}=O$ (**20**, λ_{max} 452 nm) 69

2.15 The oxidation of $Cl_{16}TSPPMnCl$ by *m*CPBA at pH 2 74

2.16 The oxidation of TDCSPPFeCl (λ_{max} 424 nm) to the λ_{max} 432 nm intermediate by NaClO at pH 10 76

2.17 The oxidation of $Cl_{16}TSPPFeCl$ (λ_{max} 422 nm) to the λ_{max} 448 nm intermediate by NaClO at pH 12 78

2.18 The UV-vis spectra of $Cl_{16}TSPPFeCl$ (λ_{max} 422 nm) and $Cl_{16}TSPPFe^{II}$-O_2 (λ_{max} 446 nm) 79

2.19 The reaction of CO and $Cl_{16}TSPPFe^{II}$-O_2 formed after the oxidation of veratryl alcohol to give $Cl_{16}TSPPFe^{II}$-CO (λ_{max} 440 nm) 80

2.20 The oxidation of veratryl alcohol by TDCSPPFeCl and *m*CPBA at various pH values at room temperature 83

2.21 The oxidation of veratryl alcohol by TDCSPPFeCl and *m*CPBA at pH 5 at room temperature, the same amount of *m*CPBA was added at time = 0, and time = 1 minute. 84

2.22 The oxidation of veratryl alcohol by TDCSPPFeCl and NaClO at various pH values at room temperature 85

2.23 The oxidation of veratryl alcohol by TDCSPPFeCl and NaClO at pH 6 at room temperature, NaClO added at time = 0 and time = 90 seconds 86

2.24 The oxidation of veratryl alcohol by t-BuOOH catalyzed by TDCSPPFeCl at various pH values at room temperature 87

2.25 The oxidation of veratryl alcohol by TDCSPPFeOH and t-BuOOH in pH 3 phosphate buffer containing various concentrations of sodium chloride 89

2.26 The oxidation of veratryl alcohol by TDCSPPFeOH and t-BuOOH in pH 3 buffer containing sodium sulfate and sodium chloride 90

2.27 The oxidation of veratryl alcohol by TDCSPPFeOH and t-BuOOH in pH 3 phosphate buffer of various concentrations 91

2.28 The oxidation of veratryl alcohol by TDCSPPFeCl and hydrogen peroxide at various pH values at room temperature 93

2.29 The oxidation of veratryl alcohol by Cl_{16}TSPPFeCl and *m*CPBA at various pH values at room temperature 94

2.30 The oxidation of veratryl alcohol by Cl_{16}TSPPFeCl and *m*CPBA at pH 5 at room temperature, *m*CPBA added at time = 0 and time = 90 seconds 95

2.31 The oxidation of veratryl alcohol by Cl_{16}TSPPFeCl and t-BuOOH at various pH values at room temperature 96

2.32 The oxidation of veratryl alcohol by Cl_{16}TSPPFeCl and NaClO at various pH values at room temperature 97

2.33 The oxidation of veratryl alcohol by TDCSPPMnCl and *m*CPBA at various pH values at room temperature 99

2.34 The oxidation of veratryl alcohol by TDCSPPMnCl and hydrogen peroxide at pH 10 and pH 9.2 at room temperature 100

2.35 The oxidation of veratryl alcohol by TDCSPPMnCl and NaClO at various pH values at room temperature 101

2.36 The oxidation of veratryl alcohol by TDCSPPMnCl and *m*CPBA at pH 5 at room temperature, *m*CPBA added at time = 0 and time = 240 seconds 102

2.37 The oxidation of veratryl alcohol by Cl_{16}TSPPMnCl and NaClO at various pH values at room temperature 103

2.38 The oxidation of veratryl alcohol by Cl_{16}TSPPMnCl and hydrogen peroxide at pH 8, 9.2 and 10 at room temperature 104

2.39 The oxidation of veratryl alcohol by Cl_{16}TSPPMnCl and *m*CPBA at various pH values at room temperature 105

2.40 The effect of manganese(II)-lactate on the oxidation of veratryl alcohol by TDCSPPFeCl and *m*CPBA, 1, pH 5 in the presence of Mn^{2+}; 2, pH 6 in the presence of Mn^{2+}; 3, pH 5 in the absence of Mn^{2+}; 4, pH 6 in the absence of Mn^{2+} 114

2.41 The effect of manganese(II)-lactate on the oxidation of veratryl alcohol by Cl_{16}TSPPMnCl and *m*CPBA, 1, pH 5 in the presence of Mn^{2+}; 2, pH 5 in the absence of Mn^{2+}; 3, pH 6 in the presence of Mn^{2+}; 4, pH 6 in the absence of Mn^{2+} 115

2.42 The effect of imidazole on the oxidation of veratryl alcohol by hydrogen peroxide and Cl_{16}TSPPMnCl at pH 9.2, Imidazole/ Cl_{16}TSPPMnCl (molar ratio): 1, 0; 2, 50; 3, 100; 4, 200 118

2.43 The effect of imidazole on the oxidation of veratryl alcohol by hydrogen peroxide and Cl_{16}TSPPMnCl at pH 10, Imidazole/ Cl_{16}TSPPMnCl (molar ratio): 1, 0; 2, 100; 3, 200 119

3.1 The structure of TDCSPPFeCl 131

3.2	The oxidation of veratryl alcohol by lignin peroxidase or biomimetic systems	134
3.3	Proposed mechanism for the oxidation of veratryl alcohol	135
3.4	The oxidation of veratryl acetate in pH 3 aqueous buffer by TDCSPPFeCl and *m*CPBA	136
3.5	Possible mechanism for the formation of compound **36**	137
3.6	The oxidation of veratryl alcohol by TDCSPPFeCl/*m*CPBA in methanol	138
3.7	Possible mechanism for the formation of compound **37**	140
3.8	The oxidation of 1-(4-ethoxy-3-methoxyphenyl)propane (**44**) by TDCSPPFeCl and t-BuOOH in aqueous acetonitrile	143
3.9	Proposed mechanism for alkyl-phenyl cleavage of phenolic model compounds	143
3.10	Possible mechanism for the formation of compound **48**	144
3.11	The oxidation of 1-(4-ethoxy-3-methoxyphenyl)-1-propene (**52**) by TDCSPPFeCl and t-BuOOH in aqueous acetonitrile	146
3.12	Possible mechanism for the oxidation of 1-(4-ethoxy-3-methoxyphenyl)propene (**52**)	148
3.13	The oxidation of 1-(4-ethoxy-3-methoxyphenyl)-2-(4-methoxyphenyl) propane-1,3-diol (**55**) by TDCSPPFeCl and t-BuOOH	149
3.14	The oxidation of 4-ethoxy-3-methoxyphenylglycerol-ß-guaiacyl ether (**62**) by TDCSPPFeCl and t-BuOOH	151
3.15	The oxidation of 4-O-ethyldehydrodiisoeugenol (**64**) by TDCSPPFeCl and t-BuOOH	153
3.16	The oxidation of 4,4′-diethyldehydrodivanillin (**74**) by	

	TDCSPPFeCl and t-BuOOH	156
3.17	The oxidation of pyrene by TDCSPPFeCl and *m*CPBA	157
3.18	The oxidation of 2,4,6-trichlorophenol by TDCSPPFeCl and *m*CPBA	158
4.1	The electrochemical decolorization of Poly B-411 in 0.1 M acetate buffer at room temperature in the presence of manganese sulfate (0.1 mM) and various concentrations of (L)-lactic acid (mM), 1, 0; 2, 10; 3, 20; 4, 30; 5, 50; 6, 60; 7, 70	200
4.2	The electrochemical decolorization of Poly B-411 (0.02%) in 0.1 M pH 4.5 acetate buffer at room temperature in the presence of manganese sulfate (0.1 mM) and various concentrations of malic acid (mM), 0, 1, 10; 2, 15; 3, 5	202
4.3	The electrochemical decolorization of Poly B-411 (0.02%) in 0.1 M pH 4.5 acetate buffer at room temperature in the presence of manganese sulfate (0.1 mM) and various concentrations of (D)-tartaric acid (mM), 1, 10; 2, 20; 3, 25	203
4.4	The electrochemical decolorization of Poly B-411 in 0.1 M pH 4.5 acetate buffer at room temperature in the presence of manganese sulfate (0.1 mM) and various concentrations of citric acid (mM), 1, 10; 2, 20; 3, 5	204
4.5	The electrochemical decolorization of Poly B-411 (0.02%) in 0.1 M pH 4.5 acetate buffer at room temperature in the presence of manganese sulfate (0.1 mM) and various concentrations of malic acid (mM), 1, 10; 2, 50, 3, 60; 4, 40	205
4.6	The electrochemical decolorization of Poly B-411 (0.02%)	

in 0.1 M pH 4.5 acetate buffer at room temperature in the presence of manganese sulfate (0.1 mM) and various carboxylic acids at their optimum concentrations, 1, no ligand; 2, 5 mM citric acid; 3, 20 mM (D)-tartaric acid; 4, 60 mM (L)-lactic acid; 5, 10 mM malic acid; 6, 50 mM malonic acid 206

4.7 The decolorization of Poly B-411 (0.005% in 25 mL 0.1 M pH 4.5 acetate buffer) by TDCSPPFeCl (1×10^{-8} mole) and *m*CPBA (2.5×10^{-5} mole) in the presence of manganese sulfate (2.5×10^{-5} mole) and lactic acid (1.5×10^{-4} mole), 1, without TDCSPPFeCl 2, without manganese sulfate ; 3, complete reaction 207

4.8 The oxidation of anisyl alcohol (3×10^{-5} mole in 6 mL pH 3 0.1 M phosphate buffer) by TDCSPPFeCl (5×10^{-8} mole) and *m*CPBA (3×10^{-5} mole) in the presence of veratryl alcohol 211

4.9 The oxidation of anisyl alcohol (3×10^{-5} mole in 6 mL pH 3 0.1 M phosphate buffer) by TDCSPPFeCl (5×10^{-8} mole) and *m*CPBA (3×10^{-5} mole) in the presence of 1,4-dimethoxybenzene 212

4.10 The electrochemical decolorization of Poly B-411 (0.005%) in 0.1 M pH 3 phosphate buffer at room temperature in the presence of various amounts of veratryl alcohol (mM), 1, 0; 2, 0.1; 3, 1; 4, 10 214

A-1 Difference spectra and reduced-difference spectra of Lignin Indulin AT treated with Cl_{16}TSPPMnCl and t-BuOOH at pH 2 226

A-2 Difference and reduced-difference spectra of Lignin Indulin AT treated with Cl_{16}TSPPMnCl and H_2O_2 at pH 2 227

A-3 Difference and reduced-difference spectra of Lignin Indulin AT treated with Cl_{16}TSPPMnCl and t-BuOOH at pH 10 228

A-4 Difference and reduced-difference spectra of Lignin Indulin AT treated with Cl_{16}TSPPMnCl and H_2O_2 at pH 10 229

A-5 The Oxidation of **62** by TSPCMnCl (or TSPCFeCl) and *m*CPBA in aqueous acetonitrile (pH 3) 236

A-6 The oxidation of **55** by TSPCMnCl (or TSPCFeCl) and *m*CPBA in aqueous acetonitrile 237

A-7 UV-vis spectral changes of TSPCMnCl and TSPCFeCl (1×10^{-7} mole in 3 mL 0.1 M phosphate buffer) upon addition of one equivalent of oxidant (1×10^{-7} mole) in the presence of veratryl alcohol (5×10^{-6} mole) over a time period of 2 minutes, 10 seconds between scan 239

List of schemes

Scheme		
1.1	The biosynthesis of lignin	1
1.2	C_α-C_β double bond hydroxylation	26
2.1	The redox cycle of TDCSPPMnCl	58
2.2	The redox cycle of Cl_{16}TSPPMnCl	61
2.3	The effect of superoxide on the catalytic cycle of Cl_{16}TSPPMnCl during the oxidation of veratryl alcohol	112
3.1	The hydrolysis of compound **37**	139
3.2	The biodegradation of dehydrodivanillic acid	155

List of Abbreviations

ABTS	2,2′-azinobis(3-ethylbenzthiazoline-6-sulfonate)
*m*CBA	*meta*-chlorobenzoic acid
Cl_{16}TSPPFeCl	*meso*-tetra(2,6-dichloro-3-sulfonatophenyl)-ß-octachloroporphyrin iron chloride
Cl_{16}TSPPMnCl	*meso*-tetra(2,6-dichloro-3-sulfonatophenyl)-ß-octachloroporphyrin manganese chloride
*m*CPBA	*meta*-chloroperbenzoic acid
CV	cyclic voltammetry
DCI	desorption chemical ionization
DDT	dithiothreitol
DMF	N,N-dimethylformide
ESR	electron spin resonance spectroscopy
FTIR	Fourier Transform Infrared spectroscopy
GC	gas chromatography
GCMS	gas chromatography-mass spectroscopy
GSH	glutathione, reduced form
HHIB	hydroxyhexafluoroisobutyrate
HPLC	high performance liquid chromatography
HRMS	high resolution mass spectroscopy
HRP	horse radish peroxidase
IR	infrared spectroscopy
LiP	lignin peroxidase
MnP	manganese-dependent peroxidase
M.P.	melting point

MS	mass spectroscopy
MWL	milled wood lignin
NADPH	nicotinamide adenine dinucleotide phosphate, reduced form
NMR	nuclear magnetic resonance spectroscopy
NOE	nuclear overhauser effect
PCBs	polychlorinated biphenyl's
P. chrysosporium	*Phanerochaete chrysosporium*
TBAP	tetrabutylammonium perchlorate
TDCPPFeCl	*meso*-tetra(2,6-dichlorophenyl)porphyrin iron chloride
TDCPPFeOH	*meso*-tetra(2,6-dichlorophenyl)porphyrin iron hydroxide
TDCSPPFeCl	*meso*-tetra(2,6-dichloro-3-sulfonatophenyl)porphyrin iron chloride
TDCSPPFeOH	*meso*-tetra(2,6-dichloro-3-sulfonatophenyl)porphyrin iron hydroxide
TDCSPPMnCl	*meso*-tetra(2,6-dichloro-3-sulfonatophenyl)porphyrin manganese chloride
THF	tetrahydrofuran
TLC	thin layer chromatography
TPP	*meso*-tetraphenylporphyrin
TPPFeCl	*meso*-tetraphenylporphyrin iron chloride
TSPCCo	cobalt tetrasulfonatophthalocyanine
TSPCCu	copper tetrasulfonatophthalocyanine
TSPCFeCl	tetrasulfonatophthalocyanine iron chloride
TSPCMnCl	tetrasulfonatophthalocyanine manganese chloride
TSPCNi	nickel tetrasulfonatophthalocyanine
TSPPFe	iron *meso*-tetra(4-sulfonatophenyl)porphyrin
UV-vis	ultraviolet-visible
λ_{max}	absorption maximum in nanometres

List of identification of compounds and structures

The following numbering system will be used for the compounds and general structures referred to in this thesis.

1 *p*-coumaryl alcohol (3-(4-hydroxyphenyl)-2-propenol)

2 coniferyl alcohol (3-(4-hydroxy-3-methoxyphenyl)-2-propenol)

3 sinapyl alcohol (3-(4-hydroxy-3,5-dimethoxyphenyl)-2-propenol)

4 ß-O-4 substructure (ß-aryl ether)

5 α-O-4 substructure (α-aryl ether)

6 5-5′ biphenyl substructure

7 ß-1 substructure

8 ß-5 (phenylcoumaran) substructure

9 5-O-4 substructure

10 TPPFeCl

11 iron protoporphyrin

12 TDCSPPFeCl

13 TDCSPPMnCl

14 Cl_{16}TSPPFeCl

15 Cl_{16}TSPPMnCl

16 TDCSPPMn^{IV}=O

17 TDCSPPMn^{V}=O

18 Cl_{16}TSPPMn^{II}

19 Cl_{16}TSPPMn^{V}=O

20	$Cl_{16}TSPPMn^{IV}=O$
21	oxidized intermediate of TDCSPPFeCl
22	Oxidized intermediate of $Cl_{16}TSPPFeCl$
23	$Cl_{16}TSPPFe^{II}-O_2$
24	iron *meso*-tetra(2,6-dimethyl-3-sulfonatophenyl)porphyrin
25	manganese *meso*-tetra(2,6-dimethyl-3-sulfonatophenyl)porphyrin
26	methyl (Z)-furan-5(2H)-one-3-butenoate
27	methyl (E)-furan-5(2H)-one-3-butenoate
28	methyl (Z)-6-oxo-2H-pyran-3(6H)-ylideneacetate
29	methyl (E)-6-oxo-2H-pyran-3(6H)-ylideneacetate
30	2-hydroxymethyl-5-methoxy-2,5-cyclohexadiene-1,4-dione
31	2-methoxy-1,4-benzoquinone
32	4,5-dimethoxy-3,5-cyclohexadiene-1,2-dione
33	dimethyl 3-hydroxymethyl-2,4-hexadienedioate
34	2-acetoxymethyl-5-methoxy-2,5-cyclohexadiene-1,4-dione
35	3,4-dimethoxyphenol
36	dimethyl 3-acetoxymethyl-2,4-hexadienedioate
37	2-hydroxymethyl-4,4,5-trimethoxy-2,5-cyclohexadiene-1-one
38	2-dimethoxymethyl-4,4,5-trimethoxy-2,5-cyclohexadiene-1-one
39	2-acetoxymethyl-4,4,5-trimethoxy-2,5-cyclohexadiene-1-one
40	4-ethoxy-2-hydroxymethyl-4,5-dimethoxy-2,5-cyclohexadiene-1-one
41	5-ethoxy-2-hydroxymethyl-4,4-dimethoxy-2,5-cyclohexadiene-1-one
42	2-dimethoxymethyl-5-ethoxy-3,4-dimethoxy-2,5-cyclohexadiene-1-one
43	phenylpropane substructure
44	1-(4-ethoxy-3-methoxyphenyl)propane

45 (6)-ethyl (1)-methyl 3-propyl-2,4-hexadienedioate

46 2-ethoxy-5-propyl-2,5-cyclohexadiene-1,4-dione

47 1-(4-ethoxy-3-methoxyphenyl)propanol

48 4-hydroxy-2-methoxy-4-propyl-2,5-cyclohexadiene-1-one

49 2-alkyl-4-hydroxy-3-methoxybenzyl alcohol

50 4-hydroxy-4-(alkylhydroxymethyl)-2-methoxy-2,5-cyclohexadiene-1-one

51 phenylpropene substructure

52 1-(4-ethoxy-3-methoxyphenyl)-1-propene

53 1-(4-ethoxy-3-methoxyphenyl)propane-1,2-diol

54 4-hydroxy-4-(4-ethoxy-3-methoxyphenyl)-3-methylbutyronitrile

55 1-(4-ethoxy-3-methoxyphenyl)-2-(4-methoxyphenyl)propane-1,3-diol

56 4-ethoxy-3-methoxybenzaldehyde

57 4′-methoxy-α-hydroxyacetophenone

58 4′-methoxyphenylglycol

59 4-ethoxy-3-methoxybenzoic acid

60 4-methoxybenzaldehyde

61 4-methoxybenzoic acid

62 4-ethoxy-3-methoxyphenylglycerol-ß-guaiacyl ether

63 guaiacol

64 4-O-ethyldehydrodiisoeugenol

65 2,3-dihydro-5-formyl-7-methoxy-3-methyl-2-(4-ethoxy-3-methoxyphenyl)-benzofuran

66 5-carboxy-2,3-dihydro-7-methoxy-3-methyl-2-(4-ethoxy-3-methoxyphenyl)-benzofuran

67 5-carboxy-2,3-dihydro-2-[(6)-ethyl (1)-methyl 2(E)-4-(Z)-2,4-hexadienedioate-3-

yl]-7-methoxy-3-methylbenzofuran

68 2,3-dihydro-5-formyl-2-[(6)-ethyl (1)-methyl 2-(E)-4-(Z)-2,4-hexadienedioate-3-yl]-7-methoxy-3-methylbenzofuran

69 2,3-dihydro-5-formyl-2-[(6)-ethyl (1)-methyl 2-(E)-4-(E)-2,4-hexadienedioate-3-yl]-7-methoxy-3-methylbenzofuran

70 2-acetyl-4-formyl-6-methoxyphenyl 4-ethoxy-3-methoxybenzoate

71 guaiacyl substructure

72 dehydrodivanillic acid

73 5-carboxyvanillic acid

74 4,4′-diethyldehydrodivanillin

75 4,4′-diethoxy-3,3′-dimethoxy-5-carboxy-5′-formylbiphenyl

76 4,4′-diethyldehydrodivanillic acid

77 (1)-ethyl (6)-methyl 2-(2-ethoxy-3-methoxy-5-formylphenyl)-4-carboxy-2,4-hexadienedioate

78 (1)-ethyl (6)-methyl 2-(2-ethoxy-3-methoxy-5-carboxyphenyl)-4-carboxy-2,4-hexadienedioate

79 pyrene

80 pyrene-1,6-dione

81 pyrene-1,8-dione

82 2,4,6-trichlorophenol

83 2,6-dichloro-1,4-benzoquinone

84 Poly B-411

85 unconjugated guaiacyl substructure

86 conjugated guaiacyl substructure

87 phthalocyanine

88 general structure of porphyrins

89 TSPCFeCl

90 TSPCMnCl

91 TSPCNi

92 TSPCCu

93 TSPCCo

94 metallo tetrasulfonatophthalocyanine

95 3-(4-ethoxy-3-methoxyphenyl)-2-(2-methoxyphenoxy)-3-oxopropanol

96 3-(4-ethoxy-3-methoxyphenyl)-2-(4-methoxyphenyl)-3-oxopropanol

Acknowledgements

I wish to express my sincere thanks to Professor David Dolphin. His guidance and encouragement have been an invaluable support throughout my research.

I am indebted to Dr. Tilak Wijesekera for kindly providing samples of *meso*-tetra(2,6-dichlorophenyl)porphyrin and *meso*-tetra(2,6-dichlorophenyl)-ß-octachloroporphyrin, for his guidance in the syntheses of the metalloporphyrins used in this study, and for reading this thesis.

I would also like to thank all the members of Professor Dolphin's research group, past and present, for their invaluable help and discussions.

I would like to take this opportunity to express thanks to my wife and my family for their support and understanding.

In memory of my father

Chapter 1

Introduction

1.1 Structure of lignin

Lignin is a three-dimensional, amorphous aromatic biopolymer occurring widely in vascular plants. It is among the most complex biopolymers in nature and the understanding of its chemical structure is based on studies of its biosynthesis and degradation. It is now known that lignin is formed in plants at the site of lignification by enzyme mediated dehydrogenative polymerization of three precursors, p-coumaryl alcohol (**1**), coniferyl alcohol (**2**) and sinapyl alcohol (**3**) as shown in Scheme 1.1. The three phenylpropanoid units in lignin are connected randomly by various C-C and C-O

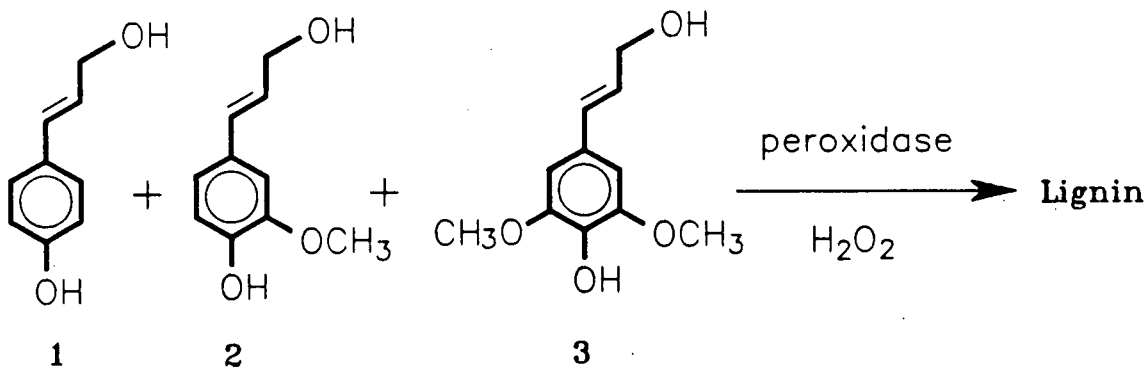

Scheme 1.1 The biosynthesis of lignin

bonds. The proportions of each phenylpropanoid unit vary with the origin of lignin. Higuchi *et al*[1] defined three major groups of lignin by their composition: guaiacyl lignin, guaiacyl-syringyl lignin, and guaiacyl-syringyl-coumaryl lignin. Guaiacyl lignin is composed of coniferyl alcohol units with small amounts of coumaryl and sinapyl alcohol derived units. Guaiacyl-syringyl lignin contains approximately equal amounts of coniferyl alcohol and sinapyl alcohol units and only small amounts of coumaryl alcohol units. Guaiacyl-syringyl-coumaryl lignin is composed of approximately equal amounts of the three cinnamyl alcohol units.

Lignin is sometimes also named by the type of plant from which it was prepared. Examples are conifer lignin, softwood lignin, hardwood lignin, and grass lignin *etc.* It should be noted that the structure of lignin varies with the specific species, age, and probably also the environment of the plant from which the lignin was obtained. As lignin is closely associated with cellulose in plants in the form of lignocellulose, physical (*i.e.* solvent extraction), chemical (*i.e.* acid treatment), or biological (*i.e.* enzyme treatment) methods have to be used to separate lignin from cellulose. The chemical and physical properties of lignin are inevitably altered to different extents by different isolation procedures. Some methods can isolate only a small portion of lignin which may not be representative of the integral sample. In addition, lignin preparations are likely to be contaminated by residual cellulose and other components such as proteins, and inorganic compounds. It is almost impossible, therefore, to obtain "natural" lignin sample. The composition, molecular weight, and chemical structure of a specific sample is also affected by its preparative procedure. Strictly speaking, it is impossible to know the exact molecular structure of a lignin molecule. It is possible, however, to roughly represent the structure of lignin by constructing a portion of a lignin molecule and Figure 1.1 shows a scheme proposed by

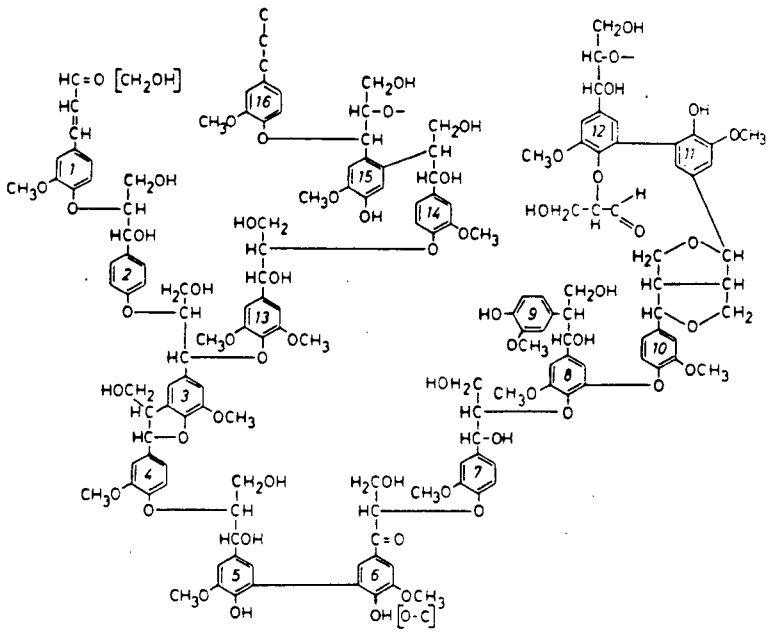

Figure 1.1 The structure of conifer lignin proposed by Adler [2]

Adler[2] representing conifer lignin. The phenylpropanoid units were connected by linkages which have been shown to occur in lignin. The proportions of various linkages shown approximate those of the lignin sample, though the importance of a few structural types is overemphasized due to the number of units that may be assembled into a scheme of this size. A scheme representing the structure of hardwood (beech) lignin proposed by Nimz[3] is shown in Figure 1.2.

From Figures 1.1 and 1.2 it can be seen that the structure of lignin is very complex and this kind of schematic presentation refers only to an "average" lignin. It is easiest to view lignin as composed of various substructures which occur in various proportions in different lignins. Figure 1.3 shows some of the most important substructures in spruce lignin. These include arylglycerol-ß-aryl ether (ß-O-4), noncyclic benzyl aryl ether (α-O-4), biphenyl (5-5′), 1,2-diarylpropane (ß-1), and

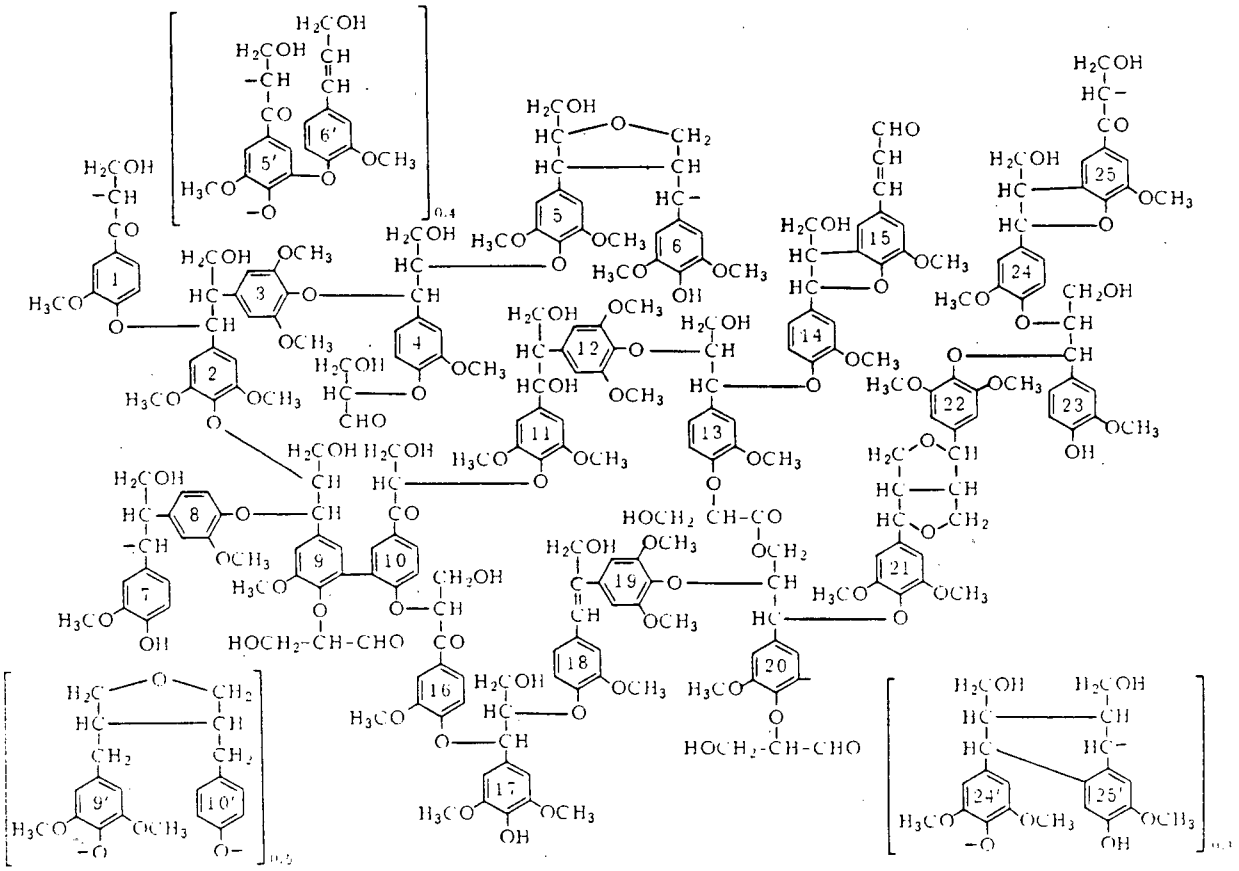

Figure 1.2 The structure of hardwood (beech) lignin proposed by Nimz [3]

phenylcoumaran (ß-5) substructures.

1.2 The importance of lignin biodegradation studies

Lignin is the second most abundant biopolymer on earth[3] and it has been estimated that 25% of the organic compounds produced by photosynthesis is eventually transformed into lignin. It is, however, one of the most persistent naturally occurring compounds and its biodegradation is probably the rate limiting step in the biospheric carbon-oxygen cycle. In addition, the most abundant biopolymer, cellulose, is protected by lignin in woody plant tissues and the efficient biodegradation of cellulose requires

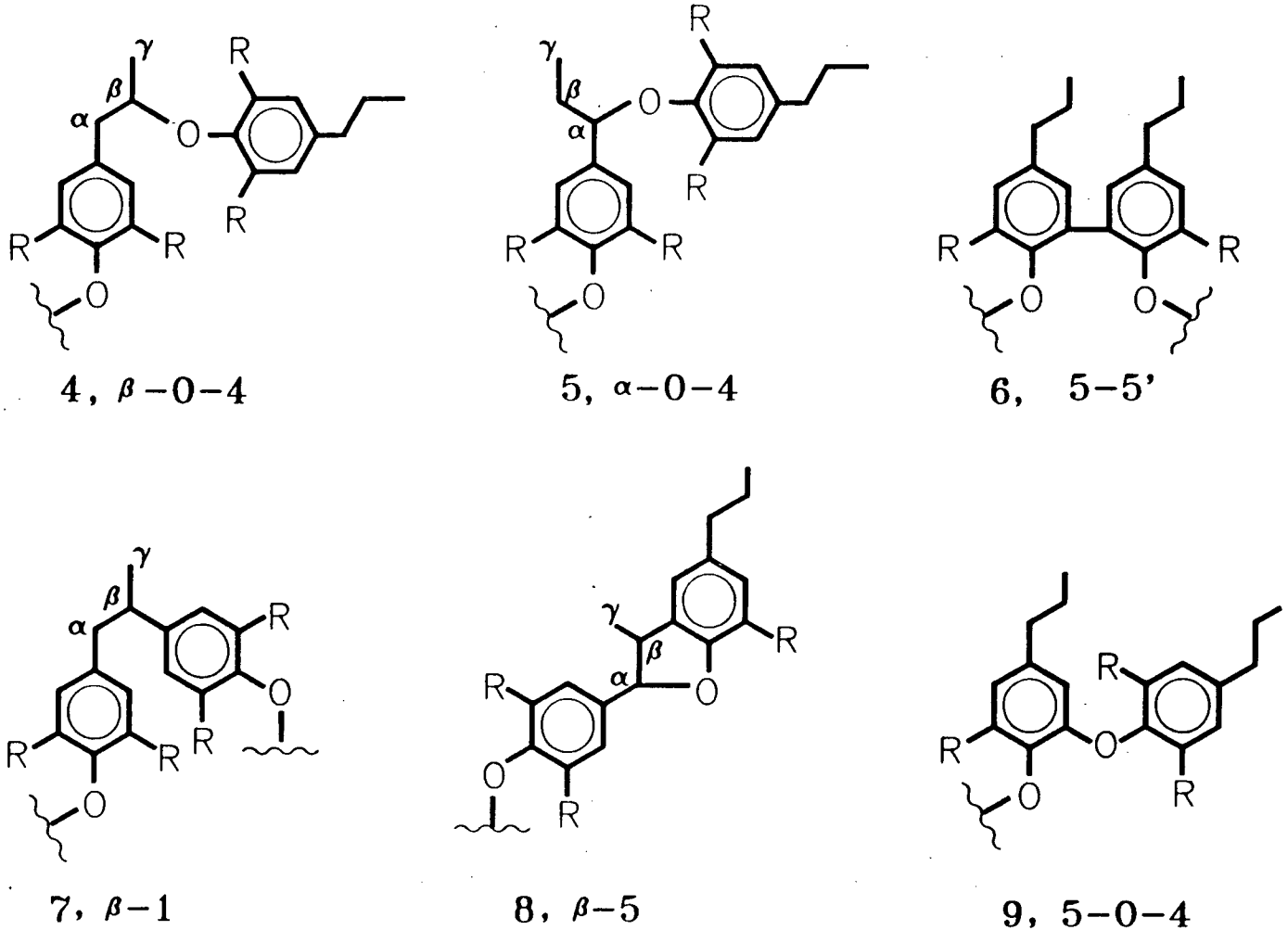

Figure 1.3 The main substructures of spruce lignin. R = H, OCH_3 or lignin

pre-disruption of the protective lignin sheath. The biodegradation of lignin, therefore, is critical for the decomposition of biomass in nature. On the other hand, the undesirable decay of lignin in woody construction materials causes enormous economical damage, and a better understanding of lignin degradation could also provide knowledge about wood preservation.

Being a renewable organic material, lignin is also an important natural resource. Billions of tons of lignocellulosic materials are produced annually in the world. Biotechnology holds a great potential to transform lignin into chemical raw materials[4,5,6] and animal feed stock.[7] Due to its unique molecular structure, however, lignin is difficult to handle by most enzymes and microorganisms. Attempts to develop industrial processes for the conversion of lignin into useful products have been unsuccessful. Biological degradation of lignin into low molecular weight aromatics is probably the bottleneck for the industrial utilization of this abundant valuable resource.

In the pulp and paper industry, chemical or mechanical methods are used to remove lignin from the desired cellulose (the pulping process). Chemical pulping gives high quality pulp, but pulp yield is low. The mechanical pulping process gives pulp in high yield without much pollution but the pulp quality is not acceptable in most applications and needs high energy input for its prodution. Pulp bleaching nowadays also depends on chemicals and produces environmentally hazardous chlorinated materials in the process. Biomechanical pulping, using microorganisms or enzymes in combination with mechanical methods as the means of delignification, has been proposed as an alternative pulping process. Thanks to the rapid progress of lignin biodegradation studies, one of the lignin degrading white-rot fungi, *Phanerochaete chrysosporium*, has been used successfully in the laboratory scale to pre-treat wood chips[8] in order to reduce the energy input for the subsequent mechanical pulping and to

increase the pulp quality. Microorganism cultures[9] and biomimetic catalysts[10] have also been used for pulp bleaching on a bench scale. Successful application of biotechnology in this area could revolutionize the pulp and paper industry in the near future.

Added to the importance of lignin biodegradation studies is the possible application of lignin degrading systems in the degradation of environmentally persistent pollutants. Chlorinated lignin, polychlorinated biphenyls (PCBs), and polycyclic aromatics are slowly metabolized by ligninolytic *P. chrysosporium* culture to give carbon dioxide. Dark pulp mill effluent is also decolorized by *P. chrysosporium.*

1.3 Lignin degrading microorganisms

1.3.1 Bacteria

A variety of bacteria, including strains of *Norcardia* and *Streptomyces*, have been reported to be able to degrade lignin.[11-13] Studies using [^{14}C]-lignin specifically labelled at side-chain, aromatic ring, and methoxyls, respectively, showed that all the three structural components are converted to $^{14}CO_2$ to various extents.[14] Bacteria, however, seem to play a secondary role in lignin degradation. None of the bacterial strains can cause rapid and extensive degradation of lignin compared to the white-rot fungi.

1.3.2 Fungi

Lignin degrading fungi are classified as white-rot (Basidiomycetes), brown-rot (Basidiomycetes), and soft-rot (Ascomycetes) depending on the pattern of their action

on wood. Brown-rot fungi mainly decompose the carbohydrate in wood, leaving a modified, brown lignin residue. Analysis of the resulting lignin residue showed that the major consequence of brown-rot attack is demethoxylation of aromatic methoxyl groups and direct hydroxylation of the aromatic nucleus. The carbonyl and carboxylic acid groups also increased after the attack, indicating the oxidative nature of the brown-rot attack.[15,16] Studies using [^{14}C]-lignin showed that brown-rot fungi have limited ability to degrade the lignin polymer backbone.[17]

Soft-rot fungi cause a softening of the surface layer of wood, resulting in significant weight loss at the same time. The soft-rot fungi are able to mineralize all the three structural moieties of lignin (aromatic nucleus, side chain, and aromatic methoxyls) in wood, the polysaccharide fraction, however, seem to be preferentially degraded. Lignin decomposition by soft-rot fungi seems to be slow compared to that by white-rot fungi. The soft-rot fungi, however, have not received extensive study and their potential for lignin degradation is still not clear.

White-rot fungi can degrade all the major components of wood and are generally believed to be the major microorganisms responsible for lignin degradation in nature. The polysaccharide and lignin fractions of wood are often degraded simultaneously by white-rot fungi. The relative rates at which cellulose, hemicellulose and lignin are degraded depend on the species of fungus and the culture condition. Species are known which selectively degrade lignin and hemicellulose. Of the many species of lignin degrading white-rot fungus, *Phanerochaete chrysosporium* is the most widely studied and the best lignin degrader found so far. Culture conditions for lignin biodegradation by *P. chrysosporium* have been optimized by Kirk and coworkers.[18] The lignin degrading enzymes of *P. chrysosporium* are produced only during secondary metabolism. Veratryl alcohol (3,4-dimethoxybenzyl alcohol), a secondary metabolite of

P. chrysosporium, was found to be able to induce the biosynthesis of lignin degrading enzymes.[19,20] Studies have shown that added lignin also increases the titers of lignin degrading enzymes.[21,22]

1.4 Lignin degrading enzymes

The complex chemical structure of lignin required that its mechanism of degradation differ from that of other biopolymers, such as cellulose and proteins which are linear molecules composed of repeating units connected by a single, hydrolysable, chemical bond. The heterogeneous nature of lignin determined that its degradation can not be handled by enzymes which have substrate specificity. The subunits of lignin are connected by stable C-C and C-O bonds and are not easily broken down by hydrolysis. The lack of knowledge about lignin degrading enzymes led to the proposal that activated oxygen species, superoxide ($O_2^{\cdot-}$), and hydroxy radical ($HO^{\cdot}$) were involved in lignin biodegradation.[23] Later studies showed, however, that these species play at most a minor role.[24,25]

The first lignin degrading enzyme, lignin peroxidase (LiP), was isolated from *P. chrysosporium* in 1983.[26,27] It is a hemoprotein containing one iron protoporphyrin IX (protohemin) per molecule. A manganese-dependent peroxidase (MnP), which is also a hemoprotein, was isolated later from the ligninolytic culture of the same white-rot fungus.[28,29] Detailed studies[30] of the extracellular enzymes of the *P. Chrysosporium* ligninolytic culture by analytical electric focusing revealed the presence of twenty-one enzymes, fifteen of them are isoenzymes of the previously isolated lignin peroxidase[26,27] and six of them belong to the family of the manganese-dependent peroxidase.[28,29]

The lignin peroxidase isoenzymes[31] have similar molecular weights, between 38,000 and 43,000, but different isoelectric points, varying between pI 4.7 and 3.3. All the lignin peroxidase are able to oxidize veratryl alcohol to veratraldehyde in the presence of hydrogen peroxide. The isoenzymes, however, have different kinetic properties towards various substrates, suggesting different substrate affinities or active site accessibilities.

The similarities and differences of the MnP isoenzymes have not been studied in detail. Preliminary studies[30,31] showed that they could not oxidize veratryl alcohol, but could oxidize vanillylacetone and phenol red in the presence of Mn(II) and hydrogen peroxide.

The importance of the multiplicity of the lignin degrading enzymes is still not clear. The fact that the lignin peroxidases differ in their kinetic properties[31], stabilities[32] and in their relative concentrations at different culture times[31] indicates that some of them might be more important than others for lignin biodegradation. Genetic studies of the isoenzymes suggested that they may have different functions.[33] The abilities of different lignin peroxidase isoenzymes to cleave the various linkages in lignin model compounds have not been demonstrated. Comparison of the reactions catalyzed by the major molecular form of lignin peroxidase, LiP1, and the major isoenzyme of the MnP, named MnP1, using the nomenclature system suggested by Farrell *et al*[31], seems to suggest that these two groups of enzymes catalyze different reactions. MnP1 normally catalyzes the oxidation of phenolic model compounds only,[34] though the oxidation of non-phenolic model compounds was also reported recently.[35] While LiP1 was reported to be able to oxidize a variety of non-phenolic model compounds and to partially depolymerize lignin, the degradation of phenolic model compounds has not been reported. The fact that lignin peroxidase and manganese-dependent peroxidase appear

to reach their maximal activities at different culture times[30] also suggests that they have different functions in lignin biodegradation.

The major lignin peroxidase isoenzyme, LiP1, has a molecular weight of 42,000 daltons and contains about 13% carbohydrate.[36] A single crystal was obtained[37] but the crystal structure is still unavailable. The spectral properties of the hydrogen peroxide-oxidized species of LiP1 were very similar to those of typical peroxidases.[36,38] Like horseradish peroxidase (HRP) compounds I and II, the compounds I and II of LiP1 contains 2 and 1 oxidizing equivalents, respectively, over the ferric resting state of the enzyme.[39] Resonance Raman spectra[40,41] showed that the local heme environment of LiP1 greatly resembles those of other peroxidase. At about 25°C, the ferric iron of LiP1 is mainly high spin, pentacoordinate, but the high spin hexacoordinate state dominates at below 2°C. Like horseradish peroxidase, LiP1 has a vacant coordination site, trans to the proximal fifth ligand, which is histidine,[40,42] at ambient temperature. The Resonance Raman spectra of LiP1 compound II are also very similar to that of HRP compound II, indicating a low spin, hexacoordinate Fe^{IV}=O structure of LiP1 Compound II.

LiP1 was first thought to be an oxygenase.[36] It was found later, however, that oxygen was not consumed in substrate amounts in the oxidation of veratryl alcohol by LiP1 and hydrogen peroxide.[43] Diarylpropane model compounds can be oxidized by LiP1 under both aerobic and anaerobic conditions.[44,45] ^{18}O from $H_2{}^{18}O$ was found to be incorporated into the products under anaerobic conditions.[45] Single-electron transfer agents are able to oxidize lignin model compounds in a manner similarly to LiP1.[43] LiP1, therefore, does not catalyze the oxidation of lignin model compounds by oxygen activation. It is a peroxidase rather than an oxygenase and oxidizes lignin model compounds by single-electron oxidations. The catalytic cycle of lignin peroxidase has been proposed and is shown in Figure 1.4.[39,46] In the absence of a readily oxidizable

substrate, excess hydrogen peroxide converts LiP1 to its inactive form, compound III.[39,46,47] Superoxide can convert the native enzyme directly to compound III. (see Figure 1.4)

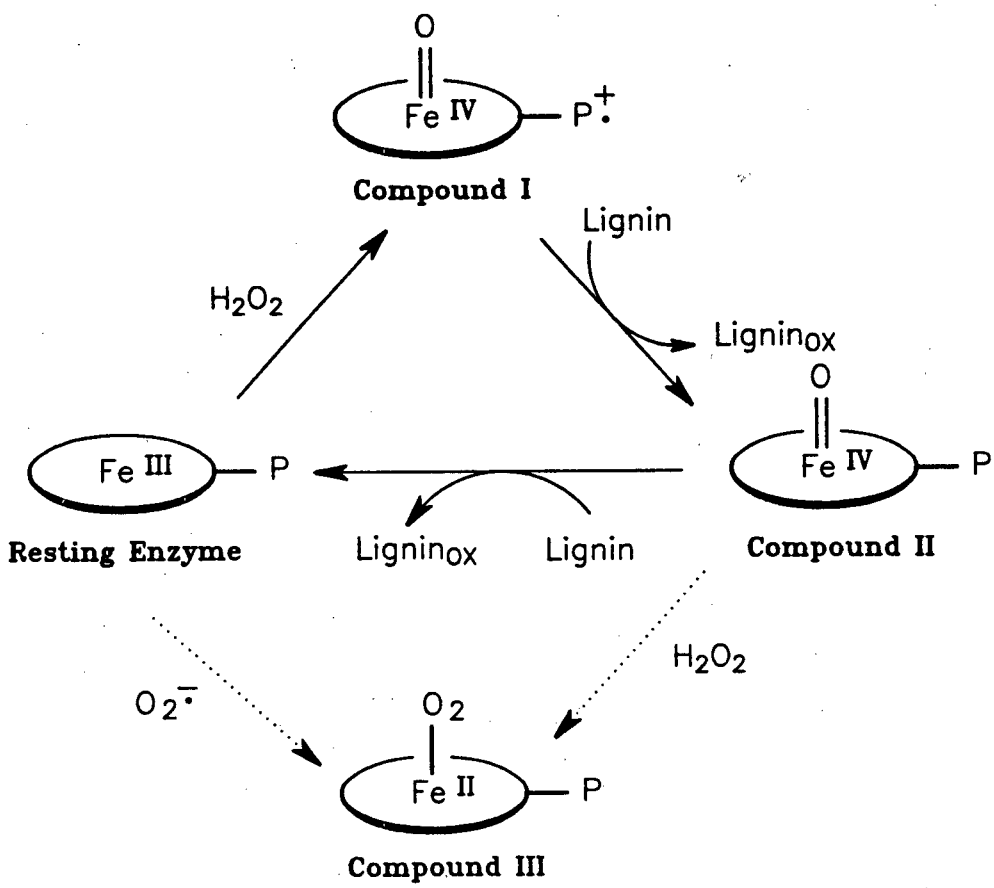

Figure 1.4 Proposed catalytic cycle of lignin peroxidase[39,46]

The isoenzyme of MnP, MnP1, has a molecular weight of 46,000 daltons and has a protohemin as its prosthetic group.[28] Enzyme activity is stimulated by α-hydroxycarboxylic acids and absolutely depends on Mn(II) for its activity. Maximal enzyme activity appears at pH 4.5. The enzyme shows properties of both an oxidase and peroxidase.[48] As an oxidase, it oxidizes NADPH, GSH, and DDT (dithiothreitol) to give hydrogen peroxide, suggesting that it might work as a hydrogen peroxide

generating enzyme for the lignin degrading enzymes of *P. chrysosporium.* As a peroxidase, the hydrogen peroxide oxidized MnP1 can oxidize Mn(II) to give Mn(III), which in turn oxidizes organic substrates. In the presence of hydrogen peroxide and Mn(II), MnP1 can oxidize a number of phenolic compounds and polymeric dyes.[29,48] Electronic absorption, ESR, and resonance Raman spectra studies[29,49,50] of MnP1 showed that the heme iron in the native enzyme is in the high spin pentacoordinate ferric state with histidine as the fifth ligand. The catalytic cycle of MnP has been proposed[50] and is shown is Figure 1.5. The oxidation of the native enzyme by one molecule of

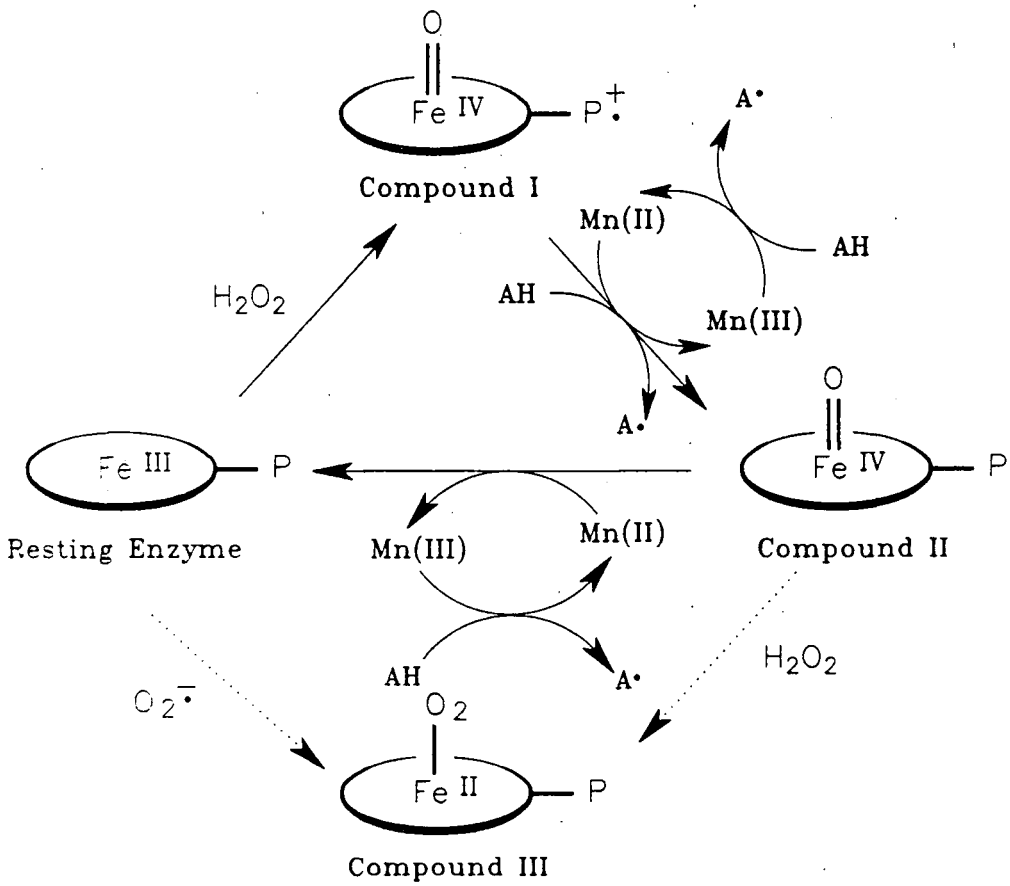

Figure 1.5 Proposed catalytic cycle of manganese-dependent peroxidase[50]

hydrogen peroxide gives MnP compound I, reduction of which by Mn(II) or other one electron acceptors (such as phenols) gives the MnP compound II. The Mn(III) generated can in turn oxidizes phenols and is itself reduced back to give Mn(II) again. The Mn(II)/Mn(III) redox couple thus acts as a mediator for the MnP catalyzed oxidations. The compound II of MnP can be reduced by one equivalent of Mn(II) to the native enzyme. Mn(II) is actually the only substrate that reduces MnP compound II efficiently and thus is necessary to maintain the catalytic cycle of MnP. In the absence of Mn(II), MnP compound II is converted to the compound III by hydrogen peroxide.

Laccase is produced by most white-rot fungi (but not by *P. chrysosporium*) and has long been the subject of research. The main effect of laccase was found to be polymerization of lignin[51,52] and related phenolics.[53] Morohoshi *et al*[54] isolated three extracellular laccases, laccase I, II, and III from *Corriolus versicolour* culture by gel filtration and ion-exchange chromatography. The main function of laccase I is to polymerize lignin while laccase III can depolymerize lignin.[55,56] The electrophoretically homogeneous laccase preparation and laccase III of *Coriolus versicolour* were reported to be able to catalyze both C_α-C_β and phenyl-alkyl cleavage reactions of phenolic ß-1 and ß-O-4 dimeric model compounds.[57,58]

1.5 Reactions catalyzed by lignin peroxidase (LiP1)

Due to the complex structure of lignin and the difficulties in obtaining well defined lignin samples, lignin model compounds, which represent a portion of a structure known to occur in lignin, are often used in lignin biodegradation studies. Although it is still uncertain that an enzyme which can degrade lignin model compounds will degrade lignin in the same way, lignin model compounds are still being used as

convenient substrates and have played important roles for the elucidation of the molecular mechanisms of lignin biodegradation. The first lignin degrading enzyme[26,27] was actually discovered by using a diarylpropane type model compound.

Lignin model compounds containing one, two, three, or even four phenylpropanoid (C_6-C_3) units have been used and are named as monomeric, dimeric, trimeric, and tetrameric model compounds, respectively. Dimeric model compounds are the most commonly used for mechanistic studies and can be classified into several groups depending on the type of linkages connecting the two phenylpropanoid units. The most frequently used dimeric model compounds are the ß-O-4 dimers representing the ß-O-4 substructure (**4**, Figure 1.3), ß-1 dimers representing substructure **7**, ß-5 dimers representing the phenylcoumaran substructure **8**, and biphenyl model compounds representing the biphenyl substructure **6** (see Figure 1.3).

1.5.1 The mechanism of lignin model compound degradation by LiP1

Lignin peroxidase is a heme peroxidase which functions by one electron oxidations. Kersten *et al*[59] first observed, by ESR, the aryl cation radical from the oxidation of alkoxybenzenes by LiP and hydrogen peroxide and suggested that lignin peroxidase degrades lignin through an aryl cation radical intermediate. Schoemaker *et al*[60] and Harvey *et al*[43] also proposed that lignin peroxidase, once oxidized by hydrogen peroxide, can abstract an electron from the electron rich oxygenated aromatic units of lignin to give cation radicals. Further non-enzymatic fragmentation of the cation radical leads to the degradation of lignin.

The single electron oxidation mechanism of lignin model compound degradation by ligninase was demonstrated by Hammel *et al.*[44] In the oxidation of a ß-1 model

compound by LiP, both C_α- and C_β-centered radicals were detected. Evidence was also obtained that the free radicals were intermediates during C_α-C_β cleavage. Radical coupling products of C_β-centered radicals were found under anaerobic conditions and a hydroperoxide derived from the C_β-centered radical was found in the presence of oxygen. A cation radical of a C_α-carbonyl ß-O-4 dimer was observed by ESR.[61] Thus, lignin peroxidase degrades lignin model compounds through a cation radical pathway. All the known reactions catalyzed by lignin peroxidase can be rationalized by this single electron oxidation mechanism.

1.5.2 Reactions catalyzed by lignin peroxidase

A. C_α-C_β cleavage

LiP catalyzes the C_α-C_β cleavage of both ß-1 and ß-O-4 dimeric model compounds[26,27,42,44,61,62] as shown in Figures 1.6 and 1.7 respectively. Substituted phenylglycols are also cleaved at the C_α-C_β bond to give aldehydes.[27] The C_α-C_β cleavage reaction of other model compounds catalyzed by LiP has not been reported so far. It is believed[63] that C_α-C_β cleavage is probably the most important reaction in lignin biodegradation. It has also been reported,[64], however, that lignin depolymerization does not occur to any significant extent even after significant oxidation. LiP was reported[26] to be able to degrade lignin to give 4.5% of veratraldehyde, a product resulting from C_α-C_β cleavage. This result, however, does not indicate extensive C-C bond cleavage as the lignin used was methylated at the free hydroxy groups, which changed the properties of the lignin sample.

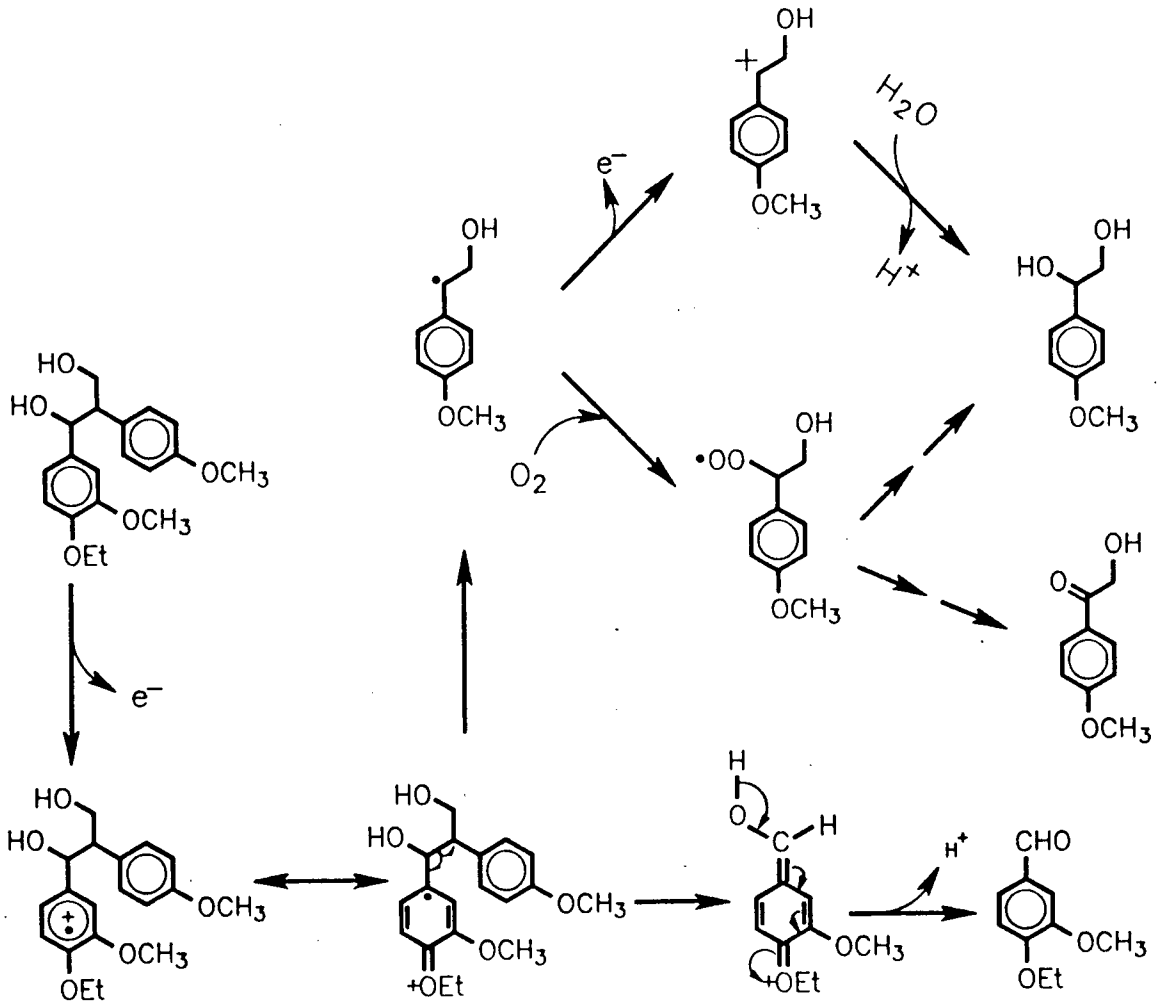

Figure 1.6 The mechanism of C_α-C_β cleavage of β-1 model compounds[26,44,62]

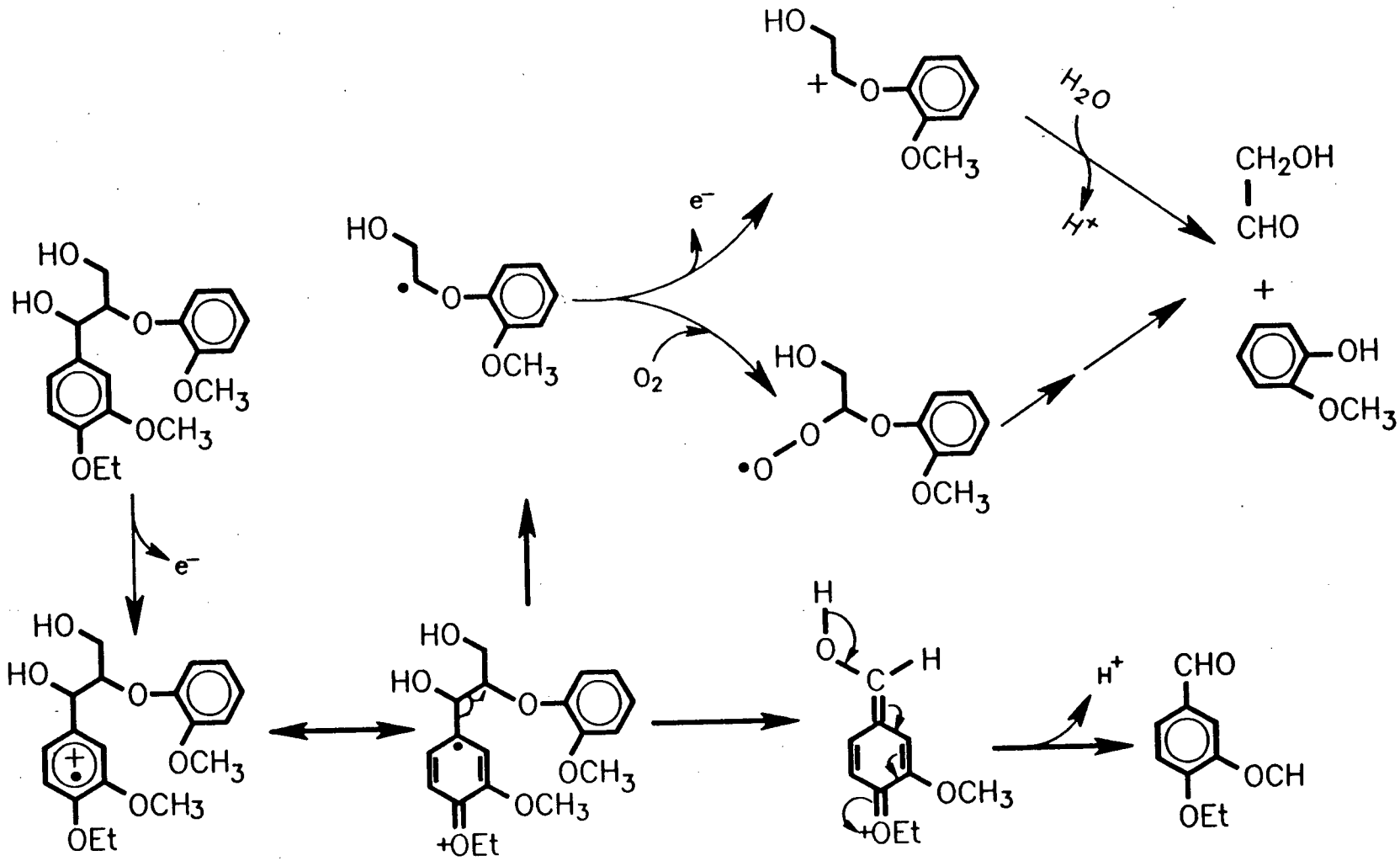

Figure 1.7 The mechanism of C_α-C_β cleavage of ß-O-4 model compounds[26,61]

B. ß-O-4 bond cleavage and dealkylation reactions

In addition to the C_α-C_β cleavage discussed above, LiP also catalyzes the ß-O-4 ether bond cleavage of ß-O-4 model compounds. The cleavage is not a simple hydrolysis but a result of a single electron oxidation[59,65] as shown in Figure 1.8. Attack of the C_α- or C_γ-hydroxy on the B-ring cation radical gives cyclic intermediates, hydrolysis of which gives the ß-O-4 ether cleavage products. Later experiments showed that rearrangement resulting from one-electron oxidation occurs[66,67] and cyclohexadiene ketals were found in the oxidation of lignin model compounds by LiP.[61,68]

Demethoxylation is an important reaction in the metabolism of lignin by *P. Chrysosporium.* A mechanism for demethoxylation was proposed[59] based on the results of oxidation of alkoxybenzenes by LiP as shown in Figure 1.9. Demethoxylation has been found to occur for alkoxybenzenes[59] and for a C_α-carbonyl ß-O-4 dimer.[61] Small amounts of a demethoxylation product was also found in the oxidation of veratryl alcohol.[69] From the experimental evidence available it would appear that demethoxylation is not a major reaction of lignin peroxidase catalysis. It becomes more pronounced when other, usually more favourable, reactions are impossible.

C. Aromatic ring cleavage reactions

The biological degradation of lignin is highly oxidative.[70] Chemical analysis of decayed lignin showed[71] a decrease in the methoxyl content and an increase in the carboxyl content, indicating oxidative aromatic ring cleavage. Degradation products containing residues resulting from aromatic ring opening have been isolated[72-74] and there is evidence[71,64,75-77] that aromatic rings can also be cleaved while still bound to the lignin

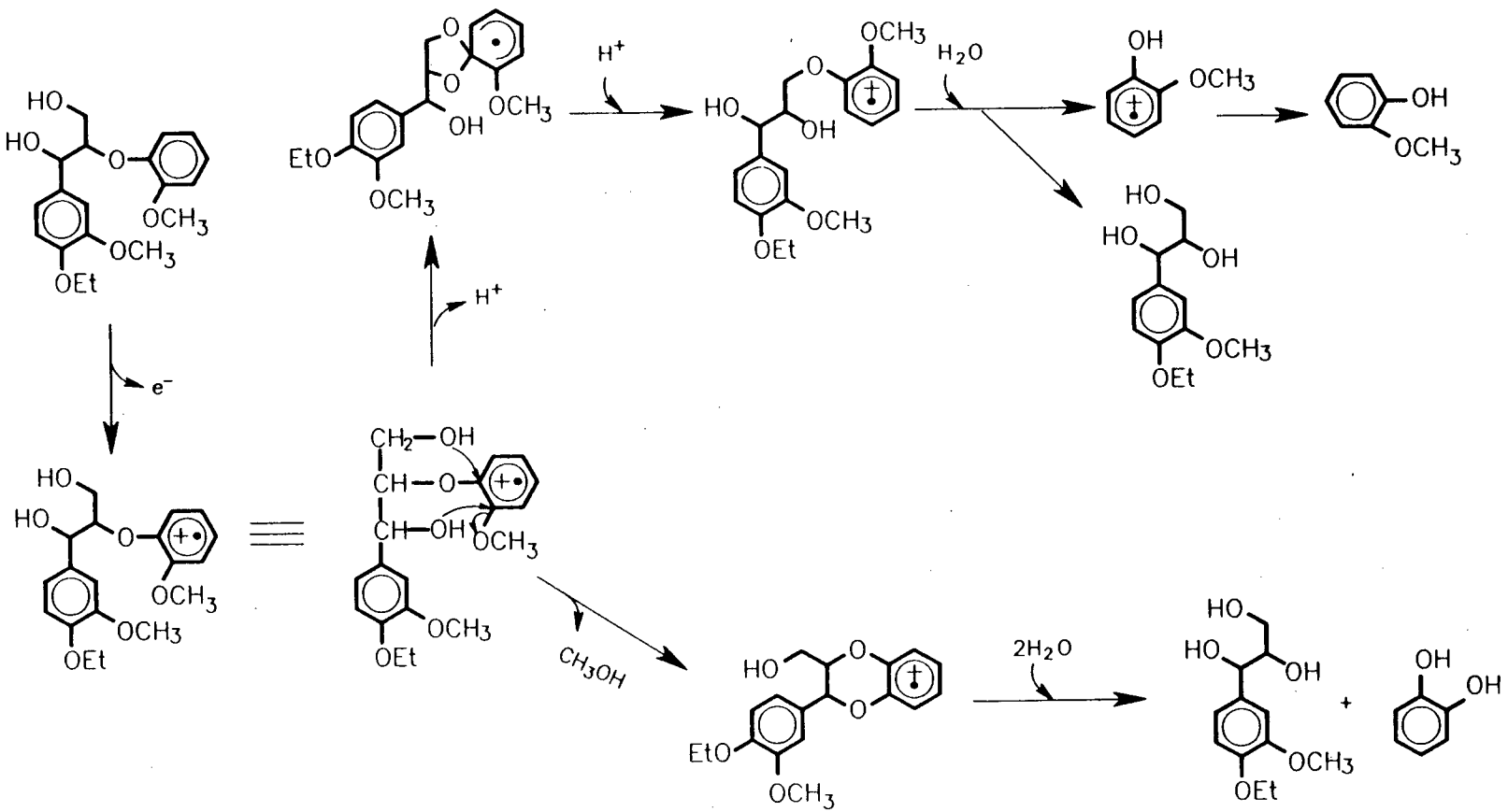

Figure. 1.8 The mechanism of β-O-4 cleavage of β-O-4 model compounds[59,65]

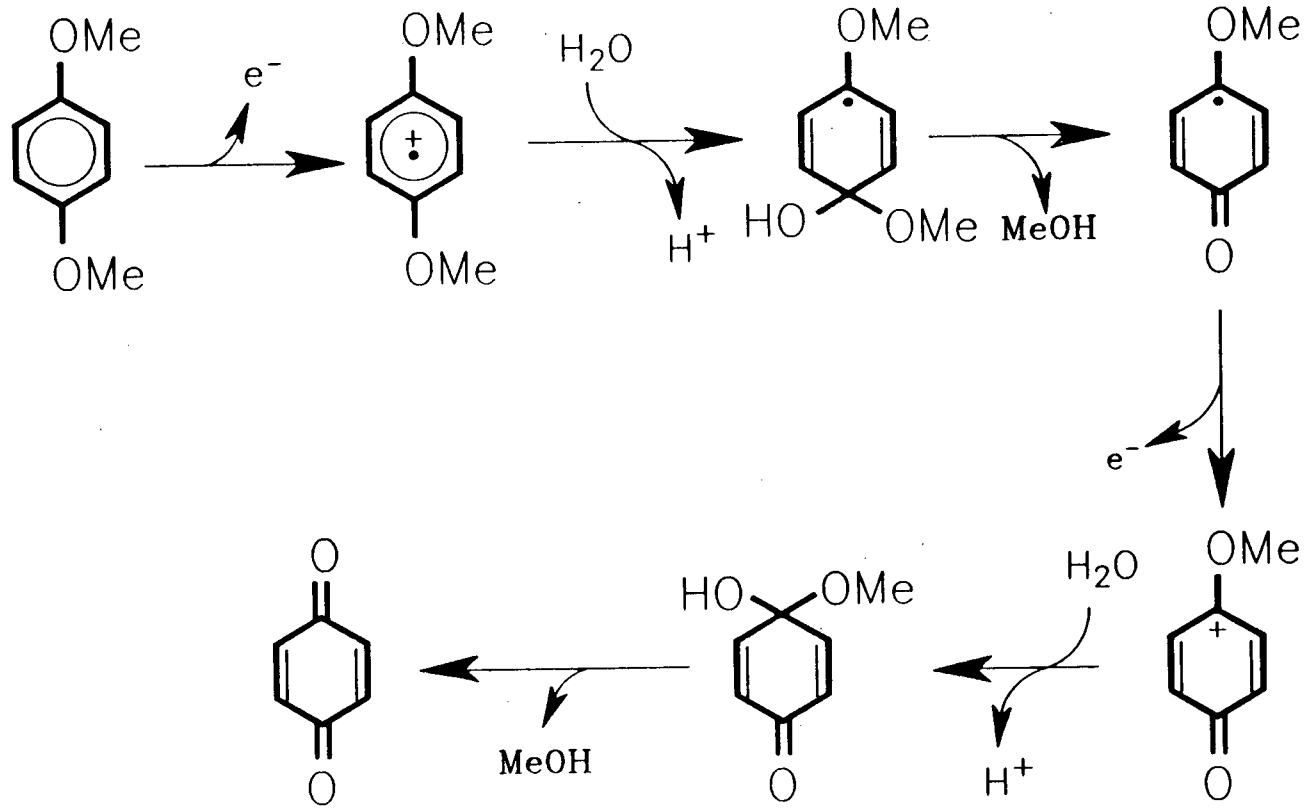

Figure 1.9 Possible mechanism of demethoxylation of lignin model compounds[59]

polymer. The molecular weight of lignin can remain virtually unchanged after extensive oxidation,[64] suggesting that aromatic ring cleavage might be a critical step for lignin degradation. It is generally believed[63,71,78,79] that the aromatic rings of lignin are first demethylated and/or hydroxylated to give *o*-diphenols, cleavage of which by dioxygenases gives aliphatic carboxylic acids. Aromatic ring cleavage of a ß-O-4 dimeric model compound by *P. chrysosporium* was reported.[70] It has been found that aromatic rings of lignin model compounds can be cleaved by lignin peroxidase without the necessity of pre-demethoxylation or hydroxylation. LiP catalyzed aromatic ring cleavage of veratryl alcohol[69,80-82] and ß-O-4 model compounds[83-89] have been studied extensively and a mechanism was proposed based on isotope labelling experiments.[86,89] As shown in Figure 1.10 using veratryl alcohol as an example, the ring opening is initiated by an one-electron oxidation. Coupling of molecular oxygen with the carbon-centered radical gives a peroxyl radical, further reaction of which gives the ring cleaved products. The isolation of direct ring-opening product (a muconate) from a ß-O-4 dimer[88] supports the mechanism described above.

D. Benzylic alcohol oxidation

Benzylic alcohol oxidation (C_α-oxidation) has been found as a reaction in the oxidation of lignin model compounds by LiP. Veratryl alcohol is oxidized to give veratraldehyde as a major product. Small amounts of C_α-carbonyl products were also found from the oxidation of the C_α-alcohol of dimeric lignin model compounds.[61,83,90] (Figure 1.11) This reaction seems to be unfavourable for lignin model compound degradation since the aromatic ring is deactivated by the C_α-carbonyl group for further oxidation.

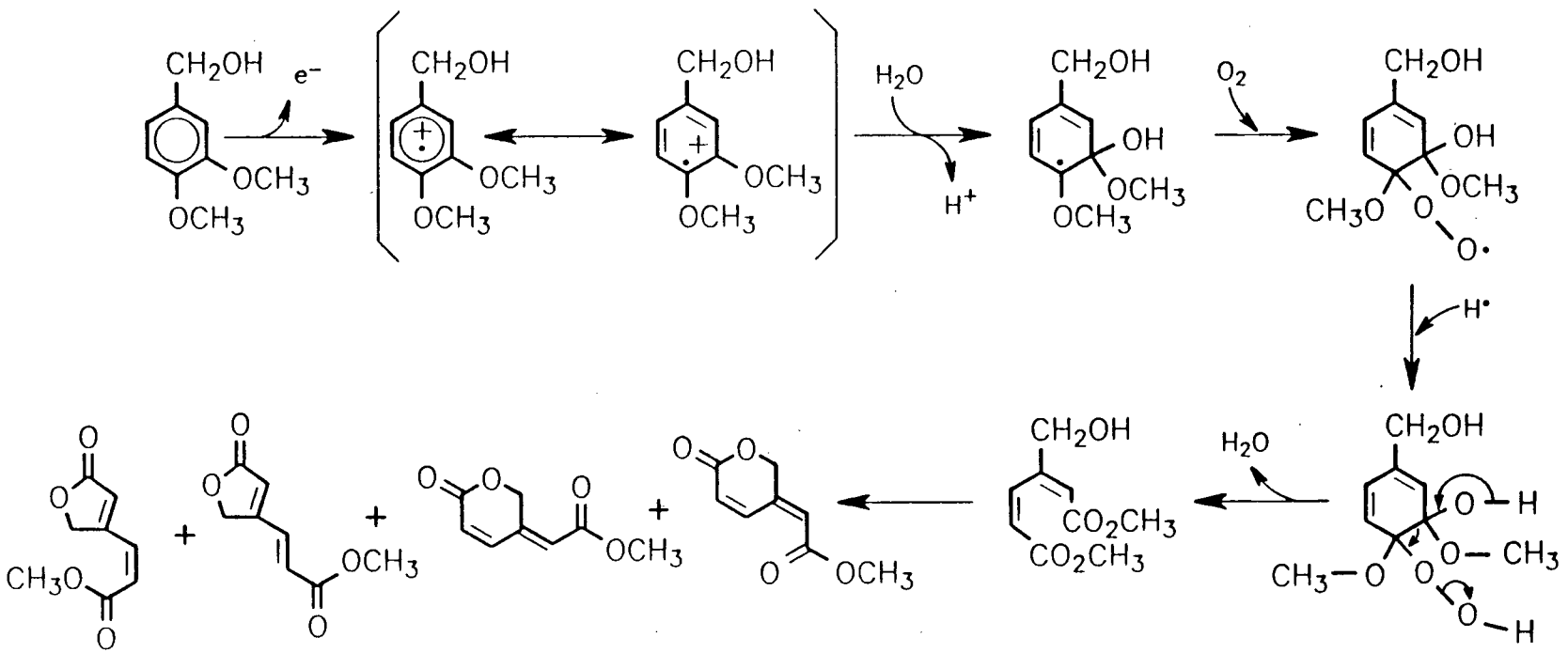

Figure 1.10 Proposed mechanism of aromatic ring cleavage of veratyl alcohol[69,80-82]

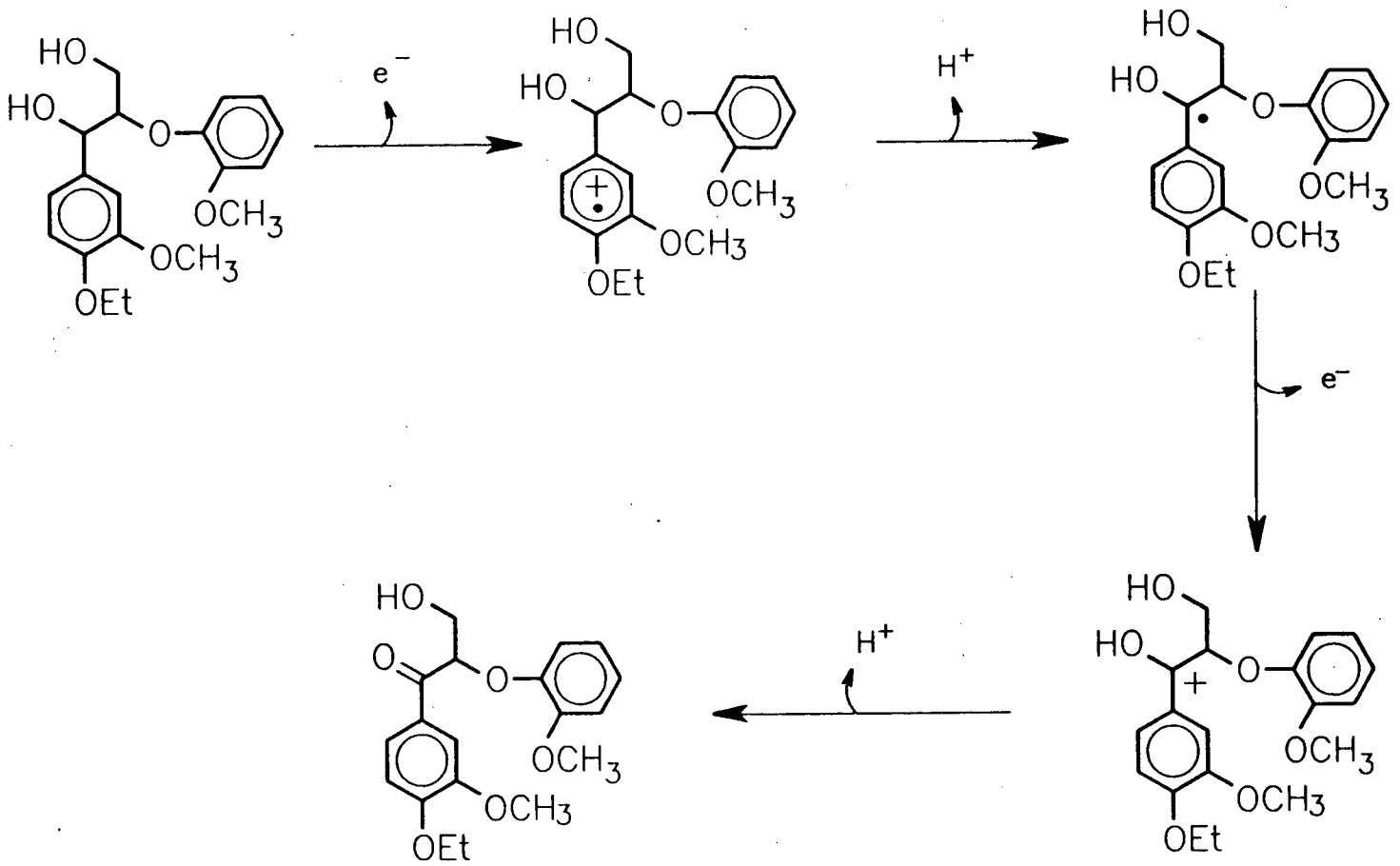

Figure 1.11 Possible mechanism of C_α-oxidation of lignin model compounds

Veratraldehyde is not oxidized by LiP. On the contrary, externally added veratraldehyde is rapidly reduced back to veratryl alcohol by the *P. chrysosporium* culture. The resulting veratryl alcohol is then metabolized to finally give carbon dioxide and water through aromatic ring cleavage and quinone intermediates.[91] The role of the oxidation of veratryl alcohol, if it happens in *vitro*, is still not clear.

Studies[71] on white-rot decayed lignin showed that C_α-carbonyl groups were prominent. Though the A-ring is deactivated by the C_α-carbonyl (Figure 1.11), the B-ring is not affected and O-C_4 (ß-O-4 ether bond) cleavage resulting from B-ring oxidation is favoured in C_α-carbonyl model compounds.[61] The aromatic ring opening of ß-1 and ß-O-4 dimers is probably also facilitated by C_α-oxidation. Another possible consequence of C_α-oxidation is the cleavage of C_α-hemicellulose ether bonds and other C_α-ether bonds in lignin.[91] The cleavage of C_α-ether bonds has been demonstrated for model compounds.[61] Shimada[92] proposed that C_α-oxidation was important for lignin biodegradation since it could destroy the chiral centers at C_α and C_β thus reducing the complexity of lignin. It was shown that C_α-oxidation of lignin enhances its depolymerization. The explanation was that the decreased steric complexity following C_α-oxidation opens up the polymer, making it more accessible to lignin degrading enzymes. Recent work[36,93] showed that lignin model compound degradation was not stereospecific. The proposed mechanism of lignin degradation by LiP also suggests that the stereocomplexity of lignin does not hinder its degradation.

E. Glycol formation from C_α-C_β double bonds

C_α-C_β double bonds are found in the terminal chains of lignin. LiP can oxidize

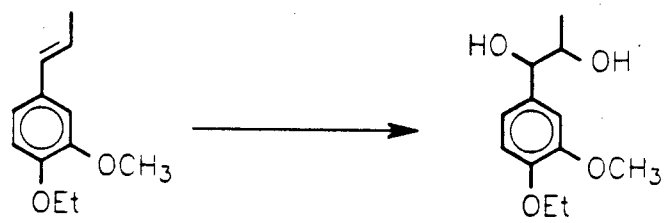

Scheme 1.2 C_α-C_β double bond hydroxylation.

these double bonds of lignin model compounds[27,38,94] to give diols which are then further oxidized (Scheme 1.2). Isotopic labelling experiments[61] showed that the oxygen of the C_β-hydroxy of the resulting diol came from molecular oxygen. Diol formation from C_α-C_β double bonds were also found in the metabolism of lignin model compounds by *P. chrysosporium* cultures.[95-98]

The formation of diols via epoxides is a well known reaction of cytochromes P-450 which are monooxygenases and function by molecular oxygen activation.[99] It seems unlikely that diol formation described above follows the mechanism of P-450 catalysis. In order for oxygen atom transfer to occur, and for epoxide to be formed, the substrate must closely approach the Fe^{IV}=O bond of the protohemin at the active site of the heme protein. Due to the complexicity of lignin structures, such steric requirements cannot be met during lignin oxidation.

F. Hydroxylation of benzylic methylene groups

Lignin peroxidase can catalyze the hydroxylation of benzylic methylene groups (C_α-hydroxylation).[36,38,45] ^{18}O from $^{18}O_2$ was found to be incorporated into the C_α-hydroxy group of the product under aerobic conditions, while under anaerobic

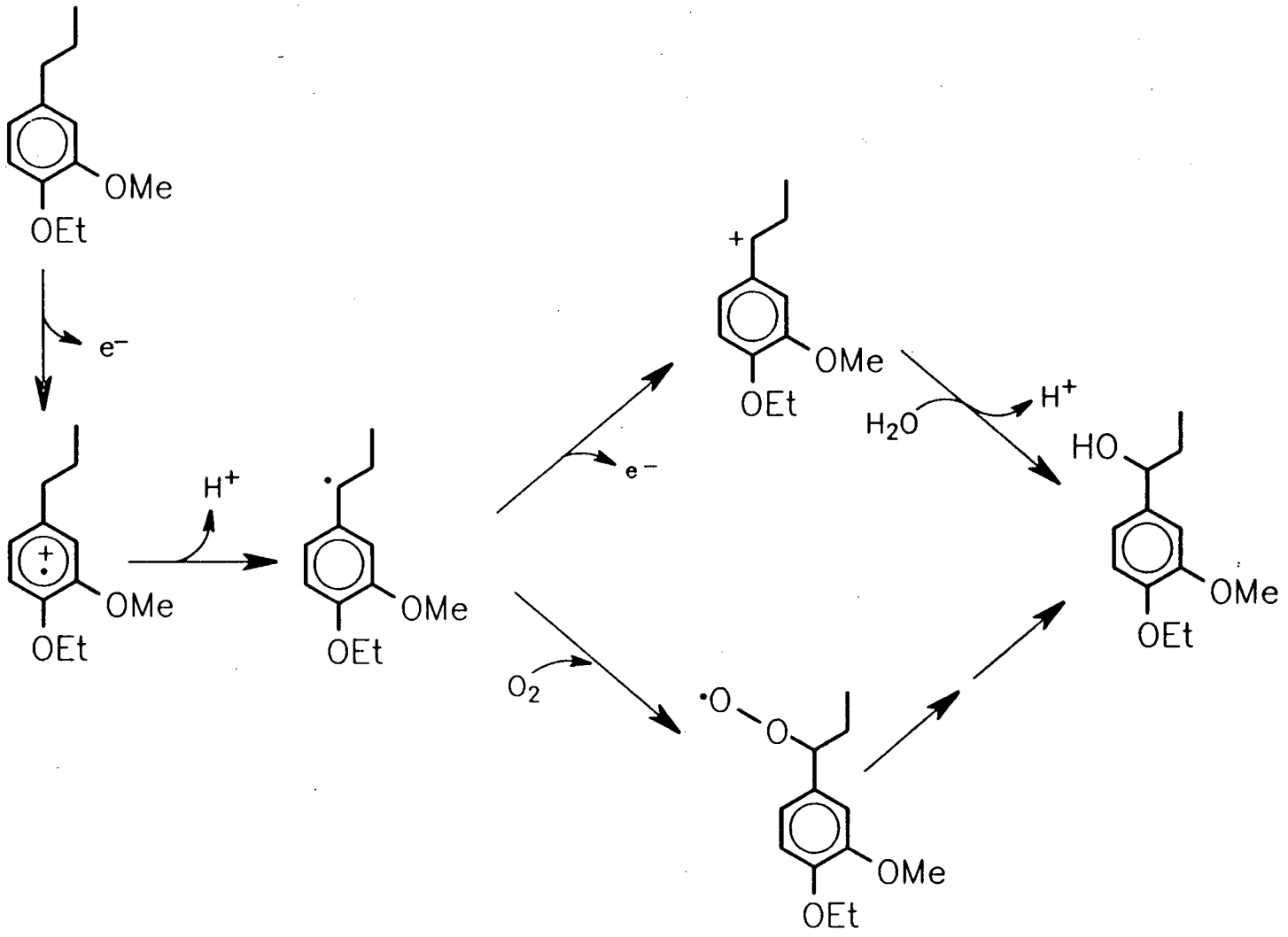

Figure 1.12 Possible mechanism of C_α-hydroxylation of lignin model compounds

conditions, the C_α-hydroxy oxygen was from water, suggesting a cation radical mechanism as shown in Figure 1.12. C_α-hydroxylation of model compounds was also found to be catalyzed by *P. chrysosporium* cultures.[100,101] The importance of this reaction in lignin degradation is still not clear.

G. Degradation and/or oxidation of lignin polymers

Tien and Kirk first studied the degradation of lignin by LiP.[26] Spruce lignin and milled wood lignin (MWL) of birch were methylated at the free hydroxyl groups with $^{14}CH_3I$. Veratraldehyde (4.5%) was isolated from spruce lignin, 0.6% veratraldehyde and 0.4% syringaldehyde were isolated from birch lignin after incubation with lignin peroxidase. These results, however, do not provide convincing evidence that lignin peroxidase alone can depolymerize lignin since fundamental properties of the lignin were changed by methylation. The absence of free hydroxy groups makes the repolymerization more difficult. It is apparent that the methylated precursors of lignin biosynthesis (Scheme 1.1, **1**, **2**, and **3**) cannot be polymerized to give methylated lignin or similar products under the conditions of lignin biosynthesis. Polymerization of lignin by enzymes from *P. chrysosporium* has been reported.[102] Glenn *et al*[27] also reported the degradation of lignin by LiP in DMF. It is not clear if lignin depolymerization occurs in aqueous solution. Dordick *et al*[103] reported that HRP and other peroxidases are able to vigorously depolymerize both natural and synthetic lignins in organic solvent, but are unable to do so in aqueous solution. A reassessment which questioned Dordick's experiment was reported later.[104] Treatment of two synthetic lignins and one ^{14}C-methylated spruce lignin with crude lignin peroxidase[105] decreased their degradation by *Xanthomonas sp* strain 99. Both polymerization and depolymerization was found for

the ^{14}C-methylated spruce lignin while only polymerization was found for the synthetic lignins.

Lignin peroxidase is unable to depolymerize lignin completely for as yet unknown reasons. Mechanism(s) must exist which can prevent the repolymerization of lignin by LiP or other enzymes. Though the degradation of lignin by *P. chrysosporium* is highly oxidative, there are enzymes in *P. chrysosporium* cultures which accomplish the reduction of acids, aldehydes, and quinones. The importance of these reductive reactions has been discussed recently.[106]

1.6 Biomimetic approaches in lignin biodegradation

Lignin peroxidase is a non-specific enzyme containing protohemin as its prosthetic group. The hydrogen peroxide-oxidized intermediate, oxoiron(IV) protoporphyrin cation radical, is a powerful oxidizing species which can initiate one-electron oxidation of its substrates. Due to the heterogeneous structure of lignin, it seems unlikely that LiP will have an "active site" which can bind all the substructures of lignin and catalyze oxidations at its active site. Metalloporphyrins, therefore, could be good models for lignin peroxidase. These biomimetic catalysts may have advantages to the enzymes.

Natural lignin is a three dimensional, water-insoluble high molecular weight polymer. Even the modified, water soluble lignin (such as lignosulfate) have compact, spheric structures in solution. The exponent α in the Mark-Houwink equation is about 0.1-0.5, corresponding to an intermediate form between an Einstein sphere and a compact coil. So a large part of lignin is not exposed to the active site of an enzyme during lignin degradation. Interaction of the lignin polymer and lignin degrading

enzymes is difficult to visualize. Being small molecules, metalloporphyrins, as lignin peroxidase models, may have an advantage in that their interactions with the lignin substrate may be easier than that with the enzyme.

The properties of the metalloporphyrins, such as redox potential and solubility in organic or aqueous solvents, can be changed as desired by structural modification. Most metalloporphyrins can be obtained in large quantities relatively easily. In contrast, lignin peroxidase is expensive and difficult to obtain in large quantity. Finally, enzymes are usually rather labile and very sensitive to pH, temperature, and solvent. Metalloporphyrins, on the other hand, can be very stable and can be used under extreme conditions.

As lignin peroxidase catalyzes reaction by one-electron oxidation, electrochemical methods, which can initiate one-electron oxidation at the electrode, can also be used for biomimetic approaches to lignin biodegradation.

1.6.1 Degradation of lignin model compounds by iron porphyrins

Shimada *et al*[90] first studied the degradation of a ß-1 model compound, 1,2-bis(4-ethoxy-3-methoxyphenyl)propane-1,3-diol by iron tetraphenylporphyrin chloride (**10**, TPPFeCl, Figure 1.13) in the presence of t-butyl hydroperoxide (t-BuOOH) or iodosylbenzene in methylene chloride. The reaction was similar to that catalyzed by lignin peroxidase. Experiments[107] in the presence of $^{18}O_2$ or $H_2{}^{18}O$ showed the same isotopic incorporation pattern as that of the enzyme catalyzed reaction, indicating similar mechanisms for the two reactions. The degradation of a ß-1 model compound by protohemin (**11**, Figure 1.13) and hydrogen peroxide was also studied,[108] C_α-C_β cleavage and C_α-oxidation were found to be the major reactions. Protohemin was also

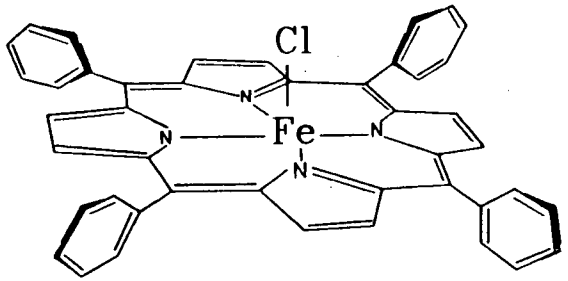

10

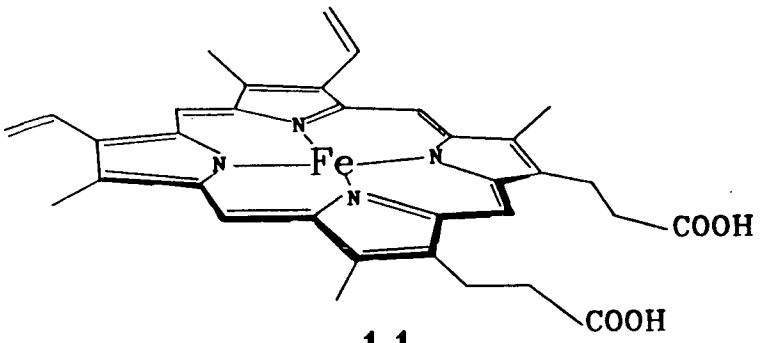

11

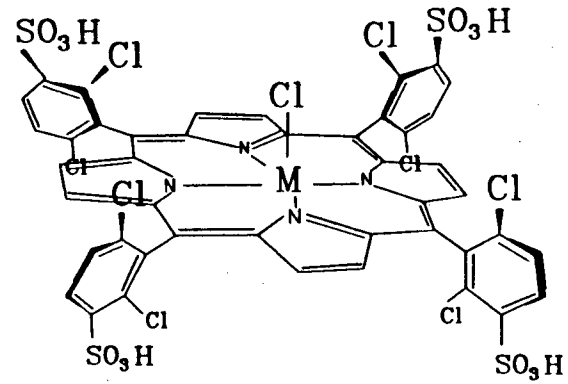

12 M=Fe

13 M=Mn

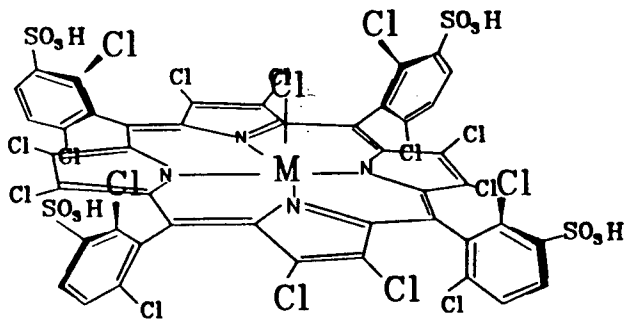

14 M=Fe

15 M=Mn

Figure 1.13 The structure of some metalloporphyrins

shown to be able to catalyze the aromatic ring cleavage of veratryl alcohol.[81] Shimada *et al*[109] studied the degradation of ß-1, ß-O-4, and ß-5 dimers by protohemin. The cation radical mechanism for the C_α-C_β cleavage of the ß-1 dimer was found to be supported by kinetic studies. While the ß-1 dimer was oxidatively cleaved by protohemin in a manner similar to the enzyme catalyzed reaction, the degradation of the ß-O-4 dimer, 4-ethoxy-3-methoxyphenylglycerol-ß-guaiacyl ether, gave products different from the enzyme catalyzed reaction.[27]

Wood *et al*[110] also reported the oxidation of a C_α-carbonyl ß-O-4 model compound by a number of iron porphyrins, including TPPFeCl, iron *meso*-tetra(2-methylphenyl)porphyrin, iron *meso*-tetra(4-sulfonatophenyl)porphyrin, iron *meso*-tetra(4-N,N,N-trimethylanilinium)porphyrin, and iron *meso*-tetra(N-methyl-4-pyridyl)porphyrin.

1.6.2 Oxidation of lignin model compounds by inorganic one-electron oxidants

It was reported[43,60] that ceric ammonium nitrate and tris(phenanthroline)iron(III) could oxidize 1,2-bis(3,4-dimethoxyphenyl)propane-1,3-diol to give veratraldehyde. An initial one-electron oxidation was suggested as the mechanism of the reaction. Further studies by Fisher and Dershem[111] showed that ceric ammonium nitrate did not cleave the ß-1 model compound by one-electron oxidations. Instead, coordination of the α-hydroxy group of the ß-1 dimer to cerium and decomposition of the resulting complex directly gave the product.

Huynh[112] reported the oxidation of several model compounds by copper peroxydisulfate in 5:1 acetic acid/water at reflux temperature. Veratrylglycerol-ß-guaiacyl ether can be degraded by this system giving products similar to that of the LiP catalyzed reaction. In the degradation of dihydroanisoin (1,2-di(4-methoxyphenyl)-1,2-

ethanediol) and veratryl alcohol, side reactions occurred.

Veratrylglycerol-ß-guaiacyl ether was reported[113] to be cleaved at the C_α-C_β bond by Co(II)/Mn(II) in 80% acetic acid under oxygen (4% oxygen in nitrogen, 500 psi) at 170°C. The C_α-C_β cleavage resulted from an initial single-electron oxidation. Treating the ß-1 model compounds, dihydroanisoin and 1,2-di(4-methoxyphenyl)propane-1,3-diol, under the same condition gave only acid-catalyzed dehydration products.

1.6.3 Electrochemical oxidation of lignin model compounds

Electrochemical methods are useful tools for studying reactions involving cation radical intermediates. It is known[114] that 3,5-dimethoxy-4-hydroxy-α-methylbenzyl alcohol can be oxidized by HRP in the presence of excess hydrogen peroxide to give 3,5-dimethoxy-*p*-benzoquinone. Phenoxy radicals of 3,5-dimethoxy-4-hydroxy-α-methylbenzyl alcohol and of 3,5-dimethoxy-4-hydroxyacetophenone were detected during the reaction. When less than one equivalent of hydrogen peroxide was used the phenoxy radical of 3,5-dimethoxyacetophenone was not detected but 3,5-dimethoxy-*p*-benzoquinone was still found as a product. By oxidizing the substrate at different potentials, electrochemical techniques showed that the quinone can be formed directly from the starting material without requiring 3,5-dimethoxy-4-hydroxyacetophenone as an intermediate.[115] The demethylation mechanism of 3,5-dimethoxy-4-hydroxyacetophenone was also readily established by electrochemical methods.[116]

Electrochemical oxidation of alkoxyphenols[117-119] indicated that two pathways were involved. They can be oxidized by removing two electrons to give the phenoxonium ions, reaction of which with water or other nucleophiles gives the final products. The second pathway, which is favoured in the presence of base, involves one-electron

oxidation to give a phenoxy radical, subsequent coupling of the radical gives polymerized products.

Limosin *et al*[120] have studied the electrochemical oxidation of over 20 dimeric lignin model compounds in acetonitrile. The major reaction was polymerization. The oxidation of a ß-O-4 model compound in aqueous acetonitrile,[121] however, gave cleavage products.

The electrochemical oxidation of lignin in basic aqueous solution has been studied.[122] A decrease in phenyl groups and an increase in carboxylic acid group content was found and aromatic ring cleavage was also found. A review addressing the practical aspects of the electrochemistry of lignin was prepared by Chum *et al.*[123] Lignins can be effectively degraded to small molecules by anodic oxidation. The reactions are probably different from LiP catalyzed reactions as the reaction conditions (pH) are different.

1.7 The purpose of this study

Although simple metalloporphyrins have been used as models for lignin peroxidase,[81,91,107-110] metalloporphyrin catalyzed degradation of model compounds representing all the major substructures of lignin have not been reported. Protohemin[81] (**11**) and iron *meso*-tetraphenylporphyrin chloride (TPPFeCl, **10**) were able to mimic lignin peroxidase in the degradation of veratryl alcohol and ß-1 model compounds. The degradation of a ß-O-4 model compound, which represents the most abundant substructure of lignin, by protohemin and lignin peroxidase gave different products.[109] The oxidation of this important model compound by metalloporphyrins needed to be re-examined.

The degradation of ß-5 and 5-5′ biphenyl compounds by iron porphyrins have not been studied. Reactions such as hydroxylation of benzylic methylene groups and glycol formation from C_α-C_β double bonds have not been reported for metalloporphyrin catalyzed reactions. These reactions have to be studied in order to demonstrate that metalloporphyrins mimic lignin peroxidase in all cases.

The metalloporphyrins used in previous studies[81,90,107-110] suffer a great disadvantage in that they are very unstable towards excess oxidants. A catalyst to substrate ratio of 1:10 had to be used.[109] In addition, most of the reactions were performed in organic solvents and reactions in organic and aqueous solutions may follow different pathways. Dramatic solvent effect has been observed for enzyme catalyzed oxidations of lignin.[103]

Biotechnology holds great potential in the pulp and paper industry. Biomimetic catalysts such as metalloporphyrins provide an alternative for using enzymes and microorganism cultures in pulping and pulp bleaching processes. The metalloporphyrins, however, have to be made stable and water soluble before they can be used in industry.

Water soluble, sterically protected metalloporphyrins, the iron(III) and manganese(III) complexes of *meso*-tetra(2,6-dichloro-3-sulfonatophenyl)porphyrin (TDCSPPFeCl, **12**; TDCSPPMnCl, **13**; Figure 1.13), and *meso*-tetra(2,6-dichloro-3-sulfonatophenyl)-ß-octachloroporphyrin (Cl_{16}TSPPFeCl, **14**; Cl_{16}TSPPMnCl, **15**; Figure 1.13) have been synthesized and used as models for lignin peroxidase. Factors affecting the catalytic activities of these metalloporphyrins have been studied. The degradation of a number of lignin model compounds, including veratryl alcohol, ß-1, ß-O-4, ß-5, 5-5′ biphenyl, phenylpropane and phenylpropene model compounds, are presented. Preliminary studies on the oxidation of environmental pollutants, pyrene and

2,4,6-trichlorophenol, are reported.

Metallophthalocyanines, a class of compounds closely related to the metalloporphyrins, have also been examined as models for lignin peroxidase.

Manganese(II)-complexes and veratryl alcohol have been suggested to function as mediators for the manganese-dependent peroxidase and lignin peroxidase, respectively. Metalloporphyrins and electrochemical techniques have been used to study the mediating effects of manganese(II)-complexes and veratryl alcohol.

References for Chapter 1

1. T. Higuchi, M. Shimada, F. Nakatsubo, and M. Tanahashi, Wood Sci. Technol. **11**, 153, 1977.
2. E. Adler, Wood Sci. Technol. **11**, 169, 1977.
3. H. Nimz, Angew. Chem. **86**, 336, 1974.
4. D. W. Ribbons, Phil. Trans. R. Soc. Lond. **A321**, 485, 1987.
5. D. Feldman, L. Lacasse, and M. Beznaczuk, Prog. Polym. Sci. **12**, 271, 1986.
6. B. E. Dale, Trends in Biotechnol. **5**, 287, 1987.
7. M. Tanaka, R. Matsuno, Enzyme Microb. Technol. **7**, 197, 1985.
8. G. F. Leatham, G. C. Myers, T. H. Wegner, and R. A. Blanchette, In proceedings of the Fourth International Conference on Biotechnology in the Pulp and Paper Industry. Raleigh, N.C., USA, 1989, in press.
9. M. G. Paice, L. Jurasek, C. Ho, R. Bourbonnais, and F. Archibald, see Ref. 8.
10. P. S. Skerker, R. L. Farrell, D. Dolphin, F. Cui and T. Wijesekera, see Ref. 8.
11. D. L. Crawford, and R. L. Crawford, Enzyme Microb. Technol. **2**, 11, 1980.
12. R. L. Crawford, and D. L. Crawford, Enzyme Microb. Technol. **6**, 434, 1984.
13. R. Vicuna, Enzyme Microb. Technol. **10**, 646, 1988.
14. J. Trojanowski, K, Haider, and V. Sundman, Arch. Microbiol. **114**, 149, 1977.
15. T. K. Kirk, and E. Adler, Acta Chem. Scand. **24**, 3379, 1970.
16. T. K. Kirk, Holzforschung, **29**, 99, 1975.
17. T. K. Kirk, W. J. Connors, R. D. Bleam, W. F. Hackett, J. K. Zeikus, Proc. Natl. Acad. Sci. USA, **72**, 2515, 1975.

18. T. K. Kirk, and R. L. Farrell, Ann. Rev. Microbiol. **41**, 465, 1987.

19. B. D. Faison, T. K. Kirk, and R. L. Farrell, Appl. Environ. Microbiol. **52**, 251, 1986.

20. M. S. A. Leisola, D. C. Ulmer, R. Waldner, A. Fiechter, J. Biotechnol. **1**, 331, 1984.

21. B. D. Faison, and T. K. Kirk, Appl. Environ. Microbiol. **49**, 299, 1985.

22. D. C. Ulmer, M. S. A. Leisola, and A. Fiechter, J. Biotechnol. **1**, 13, 1984.

23. P. Hall, Enzyme Microb. Technol. **2**, 170, 1980.

24. T. K. Kirk, M. D. Muzuch, and M. Tien, Biochem. J. **266**, 455, 1985.

25. T. K. Kirk, F. Nakatsubo, and I. D. Raid, Biochem. Biophys. Res. Comm. **111**, 200, 1983.

26. M. Tien, and T. K. Kirk, Science, **221**, 661, 1983.

27. J. K. Glenn, M. A. Morgan, M. B. Mayfield, M. Kuwahara, and M. H. Gold, Biochem. Biophys. Res. Commun. **114**, 1077, 1983.

28. M. Kuwahara, J. K. Glenn, M. A. Morgan, and M. H. Gold, FEBS Letters, **169**, 247, 1984.

29. J. K. Glenn, and M. H. Gold, Arch. Biochem. Biophys. **242**, 329, 1985.

30. M. S. A. Leisola, B. Kozulic, F. Menssdoerffer, and A. Fiechter, J. Biol. Chem. **262**, 419, 1987.

31. R. L. Farrell, K. E. Murtagh, M. Tien, M. D. Mozuch, and T. K. Kirk, Enzyme Microb. Technol. **11**, 322, 1989.

32. F. Tonon, and E. Odier, Appl. Environ. Microbiol. **54**, 466, 1988.

33. M. Tien, see Ref. 8.

34. H. Wariishi, K. Valli, and M. H. Gold, Biochem. **28**, 6017, 1989.

35. M. H. Gold, H. Wariishi, K. Valli, M. B. Mayfield, V. J. Nipper, and D.

Pribnow, see Ref. 8.

36. M. Tien, and T. K. Kirk, Proc. Natl. Acad. Sci. USA, **81**, 2280, 1984.

37. J. Troller, J. D. G. Smit, M. S. A. Leisola, J. Kallen, K. H. Winterhalter, and A. Fiechter, Bio/technol. **6**, 571, 1988.

38. V. Renganathan, K. Miki, and M. H. Gold, Arch. Biochem. Biophys. **241**, 304, 1985.

39. V. Renganathan, and M. H. Gold, Biochem. **25**, 1626, 1986.

40. D. Kuila, M. Tien, J. A. Fee, and M. R. Ondrias, Biochem. **24**, 3394, 1985.

41. L. A. Anderson, V. Renganathan, T. M. Loehr, and M. H. Gold, Biochem. 26, 2258, 1987.

42. L. A. Anderson, V. Renganathan, A. A. Chiu, T. M. Loehr, and M. H. Gold, J. Biol. Chem. **260**, 6080, 1985.

43. P. J. Harvey, H. E. Schoemaker, R. M. Bowen, and J. M. Palmer, FEBS Letters, **183**, 13, 1985.

44. K. E. Hammel, M. Tien, B. Kalyanaraman, and T. K. Kirk, J. Biol. Chem. **260**, 8348, 1985.

45. V. Renganathan, K. Miki, and M. H. Gold, Arch. Biochem. Biophys. **246**, 155, 1986.

46. J. M. Palmer, P. J. Harvey, and H. E. Schoemaker, Phil. Trans. R. Soc. Lond. **A321**, 495, 1987.

47. M. Tien, T. K. Kirk, C. Bull, and J. A. Fee, J. Biol. Chem. **261**, 1687, 1986.

48. A. Pasczynski, V.-B. Huynh, and R. Crawford, Arch. Biochem. Biophys. **244**, 750, 1986.

49. Y. Mino, H. Wariishi, N. J. Blackburn, T. M. Loehr, and M. H. Gold, J. Biol. Chem. **263**, 7029, 1988.

50. H. Wariishi, L. Akileswaran, and M. H. Gold, Biochem. **27**, 5365, 1988.

51. A. Haars, and A. Huttermann, Naturwissenschaften, **67**, 39, 1980.

52. A. Huttermann, C. Herche, and A. Haars, Holzforschung, **34**, 64, 1980.

53. A. Haars, and A. Huttermann, Arch. Microbiol. **125**, 233, 1980.

54. N. Morohoshi, H. Wariishi, C. Muraiso, T. Nagai, and F. Haraguchi, Mokuzai Gakkaishi, **33**, 218, 1987.

55. N. Morohoshi, and T. Haraguchi, Mokuzai Gakkaishi, **33**, 143, 1987.

56. N. Morohoshi, K. Fujita, H. Wariishi, and H. Haraguchi, Mokuzai Gakkaishi, **33**, 310, 1987.

57. S. Kawai, T. Umezawa, M. Shimada, T. Higuchi, K. Koide, T. Nishida, N. Morohoshi, and T. Haraguchi, Mokuzai Gakkaishi, **33**, 792, 1987.

58. H. Wariishi, N. Morohoshi, and T. Haraguchi, Mokuzai Gakkaishi, **33**, 892, 1987.

59. P. J. Kersten, M. Tien, B. Kalyanaraman, and T. K. Kirk, J. Biol. Chem. **260**, 2609, 1985.

60. H. E. Schoemaker, P. J. Harvey, R. M. Bowen, and J. M. Palmer, FEBS Letters, **183**, 7, 1985.

61. T. K. Kirk, M. Tien, P. J. Kersten, M. D. Mozuch, and B. Kalyanaraman, Biochem. J. **236**, 279, 1986.

62. K. E. Hammel, B. Kalyanaraman, and T. K. Kirk, Proc. Natl. Acad. Sci. USA, **83**, 3708, 1986.

63. C.-L. Chen, and H.-M. Chang, in Biosynthesis and Biodegradation of Wood Components, Ed. T. Higuchi, San Diego, CA: Academic Press, 1985, Chp. 19.

64. T. K. Kirk, and H.-M. Chang, Holzforschung, **28**, 217, 1974.

65. T. Umezawa, and T. Higuchi, Agric. Biol. Chem. **48**, 1917, 1984.

66. K. Miki, V. Renganathan, and M. H. Gold, FEBS Letters, **203**, 235, 1986.

67. V.-B. Huynh, A. Paszczynski, P. Olson, and R. Crawford, Arch. Biochem. Biophys. **250**, 186, 1986.

68. S. Kawai, T. Umezawa, and T. Higuchi, FEBS Letters, **210**, 61, 1987.

69. S. D. Haemmerli, H. E. Schoemaker, H. W. H. Schmidt, and M. S. A. Leisola, FEBS Letters, **220**, 149, 1987.

70. T. Umezawa, and T. Higuchi, FEBS Letters, **182**, 257, 1985 .

71. T. K. Kirk, and H.-M. Chang, Holzforschung, **29**, 56, 1975.

72. C.-L. Chen, H.-M. Chang, and T. K. Kirk, Holzforschung, **36**, 3, 1982.

73. C.-L. Chen, H.-M. Chang, and T. K. Kirk, J. Wood Chem. Technol. **3**, 35, 1983.

74. D. Tai, M. Terasawa, C.-L. Chen, H.-M. Chang, and T. K. Kirk, in Recent advances in Lignin Biodegradation Research, Ed. T. Higuchi, H.-M. Chang, and T. K. Kirk, 1983, p44.

75. M. G. S. Chua, C.-L. Chen, H.-M. Chang, and T. K. Kirk, Holzforschung, **36**, 165, 1982.

76. K. Haider, H. W. Kern, and L. Ernst, Holzforschung, **39**, 23, 1985.

77. H. Junshekar, C. Brown, T. Haltmeier, M. S. A. Leisola, and A. Fiechter, Arch. Microbiol. **132**, 14, 1982.

78. R. L. Crawford, Lignin Biodegradation and Transformation, John Wiley & sons, New York, 1981, p42, p107.

79. D. L. Crawford and R. L. Crawford, Enzyme Microb. Technol. **2**, 11, 1980.

80. M. S. A. Leisola, B. Schmidt, V. Thanei-Wyss, and A. Fiechter, FEBS Letters, **189**, 267, 1985.

81. M. Shimada, T. Hattori, T. Umezawa, T. Higuchi, and T. Okamoto, Colloq. INRA **40** (Lignin Enzymic Microb. Degrad.), 151, 1987.

82. M. S. A. Leisola, S. D. Haemmerli, J. D. G. Smit, J. Troller, R. Waldner, H. E. Schoemaker, and H. Schmidt, Collq. INRA **40** (Lignin Enzymic Microb. Degrad.), 81, 1987.

83. T. Umezawa, M. Shimada, T. Higuchi, and K. Kusai, FEBS Letters, **205**, 287, 1986.

84. T. Umezawa, and T. Higuchi, FEBS Letters, **205**, 293, 1986.

85. K. Miki, V. Renganathan, M. B. Mayfield, and M. H. Gold, FEBS Letters, **210**, 199, 1987.

86. T. Umezawa, and T. Higuchi, Colloq. INRA **40** (Lignin Enzymic Microb. Degrad.), 63, 1987.

87. K. Miki, V. Renganathan, M. B. Mayfield, and M. H. Gold, Colloq. INRA **40** (Lignin Enzymic Microb. Degrad.), 69, 1987.

88. T. Umezawa, and T. Higuchi, Agric. Biol. Chem. **51**, 2281, 1987.

89. K. Miki, R. Kondo, V. Renganathan, M. B. Mayfield, and M. H. Gold, Biochem. **27**, 4787, 1988.

90. M. Shimada, T. Habe, T. Umezawa, and T. Higuchi, Biochem. Biophys. Res. Commun. **122**, 1247, 1984.

91. M. S. A. Leisola, S. D. Haemmerli, R. Waldner, H. H. Schoemaker, H. W. H. Schmidt, and A. Fiechter, Cellulo. Chem. Technol. **22**, 267, 1988.

92. M. Shimada, in Lignin Biodegradation: Microbiol. Chem. and Potential Appl. Ed. T. K. Kirk, T. Higuchi, and H.-M. Chang, CRC Press, 1980, pp195.

93. F. Nakatsubo, I. D. Reid, and T. K. Kirk, Biochim. Biophys. Acta, **719**, 284, 1982.

94. M. H. Gold, M. Kuwahara, A. A. Chiu, and J. K. Glenn, Arch. Biochem. Biophys. **234**, 353, 1984.

95. T. Umezawa, F. Nakatsubo, and T. Higuchi, Agric. Biol. Chem. **47**, 2677, 1983.

96. T. Higuchi, Wood Res. **67**, 47, 1981 .

97. T. Katagama, and T. Higuchi, Abst. 25th Symp. Lignin Chem. Fukuoko, Japan, 1980, pp5.

98. F. Nakatsubo, T. K. Kirk, M. Shimada, and T. Higuchi, Arch. Microbiol. **128**, 416, 1981.

99. B. W. Griffin, J. A. Peterson, and R. W. Estabrook, in The Porphyrins, Ed. D. Dolphin, Academic Press, 1979, Vol. VII, p333.

100. G. P. Goldsby, A. Enoki, and M. H. Gold, Arch. Microbiol. **128**, 190, 1980.

101. A. Enoki, and M. H. Gold, Arch. Microbiol. **132**, 123, 1982.

102. S. D. Haemmerli, M. S. A. Leisola, and A. Fiechter, FEBS Microbiol. Letters, **35**, 33, 1986.

103. J. S. Dordick, M. A. Marletta, and A. M. Klibanov, Proc. Natl. Acad. Sci. USA, **83**, 6255, 1986.

104. N. G. Lewis, R. A. Razal, and E. Yamamoto, Proc. Natl. Acad. USA, **84**, 7925, 1987.

105. H. W. Kern, and T. K. Kirk, Appl. Environ. Microbiol. **53**, 2242, 1987.

106. H. E. Schoemaker, E. M. Meijer, M. S. A. Leisola, S. D. Haemmerli, R. Waldner, D. Sanglard, and H. W. H. Schmidt, in Plant Cell Wall Polymers, Biogenesis and Biodegradation. Ed. N. G. Lewis, and M. G. Paice, Am. Chem. Soc. Washington DC, 1989, chp33.

107. T. Habe, M. Shimada, T. Okamoto, B. Panijpan, and T. Higuchi, J. Chem. Soc. Chem. Commun. 1323, 1985.

108. T. Habe, M. Shimada, and T. Higuchi, Mokuzai Gakkaishi, **31**, 54, 1985.

109. M. Shimada, T. Habe, T. Higuchi, T. Okamoto, and B. Panijpan, Holzforschung,

41, 277, 1987.

110. J. W. Wood, B. R. Folsom, and W. W. Eudy, in Biotechnology in the Pulp and Paper Industry (3rd international conference), Stockholm, Sweden, June 16-19, 1986, p31.

111. T. M. Fisher, and S. M. Dershem, J. Org. Chem. **53**, 1504, 1988.

112. V.-B. Huynh, Biochem. Biophys. Res. Commun. **139**, 1104, 1986.

113. R. Dicosimo, and H.-C. Szabo, J. Org. Chem. **53**, 1673, 1988.

114. M. Young, and C. Steelink, Phytochem. **12**, 2851, 1973.

115. C. Steelink, and W. E. Brritton, Tetrahedron Letters, **33**, 2869, 1974.

116. W. E. Britton, and C. Steelink, Tetrahedron Letters, **33**, 2873, 1974.

117. F. Sundholm, Holzforschung, **36**, 1982.

118. F. J. Vermillion, and J. A. Pearl, J. Electrochem. Soc. **111**, 1392, 1964.

119. B. Chaband, F. Sundholm, and G. Sundholm. Electrochimica Acta, **23**, 659, 1978.

120. D. Limosin, G. Pierre, and G. Canquis, Holzforschung, **39**, 91, 1985.

121. L. Y. Dudenko, M. I. Anisimova, V. V. Yanilxin, V. A. Babkin, S. Z. Ivanova, L. N. Spirridonova, and V. G. Gorokhova, Khim. Drev. **5**, 70, 1985.

122. D. Limosin, G. Pierre, and G. Cauguis, Holzforschung, **40**, 31, 1986.

123. H. L. Chum, D. W. Sopher, and H. Schroeder, in Fundamentals of Thermochemical Biomass Conversion, Ed. R. P. Overend, R. A. Milne, and L. K. Mudge, Elsevier Appl. Sci., New York, 1985, chp. 62.

Chapter 2

Metalloporphyrins as lignin peroxidase models

2.1 Results and discussion

2.1.1 Stability of the metalloporphyrins towards excess oxidant

Enzymes are proteins that catalyze chemical reactions in biological systems with enormous catalytic power. Most enzymes are substrate specific and this substrate specificity is determined by the three-dimensional structure of the enzyme active site, which is provided by a certain conformation of the protein. The amino acid residues near the active site also provide a special chemical environment (*i. e.* hydrophobic, hydrophillic) to facilitate the reaction, and to contribute special groups participating in the catalytic process.

Lignin peroxidase is an unusual enzyme which has little or no substrate specificity. It works by one-electron oxidation and oxidizes a wide variety of substrates, including various lignin model compounds, alkoxybenzenes, and polycyclic aromatic hydrocarbons. It is unlikely that lignin peroxidase will have an "active site" which can bind all the lignin substructures and other substrates. The protein part of lignin peroxidase, therefore, may not be as important as that of other enzymes for the catalytic process. However, it probably plays an important role in protecting the

oxidized prosthetic group of the enzyme. Without such protection, simple iron porphyrins such as protohemin are rapidly self-destroyed in the presence of excess oxidants.

Metalloporphyrins, especially iron, manganese, chromium, and ruthenium complexes of *meso*-tetraphenylporphyrin derivatives (TPP's) have been used as models for peroxidases and cytochrome P-450. Various substituents can be introduced at the phenyl ring and/or the ß-position of TPP's to increase their stability. The metal complexes of the following porphyrins have been used as models for various enzymes: *meso*-tetramesitylporphyrin, *meso*-tetra(pentafluorophenyl)porphyrin, *meso*-tetra(*o*-phenylphenyl)porphyrin, *meso*-tetra(2,6-dichlorophenyl)porphyrin, *meso*-tetra(2,6-dichlorophenyl)-ß-octachloroporphyrin, and *meso*-tetra(2,6-dichlorophenyl)-ß-octabromoporphyrin. Chloro-substituted, water soluble TPP derivatives, **12**, **13**, **14**, and **15** (Figure 1.13) were used in this study. Iron *meso*-tetra(4-sulfonatophenyl)porphyrin chloride (TSPPFeCl) was synthesized and used for comparison.

Figure 2.1 shows the relative stability of TDCSPPFeCl (**12**), Cl_{16}TSPPFeCl (**14**), TDCSPPMnCl (**13**), Cl_{16}TSPPMnCl (**15**) (Figure 1.13), and TSPPFeCl at pH 3 towards 100 fold excess (molar ratio) of hydrogen peroxide in the presence of veratryl alcohol. TSPPFeCl is the least stable and about 70% of it is destroyed in 10 minutes. The chloro-substituted metalloporphyrins **12-15** are much more stable and less than 10% of them are destroyed under the same condition. Figure 2.1 shows clearly that both manganese porphyrins are more stable than the iron porphyrins and the octachloroporphyrins (TDCSPPFeCl, TDCSPPMnCl) are more stable than their corresponding ß-octachloro analogues (Cl_{16}TSPPFeCl, Cl_{16}TSPPMnCl). This stability order seems to be in conflict with that reported in the literature[1] and the reasons are not clear. Iron *meso*-tetra(2,6-dichlorophenyl)-ß-octabromoporphyrin was more stable than

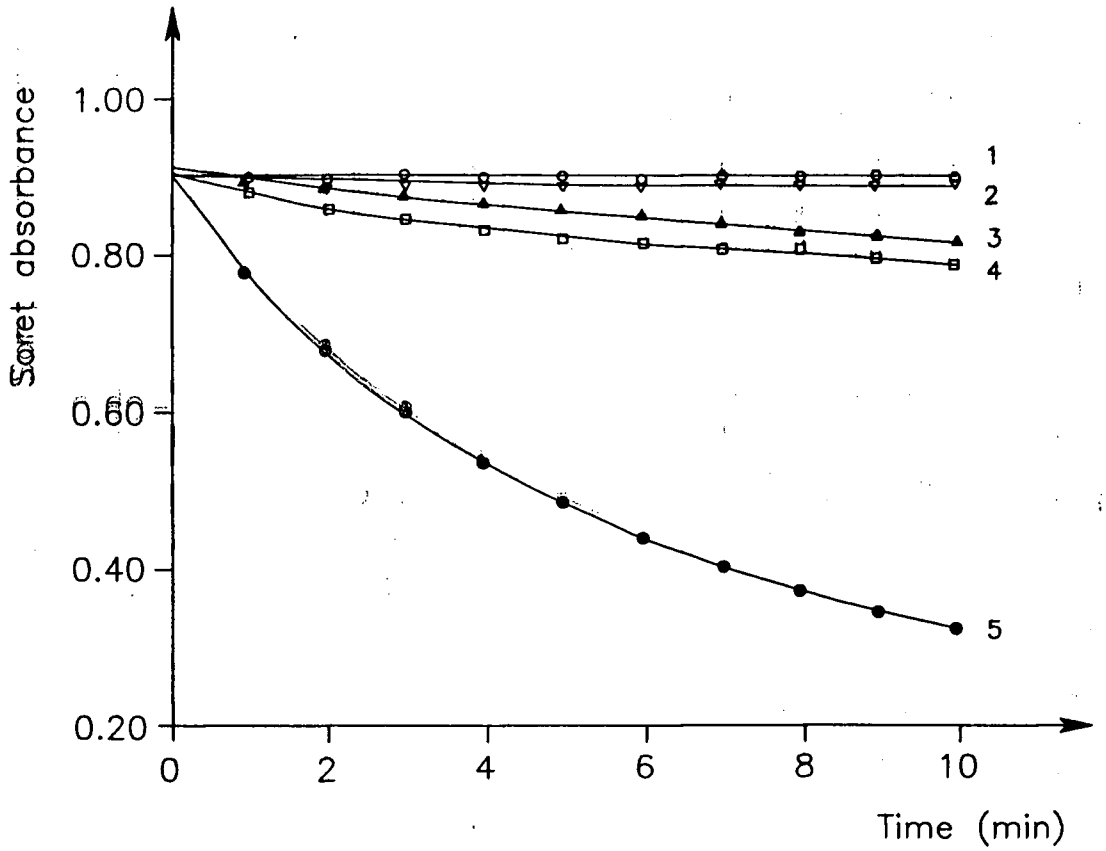

Figure 2.1 The relative stability of metalloporphyrins (7.5×10^{-6} M) towards 100 fold excess of hydrogen peroxide (7.5×10^{-4} M) at pH 3 (0.1 M phosphate buffer) in the presence of veratryl alcohol (2.5×10^{-3} M) at room temperature: 1, TDCSPPMnCl; 2, Cl_{16}TSPPMnCl; 3, TDCSPPFeCl; 4, Cl_{16}TSPPFeCl; 5, TSPPFeCl;

iron *meso*-tetra(2,6-dichlorophenyl)porphyrin, iron *meso*-tetramesitylporphyrin, and iron *meso*-tetra(pentafluorophenyl)porphyrin towards pentafluoroiodosylbenzene in organic solvents.

The stability of the metalloporphyrins depends on the pH of the solvent and Figure 2.2 shows the relative stability of the metalloporphyrins at pH 10 in the presence of veratryl alcohol and 100 fold excess (molar ratio) of hydrogen peroxide. The results are plotted as $(A_{Soret})/(A_{Soret})_0$ against time t, where $(A_{Soret})_t$ is the Soret absorption at time t, and $(A_{Soret})_0$ is the Soret absorption at time 0. The stability order is the same as that at pH 3: TDCSPPMnCl > Cl_{16}TSPPMnCl > TDCSPPFeCl > Cl_{16}TSPPFeCl. It can be seen by comparing Figure 2.1 and Figure 2.2 that all the metalloporphyrins (**12-15**) are more stable at lower pH. It was reported[2], however, that manganese porphyrins were more stable towards oxidant at higher pH in the absence of substrate.

The stability of TDCSPPFeCl towards *m*CPBA in the absence of veratryl alcohol is shown in Figure 2.3. As expected, the iron porphyrin is indeed more stable at higher pH in the absence of substrates. When hydrogen peroxide is the oxidant, however, TDCSPPFeCl is relatively more stable at lower pH (Figure 2.4).

The stability of the metalloporphyrins also depends on the type of oxidant used. As shown in Figure 2.5, Cl_{16}TSPPFeCl is much more stable towards t-BuOOH than towards hydrogen peroxide.

These results indicate that both the relative and absolute stabilities of the chloro-substituted porphyrins depend on several factors including the type of oxidant, pH, and the presence or absence of substrates.

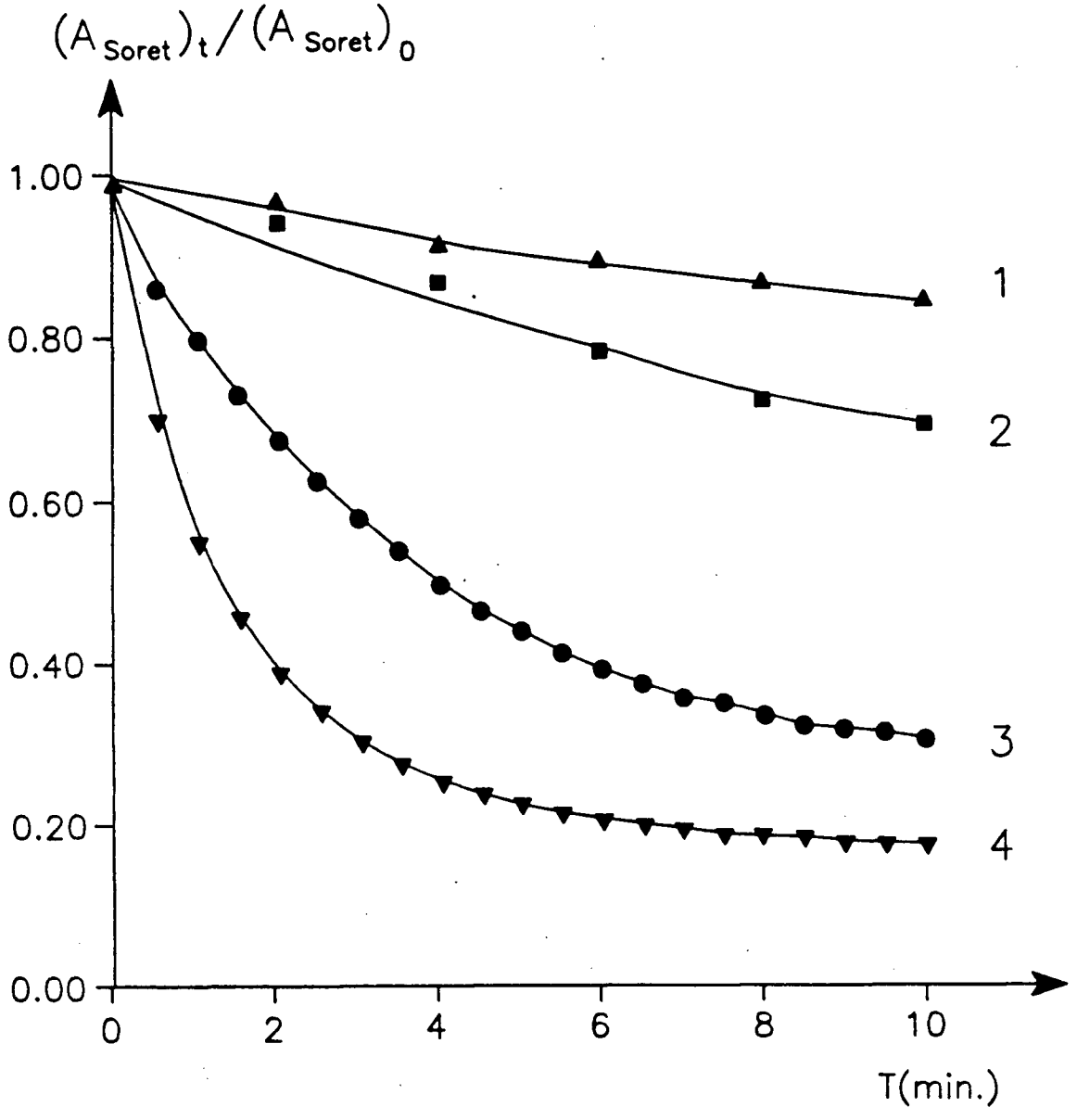

Figure 2.2 The relative stability of the metalloporphyrins (7.5×10^{-6} M) towards 100 fold excess of hydrogen peroxide (7.5×10^{-4} M) at pH 10 (0.1 M phosphate buffer) in the presence of veratryl alcohol (2.5×10^{-3} M) at room temperature: 1, TDCSPPMnCl; 2, Cl_{16}TSPPMnCl; 3, TDCSPPFeCl; 4, Cl_{16}TSPPFeCl;

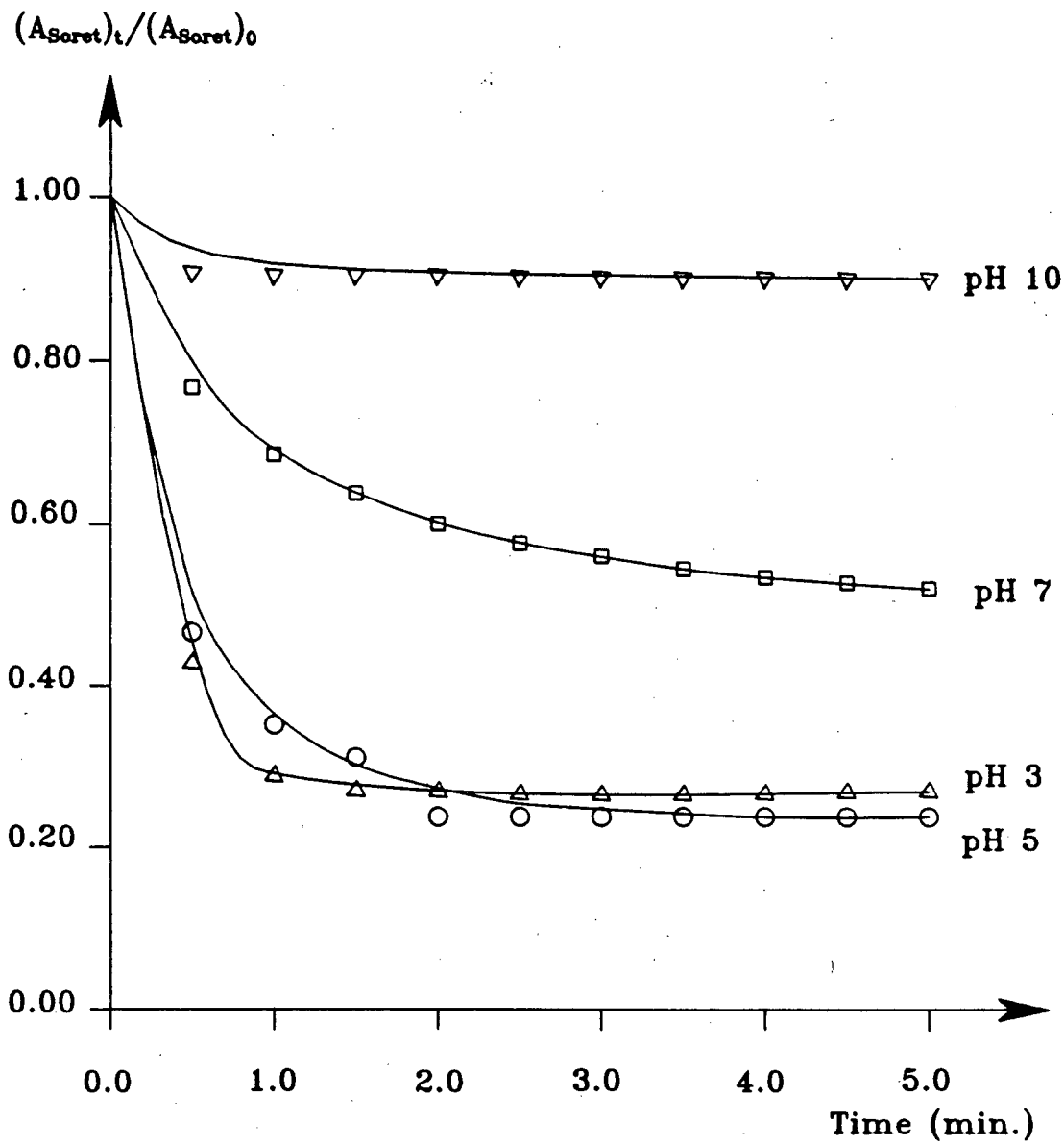

Figure 2.3 The stability of TDCSPPFeCl (1×10^{-5} M) towards *m*CPBA (1×10^{-4} M) in 0.1 M phosphate buffer at room temperature in the absence of veratryl alcohol

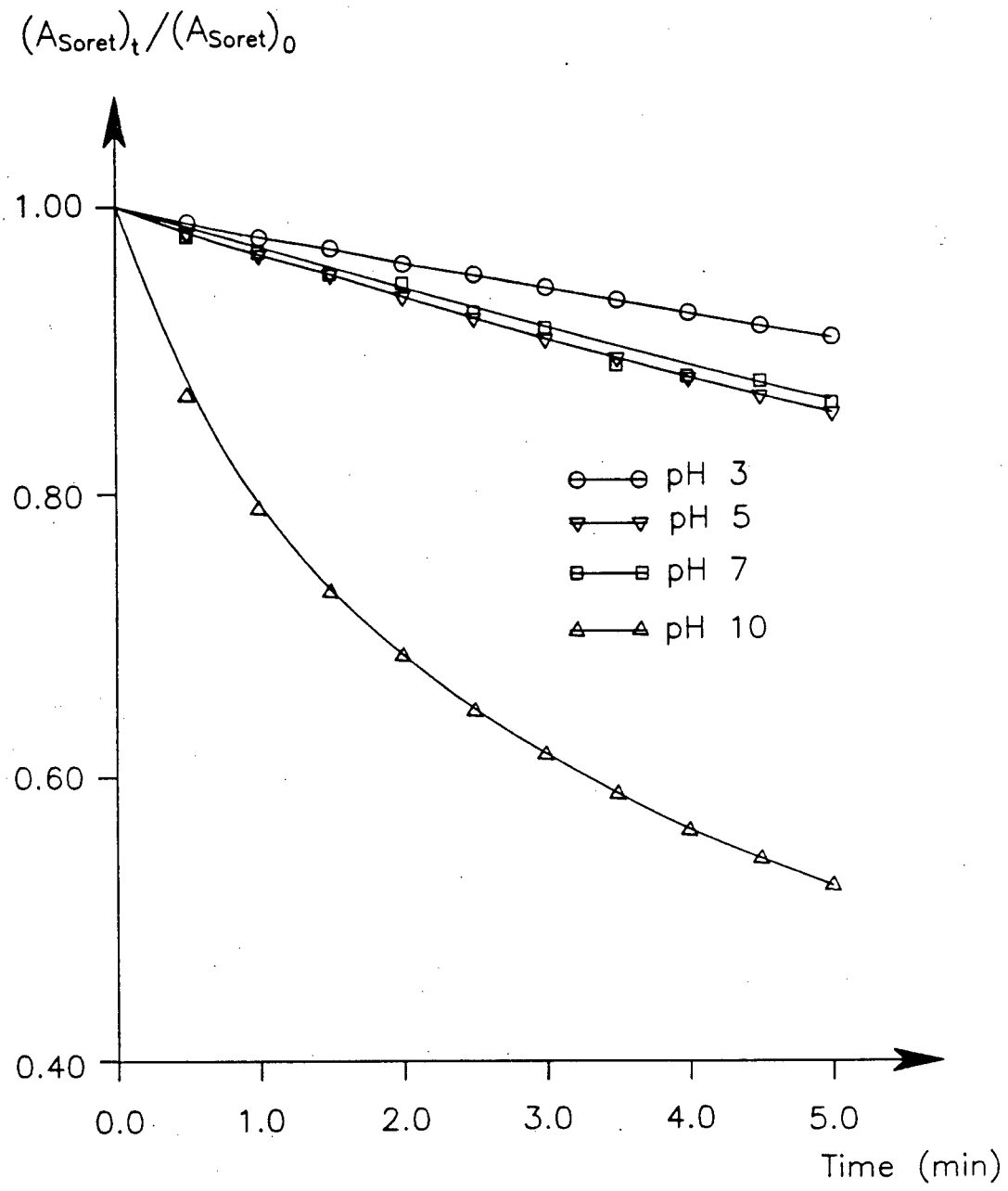

Figure 2.4 The stability of TDCSPPFeCl (1×10^{-5} M) towards hydrogen peroxide (1×10^{-4} M) in 0.1 M phosphate buffer at room temperature in the absence of veratryl alcohol

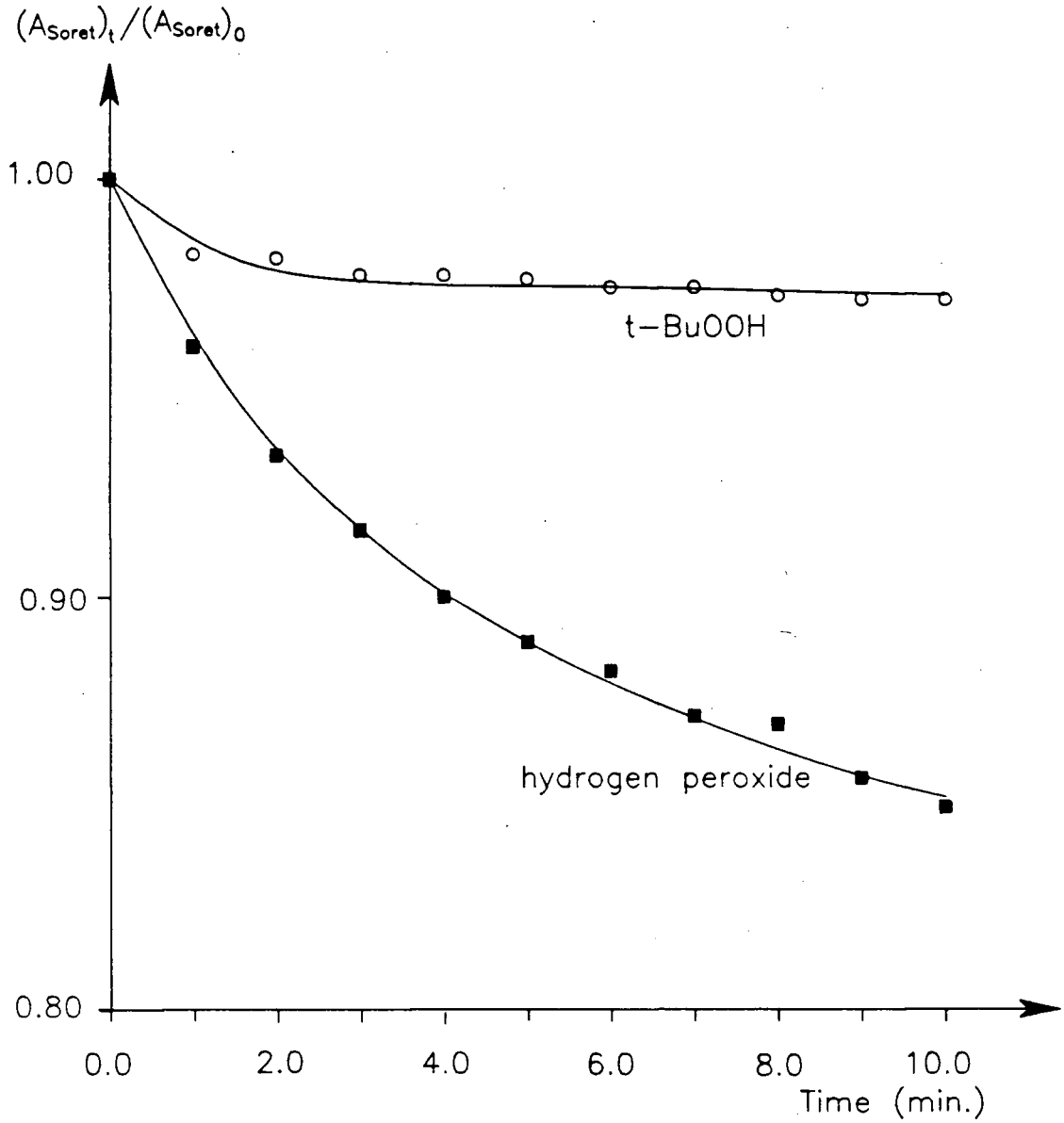

Figure 2.5 The stability of $Cl_{16}TSPPFeCl$ towards t-BuOOH and H_2O_2 at pH 3 in the presence of veratryl alcohol at room temperature, the reaction mixture contains in 3 mL 0.1 M phosphate buffer 3×10^{-8} mole of $Cl_{16}TSPPFeCl$, 3×10^{-6} mole of t-BuOOH or H_2O_2, and 1×10^{-5} mole of veratryl alcohol.

2.1.2 Oxidized intermediates of the metalloporphyrins

Biological systems use a variety of heme containing enzymes to carry out various efficient and selective oxidations. Understanding the function and mechanism of these enzymes is of great theoretical and industrial importance. Synthetic metalloporphyrins have been extensively studied as biomimetic models for monooxygenases and peroxidases and have provided a means to isolate and characterize reactive intermediates implicated in these biological systems.

Oxidation of iron porphyrins by iodosylbenzene or peracids at low temperature[3-6] gives an oxoiron(IV) porphyrin cation radical (corresponding to compound I of peroxidase), one electron reduction of which gives a second intermediate, oxoiron(IV) porphyrin (corresponding to compound II of peroxidase). Both intermediates are very reactive and are responsible for the oxidations catalyzed by heme.[3-6]

Two oxidized intermediates of manganese(III) porphyrins, oxomanganese(IV) and oxomanganese(V) were suggested to be involved in manganese(III) porphyrin catalyzed alkane hydroxylation and alkene epoxidation reactions. Oxomanganese(IV) porphyrins (or hydroxide adducts) seem to be fairly stable and have been characterized by UV-vis, resonance Raman, IR, and ESR spectroscopy.[7-10] X-ray crystal structure of a manganese(IV) porphyrin μ-oxo dimer, μ-oxo bis[azidotetraphenylporphyrinato-manganese(IV)], has been reported.[11] Manganese(IV) porphyrin-iodosylbenzene adducts, $TPPMn^{IV}$-bis(iodosylbenzene) and a μ-oxo dimer, $(TPPMn^{IV})_2$-O-bis(iodosylbenzene) have been shown to be able to functionalize both alkenes and alkanes.[12] The second oxidized intermediate of manganese porphyrin, believed to be an oxomanganese(V) porphyrin, was suggested to be involved in manganese porphyrin catalyzed reactions.[7,8,13,14] This species seems to be very unstable and has not been fully

characterized. When produced by reacting *meso*-tetramesitylporphyrin manganese hydroxide with *m*CPBA at -78°C in methylene chloride, it decays to give the oxomanganese(IV) porphyrin in a few minutes.[14] Physical and chemical evidence[7,8,13,14] suggest that this second oxidized intermediate, which is believed to be an oxomanganese(V) porphyrin, is different from the well characterized oxomanganese(IV) porphyrin species. It is more reactive than oxomanganese(IV) porphyrins for alkene epoxidation. The stereoselectivity and isotope incorporation pattern of alkene epoxidation in the presence of $H_2{}^{18}O$ or $^{18}O_2$ catalyzed by oxomanganese(IV) porphyrin and the second oxidized species are different. Oxomanganese(IV) porphyrins have ESR signals while the second intermediate is ESR silent. It has been shown that decomposition of acylperoxomanganese(III)[15,16] and manganese(III)-peroxycarbonate porphyrins[10] also gave oxomanganese(V) porphyrin species. The oxomanganese(V) porphyrin thus generated[15] has two oxidizing equivalents over the manganese(III) porphyrin. All these facts supports the suggestion that the second oxidized intermediate of manganese porphyrin is an oxomanganese(V) complex. The oxidation of water soluble manganese porphyrins were also studied[2,17], under basic conditions both manganese(IV) and oxomanganese(V) porphyrins were claimed to be produced. Oxomanganese(V) porphyrins seem to be more stable in basic aqueous solution than in organic solvents.[2,17]

Several oxidized intermediates of TDCSPPMnCl, Cl_{16}TSPPMnCl, TDCSPPFeCl, and Cl_{16}TSPPFeCl were observed by UV-vis spectroscopy. Due to the short life times and difficulties in handling these water soluble intermediates, no effort was made to characterize these intermediates by other physical methods.

2.1.2.1 Oxidized intermediates of TDCSPPMnCl

A. Oxidation of TDCSPPMnCl by sodium hypochlorite

TDCSPPMnCl was oxidized by sodium hypochlorite (NaClO) at various pH's in the presence or absence of veratryl alcohol at room temperature to examine the stability and reactivity of the oxidized intermediates towards veratryl alcohol. The oxidation of TDCSPPMnCl was followed using a diode array UV-vis spectrometer. When NaClO (1×10^{-6} mole) was added to TDCSPPMnCl (3×10^{-8} mole) in pH 2 phosphate buffer (3 mL), no spectral change was observed. Addition of another 5×10^{-6} mole of NaClO to the solution caused a slow decrease of the 472 nm peak of TDCSPPMnCl and a new peak at 432 nm was slowly formed. The intensity of the 472 nm peak of TDCSPPMnCl decreased by half in about 15 minutes.

At pH 3, the oxidation of TDCSPPMnCl by NaClO to the new species (**16**) which had its Soret band at 432 nm was also slow and the 472 nm peak did not disappear completely in 30 minutes after NaClO (5×10^{-6} mole) was added to TDCSPPMnCl (3×10^{-8} mole). The oxidation is very fast at pH 7 and the addition of NaClO (1×10^{-6} mole) to TDCSPPMnCl (3×10^{-8} mole in 3 mL 0.1 M phosphate buffer) brought about an instant reaction giving **16**. The intermediate **16** seems fairly stable and the 432 nm peak decreased very slowly at room temperature in air. Addition of veratryl alcohol (1×10^{-5} mole) to **16** caused its rapid reduction to give TDCSPPMnCl as shown in Figure 2.6. Veratryl alcohol was oxidized at the same time to give veratraldehyde, as seen by the increase of the absorption of veratraldehyde at 310 nm. The intermediate **16** was probably reduced by veratryl alcohol to give the Mn(III) porphyrin directly. Figure 2.6 shows clearly the presence of three isosbestic points at

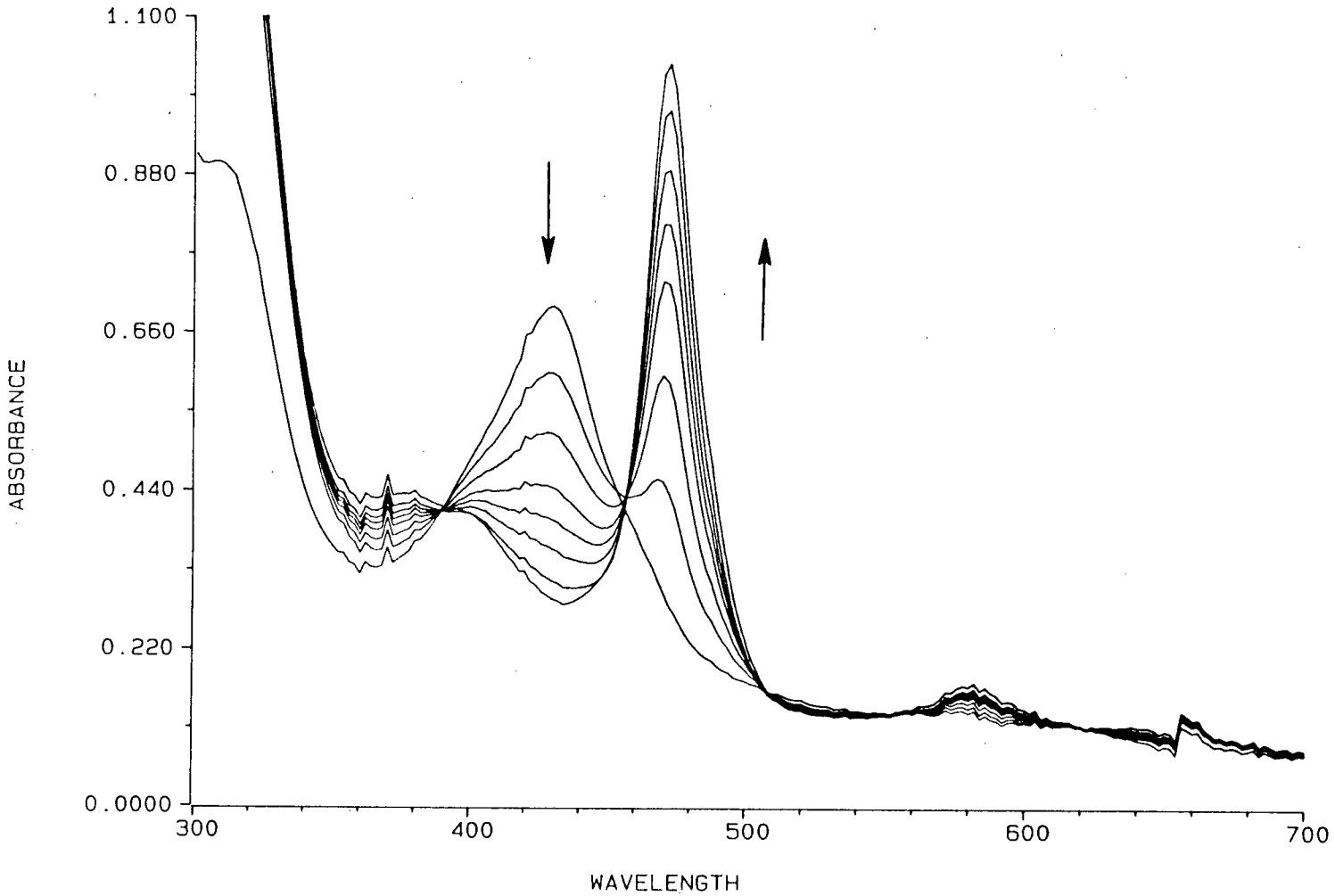

Figure 2.6 UV-vis spectral changes when veratryl alcohol was added to the oxidized intermediate **16** (TDCSPPMn^{IV}=O, λ_{max} 432 nm) in pH 7 phosphate buffer (0.1 M) at room temperature

390 nm, 456 nm, and 508 nm, respectively.

TDCSPPMnCl was rapidly oxidized by NaClO at pH 10. Addition of NaClO (1×10^{-7} mole) to TDCSPPMnCl (3×10^{-8} mole in 3 mL 0.1 M phosphate buffer) gave an intermediate **17** which absorbs at 446 nm. The newly formed 446 nm peak decreased slowly in intensity and at the same time shifted slowly to 432 nm as shown in Figure 2.7. The 472 nm peak also appeared during the process and increased in intensity. The 472 nm peak of TDCSPPMnCl was restored completely in about 19 hours. The UV-vis spectra of TDCSPPMnCl, **16**, and **17** are shown in Figure 2.8.

In the presence of veratryl alcohol, the oxidized intermediates of TDCSPPMnCl were observed less readily than in its absence. Intermediate **16** was not observed at pH 2 and pH 3 in the presence of veratryl alcohol (1×10^{-5} mole). The oxidation of veratryl alcohol was observed under these conditions. The oxidized intermediate **16** and/or **17**, therefore, was indeed formed but rapidly reduced by veratryl alcohol. At pH 7 and pH 10, the intermediate **16** was observed by UV-vis spectroscopy but **17** was not seen, suggesting that **17** was more reactive than **16**. Together with the observation that **17** decomposed to give **16** and TDCSPPMnCl, it is suggested here that **17** is probably the oxomanganese(V) complex and **16** is probably the oxomanganese(IV) complex. It has been reported[14] that the oxomanganese(V) porphyrin was much more reactive than the oxomanganese(IV) porphyrin for alkene epoxidation. The redox cycle of TDCSPPMnCl is shown in Scheme 2.1.

As shown in Figure 2.8, TDCSPPMn^{IV}=O (**16**) and TDCSPPMn^{V}=O (**17**) have distinctively different UV-vis spectra. It has been reported[2,15] that the oxomanganese(IV) and oxomanganese(V) complexes of *meso*-tetramesitylporphyrin or *meso*-tetra(4-sulfonatophenyl)porphyrin have similar UV-vis spectra. The electron-withdrawing chloro substituents of TDCSPPMnCl might be responsible for this

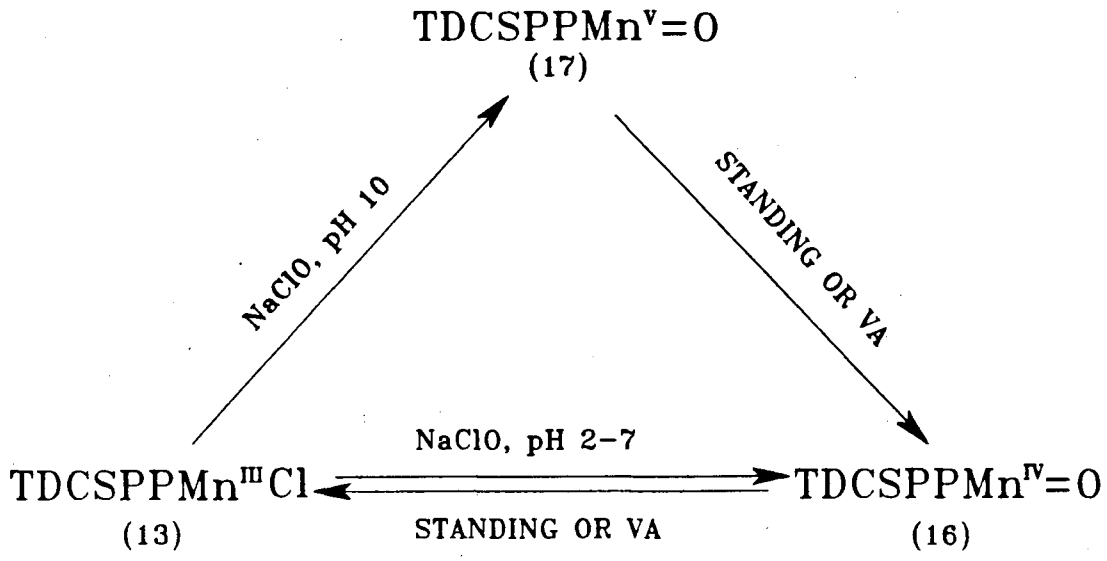

Scheme 2.1 The redox cycle of TDCSPPMnCl (VA: veratryl alcohol)

difference.

B. Oxidation of TDCSPPMnCl by H_2O_2, t-BuOOH, and *m*CPBA

Hydrogen peroxide and t-BuOOH seem to be unable to oxidize TDCSPPMnCl below pH 7 under the conditions described above for NaClO, since neither spectral change of the porphyrin nor increase in absorption at 310 nm (the oxidation of veratryl alcohol) was observed. At pH 10, both oxomanganese(V) and oxomanganese(IV) complexes were observed by UV-vis spectroscopy. *m*CPBA oxidized TDCSPPMnCl between pH 2 to pH 7 in a way similar to NaClO. At pH 10, a mixture of TDCSPPMn^{V}=O (**17**) and TDCSPPMn^{IV}=O (**16**) was observed.

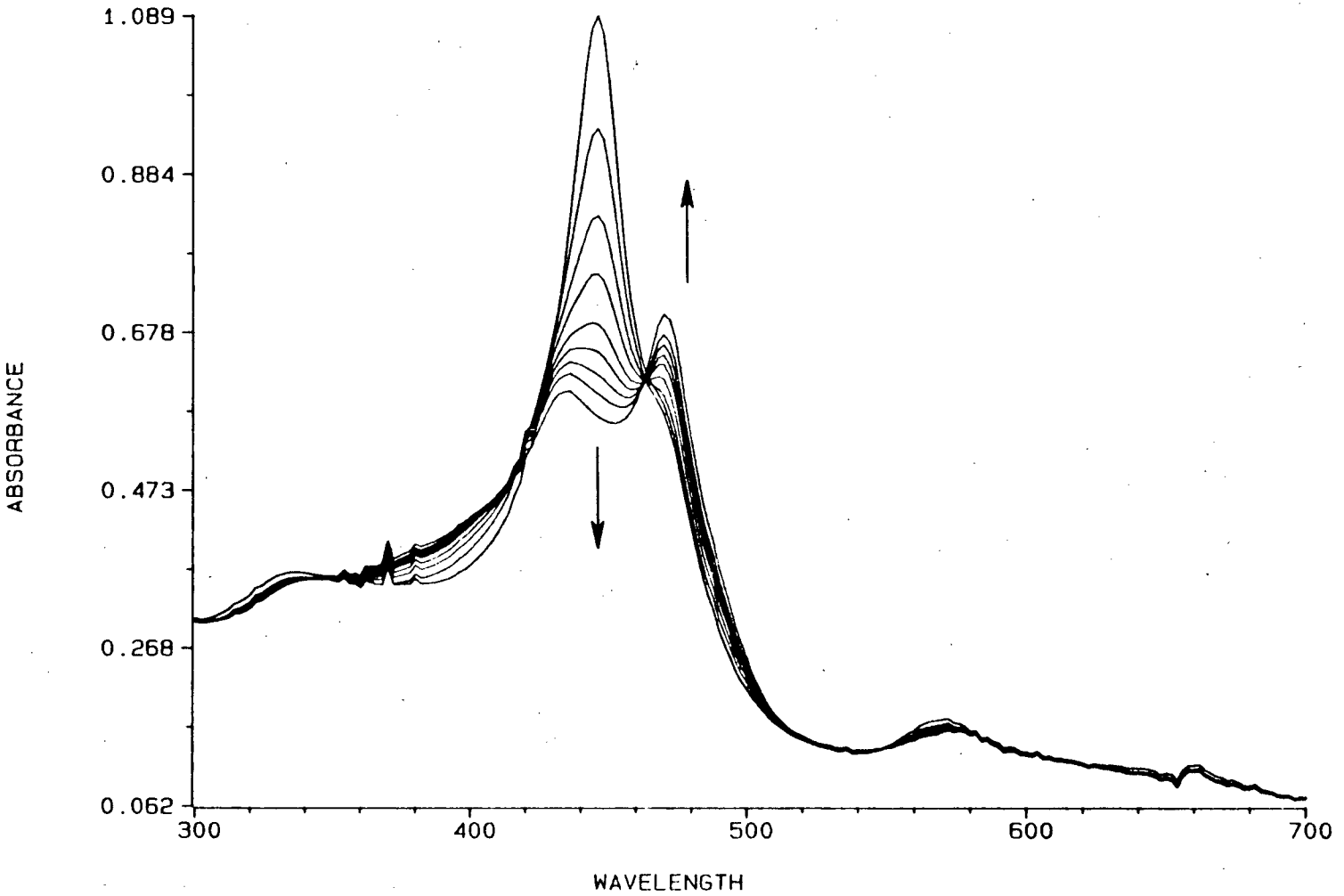

Figure 2.7 The decay of the oxidized intermediate **17** (TDCSPPMn^{V}=O, λ_{max} 446 nm) to give intermediate **16** (λ_{max} 432 nm) and the manganese(III) porphyrin (λ_{max} 472 nm) in pH 10 buffer at room temperature

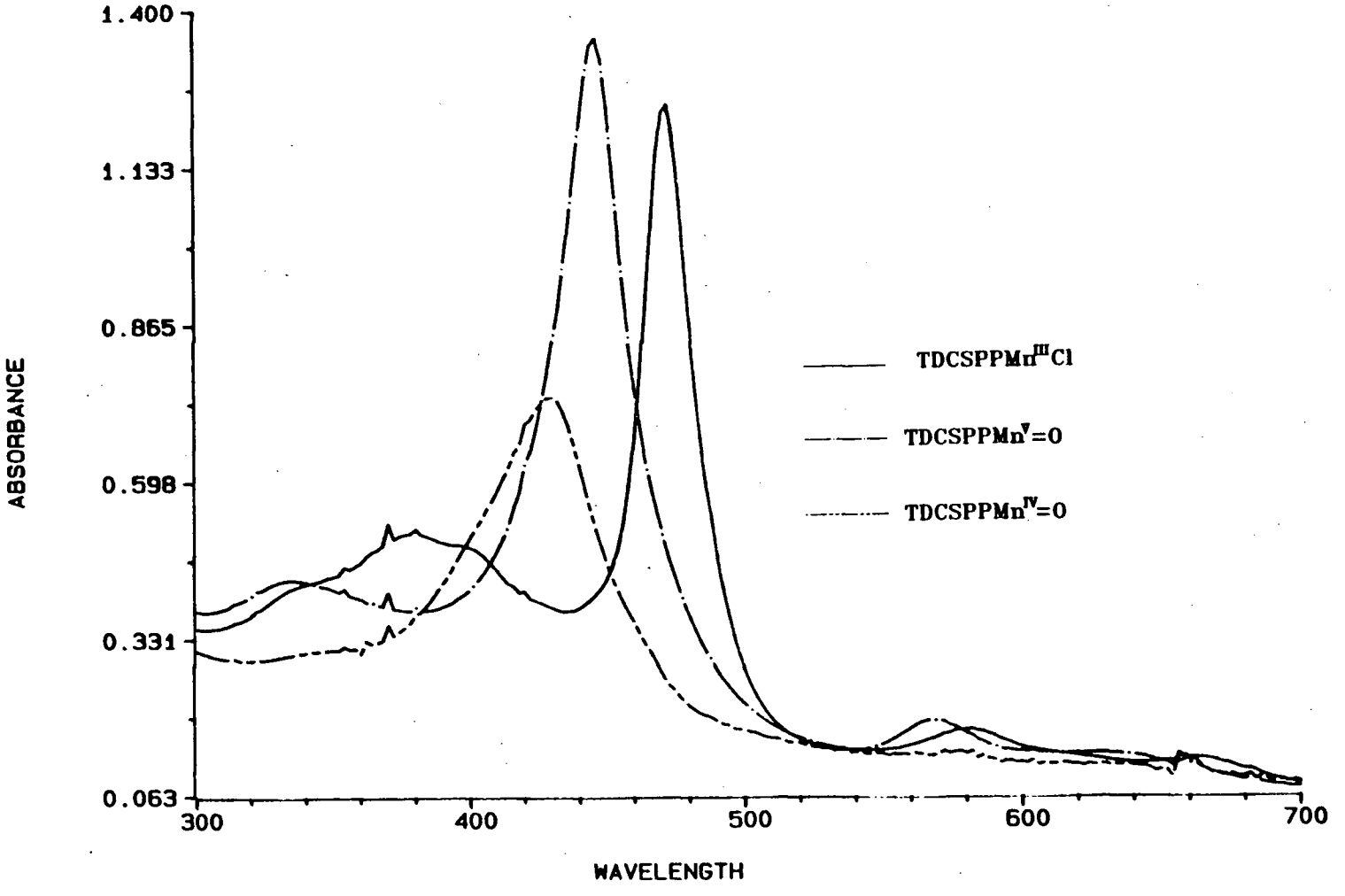

Figure 2.8 The UV-vis spectra of TDCSPPMnCl (λ_{max} 472 nm, in pH 7 buffer), TDCSPPMn^{IV}=O (**16**, λ_{max} 432 nm, in pH 7 buffer), and TDCSPPMn^{V}=O (**17**, λ_{max} 446 nm, in pH 10 buffer)

2.1.2.2 Oxidized intermediates of Cl_{16}TSPPMnCl

A. Oxidation of Cl_{16}TSPPMnCl by NaClO

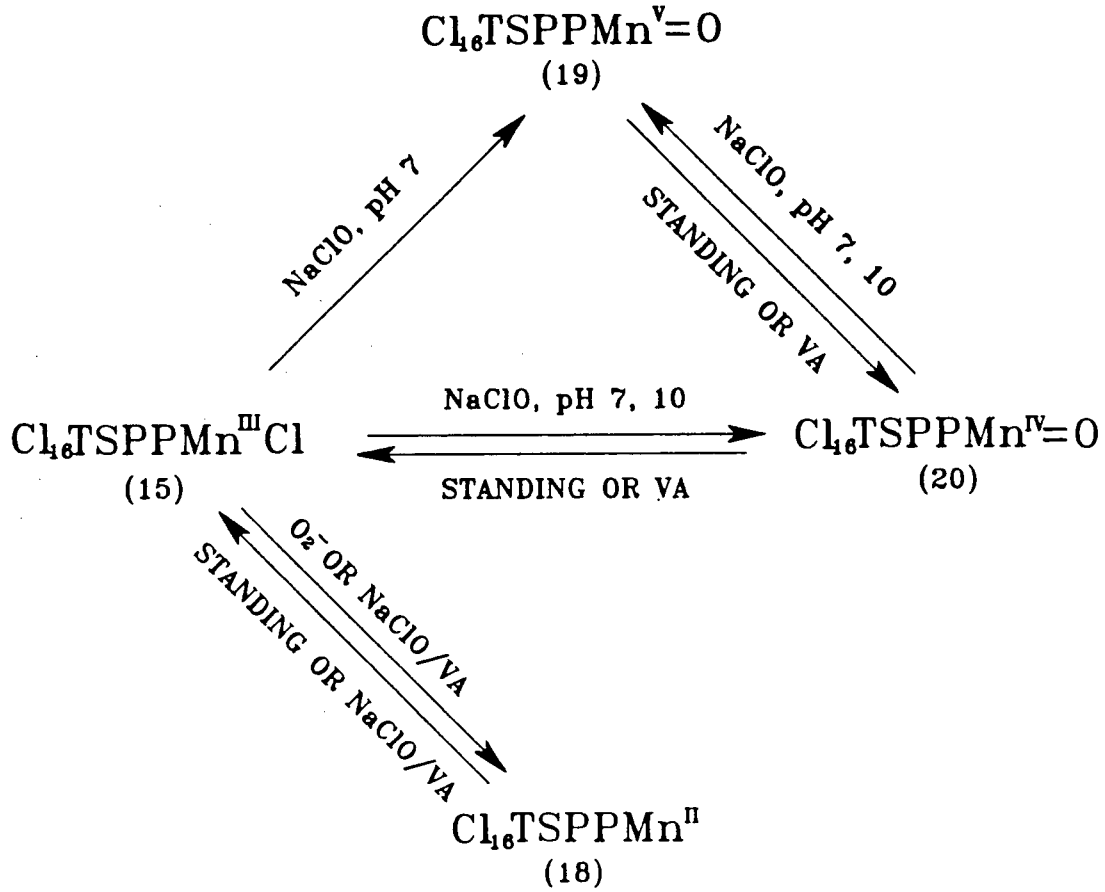

Scheme 2.2 The redox cycle of Cl_{16}TSPPMnCl (VA: veratryl alcohol)

Addition of NaClO (1×10^{-7} mole) to Cl_{16}TSPPMnCl (3×10^{-8} mole) in pH 7 buffer (3 mL, 0.1 M phosphate) resulted in the decrease of the 482 nm peak of Cl_{16}TSPPMnCl and formation of two new peaks at 428 nm and 452 nm. Both new peaks decreased rapidly in intensity and the 482 nm peak was restored. Oxidation of Cl_{16}TSPPMnCl (3×10^{-8} mole) by more NaClO (1×10^{-6} mole) at pH 7 also gave peaks at 428 nm and at 452 nm. Addition of 1×10^{-5} mole more of NaClO resulted in an

intensity increase of the 428 nm peak and decrease of the 452 nm peak. When veratryl alcohol (1×10^{-5} mole) was added to the solution, the 428 nm peak decreased in intensity and the 452 nm peak increased at first, then the 452 nm peak decreased and 482 nm peak appeared. The 310 nm peak of veratraldehyde increased rapidly until the 482 nm peak appeared. Interestingly, when the 310 nm peak stopped increasing and the 482 nm peak nearly returned to its original intensity, the 482 nm peak started to decrease and finally gave a new peak at 452 nm as shown in Figure 2.9. This mysterious intermediate (**18**) formed after veratryl alcohol oxidation had stopped (310 nm peak stopped increasing) was fairly stable and decayed to give the 482 nm peak of Cl_{16}TSPPMnCl after overnight. It was inactive towards veratryl alcohol.

Oxidation of Cl_{16}TSPPMnCl (3×10^{-8} mole) by NaClO (3×10^{-5} mole) in pH 7 buffer (3 mL) gave a intermediate **19** which has its Soret band at 428 nm. The 428 nm peak decreased in intensity slowly at room temperature in air. Intermediate **19** oxidized veratryl alcohol rapidly, the 428 nm peak decreased in intensity and a peak at 452 nm appeared (Figure 2.10). After that, the 482 nm peak also appeared and its intensity increased rapidly, the 452 nm peak and the 428 nm peak disappeared (Figure 2.11). The inactive intermediate **18** appeared again after the 482 nm peak was restored to its original intensity.

Oxidation of Cl_{16}TSPPMnCl (3×10^{-8} mole) by NaClO (1×10^{-6} mole) at pH 10 (3 mL phosphate buffer) gave a species **20** which has its Soret peak at 452 nm. This species was stable and decayed to give the 482 nm peak of Cl_{16}TSPPMnCl overnight. When veratryl alcohol was added to a solution containing **20**, the 452 nm peak decreased rapidly to give a peak at 482 nm (Figure 2.12). After the 310 nm peak of veratraldehyde stopped increasing and the 482 nm peak increased to its original intensity, again, the inactive intermediate **18** was formed. Though having their Soret

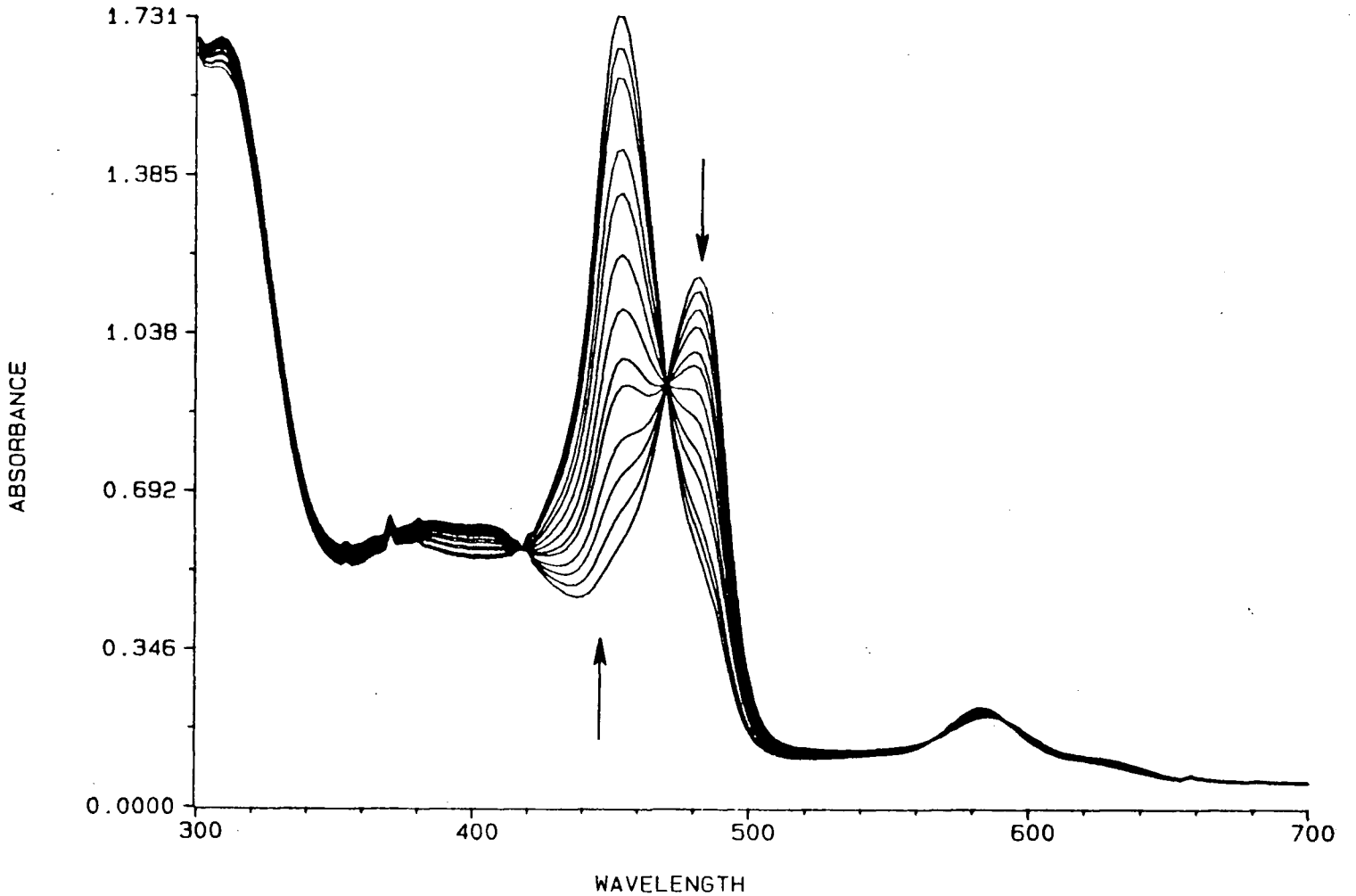

Figure 2.9 The conversion of $Cl_{16}TSPPMnCl$ (λ_{max} 482 nm) to the intermediate **18** ($Cl_{16}TSPPMn^{II}$, λ_{max} 452 nm) in pH 7 phosphate buffer at room temperature after veratryl alcohol oxidation stopped

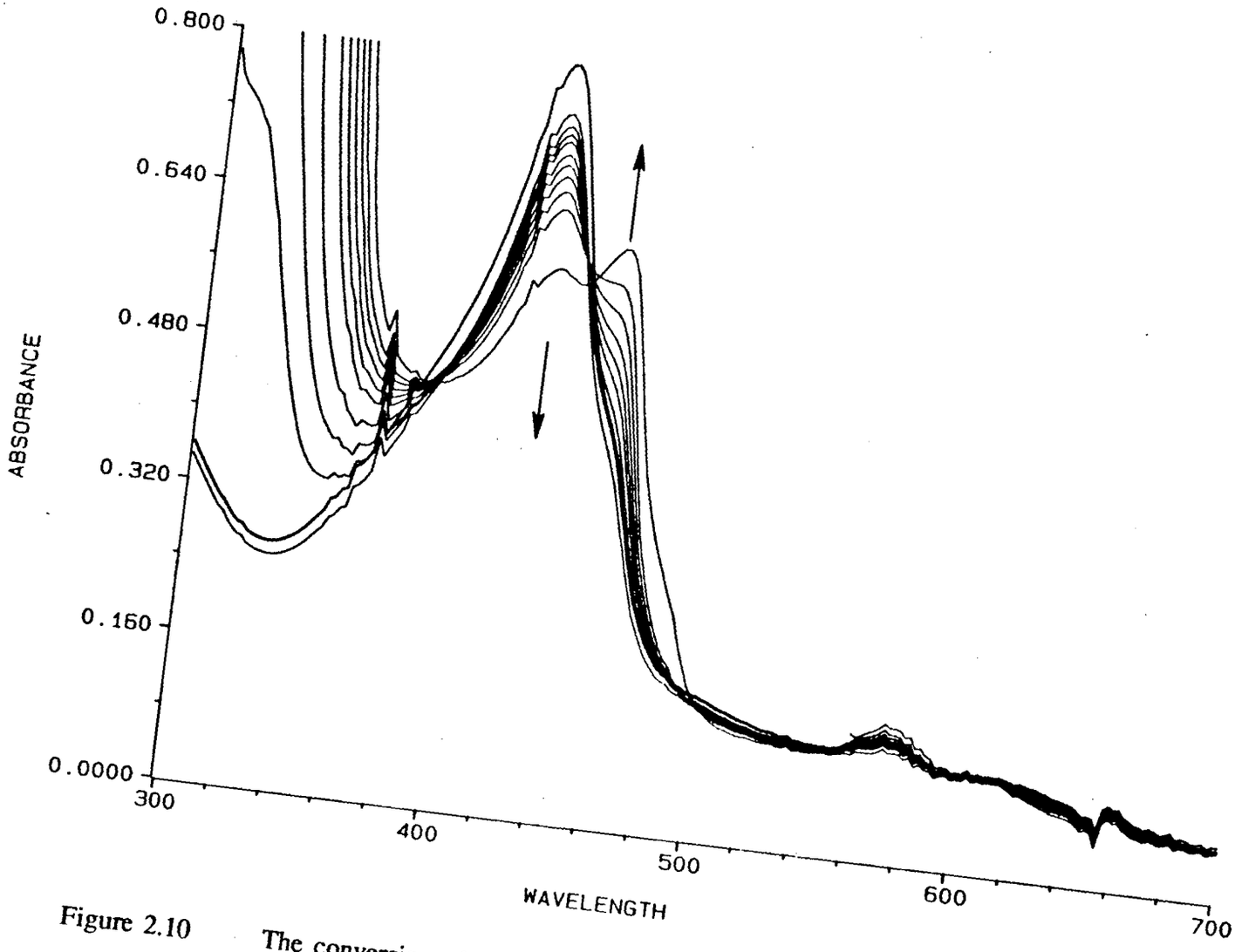

Figure 2.10 The conversion of the oxidized intermediate **19** (λ_{max} 428 nm) to intermediate **20** (λ_{max} 452 nm) in pH 7 buffer at room temperature upon addition of veratryl alcohol

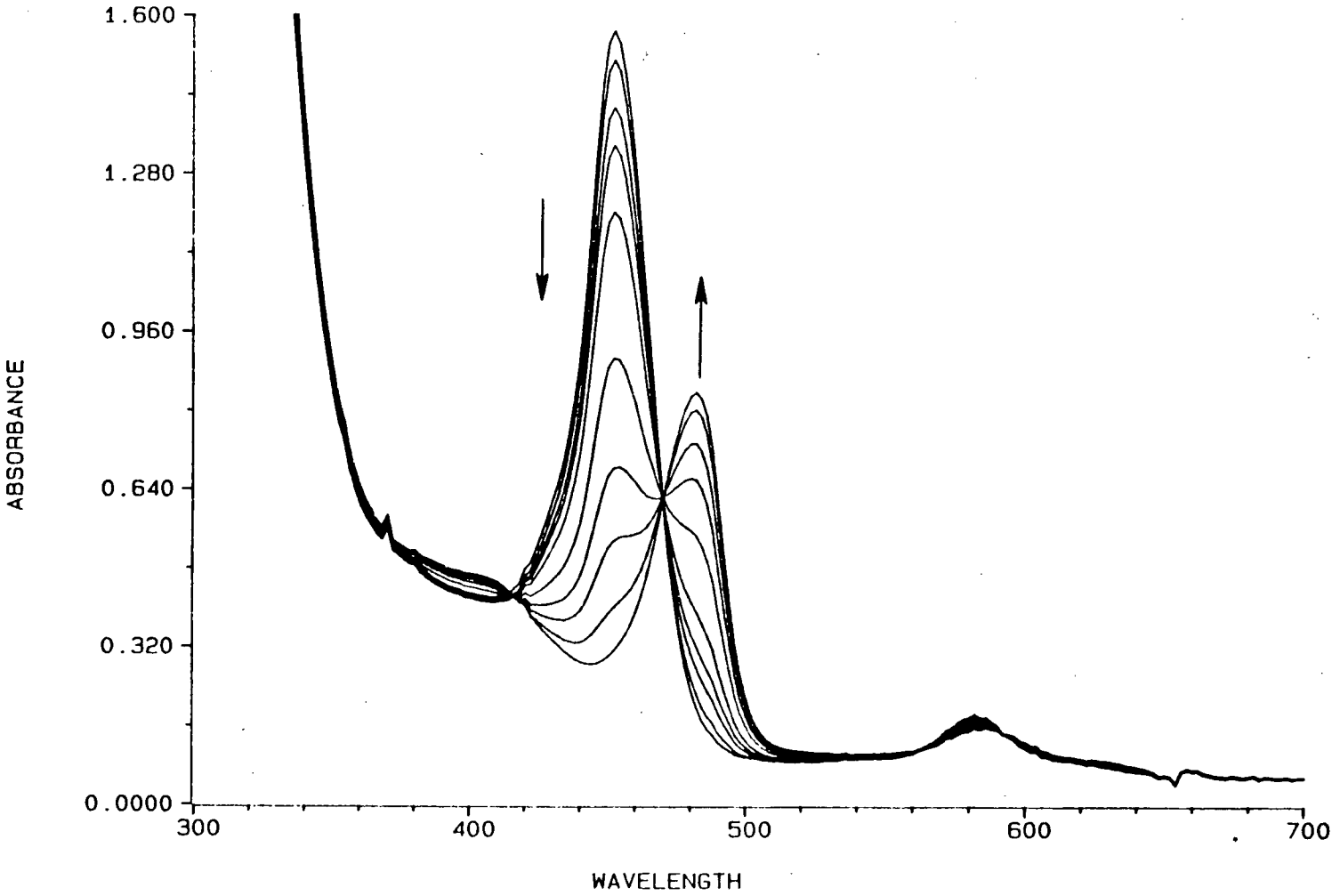

Figure 2.11 The reduction of intermediate **20** (λ_{max} 452 nm) to Cl_{16}TSPPMnCl (λ_{max} 482 nm) by veratryl alcohol in pH 7 buffer at room temperature

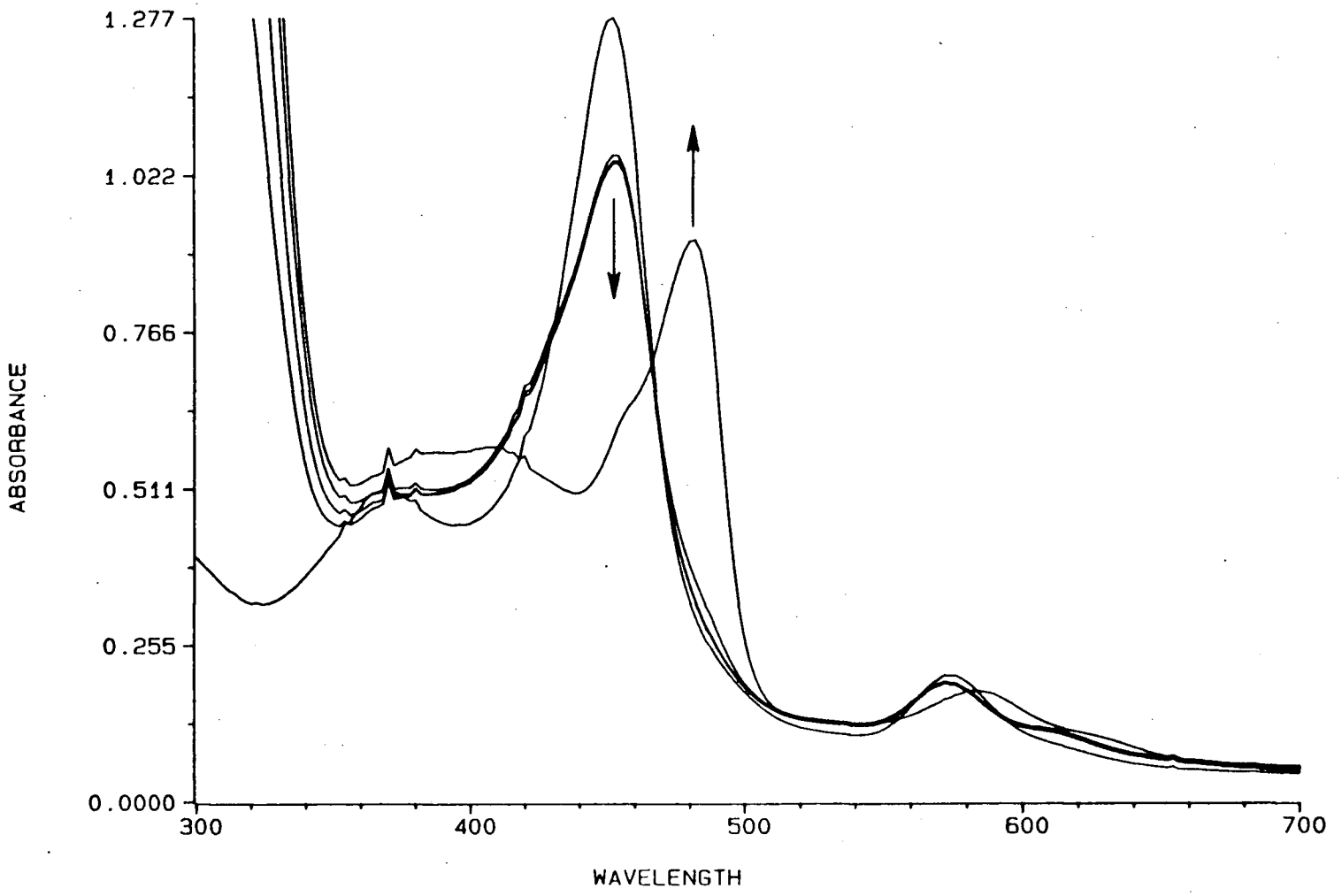

Figure 2.12 The reduction of intermediate **20** (λ_{max} 452 nm) to Cl_{16}TSPPMnCl (λ_{max} 482 nm) by veratryl alcohol in pH 10 buffer at room temperature

bands at the same position, the inactive intermediate **18** and the one (**20**) which can oxidize veratryl alcohol have different extinction coefficients as shown in Figure 2.13.

No spectral changes were observed when NaClO was added to Cl_{16}TSPPMnCl at pH 2 or pH 3.

It is proposed here that intermediate **19** which is very reactive and decays to give the intermediate **20** is $Cl_{16}TSPPMn^{V}=O$. The intermediate **20** which is able to oxidize veratryl alcohol is probably $Cl_{16}TSPPMn^{IV}=O$. The UV-vis spectrum of manganese(III), oxomanganese(IV) (**20**), and oxomanganese(V) (**19**) porphyrins are shown in Figure 2.14. The inactive intermediate **18** was found to be Cl_{16}TSPPMn(II) as rationalized below.

As this intermediate was unable to oxidize veratryl alcohol but was observed only in the presence of veratryl alcohol, it must be a product of the reaction between the manganese(III) porphyrin and veratryl alcohol or one of the oxidation products of veratryl alcohol. It was noted that at pH 10, the UV-vis spectrum of Cl_{16}TSPPMnCl had a shoulder around 452 nm. Addition of sodium hydroxide to the solution shifted the 482 nm peak of Cl_{16}TSPPMnCl to 456 nm. This 456 nm species was believed to be a hydroxide adduct of the manganese(III) porphyrin.[2] It had a similar UV-vis spectrum to that of the inactive intermediate **18**. Addition of hydrochloric acid to the 456 nm species shifted the Soret band back to 482 nm instantly. The inactive intermediate **18**, however, did not change back to 482 nm upon the addition of hydrochloric acid.

Addition of a large excess of veratryl alcohol (3×10^{-5} mole) to the manganese(III) porphyrin (3×10^{-8} mole) at pH 10 resulted in a very slow decrease of the 482 nm peak of Cl_{16}TSPPMnCl and a correspondingly slow formation of a new peak at around 450 nm. The shifting from 482 nm to 450 nm was not complete even

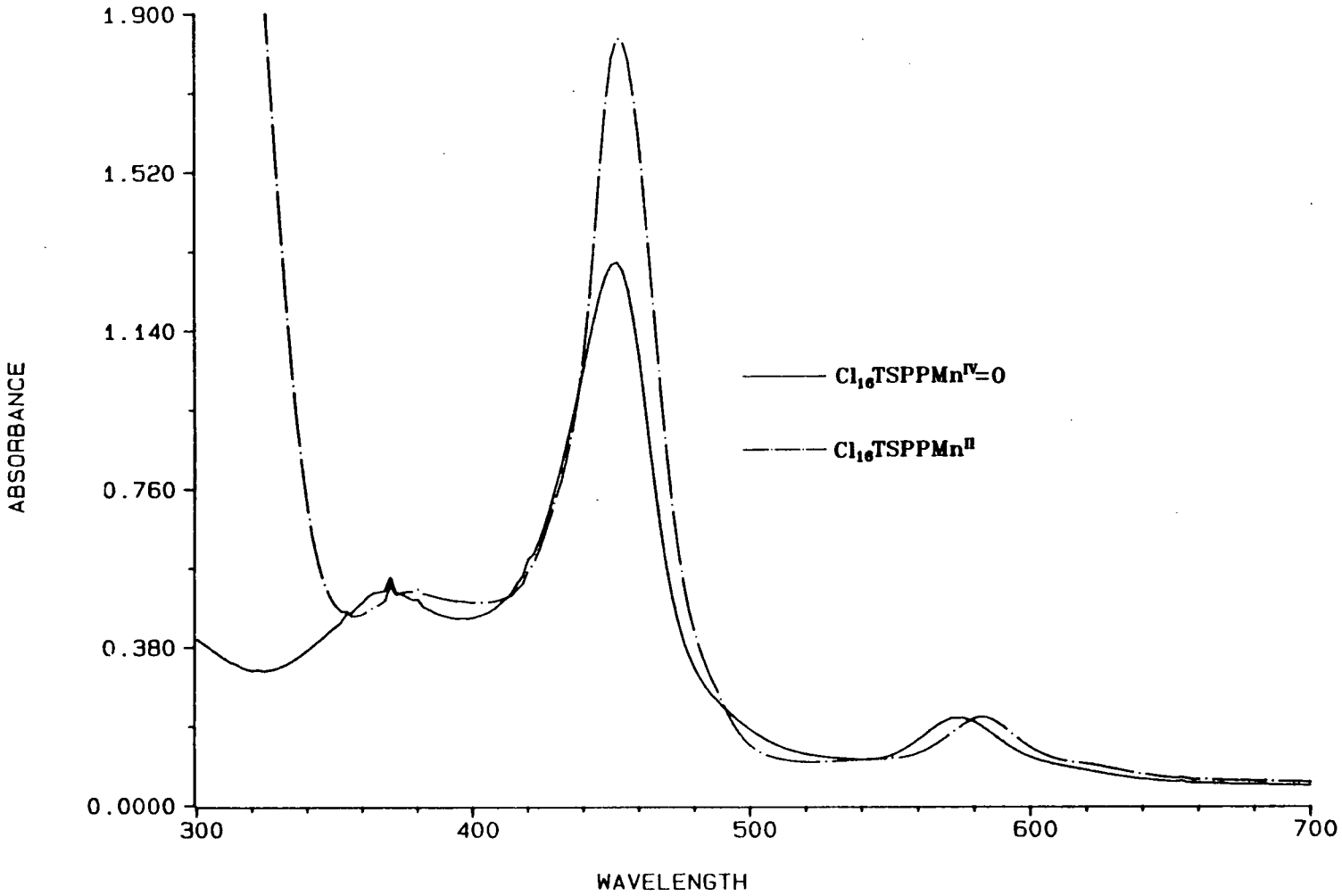

Figure 2.13 The UV-vis spectra of intermediate **18** ($Cl_{16}TSPPMn^{II}$, in pH 10 buffer) and **20** ($Cl_{16}TSPPMn^{IV}$=O, in pH 10 buffer)

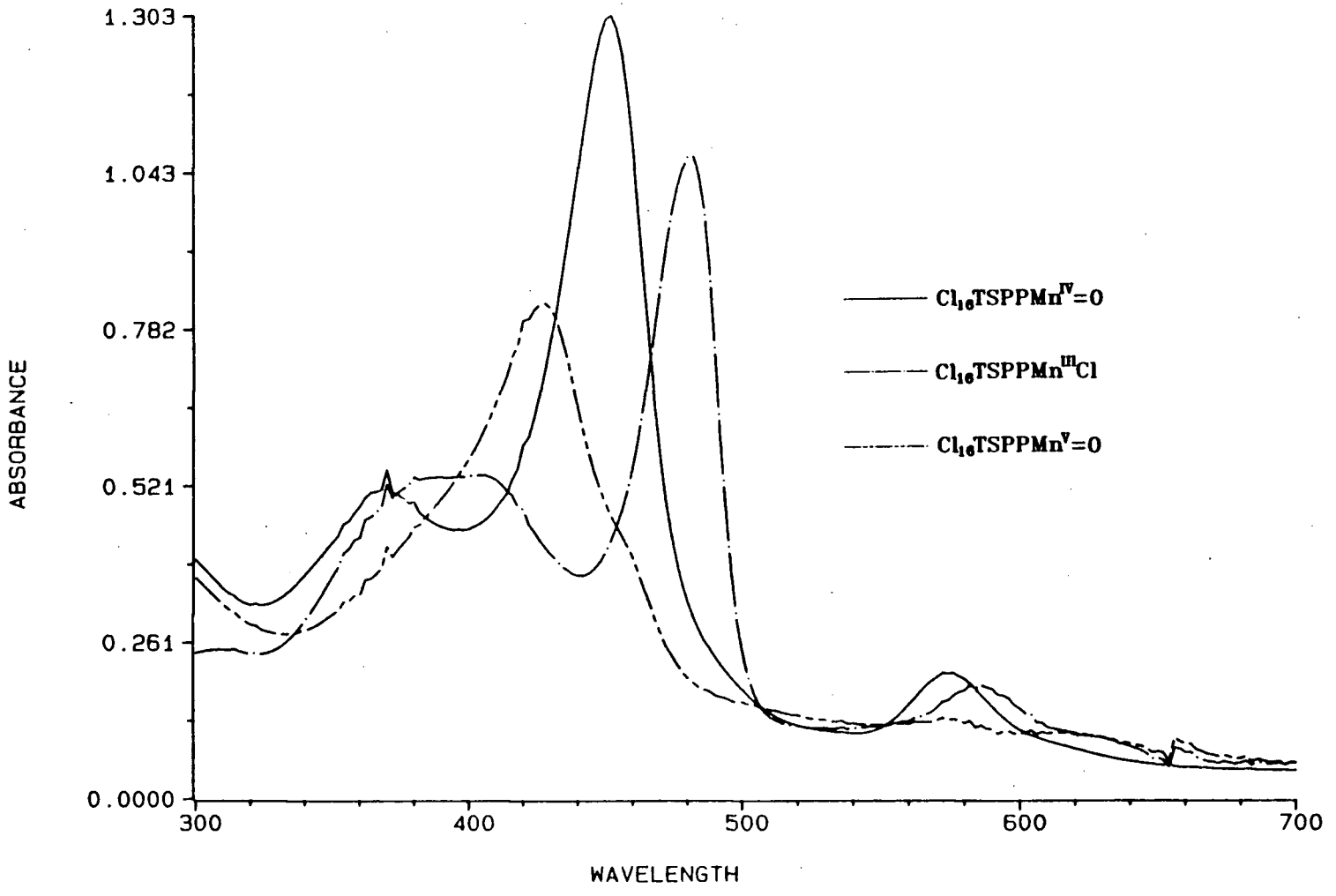

Figure 2.14 The UV-vis spectra of $Cl_{16}TSPPMnCl$ (λ_{max} 482 nm, in pH 7 buffer), $Cl_{16}TSPPMn^{V}=O$ (**19**, λ_{max} 428nm, in pH 7 buffer), and $Cl_{16}TSPPMn^{IV}=O$ (**20**, λ_{max} 452 nm, in pH 10 buffer)

after standing overnight. The formation of the 450 nm species, which was probably a veratryl alcohol-porphyrin complex, was much slower than the formation of the inactive intermediate **18**. Addition of veratraldehyde (3×10^{-5} mole), the major product of veratryl alcohol oxidation, to Cl_{16}TSPPMnCl (3×10^{-8} mole) at pH 10 (3 mL 0.1 M phosphate buffer) did not change the UV-vis spectrum of the manganese(III) porphyrin.

It has been reported that oxidation of veratryl alcohol by lignin peroxidase produced superoxide.[18] Manganese porphyrins could also catalyze the oxidation of veratryl alcohol and give superoxide. Reaction of superoxide with the manganese(III) porphyrin can give a manganese(III)-superoxide complex, which is unstable at room temperature and decomposes to give dioxygen and the manganese(II) porphyrin as shown below:

$$Cl_{16}TSPPMn(III)Cl + O_2^- \rightarrow Cl_{16}TSPPMn(III)\text{-}O_2^- \rightarrow$$

$$Cl_{16}TSPPMn(II) + O_2$$

Reactions of manganese(III) porphyrins and superoxide in organic solvents to give manganese(II) porphyrins have been reported.[15,19] Manganese porphyrins were found to bind dioxygen reversibly at -78°C. At room temperature, however, the manganese(II) porphyrin was rapidly oxidized by dioxygen.[20] The fact that Cl_{16}TSPPMn(II) was relatively stable at room temperature suggests that it might be a much better haemoglobin model for reversible dioxygen binding than other simple manganese porphyrins previously studied.

Cl_{16}TSPPMn(II) (**18**) was oxidized rapidly to give the manganese(III) porphyrin by adding excess NaClO, explaining the fact that Cl_{16}TSPPMn(II) (**18**) was observed

only after the oxidation of veratryl alcohol had stopped, which happened when all the NaClO was consumed. Before the NaClO was depleted, Cl_{16}TSPPMn(II) could also be formed by the reaction described above. It could not be observed, however, by UV-vis spectroscopy due to its rapid oxidation by NaClO.

In order to confirm that the inactive intermediate **18** was Cl_{16}TSPPMn(II), the manganese(II) porphyrin was made by another method to compare its UV-vis spectrum with that of **18**.

Addition of small amounts of solid sodium dithionite to Cl_{16}TSPPMnCl (3×10^{-8} mole in 3 mL 0.1 M pH 7 phosphate buffer) gave a species which had its Soret band at 450 nm. This species, however, was not stable and decomposed rapidly to give an orange solution. This experiment was also very difficult to repeat since excess sodium dithionite destroyed the porphyrin instantly to give an orange solution. Experiments carried out in pH 10 phosphate buffer (0.1 M) gave similar results. Reduction of Cl_{16}TSPPMnCl (3×10^{-8} mole) by excess sodium borohydride in pH 10 phosphate buffer (3 mL) gave a complex which had its Soret band at 450 nm and another small peak at 582 nm. The UV-vis spectrum of this complex was the same as that of **18** except a 2 nm wavelength difference between the two Soret bands. Because the different solvent condition, these two spectra can be considered as the same.

The formation of Cl_{16}TSPPMn(II) by reacting the manganese(III) porphyrin and superoxide was also demonstrated. Aliquots of potassium superoxide dissolved in acetonitrile containing 18-crown-6 ether were added to a Cl_{16}TSPPMnCl solution (3×10^{-8} mole in 3 mL pH 10 phosphate buffer) until the 452 nm peak reached its maximal absorption. Further addition of potassium superoxide decreased the intensity of the 452 nm peak. It was found that the 452 nm peak thus formed had a smaller intensity compared with that of the manganese(II) porphyrin formed from the reaction of

Cl_{16}TSPPMnCl and NaClO in the presence of veratryl alcohol when the initial concentrations of the manganese(III) porphyrin were the same. It is possible that hydrogen peroxide, formed from potassium peroxide (which was present in potassium superoxide), might have interfered with the reaction. Addition of veratryl alcohol could reduce the oxidized intermediates of the manganese porphyrin, which were produced by hydrogen peroxide oxidation, to regenerate the manganese(III) porphyrin. Reaction of manganese(III) porphyrin with superoxide may produce pure manganese(II) porphyrin. Indeed, reaction of Cl_{16}TSPPMnCl (3×10^{-8} mole in 3 mL pH 10 buffer) with potassium superoxide in the presence of veratryl alcohol (1×10^{-5} mole) gave a 452 nm peak which had similar intensity as that of the manganese(II) porphyrin formed after the oxidation of Cl_{16}TSPPMnCl by NaClO in the presence of veratryl alcohol.

While no strong evidence was available to support the formation of superoxide during the oxidation of veratryl alcohol by Cl_{16}TSPPMnCl, the effect of a superoxide dismutating agent on the formation of Cl_{16}TSPPMn(II) would provide indirect evidence that superoxide was involved. Manganese(II) complexes are well known model systems of superoxide dismutase.[21,22] The effect of manganese(II)-lactate on the formation of Cl_{16}TSPPMn(II) was studied. In the presence of veratryl alcohol (1×10^{-5} mole) and manganese(II)-lactate (1mM and 60 mM concentration, respectively, in 3 mL pH 7 buffer), reaction of Cl_{16}TSPPMnCl (3×10^{-8} mole) and NaClO (2×10^{-5} mole) did not give the manganese(II) porphyrin, suggesting that the superoxide produced was effectively dismutated by manganese(II)-lactate. In the absence of manganese(II)-lactate and under otherwise the same condition, the manganese(II) porphyrin was observed by UV-vis spectroscopy.

B. Oxidation of Cl_{16}TSPPMnCl by *m*CPBA

Unlike NaClO, *m*CPBA was able to oxidize Cl_{16}TSPPMnCl over a wide range of pH. The oxidized intermediates at pH 2 and pH 3 were found to have their Soret bands at slightly different wavelengths compared with those formed by using NaClO as oxidant.

When *m*CPBA (5×10^{-6} mole) was added to Cl_{16}TSPPMnCl (3×10^{-8} mole) in 3 mL 0.1 M pH 2 phosphate buffer, the UV-vis spectrum showed a broad peak at 420 nm which had a shoulder at 474 nm (Figure 2.15). Further addition of *m*CPBA decreased the intensity of both peaks. Addition of veratryl alcohol (1×10^{-5} mole) brought the Soret peak back to 482 nm rapidly. A peak at 420 nm and another peak at 460 nm were found in the UV-vis spectrum when *m*CPBA (1×10^{-6} mole) was added to Cl_{16}TSPPMnCl (3×10^{-8} mole) at pH 3 (3 mL 0.1 M phosphate buffer). The 460 nm peak decreased in intensity and the 420 nm peak remained almost unchanged upon further addition of 5×10^{-6} mole of *m*CPBA. The intensity of both peaks decreased when the solution was allowed to stand at room temperature. When the reactions were carried out in phosphate buffer of pH 6, or higher, the oxidation of Cl_{16}TSPPMnCl by *m*CPBA was similar to that using NaClO as oxidant. Oxomanganese(V) and oxomanganese(IV) porphyrin have their Soret absorption at 430 nm and 454 nm, respectively. Cl_{16}TSPPMn(II) was formed at above pH 5 during the oxidation of veratryl alcohol by Cl_{16}TSPPMnCl and *m*CPBA. The manganese(II) porphyrin was formed very slowly at pH 5. Superoxide formed from the oxidation of veratryl alcohol probably decomposed rapidly at pH 2 and pH 3 and therefore the manganese(II) porphyrin was not formed.

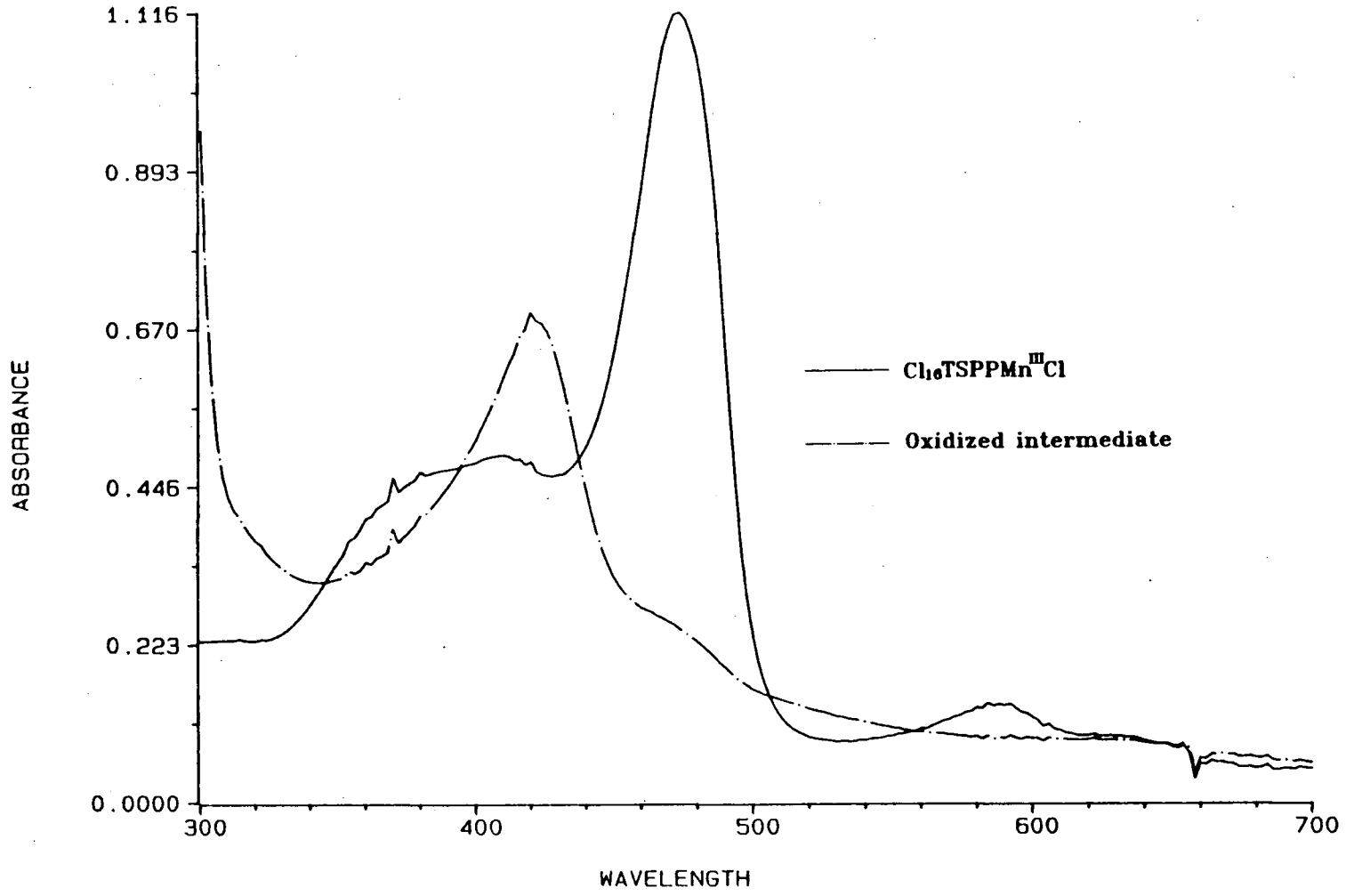

Figure 2.15 The oxidation of $Cl_{16}TSPPMnCl$ (3×10^{-8} mole) by *m*CPBA (5×10^{-6} mole) in pH 2 phosphate buffer at room temperature

2.1.2.3 Oxidized intermediates of TDCSPPFeCl

Oxidation of TDCSPPFeCl (3×10^{-8} mole) with NaClO (1×10^{-7} mole) in pH 7 phosphate buffer (3 mL, 0.1 M) shifted the Soret band from 424 nm to 430 nm. Additional NaClO (1×10^{-6} mole) further shifted the Soret band to 431 nm. The 431 nm peak shifted back to 424 nm slowly upon standing at room temperature. When NaClO (1×10^{-6} mole) was added to TDCSPPFeCl (3×10^{-8} mole in 0.1 M phosphate buffer) at pH 10, the UV-vis spectrum showed a peak at 432 nm (Figure 2.16). Further addition of NaClO caused no change in the spectrum. The 432 nm peak was also observed when TDCSPPFeCl (3×10^{-8} mole) was oxidized by NaClO (1×10^{-6} mole) at pH 12 (3 mL, 0.1 M borate buffer). The formation of oxidized intermediates of TDCSPPFeCl was not observed at pH 2 and pH 3. The oxidation of TDCSPPFeCl by *m*CPBA gave similar spectral changes. The nature of the species (**21**) which has its Soret band at 432 nm is not clear.

2.1.2.4 Oxidized intermediates of Cl_{16}TSPPFeCl

The Soret band of Cl_{16}TSPPFeCl (3×10^{-8} mole) decreased in intensity when NaClO (1×10^{-6} mole) was added to the iron porphyrin at pH 2 or pH 3 (3 mL phosphate buffer). When NaClO (1×10^{-6} mole) was added to Cl_{16}TSPPFeCl (3×10^{-8} mole) at pH 7 or pH 10 (3 mL 0.1 M phosphate buffer), the Soret band of the iron(III) porphyrin decreased in intensity and a new peak at 448 nm was formed. The 422 nm peak did not disappear completely even in the presence of a large excess (3×10^{-5} mole) of NaClO. When Cl_{16}TSPPFeCl (3×10^{-8} mole in 3 mL 0.1 M phosphate buffer) was oxidized by NaClO (1×10^{-5} mole) at pH 12 (3 mL 0.1 M borate buffer), a peak at 448

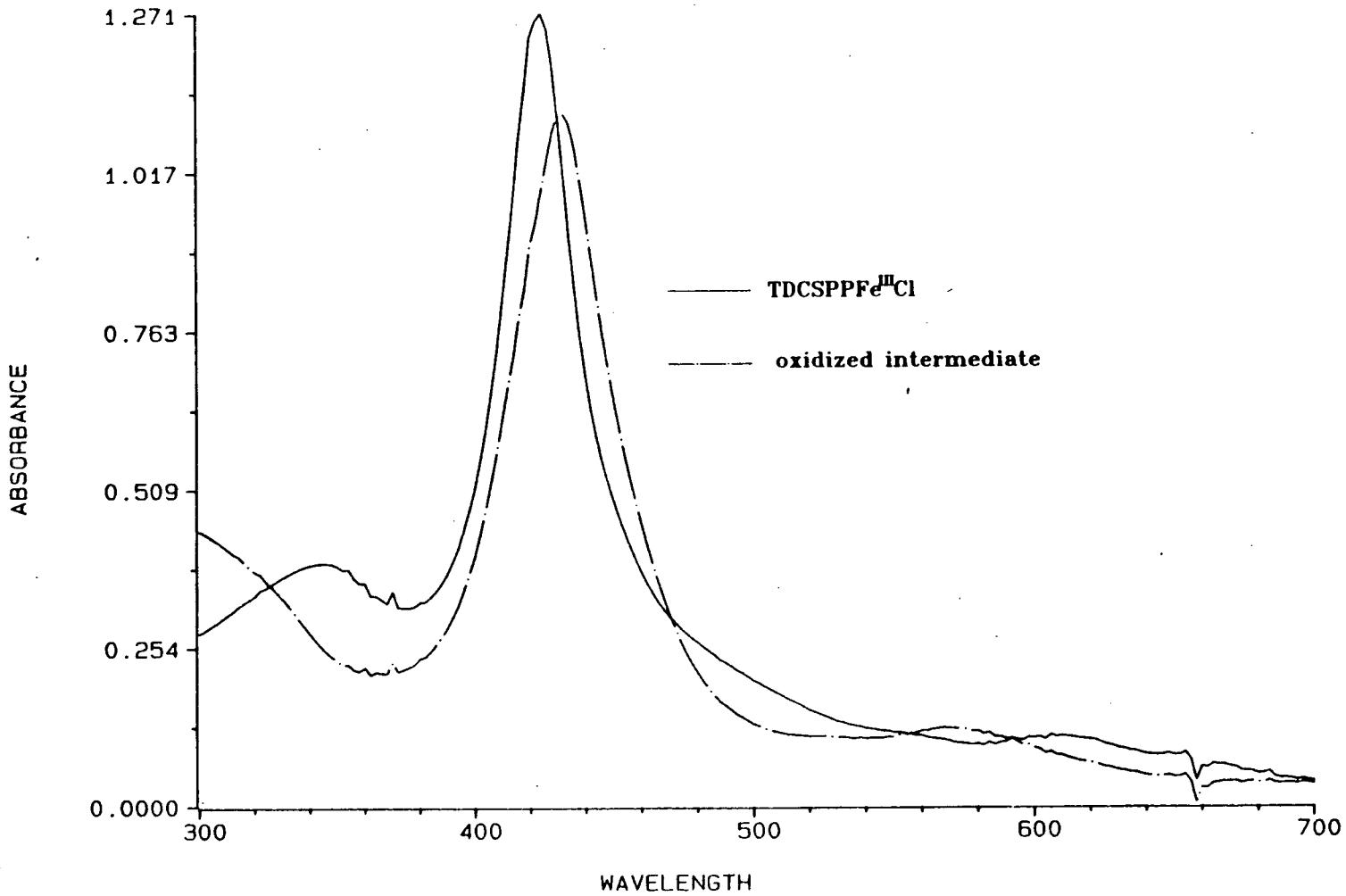

Figure 2.16 The oxidation of TDCSPPFeCl (λ_{max} 424 nm, 3×10^{-8} mole) to the λ_{max} 432 nm intermediate (**21**) by NaClO (1×10^{-6} mole) in pH 10 buffer at room temperature

nm with a shoulder at 422 nm was formed. The UV-vis spectra of Cl_{16}TSPPFeCl and that of the oxidized intermediate (**22**) are shown in figure 2.17.

A dioxygen-iron(II) porphyrin complex, Cl_{16}TSPPFe(II)-O_2 (**23**) was observed when Cl_{16}TSPPFeCl was oxidized by NaClO under basic condition (pH≥7) at room temperature in the presence of veratryl alcohol. When NaClO (5×10^{-6} mole) was added to Cl_{16}TSPPFeCl (3×10^{-8} mole in 3 mL 0.1 M pH 7 phosphate buffer) in the presence of veratryl alcohol (1×10^{-5} mole), the 422 nm peak decreased in intensity and the 448 nm peak appeared and increased in intensity. The 310 nm peak of veratraldehyde kept increasing until the 448 nm peak disappeared and the 422 nm peak was restored. The 422 nm peak decreased in intensity after that and gave the dioxygen-iron(II) porphyrin complex which had its Soret band at 446 nm (Figure 2.18).

The presence of manganese(II)-lactate, a superoxide dismutating agent, inhibited the formation of this dioxygen-iron(II) porphyrin complex, suggesting that the dioxygen complex was formed from the reaction of superoxide and the iron(III) porphyrin:

$$Cl_{16}TSPPFeCl + O_2^{\cdot-} \rightarrow Cl_{16}TSPPFe(II)\text{-}O_2$$

The dioxygen complex (**23**) reacted with excess NaClO to give a UV-vis spectrum characteristic of the iron(III) porphyrin, explaining the fact that the dioxygen complex was observed only after the oxidant (NaClO) was consumed.

The dioxygen-iron(II) porphyrin complex (**23**) reacted with carbon monoxide to give the CO-iron(II) porphyrin complex (Figure 2.19), which showed the same UV-vis spectrum as that of the complex prepared by reacting Cl_{16}TSPPFeCl with excess sodium dithionite at pH 7 followed by treating the solution with carbon monoxide.

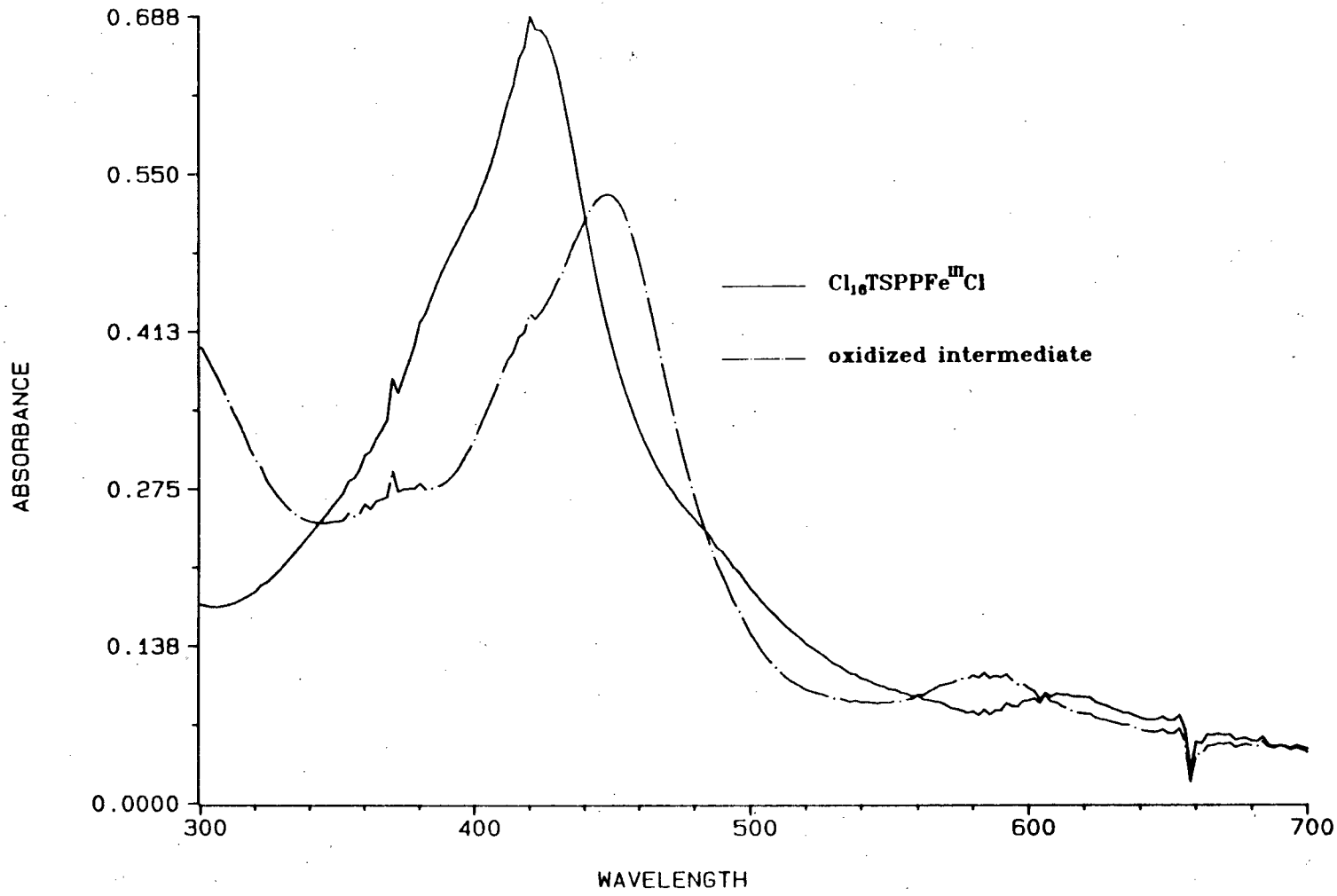

Figure 2.17 The oxidation of $Cl_{16}TSPPFeCl$ (λ_{max} 422 nm, 3×10^{-8} mole) to the λ_{max} 448 nm intermediate (**22**) by NaClO (1×10^{-5} mole) in pH 12 borate buffer (3 mL) at room temperature

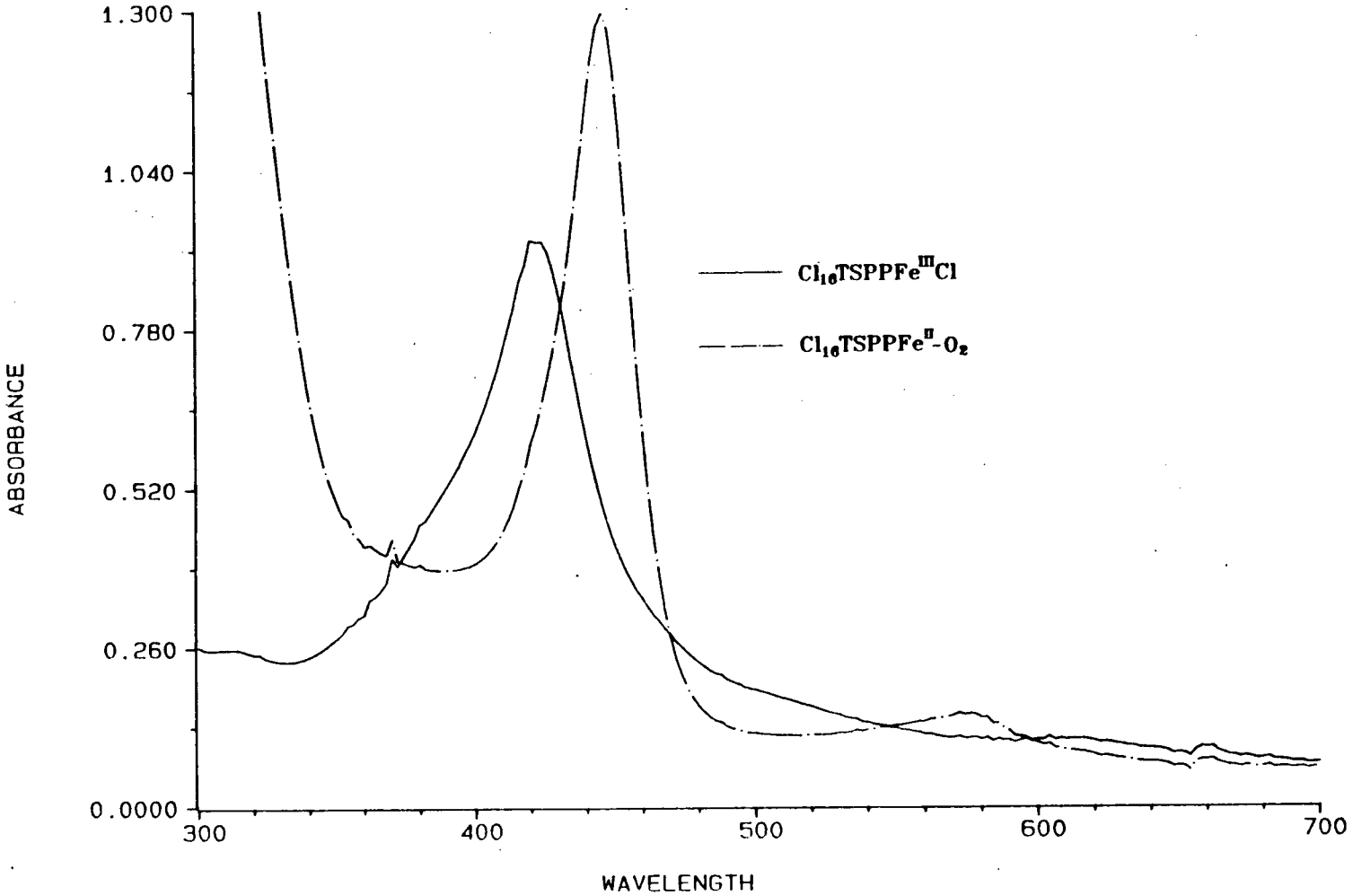

Figure 2.18 The UV-vis spectra of $Cl_{16}TSPPFeCl$ (λ_{max} 422 nm) and $Cl_{16}TSPPFe^{II}$-O_2 (**23**, λ_{max} 446 nm) in pH 7 phosphate buffer (0.1 M)

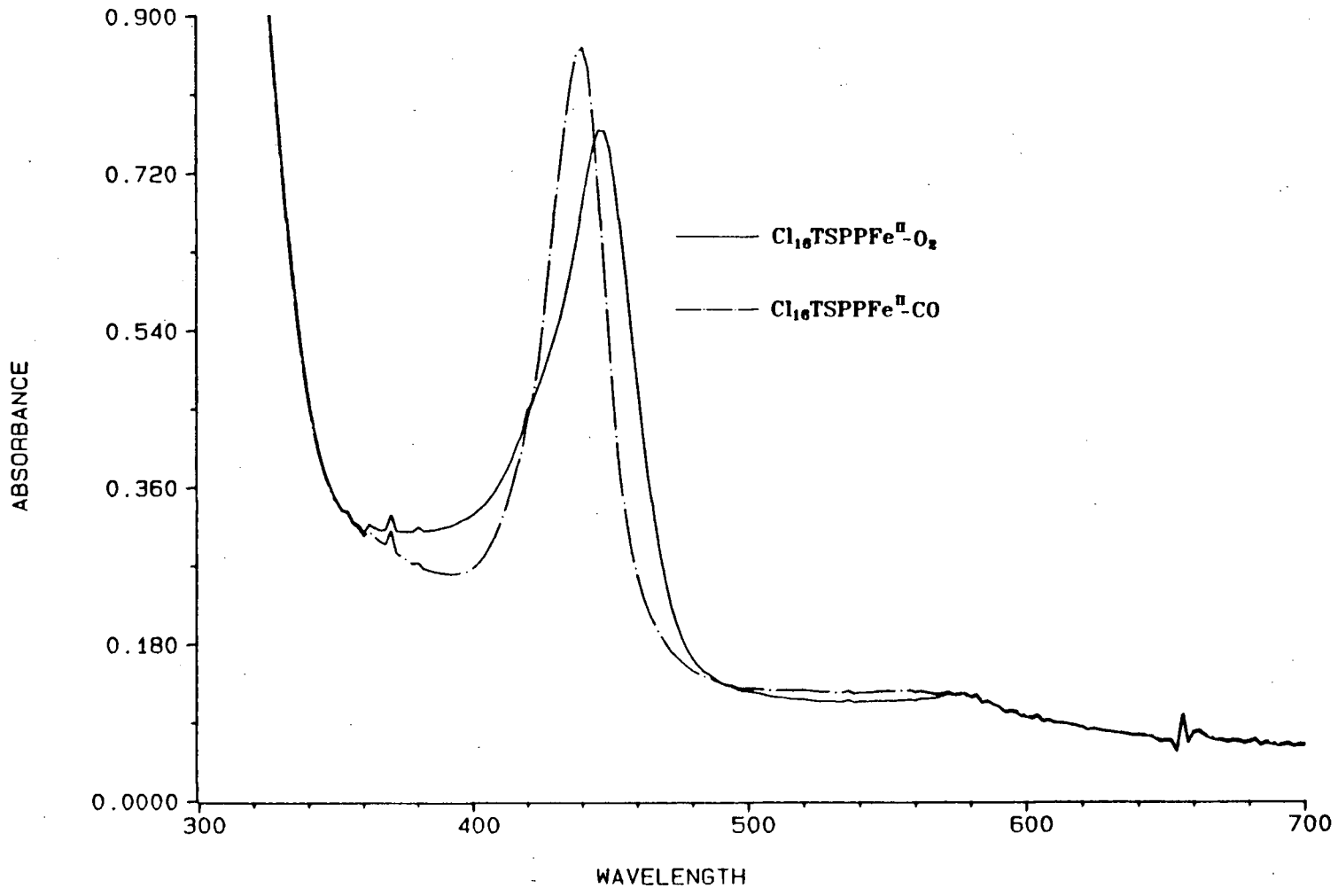

Figure 2.19 The reaction of CO and $Cl_{16}TSPPFe^{II}$-O_2 (**23**) formed after the oxidation of veratryl alcohol to give $Cl_{16}TSPPFe^{II}$-CO (λ_{max} 440 nm) in pH 7 phosphate buffer

Cl_{16}TSPPFeCl (3×10^{-8} mole) also reacted with potassium superoxide in the presence of veratryl alcohol (1×10^{-5} mole) to give the dioxygen-iron(II) porphyrin complex **23**.

Cl_{16}TSPPFeCl destruction by hydrogen peroxide was observed even in the presence of a large excess of veratryl alcohol. No spectral change was observed when Cl_{16}TSPPFeCl (3×10^{-8} mole) was treated with t-BuOOH (5×10^{-6} mole) at pH 2 and pH 3. The reaction of Cl_{16}TSPPFeCl with t-BuOOH at pH 7 or pH 10 was similar to that with NaClO. No oxidized intermediates were observed when Cl_{16}TSPPFeCl was oxidized by *m*CPBA at pH 2 and pH 3, pH 5 was the minimum pH to observe the oxidized intermediate **22** (λ_{max} 448 nm) and the dioxygen-iron(II) porphyrin in the presence of veratryl alcohol.

2.1.3 Factors affecting the catalytic activity of the metalloporphyrins

Oxidation of veratryl alcohol by lignin peroxidase gave veratraldehyde as a major product together with small amounts of quinones and aromatic ring cleaved products. The oxidation of veratryl alcohol by protohemin, TPPFeCl, or TDCSPPFeCl gave similar products as will be described in Chapter 3. Veratryl alcohol was used as a substrate in this experiment and the formation of veratraldehyde was used as a criterion for comparing the catalytic activities of metalloporphyrins under different conditions. Veratraldehyde has a strong absorption at 310 nm and its formation can be conveniently followed by using a rapid scanning Diode Array UV-vis spectrometer.

2.1.3.1 pH of the solvent

A. TDCSPPFeCl as catalyst

The pH dependency of the oxidation of veratryl alcohol by TDCSPPFeCl and *m*CPBA is shown in Figure 2.20. Both the rate and yield of veratraldehyde formation were highly dependent on the pH of the buffer solution. It can be seen from Figure 2.20 that at pH 3 and pH 5, the reaction stopped soon after addition of *m*CPBA and the final yield of veratraldehyde was lower than that at pH 2. It was found that the reaction stopped because the oxidant was consumed. The porphyrin catalyst was still active after the reaction and addition of another aliquot of *m*CPBA restarted the reaction as shown in Figure 2.21.

The oxidation of veratryl alcohol (1×10^{-5} mole) by TDCSPPFeCl (3×10^{-8} mole) and NaClO (5×10^{-6} mole) in 0.1 M aqueous buffer of various pH's is shown in Figure 2.22. The highest rate was seen at pH 5 and the highest yield was achieved at pH 7. Little reaction was observed at pH 2 and pH 3. The catalyst was also reactive after the reaction as shown in Figure 2.23.

TDCSPPFeCl (3×10^{-8} mole) catalyzed oxidation of veratryl alcohol (1×10^{-5} mole) in 0.1 M aqueous buffer of various pH's using t-BuOOH as oxidant is shown in Figure 2.24. There were no observable reactions at pH 8 and pH 10. There seemed to be an induction period at pH 2, 3, 5, and 7. It has been suggested that the displacement of chloride by *m*CPBA was a slow process and was responsible for the induction period in the oxidation of *meso*-tetramesitylporphyrin iron chloride by *m*CPBA.[6] An induction period was observed in this laboratory[23] for the oxidation of *meso*-tetra(2,6-dichlorophenyl)porphyrin iron chloride (TDCPPFeCl) but not for the corresponding

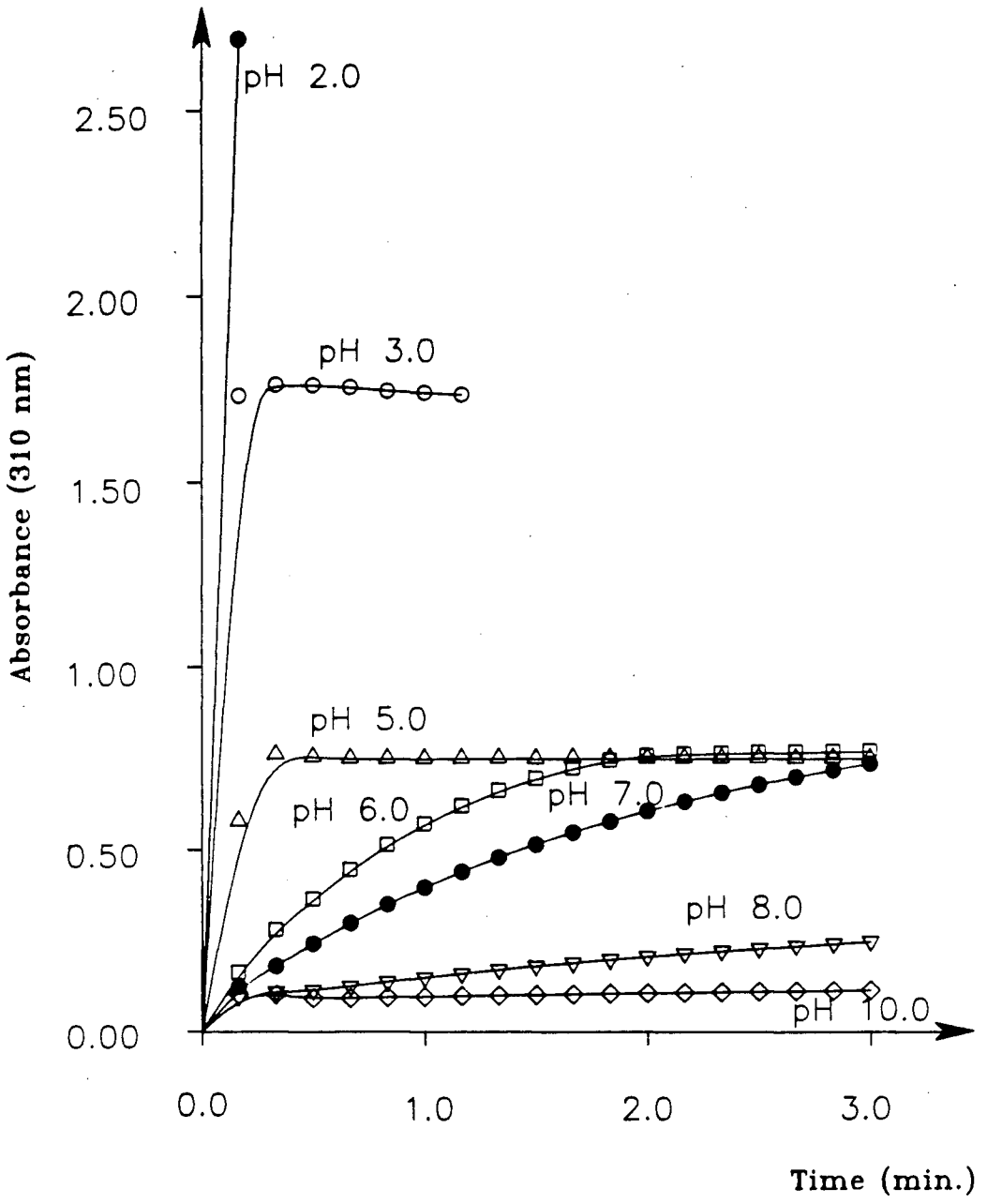

Figure 2.20 The oxidation of veratryl alcohol (5×10^{-6} mole) by TDCSPPFeCl (1×10^{-8} mole) and *m*CPBA (2×10^{-6} mole) at room temperature in 4 mL aqueous buffer of various pH values, pH 5 and 6 buffers are 0.1 M citrate and all others are 0.1 M phosphate.

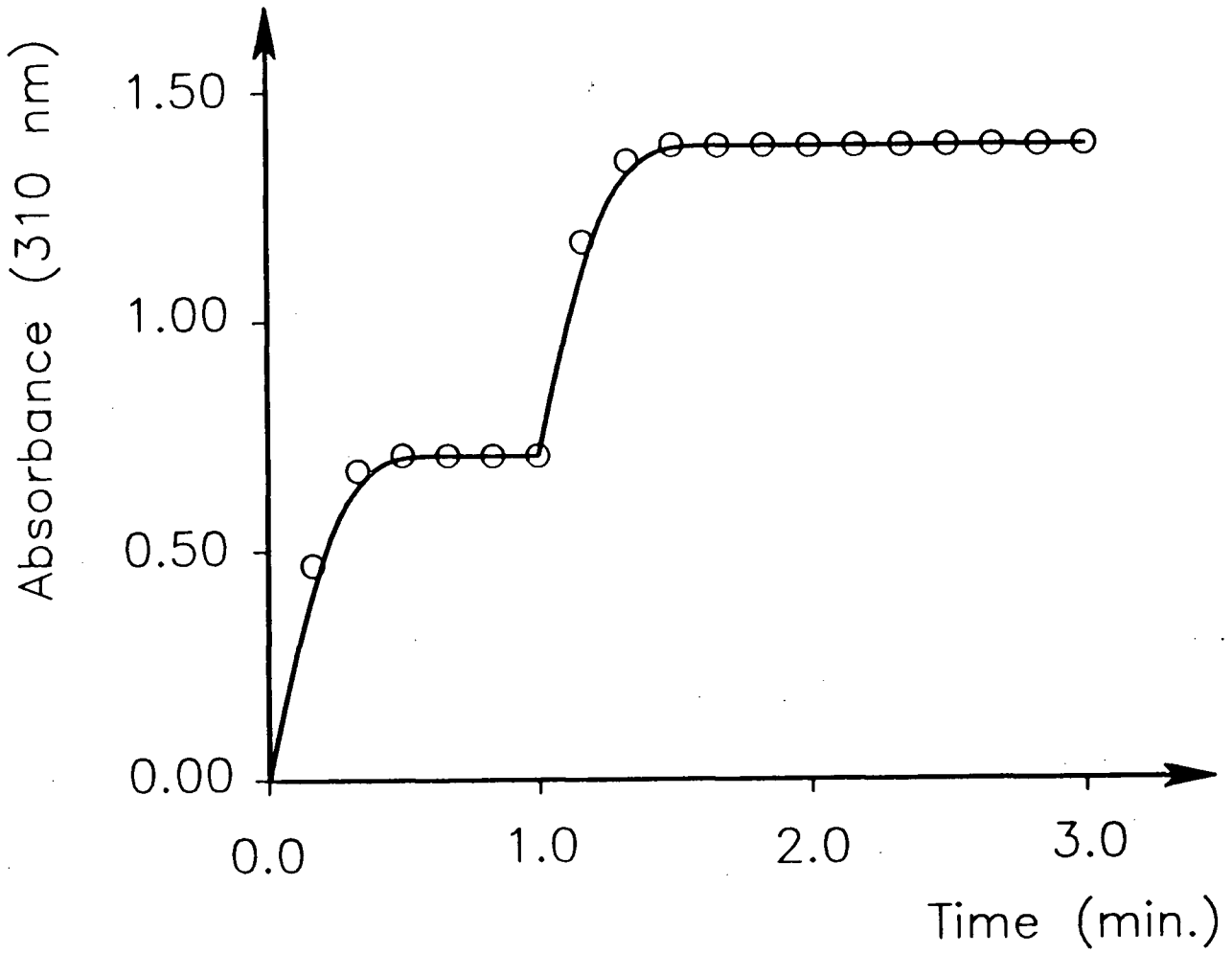

Figure 2.21 The oxidation of veratryl alcohol (5×10^{-6} mole) by TDCSPPFeCl (1×10^{-8} mole) and *m*CPBA in 4 mL 0.1 M pH 5 citrate buffer at room temperature, the same amount of *m*CPBA (2×10^{-6} mole) was added at time = 0 and time = 1 min.

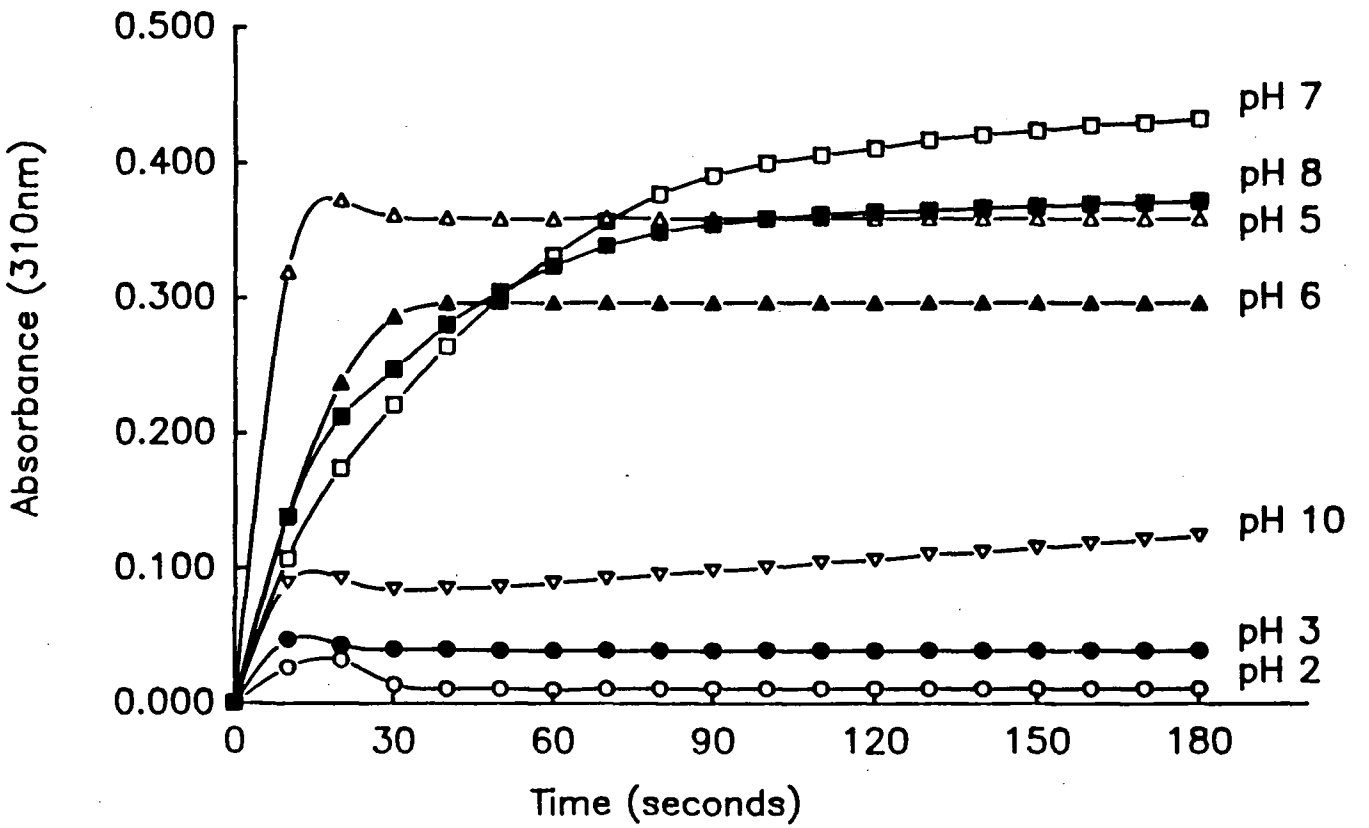

Figure 2.22 The oxidation of veratryl alcohol (1×10^{-5} mole) by TDCSPPFeCl (3×10^{-8} mole) and NaClO (5×10^{-6} mole) at room temperature in 4 mL aqueous buffer of various pH values, pH 5, and 6 buffers are 0.1 M citrate and all others are 0.1 M phosphate.

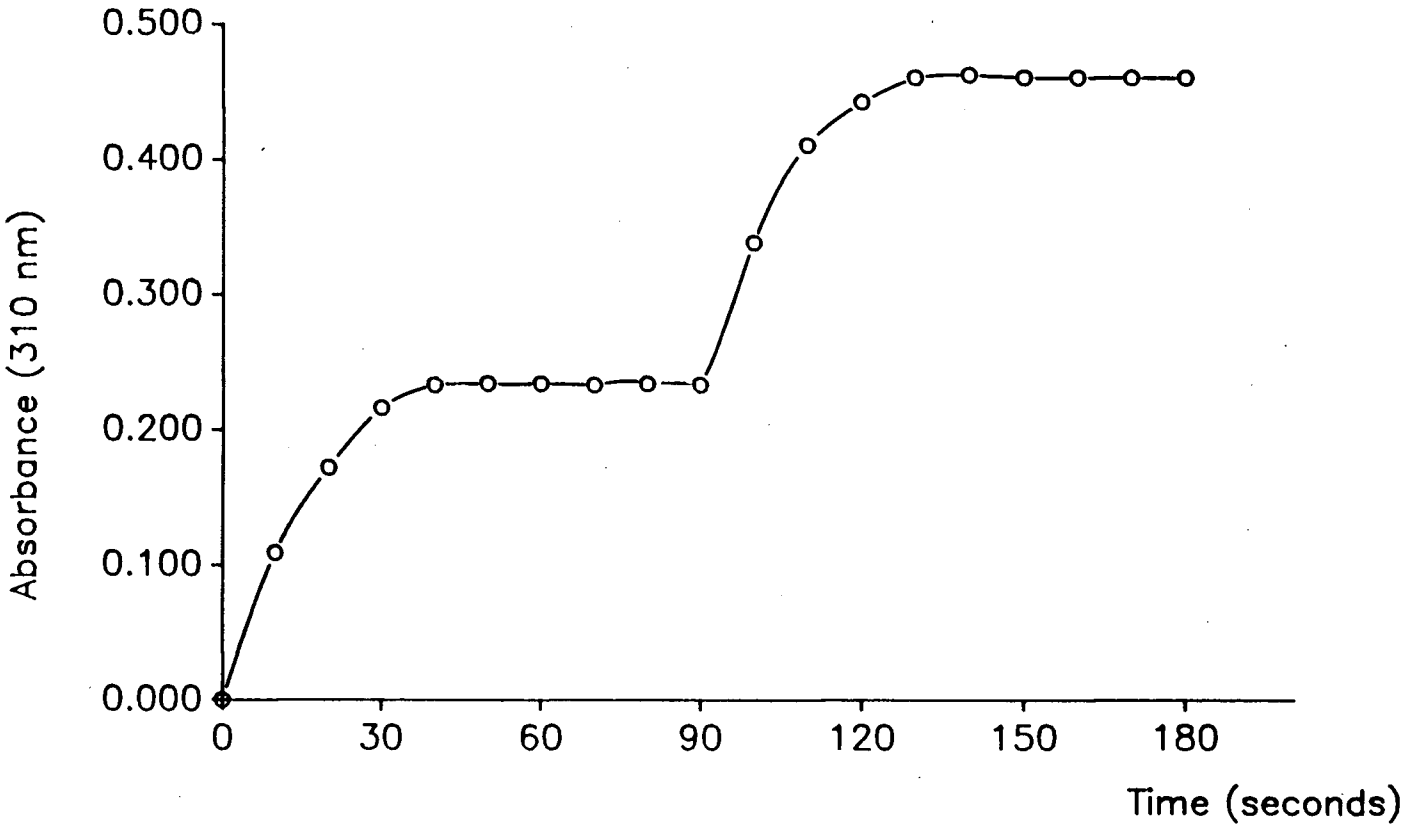

Figure 2.23 The oxidation of veratryl alcohol (1×10^{-5} mole) by TDCSPPFeCl (3×10^{-8} mole) and NaClO in 4 mL 0.1 M pH 6 citrate buffer at room temperature, NaClO (5×10^{-6} mole) added at time = 0 and time = 90 seconds

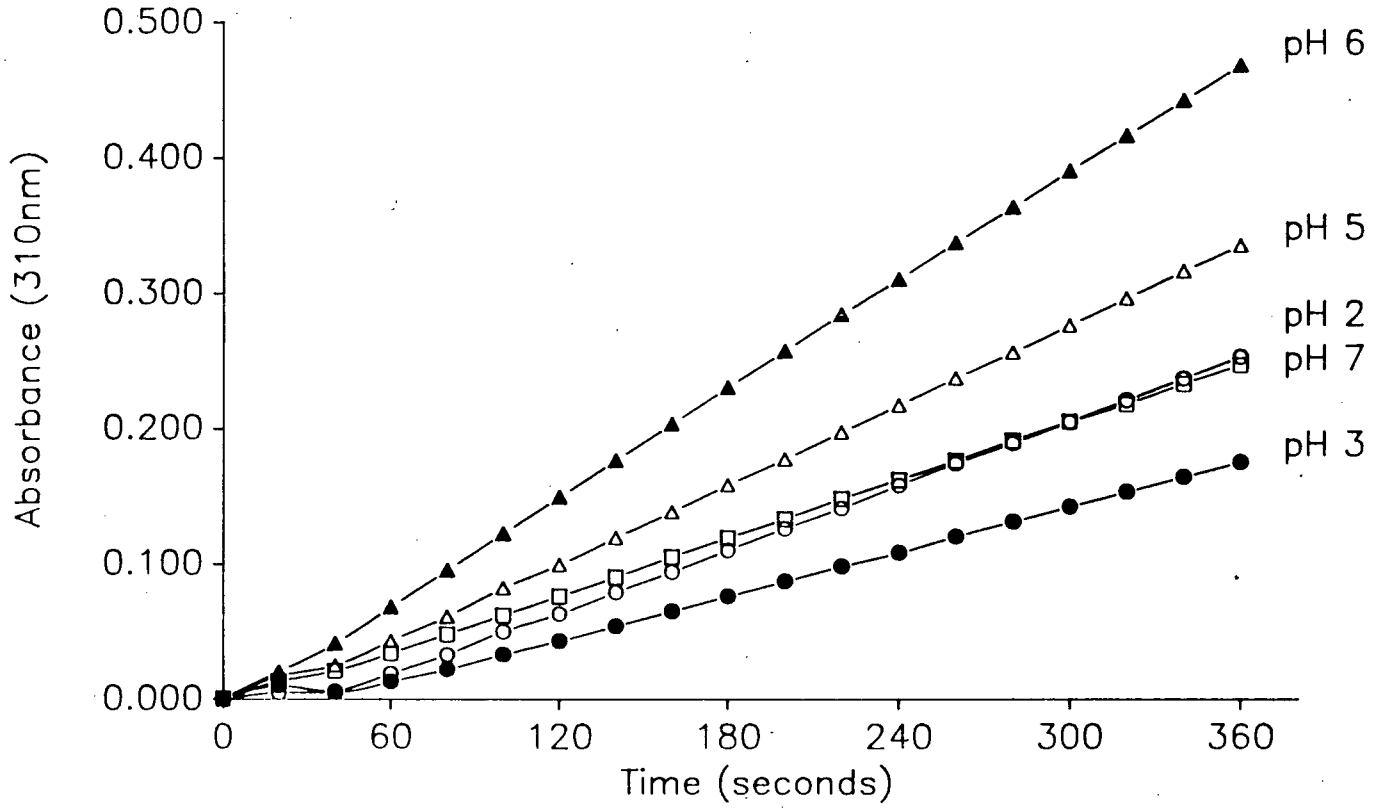

Figure 2.24 The oxidation of veratryl alcohol (1×10^{-5} mole) by t-BuOOH (5×10^{-6} mole) and TDCSPPFeCl (3×10^{-8} mole) at room temperature in 4 mL aqueous buffer of various pH values, pH 2, 3, and 7 buffers are 0.1 M phosphate, pH 5 and 6 buffers are 0.1 M citrate.

hydroxide, TDCPPFeOH. *Meso*-tetra(2,6-dichloro-3-sulfonatophenyl)porphyrin iron hydroxide (TDCSPPFeOH) was synthesized and tested for the presence of induction periods during the oxidation of veratryl alcohol. As shown in Figure 2.25 (curve 1), the induction period still exists in the oxidation of veratryl alcohol by TDCSPPFeOH and t-BuOOH at pH 3. Addition of sodium chloride, which will shift the equilibrium:

$$\text{TDCSPPFeOH} + \text{Cl}^- \rightleftharpoons \text{TDCSPPFeCl} + \text{OH}^-$$

to the right, not only failed to extend the induction period but speeded up the reaction as shown in Figure 2.25. This result indicates that chloride as axial ligand was not responsible for the induction period.

The stimulating effect for the oxidation of veratryl alcohol caused by sodium chloride is probably a simple ion effect. Lignin peroxidase and biomimetic catalysts oxidize lignin model compounds through a cation radical mechanism. Increasing ionic strength will stabilize the cation radical intermediates. The rate of the oxidation of veratryl alcohol increased with increasing concentration of sodium chloride (Figure 2.25). As shown in Figure 2.26, addition of 1 M sodium sulfate results in a 4 fold increase of the reaction rate. Not all inorganic salts increase the reaction rate. The presence of 1 M sodium fluoride or sodium nitrate (in 3 mL 0.1 M pH 3 phosphate buffer) completely inhibited the oxidation of veratryl alcohol (1×10^{-5} mole) by t-BuOOH (1×10^{-5} more) and TDCSPPFeOH (3×10^{-8} mole).

The effect of buffer concentration on the oxidation of veratryl alcohol was also studied. As shown in Figure 2.27, increasing buffer concentration also increases the rate of the oxidation of veratryl alcohol by TDCSPPFeOH and t-BuOOH.

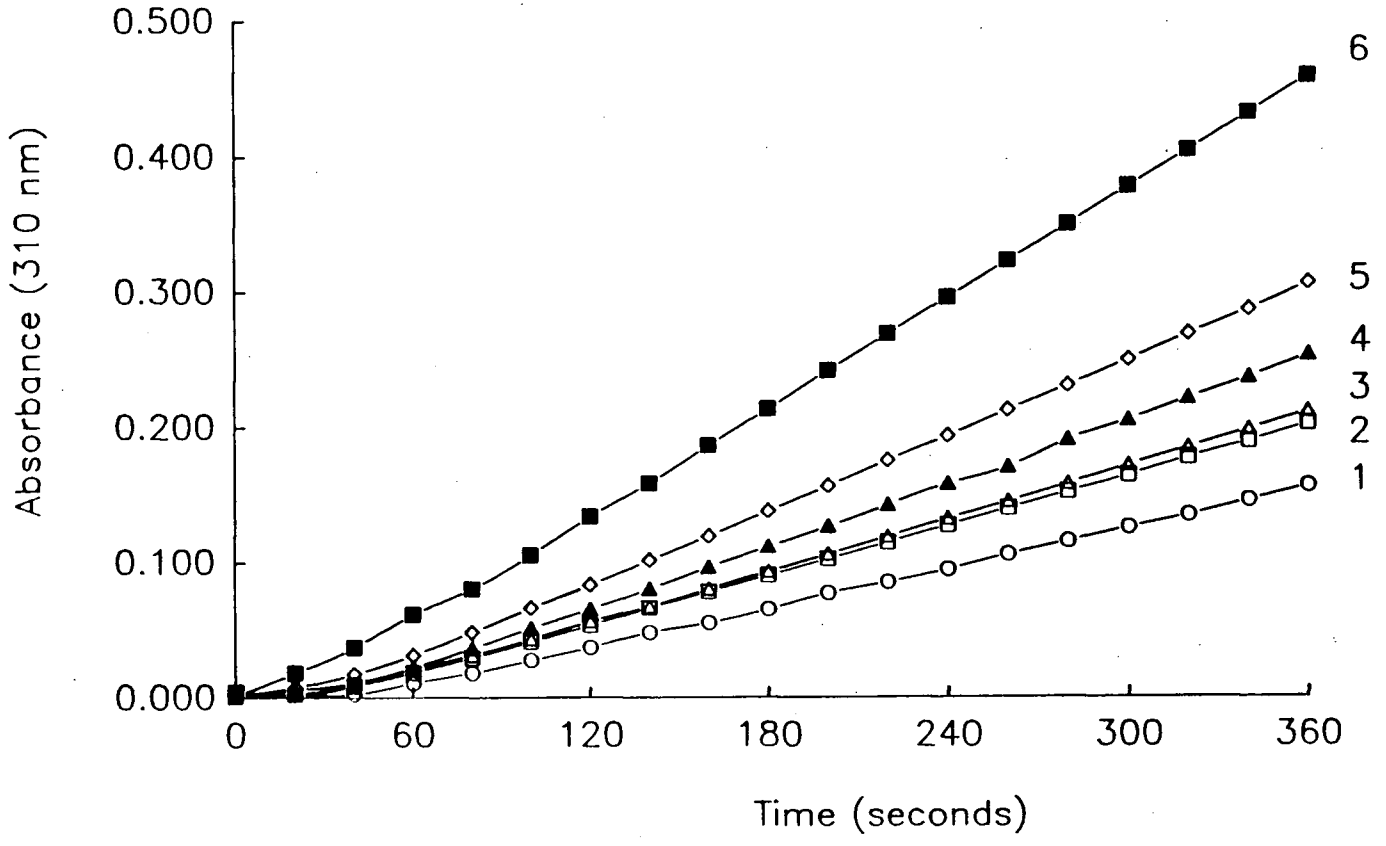

Figure 2.25 The oxidation of veratryl alcohol (1×10^{-5} mole) by TDCSPPFeOH (3×10^{-8} mole) and t-BuOOH (1×10^{-5} mole) at room temperature in 4 mL 0.1 M pH 3 phosphate buffer containing various concentrations of sodium chloride (M), 1, 0; 2, 0.1; 3, 0.2; 4, 0.5; 5, 1.0; 6, 2.0

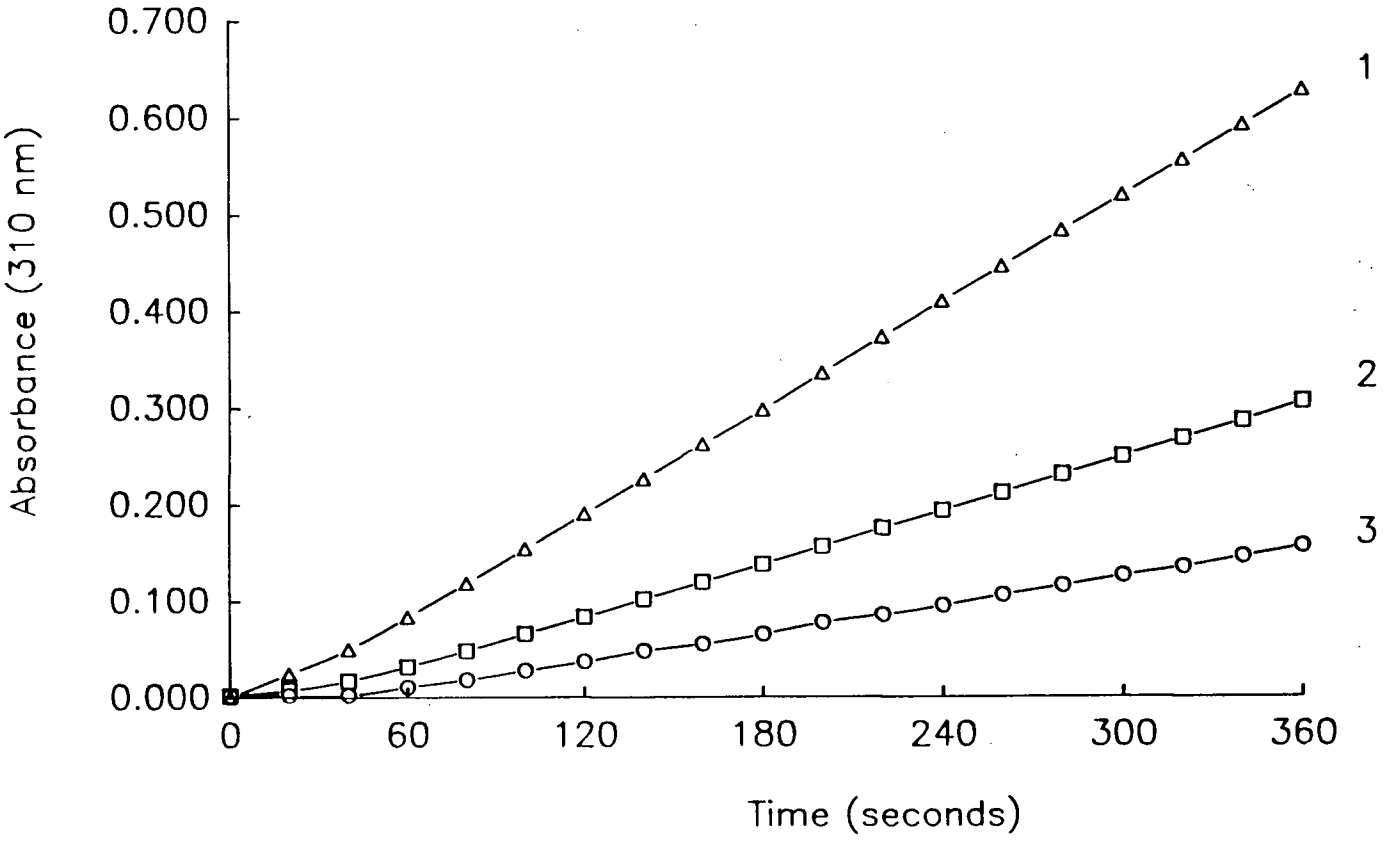

Figure 2.26 The oxidation of veratryl alcohol (1×10^{-5} mole) by TDCSPPFeOH (3×10^{-8} mole) and t-BuOOH (1×10^{-5} mole) at room temperature in 4 mL 0.1 M pH 3 phosphate buffer containing: 1, 1 M Na_2SO_4; 2, 1 M NaCl; 3, no other inorganic salts

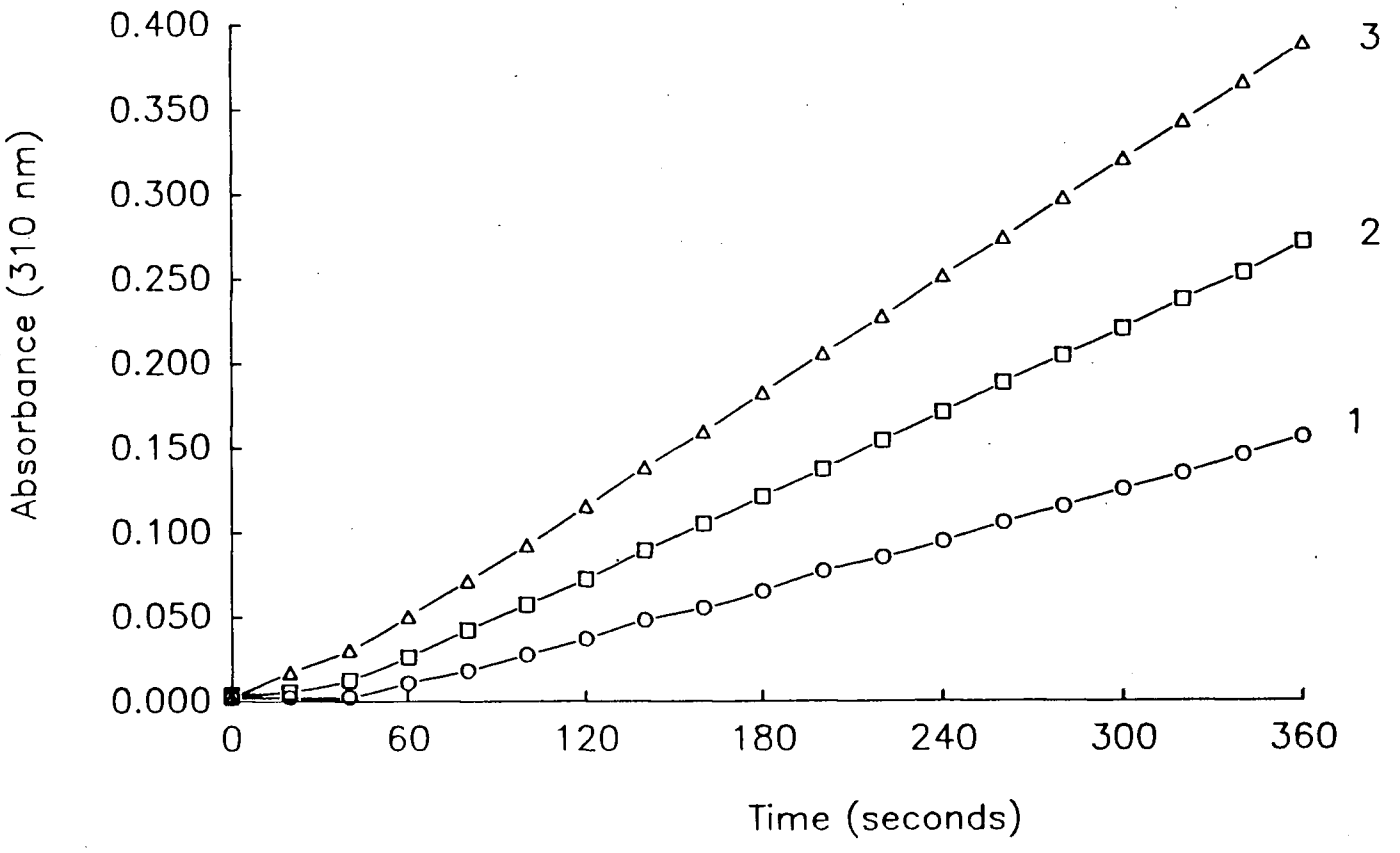

Figure 2.27 The oxidation of veratryl alcohol (1×10^{-5} mole) by TDCSPPFeOH (3×10^{-8} mole) and t-BuOOH (1×10^{-5} mole) at room temperature in 4 mL pH 3 phosphate buffer of various concentrations (M), 1, 0.1; 2, 0.5; 3, 1.0

Although purified by vacuum distillation, veratryl alcohol was shown by GC analysis to contain a trace amount of methyl 4-hydroxy-3-methoxybenzoate, which was responsible for the induction period. It was reported that the same compound delayed the oxidation of veratryl alcohol by lignin peroxidase.[24] Addition of methyl 4-hydroxy-3-methoxybenzoate (1×10^{-6} mole) dramatically slowed down the oxidation of veratryl alcohol (1×10^{-5} mole in 3 mL 0.1 M pH 3 phosphate buffer) by TDCSPPFeOH (3×10^{-8} mole) and t-BuOOH (1×10^{-5} mole). The induction period was not seen when veratryl alcohol was purified by double distillation.

Hydrogen peroxide seemed to be an inefficient oxidant for TDCSPPFeCl catalyzed veratryl alcohol oxidation. The reaction was slow at every pH (Figure 2.28).

B. Cl_{16}TSPPFeCl as catalyst

Figure 2.29 shows the pH dependency of Cl_{16}TSPPFeCl catalyzed oxidation of veratryl alcohol by *m*CPBA. The maximal catalytic activity was observed at pH 2 and the reaction was slower and the yield was lower at higher pH. The catalyst was still active after the reaction (Figure 2.30).

Cl_{16}TSPPFeCl (3×10^{-8} mole) and t-BuOOH (5×10^{-6} mole) oxidized veratryl alcohol (1×10^{-5} mole) effectively only in pH 5, 6, and 7 buffers (3 mL) as shown in Figure 2.31. The reaction was very slow at pH 2, 3, 8, and 10. Cl_{16}TSPPFeCl catalyzed oxidation of veratryl alcohol was favoured at high pH when NaClO was the oxidant (Figure 2.32). Cl_{16}TSPPFeCl was not stable towards hydrogen peroxide and the oxidation of veratryl alcohol (1×10^{-5} mole) by Cl_{16}TSPPFeCl (3×10^{-8} mole) and H_2O_2 (5×10^{-6} mole) was very slow.

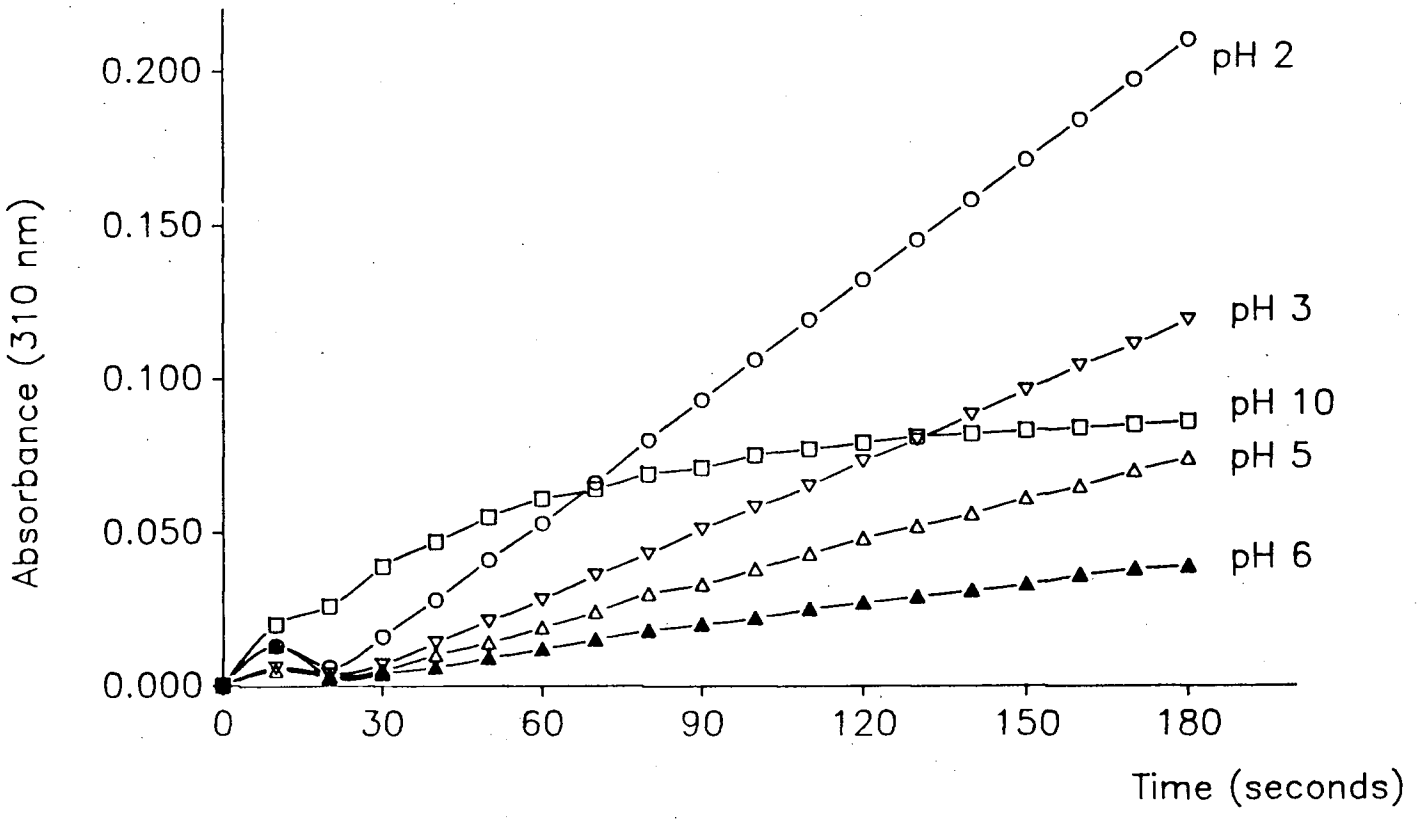

Figure 2.28 The oxidation of veratryl alcohol (1×10^{-5} mole) by TDCSPPFeCl (3×10^{-8} mole) and H_2O_2 (5×10^{-6} mole) at room temperature in 4 mL aqueous buffer of various pH values, pH 2, 3 and 10 buffers are 0.1 M phosphate, pH 5 and 6 buffers are 0.1 M citrate.

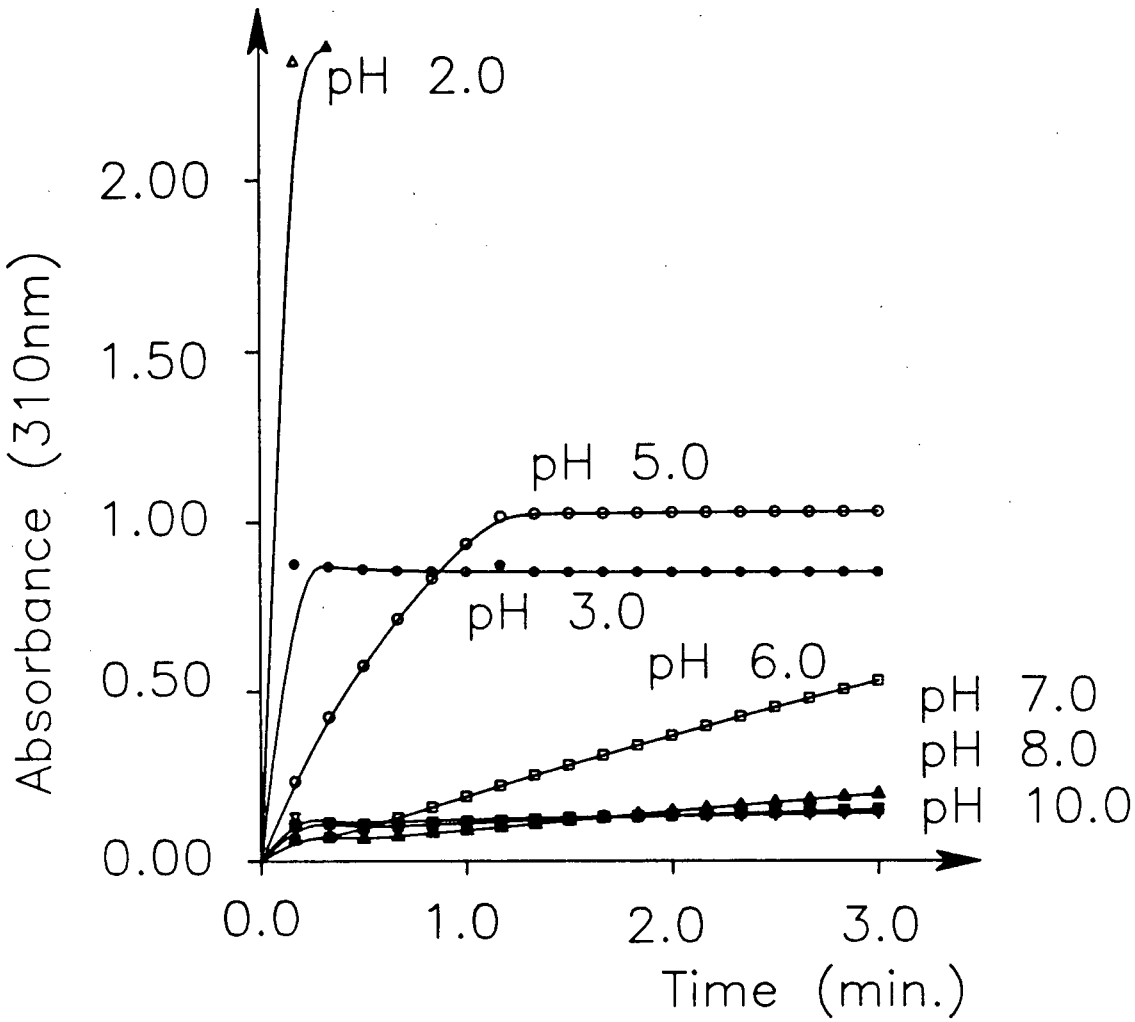

Figure 2.29 The oxidation of veratryl alcohol (5×10^{-6} mole) by Cl_{16}TSPPFeCl (1×10^{-8} mole) and *m*CPBA (2×10^{-6} mole) at room temperature in 4 mL aqueous buffer of various pH values, pH 5, and 6 buffers are 0.1 M citrate and all others are 0.1 M phosphate.

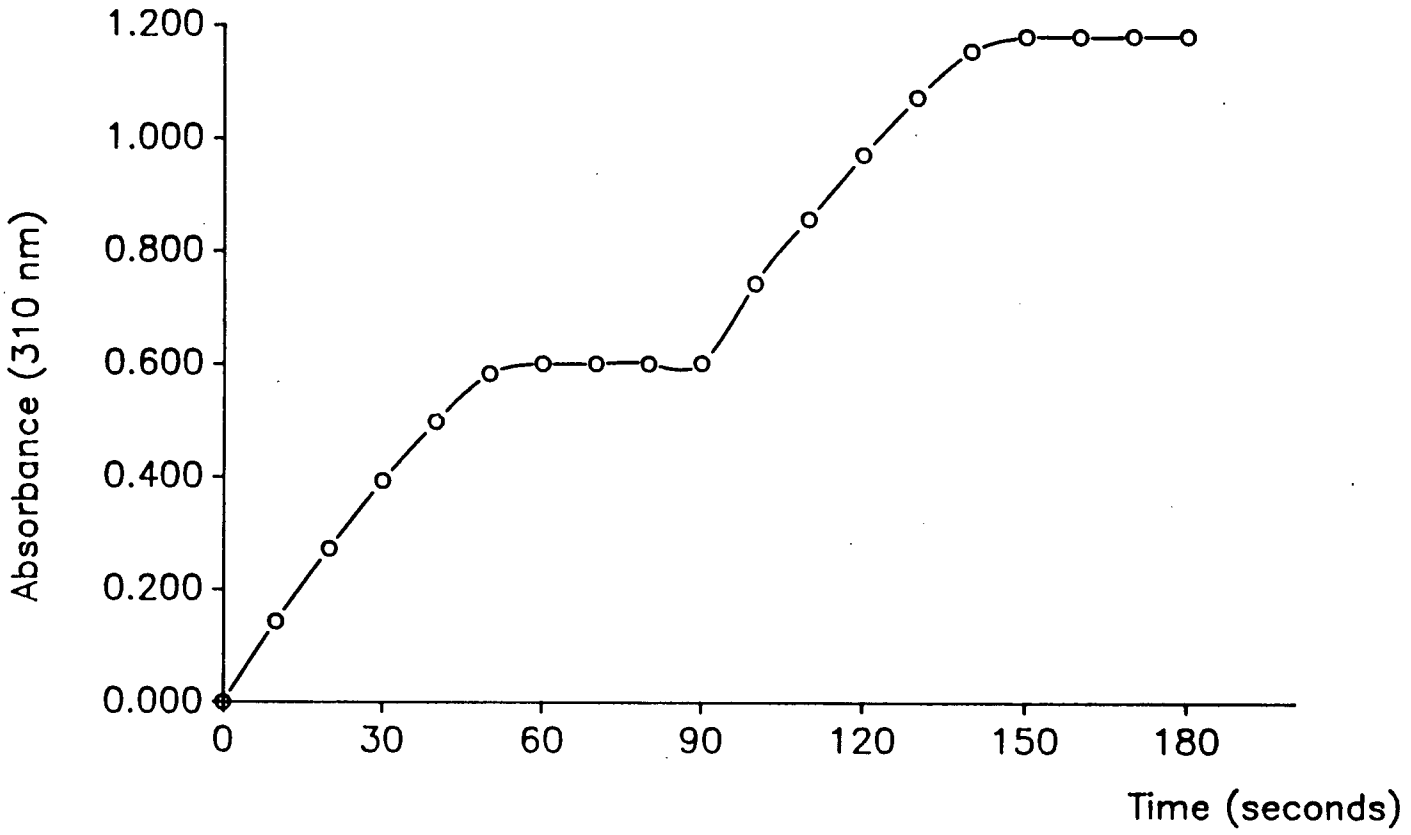

Figure 2.30 The oxidation of veratryl alcohol (1×10^{-5} mole) by Cl_{16}TSPPFeCl (1×10^{-8} mole) and *m*CPBA in 4 mL 0.1 M pH 5 citrate buffer at room temperature, *m*CPBA (1×10^{-6} mole) added at time = 0 and time =90 seconds

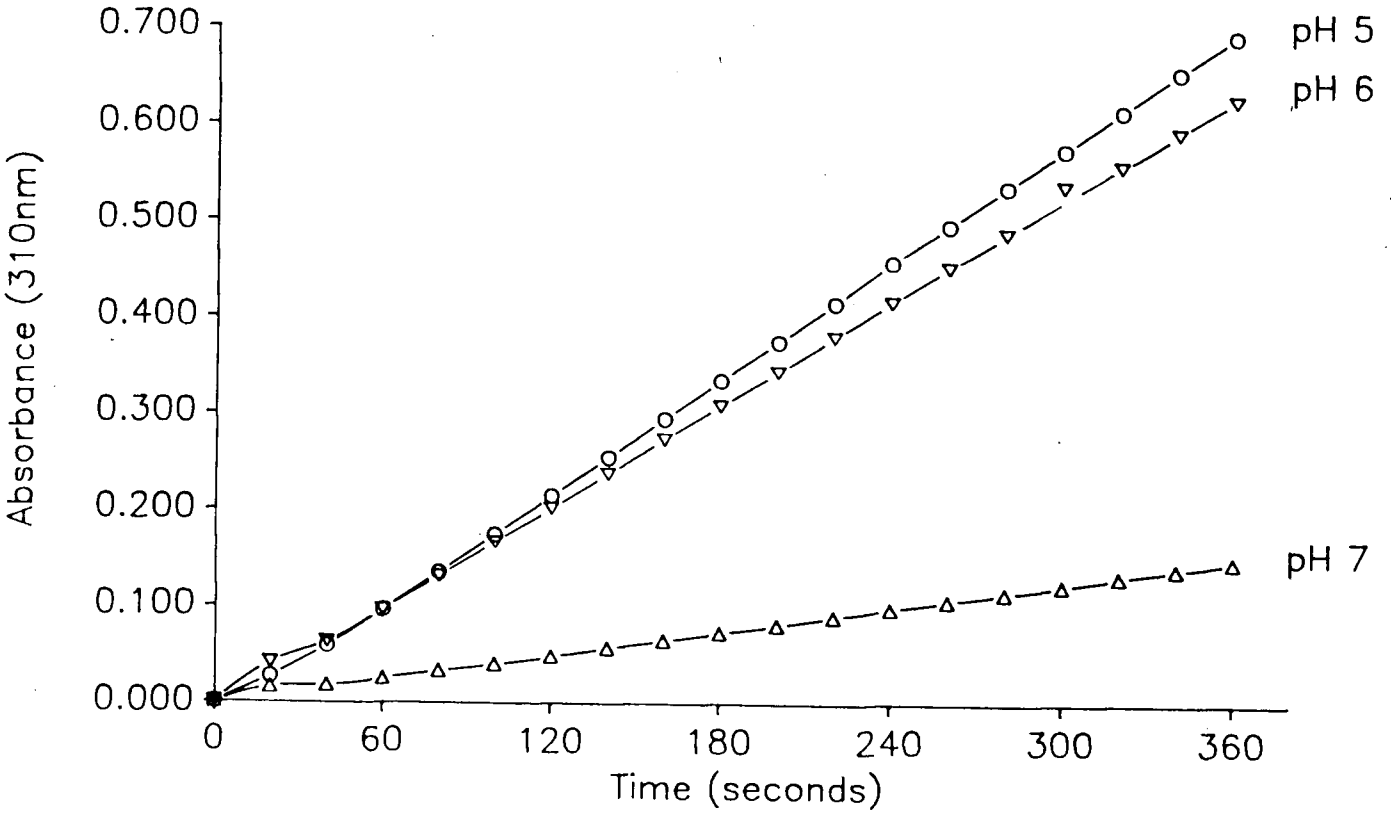

Figure 2.31 The oxidation of veratryl alcohol (1×10^{-5} mole) by $Cl_{16}TSPPFeCl$ (3×10^{-8} mole) and t-BuOOH (5×10^{-6} mole) in 4 mL 0.1 M phosphate buffer (pH 7) or 0.1 M citrate buffer (pH 5 and 6) at room temperature

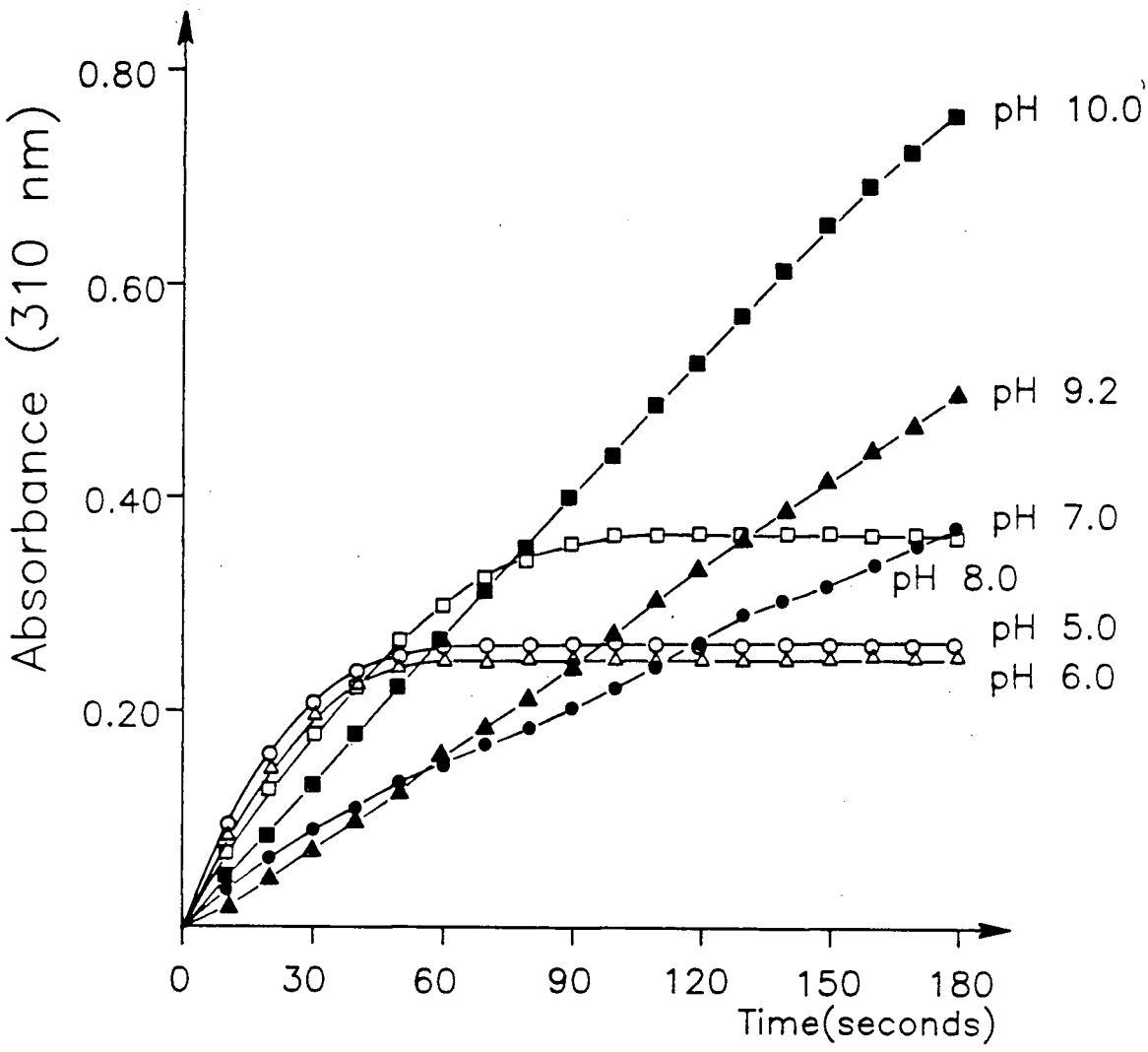

Figure 2.32 The oxidation of veratryl alcohol (1×10^{-5} mole) by $Cl_{16}TSPPFeCl$ (3×10^{-8} mole) and NaClO (5×10^{-6} mole) at room temperature in 4 mL aqueous buffer of various pH values, pH 7 and 10 buffers are 0.1 M phosphate, pH 5 and 6 buffers are 0.1 M citrate, and pH 9.2 buffer is 0.1 M borate.

C. TDCSPPMnCl as catalyst

TDCSPPMnCl catalyzed oxidation of veratryl alcohol by various oxidants was also highly dependent on the pH of the solvent as shown in Figures 2.33, 2.34, and 2.35. There was no observable loss of catalytic activity of the manganese porphyrin during the reaction. As shown in Figure 2.36, when the oxidant was consumed and the 310 nm peak stopped increasing, addition of a second aliquot of oxidant restarted the reaction and caused the same increase of 310 nm absorption.

When t-BuOOH (5×10^{-6} mole) was the oxidant, TDCSPPMnCl (3×10^{-8} mole) catalyzed oxidation of veratryl alcohol (1×10^{-5} mole) was very slow at pH 10 and no reaction was observed between pH 3 and pH 8.

D. Cl_{16}TSPPMnCl as catalyst

Cl_{16}TSPPMnCl catalyzed oxidation of veratryl alcohol was favoured at high pH when NaClO or H_2O_2 was the oxidant as shown in Figures 2.37 and 2.38. When *m*CPBA was the oxidant, the catalytic activity order was pH 3 > pH 2 > pH 5 > pH 8, pH 10, pH 7 (Figure 2.39). When t-BuOOH (5×10^{-6} mole) was the oxidant, the reaction (3×10^{-8} mole Cl_{16}TSPPMnCl, 1×10^{-5} mole veratryl alcohol in 3 mL buffer) was very slow between pH 5 and pH 10 and no reaction was observed at pH 2 and pH 3.

As discussed earlier, Cl_{16}TSPPMn(II) was produced at high pH from the reaction of the manganese(III) porphyrin and superoxide. Oxidant could be consumed in vain for oxidizing the manganese(II) porphyrin back to the manganese(III) porphyrin. It is known that the dismutation of superoxide in aqueous solution is inversely proportional to the pH. More oxidant would be consumed at higher pH by oxidizing the

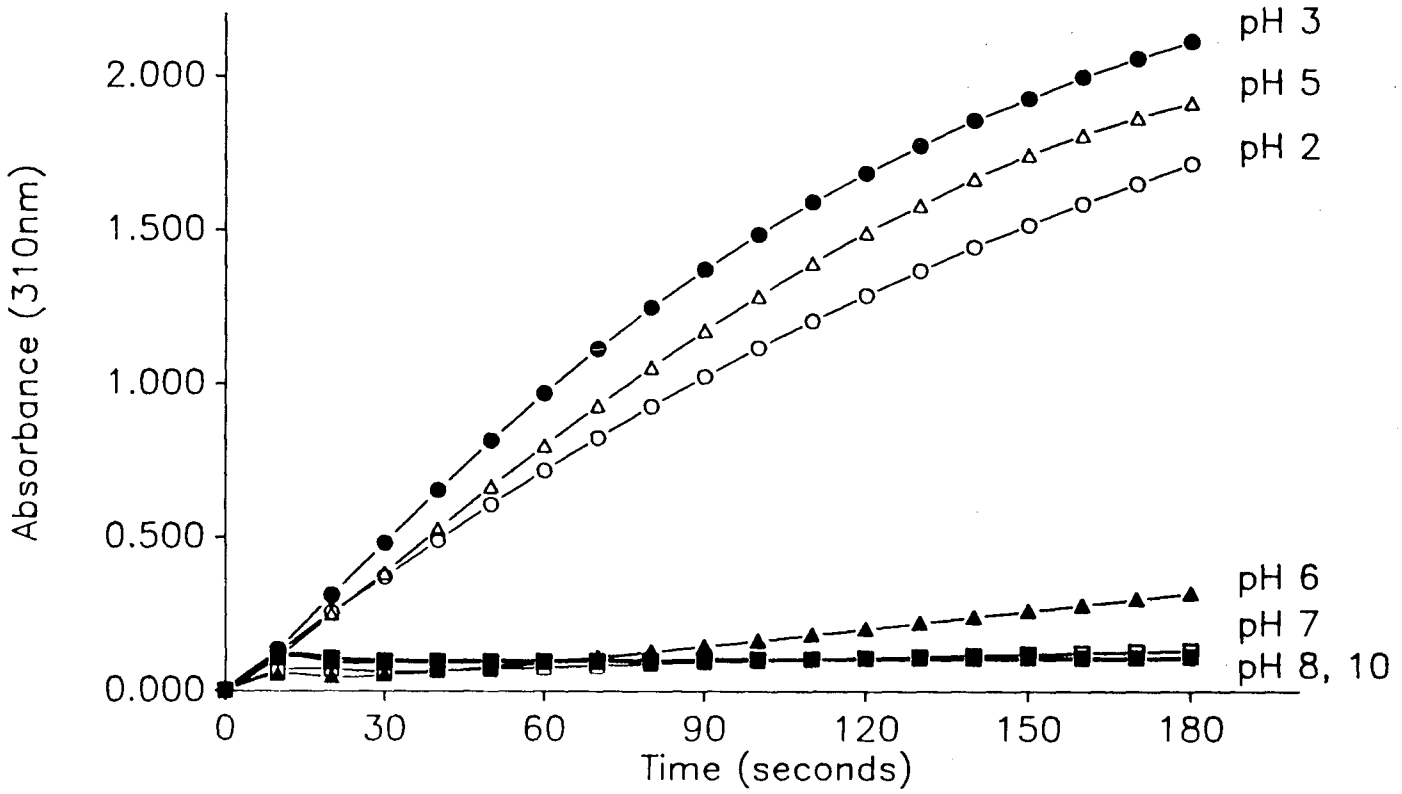

Figure 2.33 The oxidation of veratryl alcohol (5×10^{-6} mole) by TDCSPPMnCl (1×10^{-8} mole) and *m*CPBA (2×10^{-6} mole) at room temperature in 4 mL aqueous buffer of various pH values, pH 5 and 6 buffers are 0.1 M citrate and all others buffers are 0.1 M phosphate.

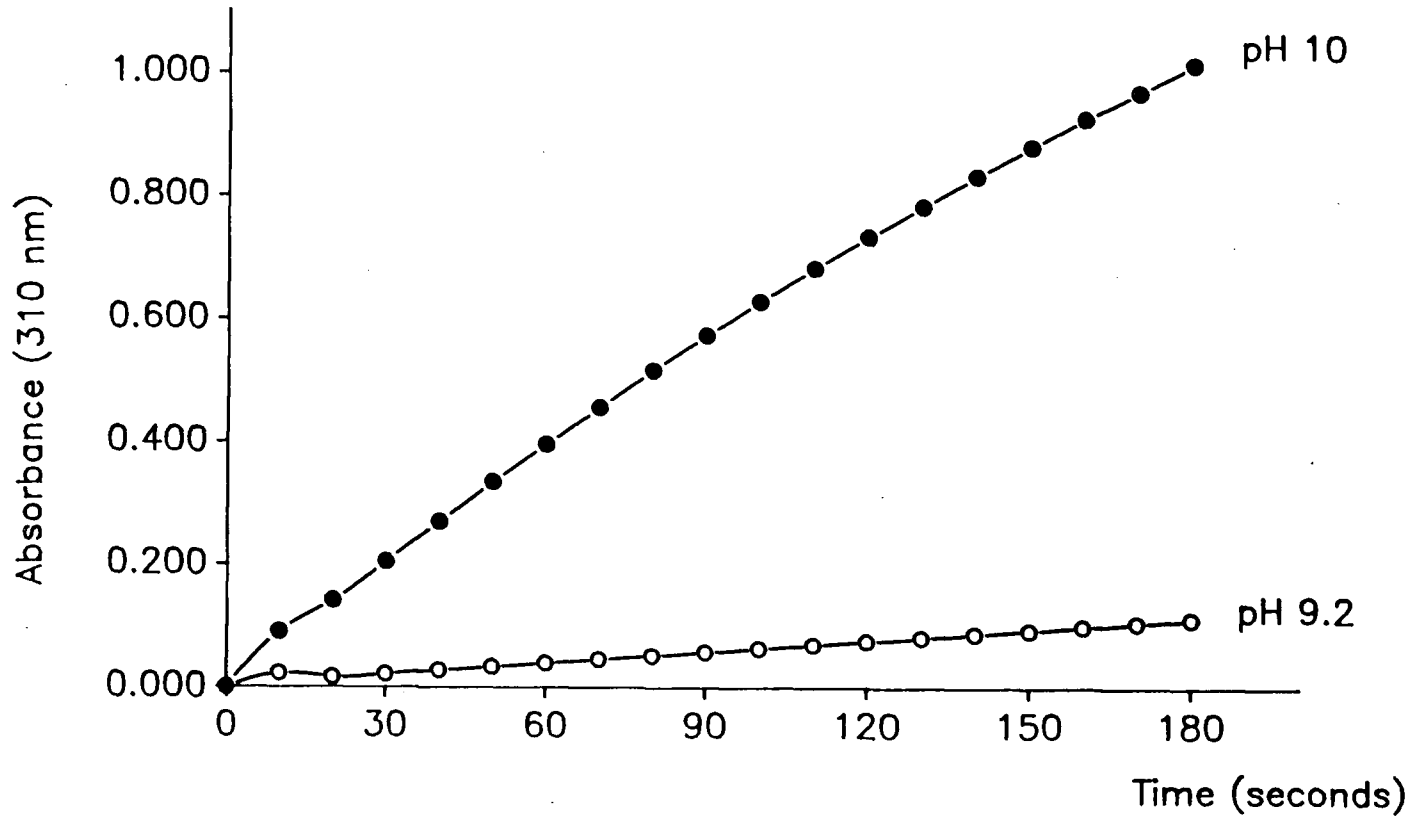

Figure 2.34 The oxidation of veratryl alcohol (1×10^{-5} mole) by TDCSPPMnCl (3×10^{-8} mole) and H_2O_2 (5×10^{-6} mole) in 4 mL 0.1 M pH 10 buffer (phosphate) or pH 9.2 buffer (borate) at room temperature

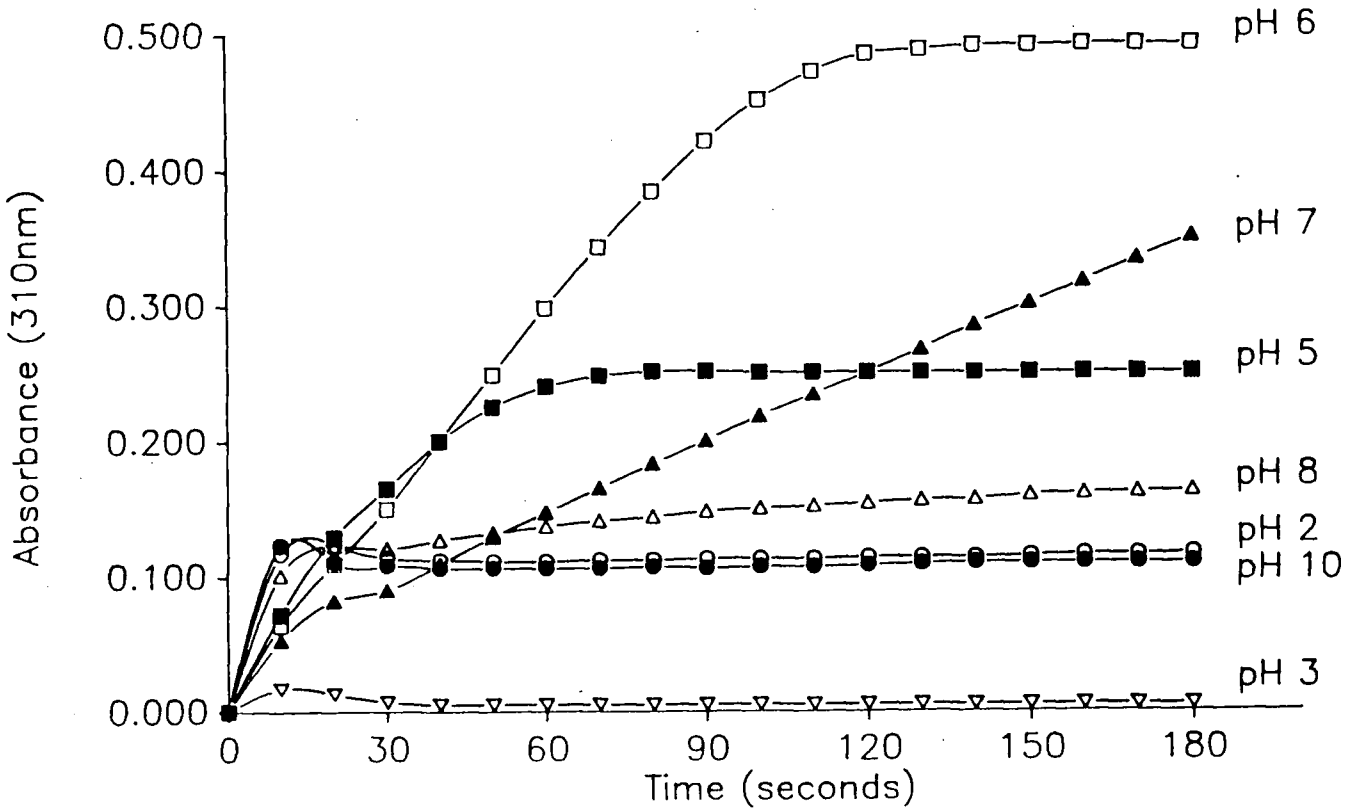

Figure 2.35 The oxidation of veratryl alcohol (1×10^{-5} mole) by TDCSPPMnCl (3×10^{-8} mole) and NaClO (5×10^{-6} mole) at room temperature in 4 mL aqueous buffer of various pH values, pH 5 and 6 buffers are 0.1 M citrate and all others are 0.1 M phosphate.

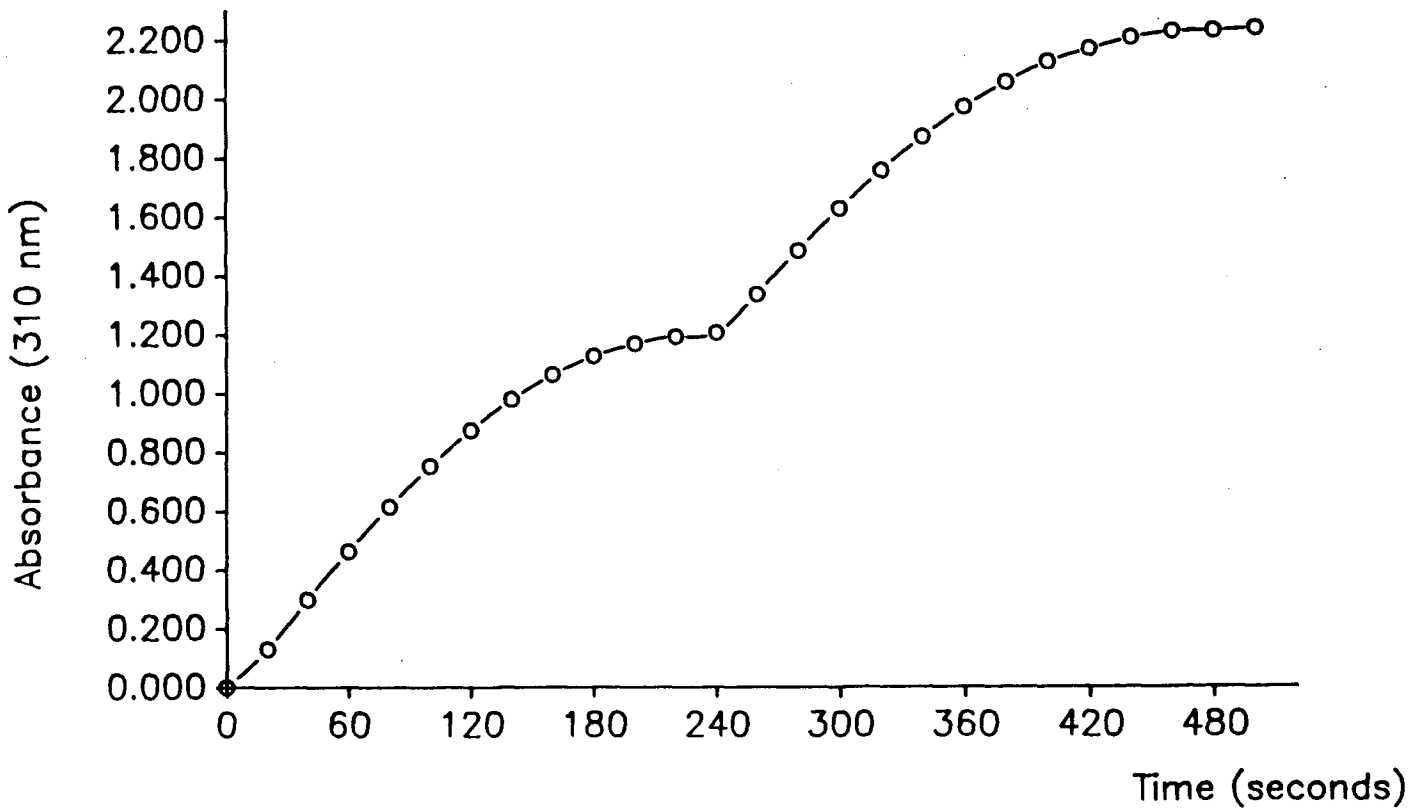

Figure 2.36 The oxidation of veratryl alcohol (5×10^{-6} mole) by TDCSPPMnCl (1×10^{-8} mole) and *m*CPBA in 4 mL 0.1 M pH 5 citrate buffer at room temperature, *m*CPBA (2×10^{-6} mole) added at time = 0 and time = 240 seconds

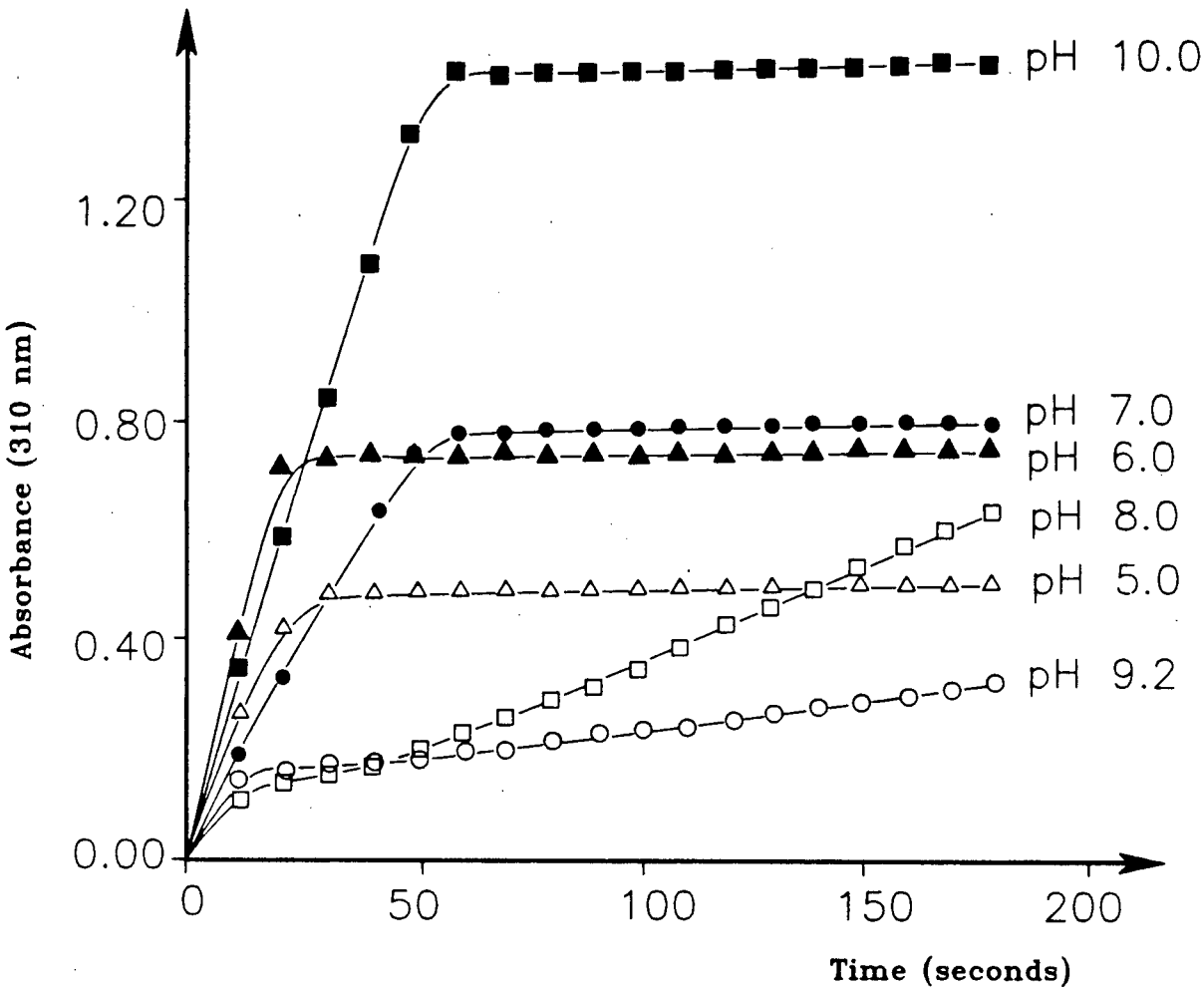

Figure 2.37 The oxidation of veratryl alcohol (1×10^{-5} mole) by $Cl_{16}TSPPMnCl$ (3×10^{-8} mole) and NaClO (5×10^{-6} mole) at room temperature in 4 mL aqueous buffer of various pH values, pH 5 and 6 buffers are 0.1 M citrate, pH 7, 8, and 10 buffers are 0.1 M phosphate, and pH 9.2 buffer is 0.1 M borate.

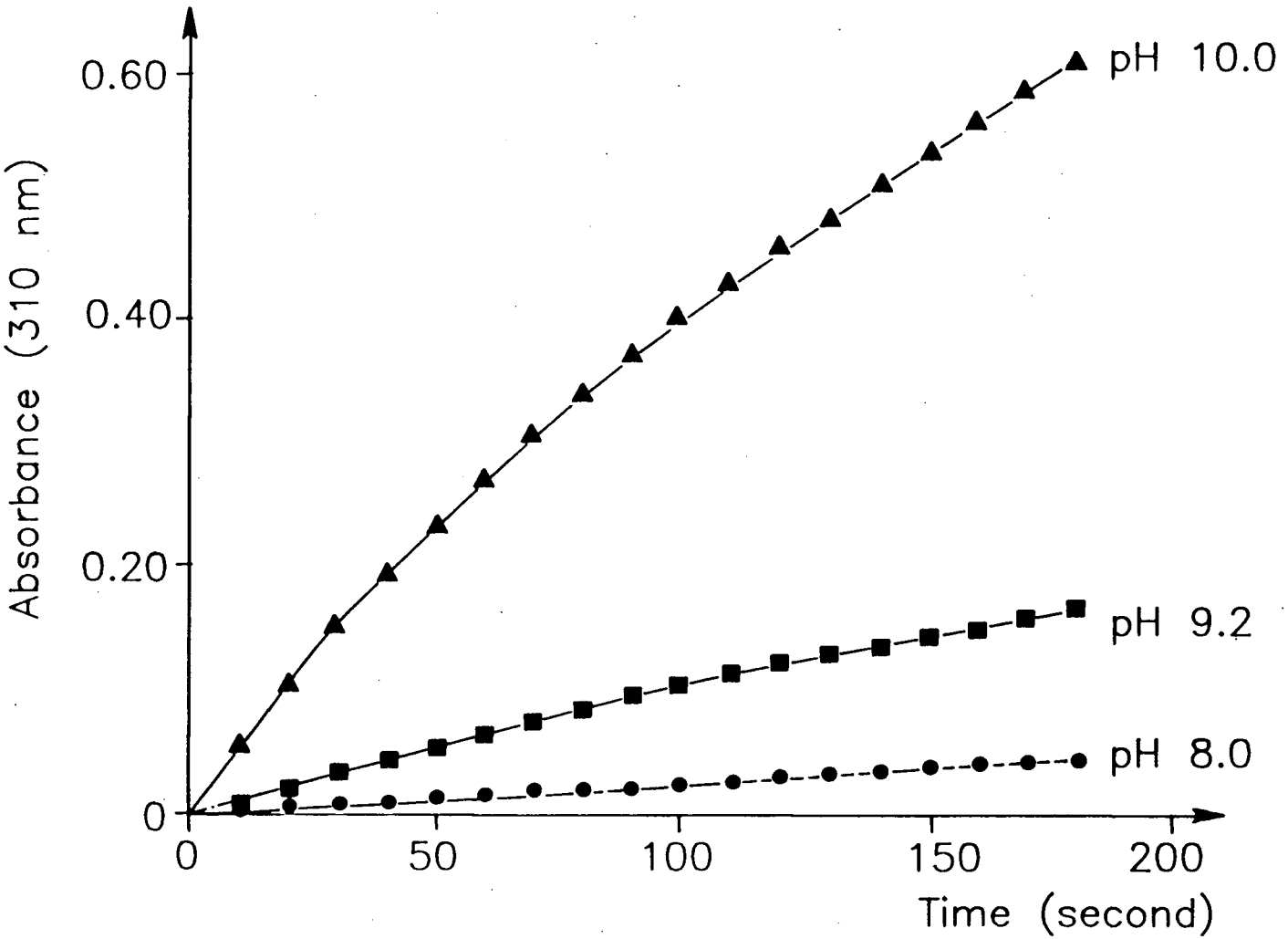

Figure 2.38 The oxidation of veratryl alcohol (1×10^{-5} mole) by $Cl_{16}TSPPMnCl$ (3×10^{-8} mole) and H_2O_2 (5×10^{-6} mole) in 4 mL 0.1 M pH 8 (phosphate), 9.2 (borate), and 10 (phosphate) buffer at room temperature

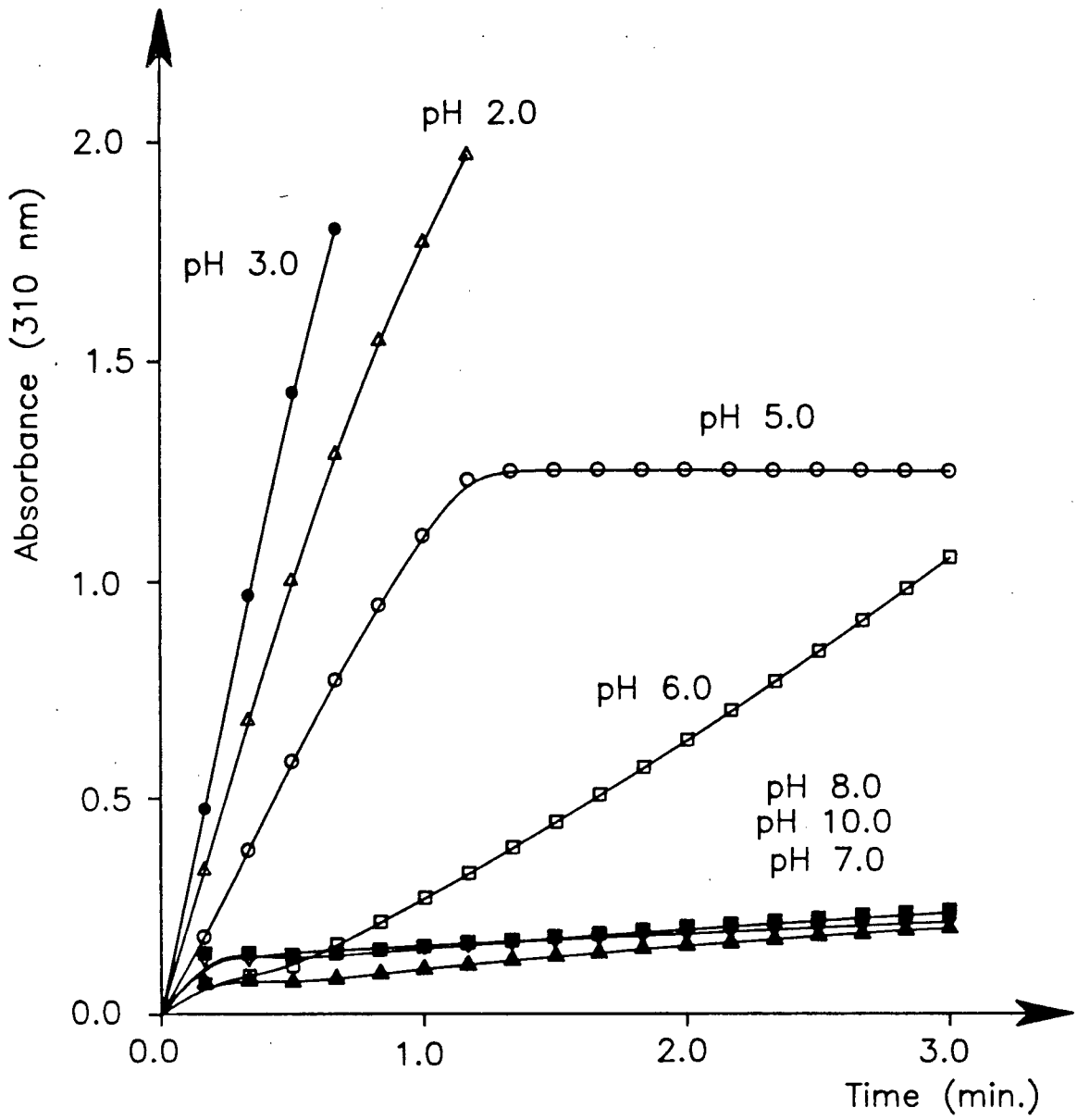

Figure 2.39 The oxidation of veratryl alcohol (5×10^{-6} mole) by Cl_{16}TSPPMnCl (1×10^{-8} mole) and *m*CPBA (2×10^{-6} mole) at room temperature in 4 mL aqueous buffer of various pH values, pH 5 and 6 buffers are 0.1 M citrate and all other buffers are 0.1 M phosphate.

manganese(II) porphyrin.

It has been shown that the oxidation of a metalloporphyrin by an oxidant was pH dependent. The rate of oxidation of iron *meso*-tetra(2,6-dimethyl-3-sulfonatophenyl)porphyrin (**24**) by hydrogen peroxide in aqueous buffer increases with increasing pH[25] (pH 1-12). The oxidation of manganese *meso*-tetra(2,6-dimethyl-3-sulfonatophenyl)porphyrin (**25**) by hydrogen peroxide was also studied[26] and the reaction rate increased with increasing pH in the pH range from 7.6 to 12.1.

The rate of the oxidation of veratryl alcohol depends on two reactions:

$$\text{MPor} + \text{oxidant} \rightarrow (\text{MPor})_{\text{oxidized}} \quad (1)$$

$$(\text{MPor})_{\text{oxidized}} + \text{veratryl alcohol} \rightarrow \text{MPor} + \text{veratraldehyde} \quad (2)$$

where MPor represents metalloporphyrin and $(\text{MPor})_{\text{oxidized}}$ is its oxidized intermediate. The rate of reaction (1) is a complex function of pH and it increases with increasing pH.[25,26] The fact that the oxidized intermediates of the iron and manganese porphyrins were observed by UV-vis spectroscopy at high pH but not at low pH in the presence of a large excess of veratryl alcohol, indicates that the rate of reaction (2) increases with decreasing pH. The optimum pH for the overall reaction will be determined by the kinetics of both reactions within the pH range of the study.

The optimal pH at which the metalloporphyrins showed maximal catalytic activity for veratryl alcohol oxidation is summarized in Table 2.1. The oxidation of veratryl alcohol by Cl_{16}TSPPMnCl/H_2O_2, Cl_{16}TSPPMnCl/t-BuOOH, TDCSPPMnCl/H_2O_2, or TDCSPPMnCl/t-BuOOH showed maximum rate at the highest pH used (pH 10), probably because reaction (1) was the rate limiting step in these systems.

Table 2.1 Optimum pH for the oxidation of veratryl alcohol by various metalloporphyrin/oxidant combinations at room temperature

Metalloporphyrin	Oxidant	Optimal pH
Cl_{16}TSPPMnCl	mCPBA	3
Cl_{16}TSPPFeCl	mCPBA	2
TDCSPPMnCl	mCPBA	3
TDCSPPFeCl	mCPBA	2
TDCSPPMnCl	NaClO	6
TDCSPPFeCl	NaClO	7
Cl_{16}TSPPFeCl	t-BuOOH	5
TDCSPPFeCl	t-BuOOH	6
Cl_{16}TSPPMnCl	t-BuOOH	10
TDCSPPMnCl	t-BuOOH	10
Cl_{16}TSPPMnCl	NaClO	10
Cl_{16}TSPPFeCl	NaClO	10
TDCSPPFeCl	H_2O_2	2
TDCSPPMnCl	H_2O_2	10
Cl_{16}TSPPMnCl	H_2O_2	10

TDCSPPMnCl and Cl_{16}TSPPMnCl have higher redox potentials than their corresponding iron porphyrins,[26] t-BuOOH and H_2O_2 are weaker oxygen donors than *m*CPBA. Both factors are responsible for a slow reaction (1).

Iron and manganese porphyrins can mimic the functions of peroxidases as well as catalases at the same time. As a peroxidase model, the two-electron oxidized metalloporphyrin oxidizes substrates by one-electron oxidation. The two-electron oxidized metalloporphyrin can also oxidize H_2O_2 to give O_2 and H_2O and thus function as a catalase. It was reported[25] that the oxidation of hydrogen peroxide to oxygen by iron porphyrin **24** competed with its peroxidase like reaction and the former reaction was favoured with increasing pH. For the manganese porphyrin **25**, just the opposite was true.[26] The peroxidase activity of **25** was higher at higher pH and its catalase activity was higher at lower pH. It is, therefore, not surprising to find that TDCSPPFeCl showed its maximal activity under acidic condition (pH 2) for veratryl alcohol oxidation by H_2O_2. TDCSPPFeCl decomposed H_2O_2 more rapidly at higher pH and had little peroxidase activity, veratryl alcohol was therefore oxidized slowly and inefficiently at high pH. Better stability of the catalyst at low pH (Fig. 2.1, 2.2) was probably also a factor.

All the reactions using *m*CPBA as oxidant are favoured at low pH. *m*CPBA is a good single oxygen donor and the oxidation of metalloporphyrins is probably reasonably fast at all pH. Reaction (2) is probably the rate limiting step when using *m*CPBA as oxidant and the overall reaction is faster at lower pH. The optimal pH for the oxidation of veratryl alcohol by Cl_{16}TSPPFeCl/t-BuOOH and TDCSPPFeCl/t-BuOOH was pH 5 and pH 6, respectively. Kinetic data for both reaction (1) and (2) are needed to give a detailed explanation of these observations.

It is obvious by examining Table 2.1 that when using the same oxidant, it is

normally true that a manganese porphyrin has a higher optimal pH than its corresponding iron porphyrin (TDCSPPMnCl compared to TDCSPPFeCl and Cl_{16}TSPPMnCl compared to Cl_{16}TSPPFeCl) and a hexadecachloroporphyrin complex has the same or higher optimal pH compared to its corresponding octachloroporphyrin complex (Cl_{16}TSPPFeCl over TDCSPPFeCl and Cl_{16}TSPPMnCl over TDCSPPMnCl). This can be explained as follows. A metalloporphyrin is oxidized more readily at higher pH since its oxidation potential decreases with increasing pH[2,25] and it is known that a manganese porphyrin has a higher oxidation potential than its iron anolog[26] and a hexadecachloroporphyrin complex (Cl_{16}TSPPFeCl or Cl_{16}TSPPMnCl) is more electron deficient than a octachloroporphyrin complex (TDCSPPFeCl or TDCSPPMnCl).[27] A higher pH will facilitate the oxidation of the metalloporphyrins with higher oxidation potentials.

2.1.3.2 Oxidant

Hydrogen peroxide, t-BuOOH, *m*CPBA, and NaClO have all been used as oxidants to oxidize various metalloporphyrins. The two-electron oxidation of metalloporphyrins by acyl- or alkylhydroperoxides (ROOH, R=acyl, alkyl, or H) involves the heterolytic O-O bond scission and the reaction is therefore accelerated by decreased electron density of R. In other words, the reaction of a metalloporphyrin and ROOH is facilitated by a decrease in the pKa value of ROH.[28-33] Among the peroxide type of oxidants used in this study, *m*CPBA should give the fastest reaction since the pKa order is *m*CBA < H_2O < t-BuOH.

It was observed that under the same conditions, the oxidation of veratryl alcohol by *m*CPBA was faster than that by t-BuOOH and H_2O_2 when the iron porphyrins (TDCSPPFeCl, Cl_{16}TSPPFeCl) were the catalysts. This is also true at low pH when the

manganese porphyrins (TDCSPPMnCl, Cl_{16}TSPPMnCl) were used as catalysts. For TDCSPPMnCl or Cl_{16}TSPPMnCl catalyzed oxidation of veratryl alcohol at high pH (>8), however, the rate of reaction is much faster with hydrogen peroxide than with *m*CPBA. This is probably because the manganese porphyrins were oxidized by *m*CPBA and hydrogen peroxide through different pathways. The oxidation of TDCSPPMnCl and Cl_{16}TSPPMnCl by hydrogen peroxide may involve homolylic cleavage[34,35] of the O-O bond of hydrogen peroxide.

The oxidation of veratryl alcohol by t-BuOOH was efficient only when the iron porphyrins, TDCSPPFeCl and Cl_{16}TSPPFeCl, were used as catalysts. TDCSPPMnCl or Cl_{16}TSPPMnCl was unable to oxidize veratryl alcohol using t-BuOOH as oxidant.

Hydrogen peroxide caused a rapid destruction of Cl_{16}TSPPFeCl and therefore was not a suitable oxidant for this catalyst. The oxidation of veratryl alcohol by hydrogen peroxide was favoured at low pH when TDCSPPFeCl was the catalyst. When the manganese porphyrins TDCSPPMnCl or Cl_{16}TSPPMnCl were the catalysts, however, the reaction was much faster at high pH as shown in Figure 2.34 and Figure 2.38. Hydrogen peroxide is a cheap, clean oxidant and would be the first choice if biomimetic catalysts are to be used in industry. The manganese porphyrins TDCSPPMnCl and Cl_{16}TSPPMnCl seem to be better catalysts than the iron porphyrins for using hydrogen peroxide as oxidant. The optimal pH of these reactions, unfortunately, is high and as described above, the oxidant is not used efficiently at high pH due to the formation of superoxide. The optimal pH of lignin peroxidase is around pH 3[36] (varies for different isoenzymes). These manganese porphyrin/hydrogen peroxide systems may not mimic the lignin peroxidase at high pH (pH 10). On the other hand, effective degradation of lignin by lignin peroxidase at pH 3 has not been reported and the pH dependency of lignin degradation and pulp bleaching by lignin peroxidase or

biomimetic catalysts has not been studied, pH 3 is not necessarily the best pH for lignin oxidation or pulp bleaching. The manganese porphyrin/hydrogen peroxide systems, therefore, may have an advantage by working at high pH where the lignin peroxidase had no activity.

The metalloporphyrins can also use NaClO as oxidant for the oxidation of veratryl alcohol. The optimal pH for the reaction was pH 10 when the hexadecachloroporphyrin complexes (Cl_{16}TSPPMnCl, Cl_{16}TSPPFeCl) were the catalysts. The reaction was favoured at around neutral pH when the octachloroporphyrin complexes (TDCSPPFeCl, TDCSPPMnCl) were the catalysts. Sodium hypochlorite is also a possible oxidant suitable for industrial applications. It is important to find out if this oxidant will lead to the formation of any chlorinated organic compounds when used in the pulp and paper industry, since elimination of chlorinated pollutants is the major goal of using biotechnology in the pulp and paper industry.

2.1.3.3 The presence of manganese complexes

As discussed earlier, superoxide is formed in the oxidation of veratryl alcohol. Under acidic conditions, superoxide dismutates rapidly giving oxygen and hydrogen peroxide and the reaction can be facilitated by the formation of additional hydrogen peroxide. At high pH, however, superoxide is relatively stable and reacts with the metalloporphyrin which decreases its catalytic activity as shown in Scheme 2.3 using Cl_{16}TSPPMnCl as an example. In the presence of superoxide, reaction B competes with reaction A for the manganese(III) porphyrin catalyst and the former reaction leads to the formation of the catalytically inactive species Cl_{16}TSPPMn(II). Though the inactive manganese(II) porphyrin can be converted back to the manganese(III) porphyrin

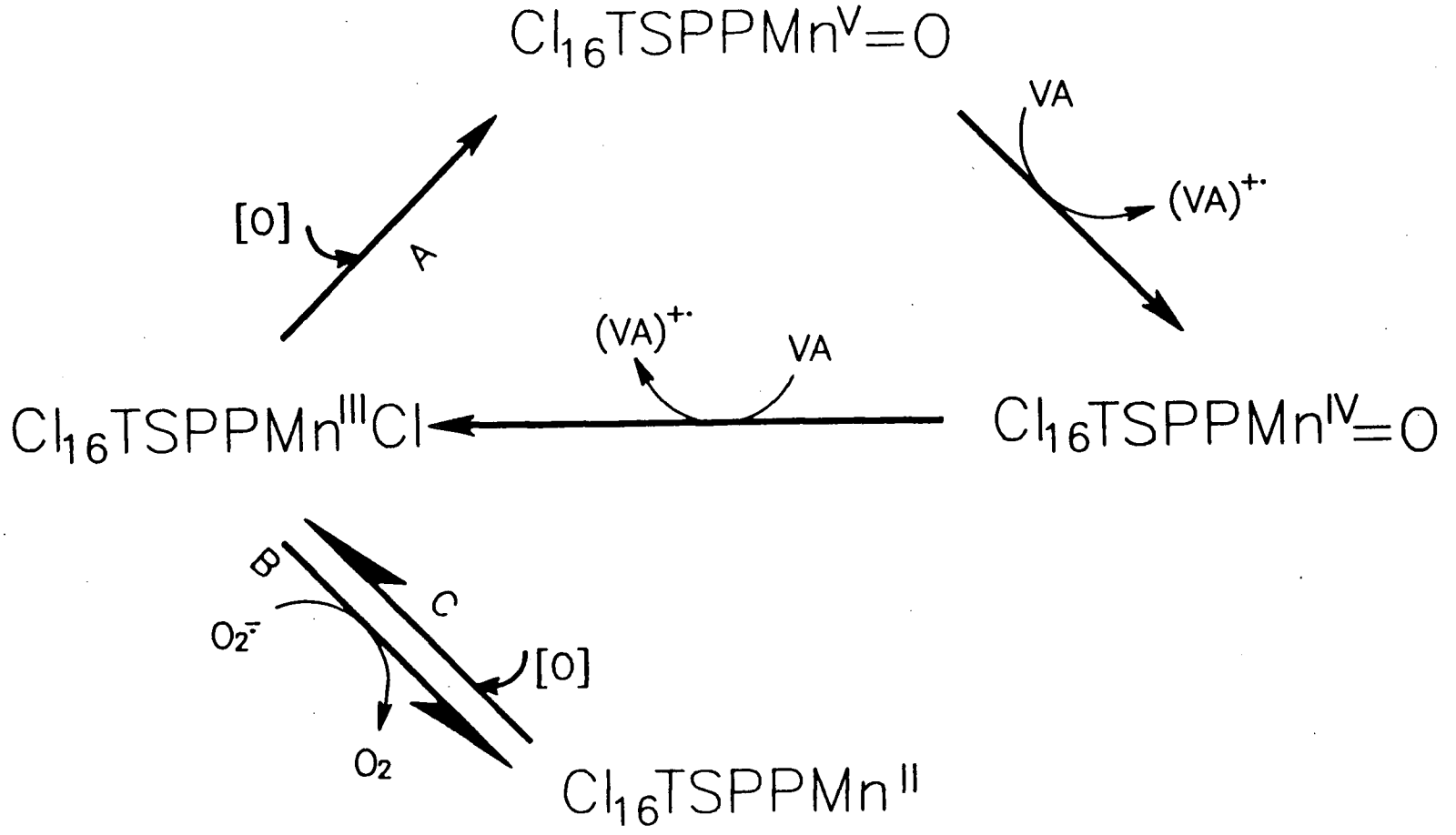

Scheme 2.3 The effect of superoxide on the catalytic cycle of Cl_{16}TSPPMnCl during the oxidation of veratryl alcohol, VA: veratryl alcohol; $(VA)^{+\cdot}$: veratryl alcohol cation radical; [O]: oxidant

(reaction pathway C), oxidant is required for this process and this reaction thus competes with the catalytic reaction pathway A for oxidant. Both the rate and yield of the oxidation of veratryl alcohol is decreased due to the formation of superoxide.

Manganese(II) complexes have been used as models for superoxide dismutase.[21,22] The presence of manganese(II)-lactate increased the activity of both lignin peroxidase and the manganese(II)-dependent peroxidase.[18] It was expected that the presence of manganese(II)-complexes could also facilitate the oxidation of veratryl alcohol by metalloporphyrins at high pH. Manganese(II)-lactate which was found to be able to stimulate the activity of the manganese(II)-dependent peroxidase was used as the manganese(II)-complex in this study. Since the mixture of manganese(II) sulfate and lactic acid (0.1 mM and 6 mM concentration, respectively) was not stable at high pH due to the formation of manganese(II) hydroxide, the effect of manganese(II)-lactate on the oxidation of veratryl alcohol was examined only at pH 5 and pH 6.

As shown in Figures 2.40 and 2.41, the presence of manganese(II)-lactate increased the rate of oxidation of veratryl alcohol by TDCSPPFeCl/*m*CPBA or Cl_{16}TSPPMnCl/*m*CPBA. It was noticed that in the presence of manganese(II)-lactate, the absorption at 310 nm (λ_{max} of veratraldehyde) started decreasing after reaching a maximum. This was due to the interference of manganese(III)-lactate, which also absorbed at 310 nm. Manganese(III)-lactate decomposed slowly in aqueous solution. The stable absorbance at 310 nm 24 hours after the reaction was still higher than that of the control experiment without manganese(II)-lactate, indicating that the yield of veratraldehyde was indeed increased by the presence of manganese(II)-complexes. The observation that manganese(III)-lactate was formed and accumulated during the reaction also suggested that manganese(II)-lactate was not a good model for superoxide dismutase in this case. Manganese(II) complexes can also be oxidized by high valent

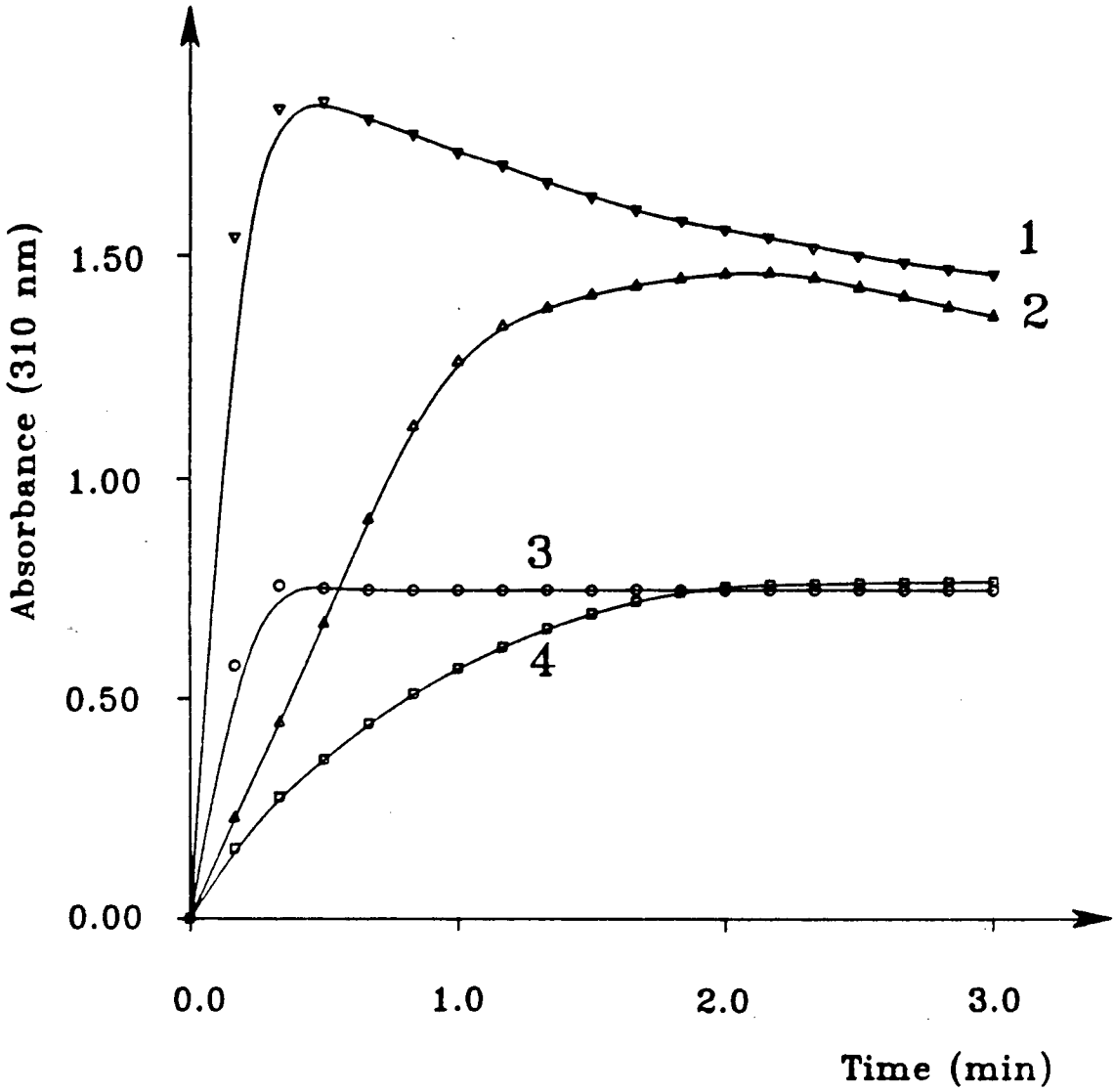

Figure 2.40 The effect of manganese(II)-lactate (4×10^{-9} mole and 2.4×10^{-7} mole, respectively) on the oxidation of veratryl alcohol (5×10^{-6} mole) by TDCSPPFeCl (1×10^{-8} mole) and *m*CPBA (2×10^{-6} mole) at room temperature in 3 mL 0.1 M citrate buffer, 1, pH 5 in the presence of Mn^{2+}; 2, pH 6 in the presence of Mn^{2+}; 3, pH 5 in the absence of Mn^{2+}; 4, pH 6 in the absence of Mn^{2+}

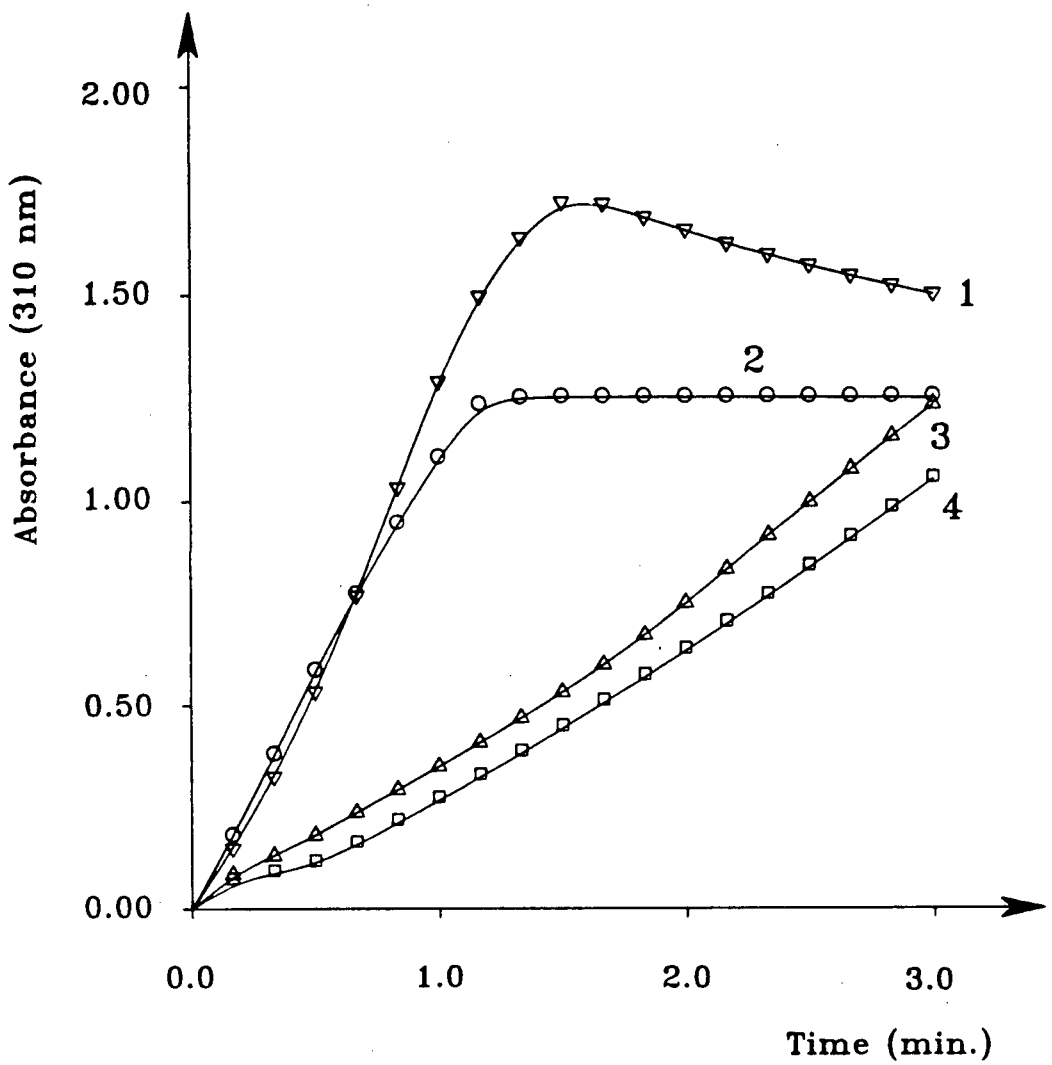

Figure 2.41 The effect of manganese(II)-lactate (4×10^{-9} mole and 2.4×10^{-7} mole, respectively) on the oxidation of veratryl alcohol (5×10^{-6} mole) by Cl_{16}TSPPMnCl (1×10^{-8} mole) and *m*CPBA (2×10^{-6} mole) at room temperature in 3 mL 0.1 M citrate buffer, 1, pH 5 in the presence of Mn^{2+}; 2, pH 5 in the absence of Mn^{2+}; 3, pH 6 in the presence of Mn^{2+}; 4, pH 6 in the absence of Mn^{2+}

metalloporphyrins to manganese(III) complexes in addition to their reaction with superoxide. The manganese(II)-lactate, therefore, competed with the veratryl alcohol substrate for the high valent metalloporphyrins. This side reaction, however, might be minimized by using a ligand other than lactate or by changing the concentration of Mn(II). No effort was made to search for a better superoxide dismutase model than manganese(II)-lactate.

It should be added that the formation and accumulation of manganese(III)-lactate is not necessarily a disadvantage to the system. The manganese(II)-dependent peroxidase uses manganese(II) complexes as mediators for the oxidation of its substrates. Although manganese(III) complexes such as Mn(III)-lactate are unable to oxidize veratryl alcohol, they can oxidize MnP substrates such as polymer dyes and phenolic compounds. Non-phenolic lignin model compounds can also be oxidized under certain conditions.[37] Further study is needed to understand the role of manganese(II) and MnP in the biodegradation of lignin.

2.1.3.4 The effect of imidazole

Peroxidases, including lignin peroxidase[38,39] and Mn(II)-dependent peroxidase[40], have an iron protoporphyrin IX with a proximal-bound imidazole group of histidine at their active sites. Imidazole has been used to facilitate metalloporphyrin catalyzed reactions.[41,42] The coordination of imidazole to the metal increases its electron density and thus aids the heterolytic O-O cleavage of bound peroxides. The epoxidation of alkenes in organic solvents by *meso*-tetraphenylporphyrin iron chloride (TPPFeCl) or *meso*-tetraphenylporphyrin manganese chloride (TPPMnCl) using either hydrogen peroxide or alkyl hydrogen peroxides as oxidant was successful only in the presence of

imidazole.[41,42] It has been reported that manganese porphyrins ligate only one imidazole per molecule[43] and in methylene chloride the rate of oxidation of TPPMnCl by alkyl hydroperoxides or percarboxylic acids was increased by 10^3-10^4 fold in the presence of imidazole.[30] In aqueous solution, however, the rate of the oxidation of manganese porphyrin **25** by hydrogen peroxide was increased by only about 10 fold by adding imidazole to the reaction mixture.[26] Metalloporphyrins with attached imidazole groups have also been used as peroxidase models.[33,44] While coordination of one imidazole group to an iron porphyrin increased its oxidation rate, attaching an additional imidazole group to the porphyrin inhibited its oxidation.[44]

The oxidation of veratryl alcohol (1×10^{-5} mole) in the presence of imidazole (0-6×10^{-6} mole) by various metalloporphyrin (TDCSPPFeCl, Cl_{16}TSPPFeCl, TDCSPPMnCl, or Cl_{16}TSPPMnCl, 3×10^{-8} mole) and oxidant (*m*CPBA, NaClO, H_2O_2, or t-BuOOH, 5×10^{-6} mole) combinations were studied. The presence of imidazole had very little effect on the rate of veratryl alcohol oxidation in most cases and the reactions were even inhibited by the presence of a large excess of imidazole. The only example where reasonable acceleration was observed was the oxidation of veratryl alcohol by Cl_{16}TSPPMnCl and H_2O_2 as shown in Figures 2.42 and 2.43. The very small stimulating effect of imidazole is probably due to the use of aqueous solution and the fact that one to one coordination of imidazole to the metalloporphyrin is difficult to achieve.[26,30]

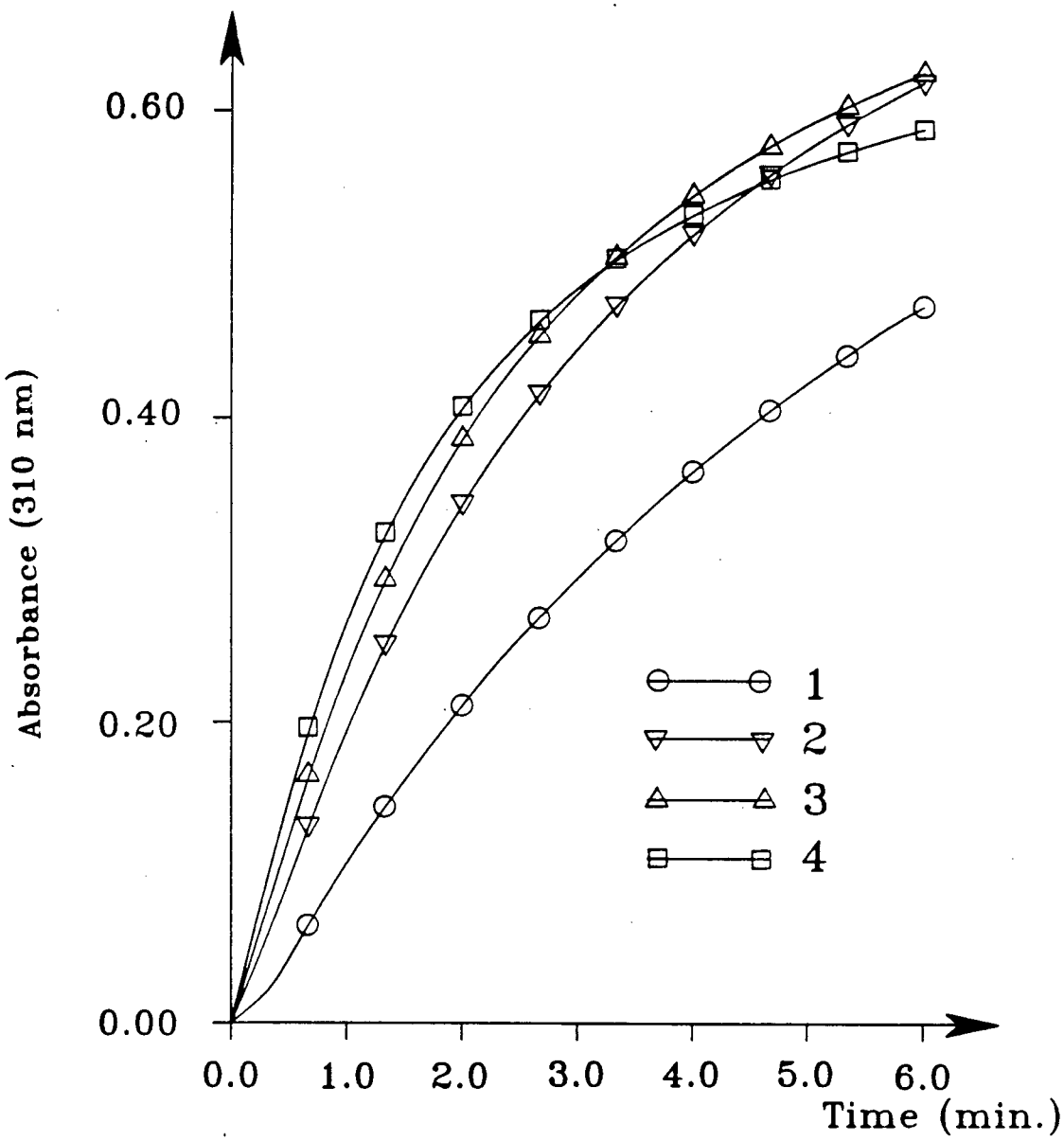

Figure 2.42 The effect of imidazole on the oxidation of veratryl alcohol (1×10^{-5} mole) by hydrogen peroxide (5×10^{-6} mole) and $Cl_{16}TSPPMnCl$ (3×10^{-8} mole) at room temperature in 3 mL 0.1 M pH 9.2 borate buffer, the amount of imidazole (mole): 1, 0; 2, 1.5×10^{-6}; 3, 3×10^{-6}; 4, 6×10^{-6}

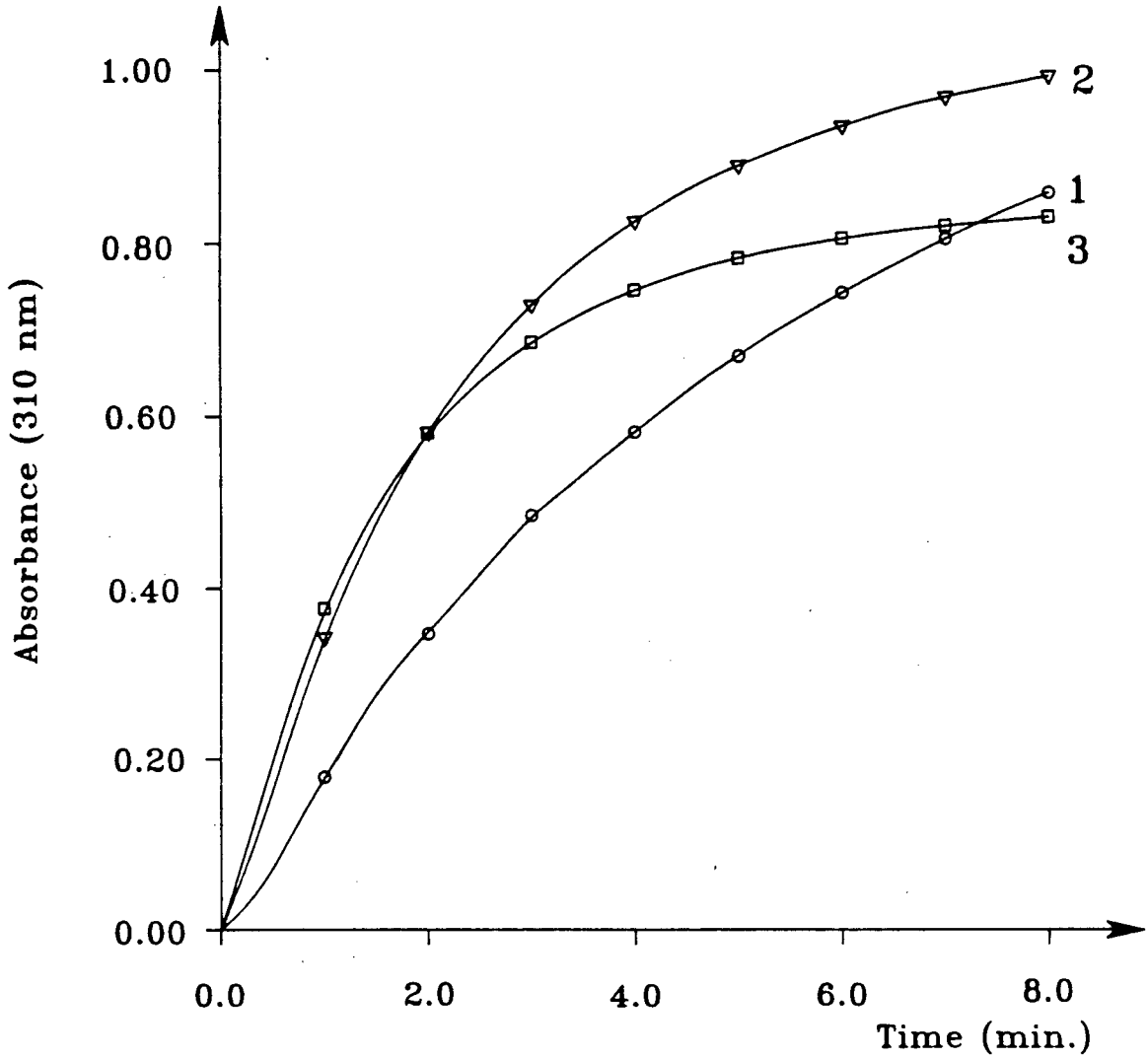

Figure 2.43 The effect of imidazole on the oxidation of veratryl alcohol (1×10^{-5} mole) by hydrogen peroxide (5×10^{-6} mole) and $Cl_{16}TSPPMnCl$ (3×10^{-8} mole) at room temperature in 3 mL 0.1 M pH 10 phosphate buffer, the amount of imidazole (mole): 1, 0; 2, 3×10^{-6}; 3, 6×10^{-6}

2.2 Conclusion

The stability of the metal complexes of TPP derivatives towards excess oxidants is dramatically increased by introducing chlorine at the phenyl ring and ß-positions. The relative and absolute stability of the metalloporphyrins also depends on pH, the type of oxidant being used, and the presence or absence of substrates.

Two oxidized intermediates, probably oxomanganese(IV) and oxomanganese(V) porphyrins, were observed spectrally when TDCSPPMnCl or Cl_{16}TSPPMnCl were oxidized. Only one oxidized intermediate of the iron porphyrins (TDCSPPFeCl or Cl_{16}TSPPFeCl) was observed and its nature is not clear. Cl_{16}TSPPMn(II) and Cl_{16}TSPPFe(III)-O_2^-, probably formed by the reaction of the metal(III) porphyrin and superoxide, were observed in the oxidation of the respective metalloporphyrin in the presence of veratryl alcohol.

The catalytic activity of the metalloporphyrins for the oxidation of veratryl alcohol depends on the oxidant being used, the pH of the solvent, and to a lesser extent, on the presence of manganese(II)-complexes and imidazole. The largest catalytic activity for the metalloporphyrins was observed at low pH using *m*CPBA as oxidant. At high pH (pH 10), TDCSPPMnCl exhibits the largest catalytic activity using hydrogen peroxide as oxidant. The optimal pH for maximal catalysis of a metalloporphyrin/oxidant combination depends on both the type of catalyst and oxidant. TDCSPPMnCl and Cl_{16}TSPPMnCl usually have a higher optimal pH than their corresponding iron porphyrins (TDCSPPFeCl and Cl_{16}TSPPFeCl) and the octachloroporphyrins (TDCSPPFeCl and TDCSPPMnCl) usually have a lower optimal pH than their corresponding hexadecachloroporphyrins (Cl_{16}TSPPFeCl and Cl_{16}TSPPMnCl) when using the same oxidant.

The oxidation of veratryl alcohol is stimulated by increasing buffer concentration or by adding some inorganic salts, supporting a cation radical mechanism of the reaction. The presence of high concentrations of sodium fluoride or sodium nitrate, however, was found to inhibit the reaction completely.

Oxidized intermediates of iron and manganese porphyrins have been observed when they are oxidized at low temperature in organic solvents.[3-10] The observation of oxidized intermediates of TDCSPPMnCl and Cl_{16}TSPPMnCl by UV-vis spectroscopy at room temperature is interesting and needs further study. Techniques such as ESR, NMR, IR, Resonance Raman spectroscopy and magnetic measurements are needed to characterize these intermediates. Only one oxidized intermediate of TDCSPPFeCl and Cl_{16}TSPPFeCl was observed, the use of stop-flow apparatus may enable the detection of the second oxidized intermediate. The formation of $Cl_{16}TSPPFe^{II}$-O_2 at room temperature indicates that it is stable and might be a good model for haemoglobin.

2.3 Experimental

2.3.1 General

Equipment. A Hewlett Packard 8452A Diode Array UV-vis spectrophotometer was used for all the UV-vis spectroscopic measurements. A HP 5890A Gas Chromatograph equipped with a HP 17 capillary column (25 meters, 0.32 millimetre ID) and a FID (flame ionization detector) detector was used for all the GC analyses.

Chemicals. Veratryl alcohol, purchased from Aldrich, was vacuum distilled before use. Purified grade *m*CPBA from Fisher Scientific Company was used in this experiment. Mixed strong acidic/strong basic ion exchange resin Amberlite MB-3 and

strong acidic ion exchange resin Amberlite IR-120 were purchased from Mallinckrodt Corporation. Strong basic ion exchange resin Rexyn® was from Fisher Scientific Company. All the ion exchange resins were washed with 5 volumes of deionized water on the column before use. Other chemicals were of reagent grade and used without further purification.

The phosphate buffers were made from appropriate amounts of phosphoric acid, KH_2PO_4, K_2HPO_4, and/or K_3PO_4 depending on the pH of the respective buffer. The final pH of the buffers were adjusted to the desired value using dilute NaOH or H_3PO_4. Citric acid was neutralized with sodium hydroxide solution to the desired pH (pH 5 or 6) and then diluted with deionized water to give a final concentration of 0.1 M. Borate buffer (pH 9.2) was made by diluting the commercially available powder from Fisher Scientific Company.

All the metalloporphyrins were synthesized following a modified procedure of Nakano *et al.*[45] *Meso*-tetra(2,6-dichlorophenyl)porphyrin and *meso*-tetra(2,6-dichlorophenyl)-ß-octachloroporphyrin, provided by Dr. Tilak Wijesekera of this laboratory were first sulfonated using fuming sulfuric acid to give *meso*-tetra(2,6-dichloro-3-sulfonatophenyl)porphyrin and *meso*-tetra(2,6-dichloro-3-sulfonatophenyl)-ß-octachloroporphyrin, respectively. The sulfonated porphyrins were then metallated in DMF to give the metalloporphyrins **12-15**.

Meso-tetra(2,6-dichlorophenyl)porphyrin (300 mg) was suspended in 14 mL of fuming sulfuric acid and heated with stirring at 165 °C for 7 hours. The reaction mixture was then cooled, added slowly to 50 mL ice cooled water, and filtered. The filtrate was further diluted with 75 mL of water and neutralized with $NaHCO_3$ (65 gram in 100 mL water). Ethanol (250 mL) was added to the solution to precipitate the sodium sulfate, which was removed by filtration. Sodium sulfate was precipitated once

more by adding 500 mL ethanol to the clear filtrate. The solution containing the product, sodium sulfate, and possibly small amount of sodium bicarbonate, was evaporated on a Rotavapor. The residue was dissolved in 10 mL deionized water and filtered. Remaining sodium bicarbonate in the filtrate was neutralized carefully with 10% HCl to neutral pH. The solution was passed slowly through a glass column (3×30 cm) packed with mixed strong acidic and strong basic ion exchange resin (Amberlite MB-3, Mallinckrodt Inc.). The eluent was dried to give a fine black microcrystalline solid.

Meso-tetra(2,6-dichlorophenyl)-ß-octachloroporphyrin was sulfonated similarly. The sulfonated porphyrins were metallated following reported procedures.[45] The purification of the metalloporphyrins[45] was considered inappropriate. The procedure was modified by using ion exchange resins. The crude product obtained via precipitation using acetone was found difficult to dissolve in water due to the presence of iron oxides. Dilute HCl was added to completely dissolve the residue in 10 mL of deionized water. The solution was then passed through a 3×30 cm ion exchange resin (strong acidic resin, Amberlite IR-120) column to remove all the free iron in the solution. Evaporating the eluent gave a fine black/blue microcrystalline powder.

Ferric ions were found to be retained efficiently on the column and the metalloporphyrin was therefore uncontaminated. After washing the column with saturated sodium chloride, addition of potassium thiocyanate to the yellow eluent gave a deep red color, indicating the presence of iron. When the metalloporphyrin solution after ion exchange was passed through a small column packed with fresh ion exchange resin, no iron was retained on the column.

The synthesis of TDCSPPFeOH. TDCSPPFeCl (10 mg) was dissolved in 1 mL of water and dilute sodium hydroxide was added until the iron porphyrin showed a

sharp single Soret band in its UV-vis spectrum. The solution was then passed through an ion exchange column (1.5×15 cm) packed with strong basic ion exchange resin (Rexyn® 201, Fisher Scientific Company). The eluent was evaporated on a Rotavapor.

2.3.2 The stability of the metalloporphyrins towards excess oxidants

The stability of the metalloporphyrins towards excess hydrogen peroxide at pH 3 in the presence of veratryl alcohol was determined as follows. Hydrogen peroxide (3×10^{-6} mole) was added to a solution (4 mL 0.1 M phosphate buffer, pH 3) containing the porphyrin (3×10^{-8} M) and veratryl alcohol (1×10^{-5} M) at room temperature. The Soret absorption changes of the metalloporphyrin with time were followed by UV-vis spectroscopy.

At pH 10, addition of hydrogen peroxide to the manganese porphyrins (TDCSPPMnCl, Cl_{16}TSPPMnCl) led to the formation of relatively stable oxidized intermediates. The extinction coefficients of these oxidized intermediates were not easy to determine and the quantification of the total concentration of the various porphyrin species was thus difficult. This problem was solved by reducing the various oxidation states of the manganese porphyrins to Mn(II) porphyrin by adding excess sodium borohydride (1 mg) immediately before the spectral measurement. The stability of the various metalloporphyrins was compared by plotting $(A_{Soret})_t/A_{Soret})_0$ against time t, where $(A_{Soret})_t$ is the Soret absorbance of the Mn(II) porphyrin produced by reducing the reaction mixture with excess $NaBH_4$ at time t, and $(A_{Soret})_0$ is the Soret absorbance of the Mn(II) porphyrin after treating the reaction mixture with $NaBH_4$ at time 0. Hydrogen peroxide (1.5×10^{-5} mole) was added to 20 mL 0.1 M pH 10 phosphate buffer containing 1.5×10^{-7} mole of TDCSPPMnCl (or Cl_{16}TSPPMnCl) and 5×10^{-5} mole of

veratryl alcohol. 3 mL of the reaction mixture was taken out at time 0, 2, 4, 6, 8 and 10 minutes, reduced with $NaBH_4$ (1 mg) and subject to UV-vis measurement. The stability of TDCSPPFeCl and Cl_{16}TSPPFeCl was determined similarly as for the experiments at pH 3.

The stability of TDCSPPFeCl towards excess *m*CPBA (or H_2O_2) at various pH in the absence of veratryl alcohol was also determined by UV-vis spectroscopy. *m*CPBA (3×10^{-7} mole dissolved in 10 μL acetonitrile) was added to a solution (3 mL 0.1 M phosphate buffer) containing 3×10^{-8} mole of TDCSPPFeCl and the change of the Soret absorption of TDCSPPFeCl with time was recorded. The results were plotted as $(A_{Soret})_t/(A_{Soret})_0$ against time t.

2.3.3 The oxidized intermediates of the metalloporphyrins

All the reactions were carried out at room temperature. The oxidation of the metalloporphyrins by various oxidants in the presence or absence of veratryl alcohol was carried out in a quartz UV-vis cell containing 3 mL solution. The metalloporphyrin (1 μmole/mL in water) and veratryl alcohol (1 M solution in water) were added. The oxidants were dissolved in appropriate solvents (*m*CPBA and t-BuOOH in acetonitrile, H_2O_2 and NaClO in water, 0.1 M in concentration) and added using a syringe. The reactions were followed by UV-vis spectroscopy.

The oxidation of Cl_{16}TSPPMn(II) by NaClO. When NaClO (1×10^{-7} mole) was added to a solution of Cl_{16}TSPPMn(II) generated by adding 2×10^{-5} mole of NaClO to a solution (3 mL 0.1 M phosphate buffer, pH 7) containing Cl_{16}TSPPMnCl (3×10^{-8} mole) and veratryl alcohol (1×10^{-5} mole), a small but very rapid decrease in the Soret band of the Mn(II) porphyrin was observed. The peak increased again in intensity afterwards.

Addition of 5×10^{-6} mole more NaClO converted the spectrum instantly to that of the Mn(III) porphyrin.

The oxidation of Cl_{16}TSPPMnCl by NaClO in the presence of manganese(II)-lactate. The reaction mixture contained in 3 mL 0.1 M citrate buffer (pH 5 or 6) 3×10^{-8} mole of Cl_{16}TSPPMnCl and 1×10^{-5} mole of veratryl alcohol. Manganese(II) sulphate and (L)-lactic acid were added to a final concentration of 1mM and 60mM, respectively. 2×10^{-5} mole of NaClO was added to start the reaction. The oxidation of Cl_{16}TSPPFeCl by NaClO in the presence of manganese(II)-lactate was carried out under similar conditions.

The oxidation of Cl_{16}TSPPFe(III)-O_2^- by NaClO was similar to the oxidation of Cl_{16}TSPPMn(II).

2.3.4 Factors affecting the catalytic activity of the metalloporphyrins

All the reactions were carried out at room temperature.

The oxidation of veratryl alcohol by mCPBA catalyzed by various metalloporphyrins. 2×10^{-6} mole of *m*CPBA dissolved in 20 μL acetonitrile was added to 4 mL solution (0.1 M phosphate or citrate buffer) containing 1×10^{-8} mole of metalloporphyrin and 5×10^{-6} mole of veratryl alcohol. The formation of veratraldehyde was followed by UV-vis spectroscopy at 310 nm.

The oxidation of veratryl alcohol by various metalloporphyrins using NaClO, t-BuOOH, or H_2O_2 as oxidants. The reaction mixture (4 mL 0.1 M phosphate, citrate or borate buffer) contained 3×10^{-8} mole of metalloporphyrin, 5×10^{-6} mole of oxidant and 1×10^{-5} mole of veratryl alcohol.

The oxidation of veratryl alcohol in the presence of manganese(II)-lactate

(Figures 2.40, 2.41). *m*CPBA (2×10^{-6} mole) was added to a solution containing 1×10^{-8} mole of metalloporphyrin (TDCSPPFeCl or Cl_{16}TSPPFeCl), 5×10^{-6} mole of veratryl alcohol, 4×10^{-9} mole of manganese(II) sulphate and 2.4×10^{-7} mole of lactic acid. The formation of veratraldehyde was followed by UV-vis spectroscopy at 310 nm.

The oxidation of veratryl alcohol in the presence of imidazole. The conditions for all the reactions were similar. A typical reaction mixture contained in 3 mL solvents 3×10^{-8} mole of metalloporphyrin, 5×10^{-6} mole of oxidant (H_2O_2 and NaClO were added as aqueous solution, t-BuOOH and *m*CPBA were added as acetonitrile solution), 1×10^{-5} mole of veratryl alcohol and various amounts of imidazole, ranging from 2 to 200 times excess (molar ratio, imidazole over metalloporphyrin), as specified in Figures 2.42 and 2.43. The formation of veratraldehyde was followed by UV-vis spectroscopy at 310 nm.

References for Chapter 2

1. T.G. Traylor, and S. Tsuchiya, Inorg. Chem. **26**, 1338, 1987.
2. N. Carnieri, A. Harriman, and G. Porter, J. Chem. Soc. Dalton Trans. 931, 1982.
3. J.T. Groves, R.T. Haushalter, M. Nakamura, T.E. Memo, and B.J. Evans, J. Am. Chem. Soc. **103**, 2884, 1981.
4. J.T. Groves, T.E. Memo, and R.S. Meyers, J. Am. Chem. Soc. **101**, 1032, 1979.
5. D. Chin, J. Del Gaudio, G.N. Lamar, and A.L. Balch, J. Am. Chem. Soc. **99**, 5486, 1977.
6. J.T. Groves, and Y. Watanabe, J. Am. Chem. Soc. **110**, 8443, 1988.
7. J.T. Groves, and M.K. Stern, J. Am. Chem. Soc. **110**, 8628, 1988.
8. J.T. Groves, and M.K. Stern, J. Am. Chem. Soc. **109**, 3812, 1987.
9. R.S. Czernuszewicz, Y.O. Su, M.K. Stern, K.A. Macor, D. Kim, J.T. Groves, and T.G. Spiro, J. Am. Chem. Soc. **110**, 4158, 1988.
10. M. Schappacher, and R. Weiss, Inorg. Chem. **26**, 1190, 1987.
11. B.C. Schardt, F.J. Hollander, and C.L. Hill, J. Chem. Soc., Chem. Commun. 765, 1981.
12. J.A. Smegal, and C.L. Hill, J. Am. Chem. Soc. **105**, 3515, 1983.
13. J.T. Groves, W.J. Kruper, and Jr. R.C. Hanshalter, J. Am. Chem. Soc. **102**, 6375, 1980.
14. J.T. Groves, and Y. Watanabe, Inorg. Chem. **25**, 4808, 1986.
15. J.T. Groves, Y. Watanabe, and T.J. McMurry, J. Am. Chem. Soc. **105**, 4489, 1983.

16. S.E. Creager, S.A. Raybuck, and R.W. Murray, J. Am. Chem. Soc. **108**, 4225, 1986.

17. N. Carnieri, A. Harriman, and G. Porter, J. Chem. Soc., Dalton Trans. 1231, 1982.

18. J.J. Bono, P. Goulas, N. Portet, and J.L. Seris, Collq INRA **40** (Lignin Enzymic Microb. Degrad.), 87, 1987.

19. J.S. Valentine, and A.E. Quinn, Inorg. Chem. **15**, 1997, 1976.

20. B.M. Hoffman, C.S. Weschler, and F. Basolo, J. Am. Chem. Soc. **98**, 5473, 1976.

21. B. Halliwell, NeuroToxicology, **5**, 113, 1984.

22. J. Epp, S. Fairchild, G. Erickson, and W.H. Koppenol, in Superoxide and Superoxide Dismutase in Chemistry, Biology, and Medicine. Ed. G. Rotilio, Elsevier Science Pub. 1986, p76.

23. Cynthia D. Millis, unpublished results.

24. M. Tien, T.K. Kirk, C. Bull, and J.A. Fee, J. Biol. Chem. **261**, 1687, 1986.

25. M.F. Zipplies, W.A. Lee, and T.C. Bruice, J. Am. Chem. Soc. **108**, 4433, 1986.

26. P.N. Balasubramanian, E.S. Schmidt, and T.C. Bruice, J. Am. Chem. Soc. **109**, 7865, 1987.

27. T. Wijesekera, A. Matsumoto, D. Dolphin, and D. Lexa, Angew. Chem. 1990, in press.

28 L.-C. Yuan, and T.C. Bruice, J. Am. Chem. Soc. **107**, 512, 1985.

29. W.A. Lee, and T.C. Bruice, J. Am. Chem. Soc. **107**, 513, 1985.

30. L.-C. Yuan, and T.C. Bruice, J. Am. Chem. Soc. **108**, 1643, 1986.

31. W.A. Lee, L.-C. Yuan, and T.C. Bruice, J. Am. Chem. Soc. **110**, 4277, 1988.

32. T.C. Bruice, P.N. Balasubramanian, R.W. Lee, and J.R.L. Smith, J. Am. Chem.

Soc. **110**, 7890, 1988.

33. T.G. Traylor, and J.P. Ciccone, J. Am. Chem. Soc. **111**, 8413, 1989.

34. T.C. Bruce, Aldrichimica Acta, **21**, 87, 1988.

35. J.R.L. Smith, P.N. Balasubramanian, and T.C. Bruice, J. Am. Chem. Soc. **110**, 7411, 1988.

36. N. Kirkpatrick, and J.M. Palmer, Appl. Microbiol. Biotechnol. **30**, 305, 1989

37. M.H. Gold, H. Wariishi, K. Valli, M.B. Mayfield, V.J. Nipper, and D. Probnow, Biotechnol. in the Pulp and Paper Industry (Proceedings of the 4th International conference), Raleigh, NC, USA, May 16-19, 1989, in press.

38. D. Kuila, M. Tien, J.A. Fee, and M.R. Ondrias, Biochem. **24**, 3394, 1985.

39. L.A. Anderson, V. Renganathan, A.A. Chiu, T.M. Lohr, and M.H. Gold, J. Biol. Chem. **260**, 6080, 1985.

40. Y. Mino, H. Wariishi, N.J. Blackburn, T.M. Lohr, and M.H. Gold, J. Biol. Chem. **263**, 7029, 1988.

41. J.-P. Renaud, P. Battioni, J.F. Bartoli, and D. Mansuy, J. Chem. Soc., Chem. Commun. 888, 1985.

42. D. Mansuy, P. Battioni, and J.-P. Renaud, J. Chem. Soc., Chem. Commun. 1255, 1984.

43. S. Neya, I. Morishima, and T. Yonezawa, Biochem. **20**, 2610, 1981.

44. T.G. Traylor, W.A. Lee, and D.V. Stynes, J. Am. Chem. Soc. **106**, 755, 1984.

45. T. Nakano, T.P. Wijesekera, D. Dolphin, T.E. Maione, T.K. Kirk, and R.L. Farrell, U.S. patent 4,892,241, 1989.

Chapter 3

Oxidation of lignin model compounds catalyzed by *meso*-tetra(2,6-dichloro-3-sulfonatophenyl)porphyrin iron chloride (TDCSPPFeCl)

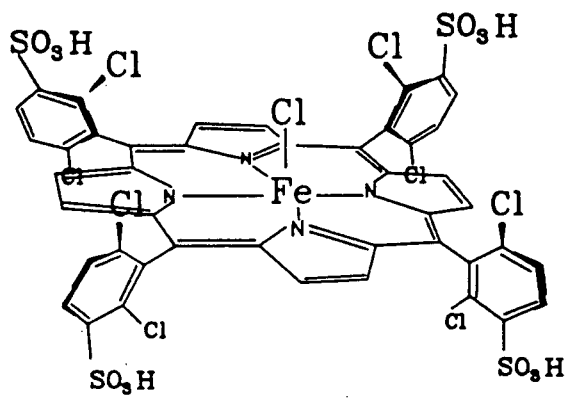

Figure 3.1 The structure of TDCSPPFeCl

3.1. Results and discussion

Due to the complex structure of lignin, model compounds representing separate portions of lignin have been widely used in lignin biodegradation studies. Though it is not clear if lignin and lignin model compounds are degraded by lignin degrading enzymes through the same pathway, lignin model compounds have played an important role in suggesting the mechanism of lignin degradation. In this study, lignin model compounds were used to study the potential of the metalloporphyrins to degrade various

substructures of lignin.

3.1.1. The oxidation of veratryl alcohol and veratryl acetate

Veratryl alcohol is a secondary metabolite of *Phanerochaete chrysosporium*[1,2] and plays a unique role in this process.[3] It was reported that veratryl alcohol could stimulate lignin degradation[4,5] and benzo(*a*)pyrene[6] oxidation by lignin peroxidase by protecting the enzyme from inactivation[7-9] in addition to functioning as a mediator at the same time (see chapter 4 of this thesis). Veratryl alcohol can also induce the biosynthesis of lignin peroxidase by *P. chrysosporium*.[10] In addition, veratryl alcohol is also a convenient lignin model compound. It is readily oxidized to give veratraldehyde by lignin peroxidase in the presence of hydrogen peroxide. On the other hand, veratraldehyde is readily reduced back to veratryl alcohol which accumulates in the *P. chrysosporium* culture.[2] This redox cycle of veratryl alcohol seemed to be energetically wasteful as the oxidizing power is used to oxidize veratryl alcohol instead of lignin. Leisola *et al*[11] first found that veratryl alcohol could be oxidized to give aromatic ring cleavage products. Later studies[12] showed that veratryl alcohol was rapidly metabolized to carbon dioxide by carbon limited cultures of *P. chrysosporium*, compared to the slow and incomplete degradation in nitrogen limited cultures. It was also shown[12] that veratraldehyde, the major oxidation product of veratryl alcohol by lignin peroxidase, could not be metabolized directly by the fungus, instead, it was reduced back to veratryl alcohol in the culture, and metabolized to carbon dioxide via intermediating quinones and aromatic ring cleavage products.

The degradation of veratryl alcohol by lignin peroxidase and biomimetic catalysts has been extensively studied[11-16] and the products including two γ-lactones, two δ-

lactones and three quinones have been found (Figure 3.2). The proposed mechanism for the production of these compounds was that initial one-electron oxidation of veratryl alcohol gave a cation radical, attack of which by water gave a carbon-centred radical, coupling of which with molecular oxygen lead to aromatic ring cleavage (pathway A) or demethoxylation products (quinones) (pathway B). Quinones can also be formed through pathway C as shown in Figure 3.3.

Oxidation of veratryl alcohol by TDCSPPFeCl/*m*CPBA at room temperature in pH 3 aqueous buffer gave veratraldehyde as the major product (>80%) along with small amounts of ring cleavage products **26**, **28**, **29**, and quinone **30** (Figure 3.2). When 4-ethoxy-3-methoxybenzyl alcohol was oxidized under the same conditions, lactones **28** and **29** were also found as products, conforming their δ-lactone structure. The quinones **31** and **32** formed in the oxidation of veratryl alcohol by lignin peroxidase were not found in this study. As will be described later, however, quinone **32** was found as a product of the oxidation of veratryl alcohol by TDCSPPFeCl/*m*CPBA using methanol as solvent.

When veratryl acetate was oxidized by TDCSPPFeCl/*m*CPBA in pH 3 aqueous buffer, quinone **34**, 3,4-dimethoxyphenol **35**, and a direct ring cleavage product **36** were isolated as the major products (Figure 3.4). Small amounts of veratraldehyde and veratryl acetate were also found.

Quinones **31** and **32** (Figure 3.2) have been found as phenyl-alkyl cleavage products of veratryl alcohol.[11,12,16] To our knowledge, this is the first time a phenol (**35**) has been found as a phenyl-alkyl cleavage product of a veratryl alcohol derivative. The quinone **34** found in this reaction is a analog of **30** found in the oxidation of veratryl alcohol, indicating that acetylation of veratryl alcohol to give veratryl acetate does not inhibit its demethoxylation.

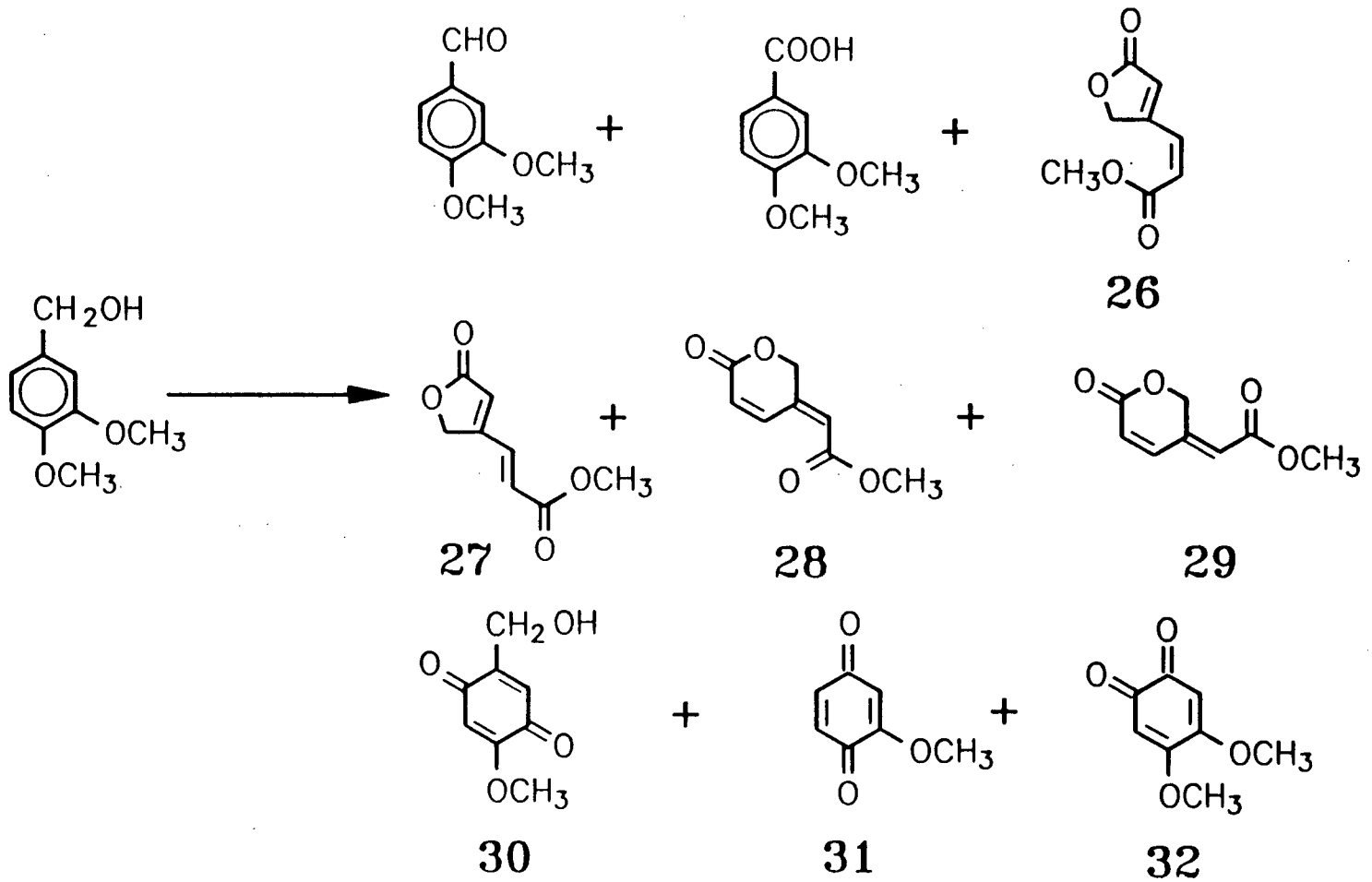

Figure 3.2 The oxidation of veratryl alcohol by lignin peroxidase or biomimetic systems

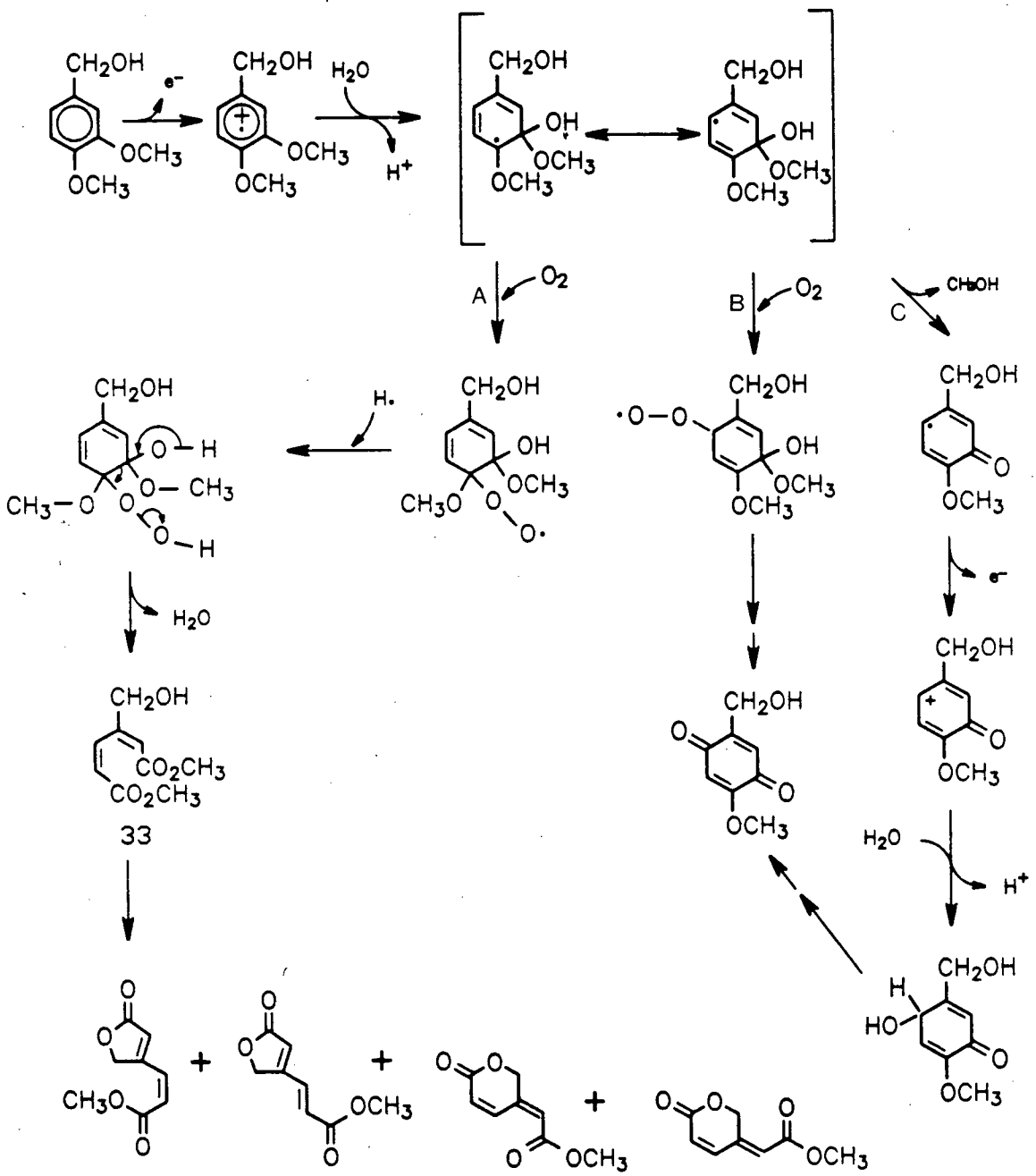

Figure 3.3 Proposed mechanisms for the oxidation of veratryl alcohol

Isolation of the direct ring cleavage product **36** supports the proposed mechanism of aromatic ring cleavage of veratryl alcohol.[13] The aromatic ring cleavage of veratryl alcohol gave initially **33** (Figure 3.3), intermolecular transesterification gave the

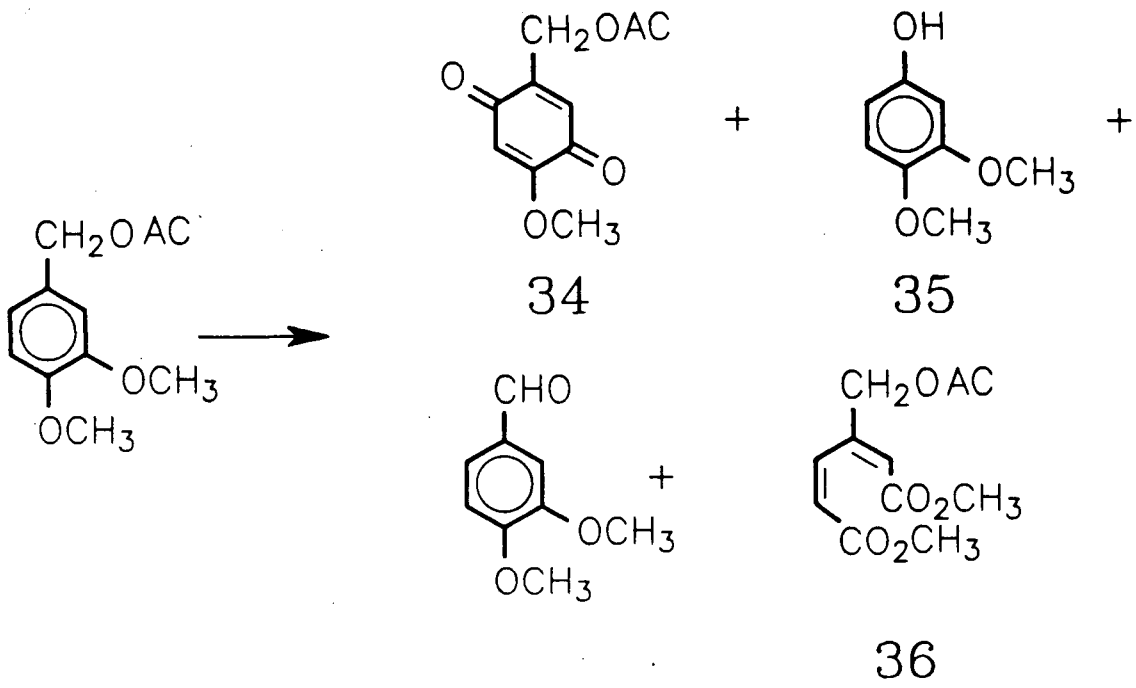

Figure 3.4 The oxidation of veratryl acetate in pH 3 aqueous buffer by TDCSPPFeCl and *m*CPBA

lactones shown in Figure 3.3. Compound **36** can be considered as a "trapped" analogue of intermediate **33**. A mechanism for the formation of **36** is proposed in Figure 3.5.

We learned after finishing this work that Schmidt *et al*[17] studied the degradation of veratryl methyl ether by lignin peroxidase and found a direct ring cleavage product similar to **36**. Veratraldehyde was the major product of veratryl methyl ether oxidation.[17] A C_α-ether bond, therefore, can be cleaved by lignin peroxidase, most probably through a one-electron oxidation mechanism.[17,18] The formation of veratraldehyde from the oxidation of veratryl acetate, though in a small amount,

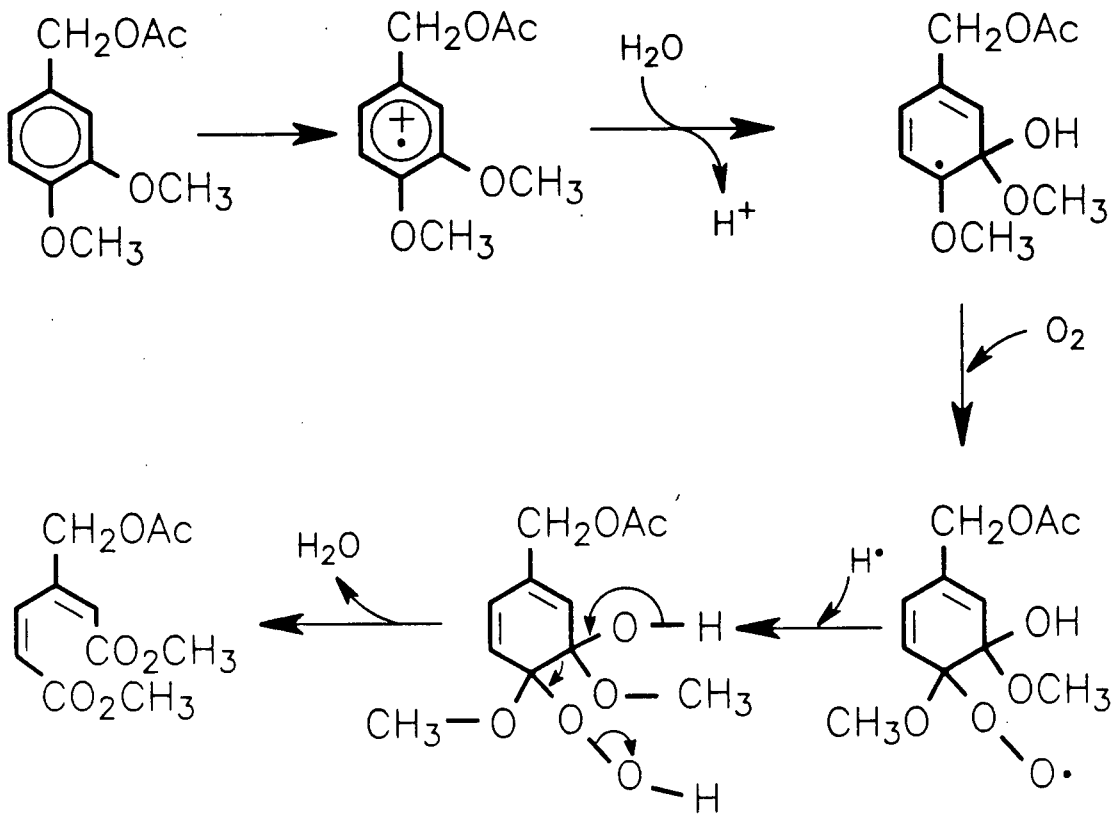

Figure 3.5 Possible mechanism for the formation of compound **36**

suggests that the C_α-ester bond of lignin model compounds can also be cleaved by lignin peroxidase in a similar way.

There have been reports that the oxidation reactions of lignin and lignin model compounds by enzymes[19,20] or biomimetic catalysts[21] vary in different solvents. As TDCSPPFeCl is soluble in both aqueous and polar organic solvents, the oxidation of veratryl alcohol and veratryl acetate in methanol was also studied to investigate possible solvent effects on lignin model compound oxidation.

Oxidation of veratryl alcohol by TDCSPPFeCl/*m*CPBA in methanol gave veratraldehyde, methanol-incorporated products **37** and **38**, and quinones **30** and **32** (Figure 3.6). The product distribution was dependent on the conditions used, when the

reaction was carried out open air with moderate stirring, veratraldehyde and **37** were produced in 47% and 42% yield, respectively. Other products were found only in very small amounts. Under highly aerobic condition (open air, vigorous stirring), the relative yield of veratraldehyde, **37**, and **38** was 51%, 11%, and 32%, respectively. Under anaerobic condition, compound **38** was found only in trace amounts.

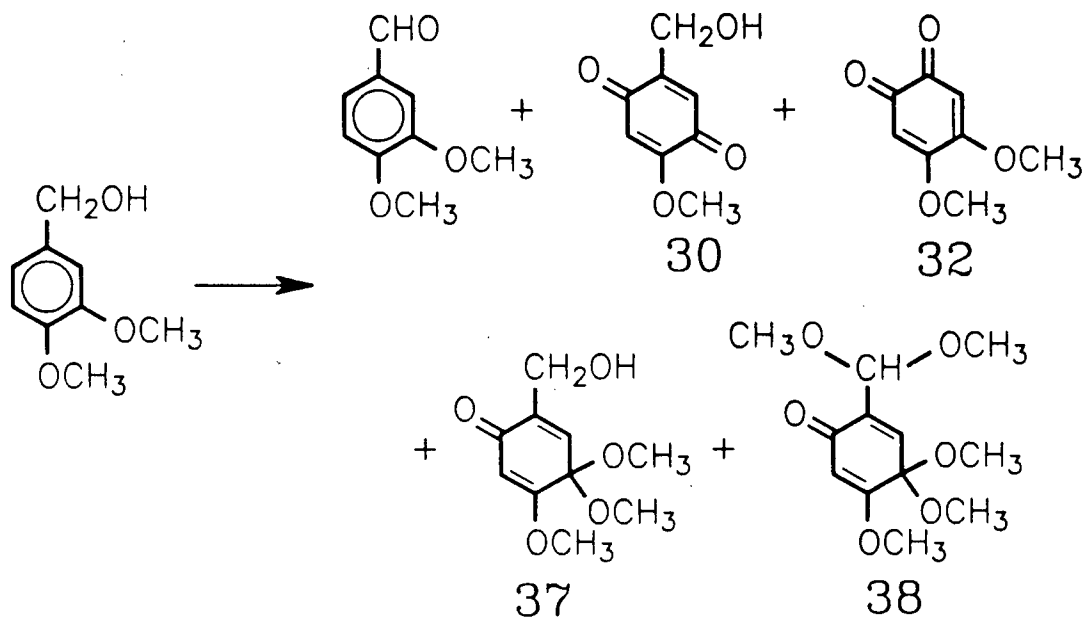

Figure 3.6 The oxidation of veratryl alcohol by TDCSPPFeCl/*m*CPBA in methanol.

The structure of the methanol incorporated product **37** was confirmed as follows. Acetylation of **37** by acetic anhydride/pyridine gave **39**. Oxidation of veratryl acetate by TDCSPPFeCl/*m*CPBA in methanol gave a product whose ^{1}H NMR and MS were the same as those of **39**. Treating **37** with concentrated HCl in aqueous THF gave compound **30** (Scheme 3.1). When veratryl alcohol was oxidized in ethanol, one solvent molecule was incorporated to give product **40**. If 4-ethoxy-3-methoxybenzyl

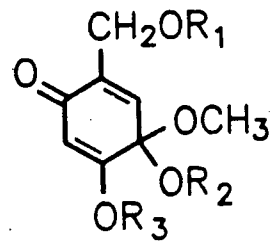

37 R_1=H, R_2=R_3=CH_3

39 R_1=$COCH_3$, R_2=R_3=CH_3

40 R_1=H, R_2=C_2H_5, R_3=CH_3

41 R_1=H, R_2=CH_3, R_3=C_2H_5

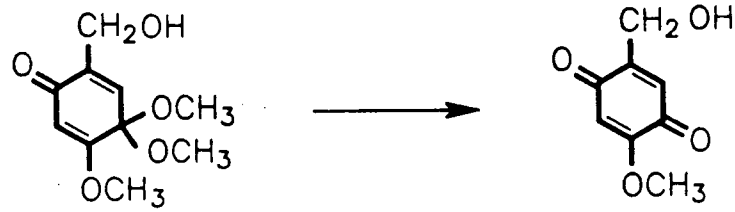

37 **30**

Scheme 3.1 The hydrolysis of compound **37**.

alcohol was used as the substrate, compound **41** instead of **37** was found as the product.

The structure of **38** was elucidated by its ^{13}C NMR and by comparing its ^{1}H

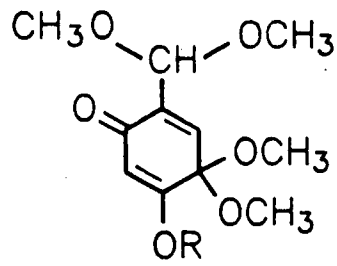

38 R=CH_3

42 R=C_2H_5

NMR and MS with those of **37**. Oxidation of 4-ethoxy-3-methoxybenzyl alcohol in methanol gave product **42**.

A mechanism for the formation of **37** is proposed in Figure 3.7. Shimada *et al*[14] proposed two possible pathways for aromatic ring cleavage of veratryl alcohol and suggested that the one in which water (or hydroxide) specifically attacked the C_3-

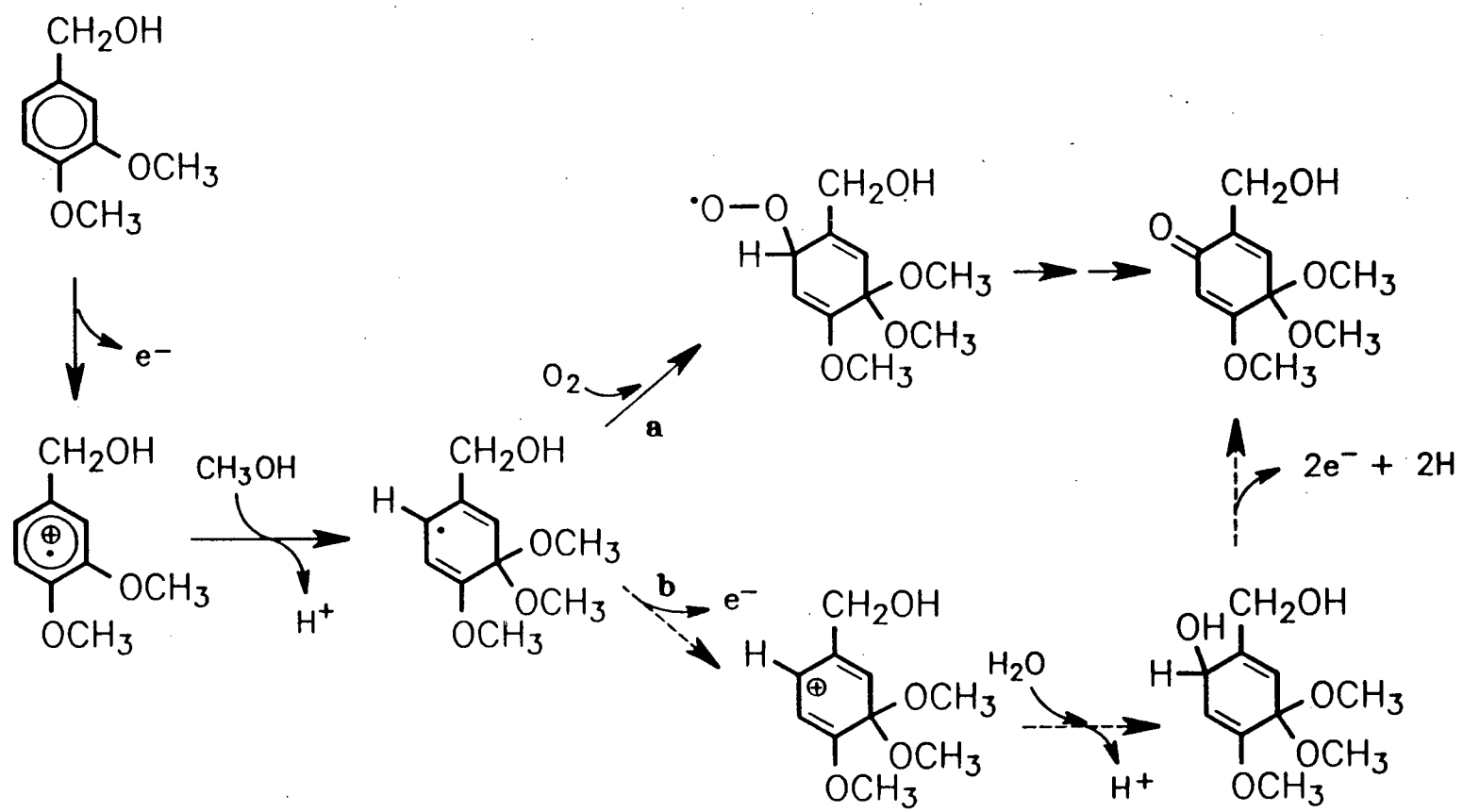

Figure 3.7 Possible mechanism for the formation of compound **37**

position of a substrate cation radical was more plausible. The specific incorporation of methanol into the C_3-position of veratryl alcohol to give compound **37** clearly indicates that the solvent methanol preferentially attacks the C_3-position of the veratryl alcohol cation radical. The formation of **37** also suggests that quinone **30** resulted from attack of water at the C_3-position of the veratryl alcohol cation radical.

Oxidation of veratryl acetate in methanol gave the methanol incorporated product **39** as a major product (82%). Small amounts of veratraldehyde and veratryl acetate were also found.

It was interesting to observe that when veratryl alcohol was oxidized in ethanol, only one solvent molecule was incorporated to give compound **40** and that the 3-methoxy group of **40** did not exchange with the solvent. Aromatic ring cleavage products were not found when veratryl alcohol or veratryl acetate were oxidized in methanol, clearly suggesting the presence of solvent effect for the oxidation of lignin model compounds.

3.1.2. Oxidation of phenylpropane model compounds

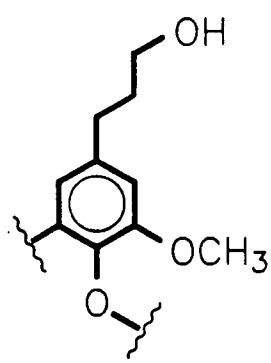

43

Alkoxy substituted phenylpropane substructure (**43**) has been suggested to be present at the terminal chains of lignin.[22] Tien and Kirk[23] first found that lignin peroxidase could catalyze hydroxylation of the benzylic methylene group (C_α-hydroxylation) of 2-(3,4-dimethoxyphenyl)ethanol to give 3,4-dimethoxyphenylglycol. C_α-hydroxylation of 1-(4-ethoxy-3-methoxyphenyl)propane by lignin peroxidase was also reported by Renganathan *et al.*[24,25] Isotopic labelling experiments[25] using $^{18}O_2$ or $H_2{}^{18}O$ showed that the oxygen of the C_α-hydroxy group was from molecular oxygen under aerobic conditions but came from water under anaerobic conditions, indicating a cation radical mechanism for the reaction.

In addition to the C_α-hydroxylation product **47** reported earlier,[24,25] oxidation of 1-(4-ethoxy-3-methoxyphenyl)propane (**44**) by TDCSPPFeCl and t-BuOOH at room temperature in aqueous acetonitrile (pH 3) gave the direct ring cleavage product **45**, quinone **46**, and **48** as major products (Figure 3.8).

The formation of the direct ring cleavage product **45** from **44** and the formation of ring cleavage product **36** from the oxidation of veratryl acetate support each other and extend our knowledge about the ring cleavage of lignin model compounds. Quinones analogous to **46** have been found in the oxidation of veratryl alcohol and veratryl acetate as described above. The formation of **48** is interesting and no similar products have been previously found from the oxidation of lignin model compounds. A mechanism for the alkyl-phenyl cleavage of phenolic model compounds has been proposed[26] as shown in Figure 3.9. The formation of **50** resulted from a one-electron oxidation process and the alkyl-phenyl cleavage of **50** needed the presence of an acidic proton. In the case of **44**, it has only an unreactive propyl side chain, hence alkyl-phenyl cleavage is unable to occur and product **48** can be considered as an analogue of the intermediate **50**. A possible mechanism for the formation of **48** is presented in

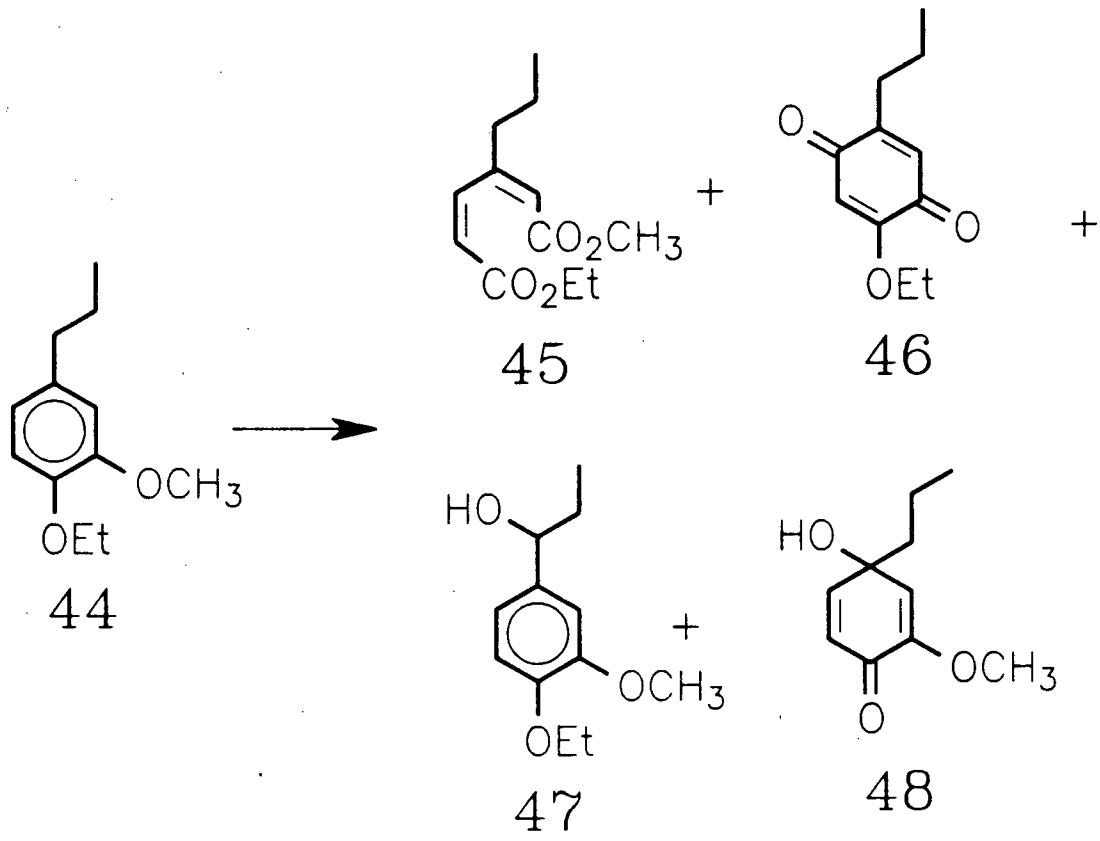

Figure 3.8 The oxidation of 1-(4-ethoxy-3-methoxyphenyl)propane (**44**) by TDCSPPFeCl and t-BuOOH in aqueous acetonitrile

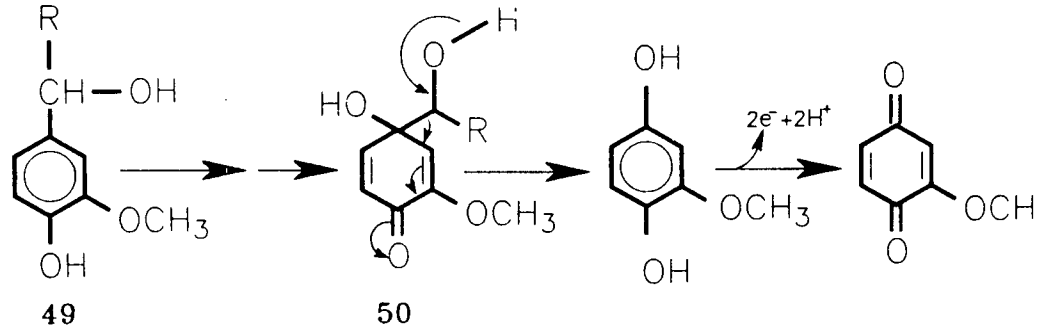

Figure 3.9 Proposed mechanism for alkyl-phenyl cleavage of phenolic model compounds

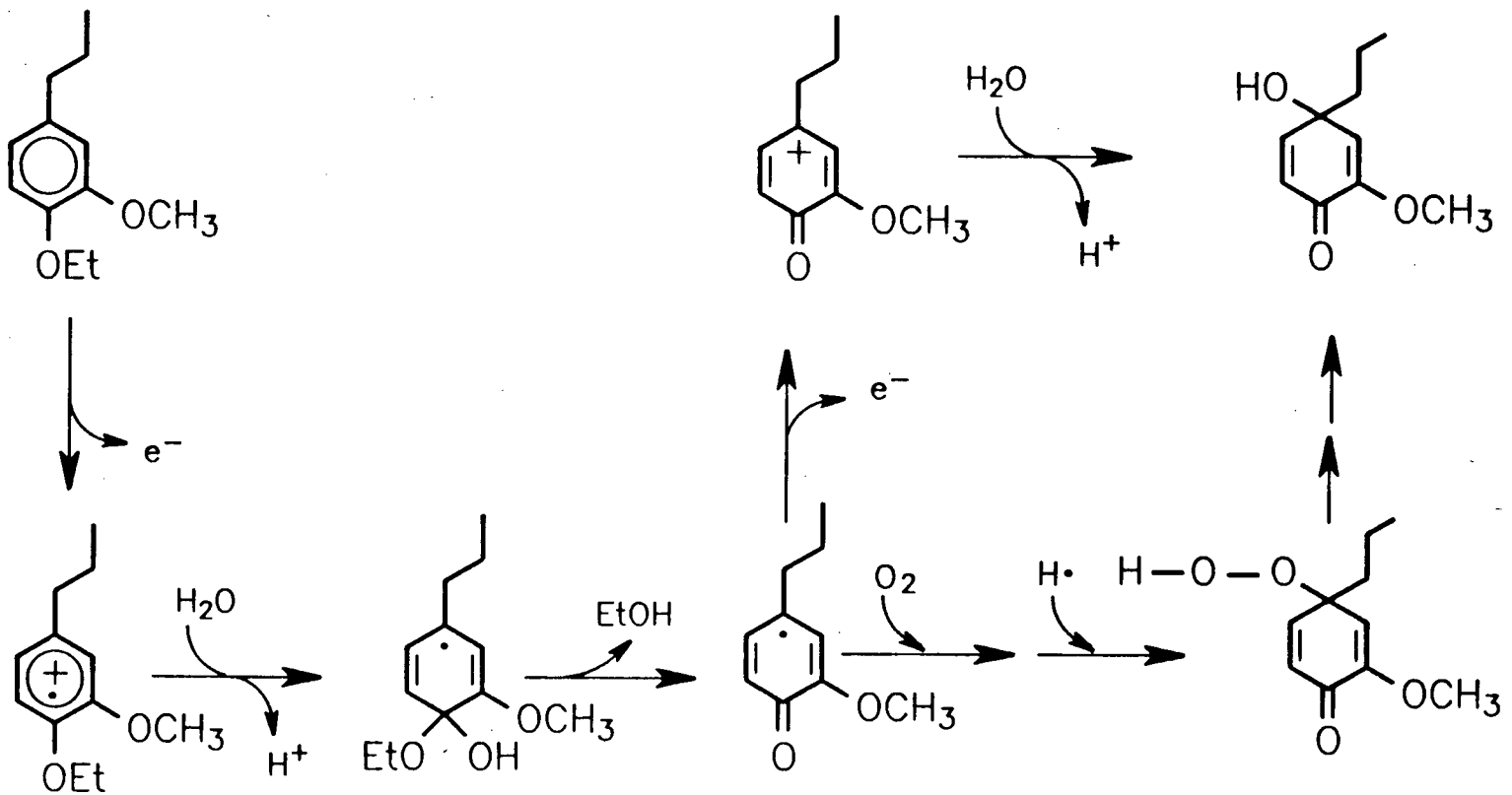

Figure 3.10 Possible mechanism for the formation of compound **48**

Figure 3.10.

Veratryl alcohol is metabolized by *P. chrysosporium* via quinones and ring cleavage products.[12] While the importance of C_α-hydroxylation to lignin biodegradation is not clear, it is quite possible that the demethoxylation and aromatic ring cleavage reactions found in this study are more important reactions than the C_α-hydroxylation previously reported for this model substructure.[24,25] The phenylpropane substructures of lignin is probably also metabolized by *P. chrysosporium* through quinone and ring cleaved intermediates.

3.1.3. Oxidation of phenylpropene model compounds

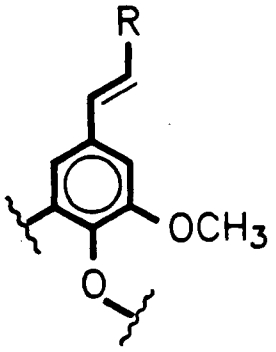

51 R = CH_2OH or CHO

Phenylpropene (**51**) is also a substructure of lignin[22] and it has been reported that hydroxylation (diol formation) of the C_α-C_β double bond of 1-(4-ethoxy-3-methoxyphenyl)-1-propene (**52**) by lignin peroxidase gives 1-(4-ethoxy-3-methoxyphenyl)propane-1,2-diol[24,27,28] (**53**). Diol formation from the C_α-C_β double bond was found to be the first step in the degradation of lignin model compounds by *P. chrysosporium*.[29-32]

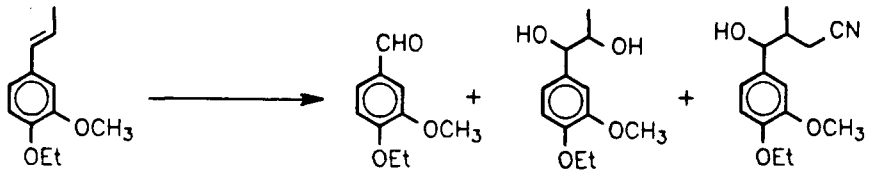

52 53 54

Figure 3.11 The oxidation of 1-(4-ethoxy-3-methoxyphenyl)-1-propene (**52**) by TDCSPPFeCl and t-BuOOH in aqueous acetonitrile

As shown in Figure 3.11, TDCSPPFeCl was able to oxidize **52** to give 4-ethoxy-3-methoxybenzaldehyde (24% yield), and **53** (33% yield) in the presence of t-BuOOH in aqueous acetonitrile. In addition, an acetonitrile incorporated product **54** (18% yield) was isolated.

It has been previously found that the oxygen of the ß-hydroxy group of **53** was derived from molecular oxygen,[33] indicating a cation radical mechanism of the reaction. The formation of **54** certainly needs a C_{β}-centred radical to be involved, supporting a cation radical mechanism of the reaction.

Cytochromes P-450 are monooxygenases and function by activating molecular oxygen.[34] They can catalyze diol formation from alkenes via an epoxide intermediate. Lignin peroxidases are peroxidases and have peroxidase and haloperoxidase activity.[35] No monooxygenase activity of lignin peroxidase has been reported. Though the fact that *P. chrysosporium* can metabolize lindane[36] (1,2,3,4,5,6-hexachlorocyclohexane) suggests the presence of other enzyme activities, it is still not clear which enzyme(s) is responsible for this reaction. Since lignin has a three-dimensional, heterogeneous structure, diol formation from lignin via an epoxide intermediate is unlikely. In order for oxygen atom to transfer and epoxide to be formed, the double bond of the substrate needs to approach closely the active site of the enzyme. It is unlikely that lignin as a substrate will meet this steric requirement. As both TDCSPPFeCl and alkene **52** are

small molecules, approach of the C_α-C_β double bond of **52** to TDCSPPFeCl is still possible, the formation of diol **53** from **52** via a epoxide intermediate cannot be excluded. The formation of **54**, however, certainly suggests radical formation for at least one of the pathways of the oxidation of **52**.

Proposed in Figure 3.12 is the mechanism for the formation of **53** and **54**. One electron oxidation of **52** gives a cation radical, reaction of which with water gives a C_β-centred radical. Reaction of the radical with dioxygen or further one electron oxidation followed by reacting with water gives the diol **53**. Coupling of the C_β-centred radical with an acetonitrile derived radical gives the acetonitrile incorporated product **54**. When **52** was oxidized under highly aerobic conditions (bubbling oxygen using a sintered glass frit), little of the solvent incorporated product **54** was detected, probably because of the competitive coupling of molecular oxygen with the C_β-centred radical.

3.1.4. Oxidation of diarylpropane model compound

Diarylpropane model compounds (ß-1) are frequently used substrates for lignin biodegradation studies. Oxidation of 1-(4-ethoxy-3-methoxyphenyl)-2-(4-methoxyphenyl)propane-1,3-diol (**55**) by lignin peroxidase gives mainly C_α-C_β cleavage products.[25,28,33]

Oxidation of **55** by TDCSPPFeCl and t-BuOOH in aqueous acetonitrile (pH 3) gave 4-ethoxy-3-methoxybenzaldehyde (**56**, 40% yield), 4′-methoxy-α-hydroxyacetophenone (**57**, 12% yield), and 4-methoxybenzaldehyde (**60**, 20% yield) as major products (Figure 3.13). Small amounts of 4-ethoxy-3-methoxybenzoic acid (**59**) and 4-methoxybenzoic acid (**61**) were also isolated by preparative TLC and detected by GC and GCMS after methylation with diazomethane of the acidic products. 4-

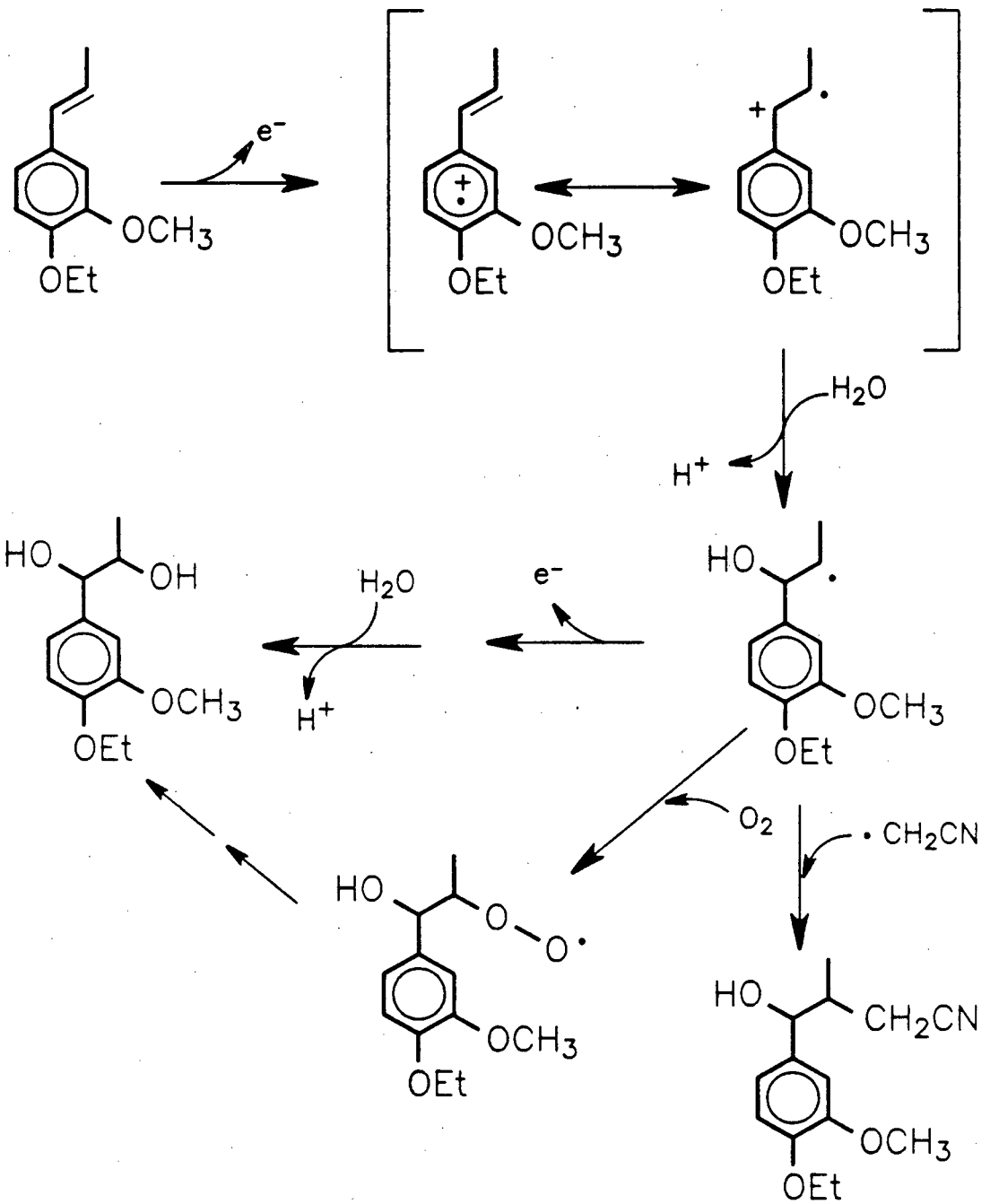

Figure 3.12 Possible mechanism for the oxidation of 1-(4-ethoxy-3-methoxyphenyl)propene

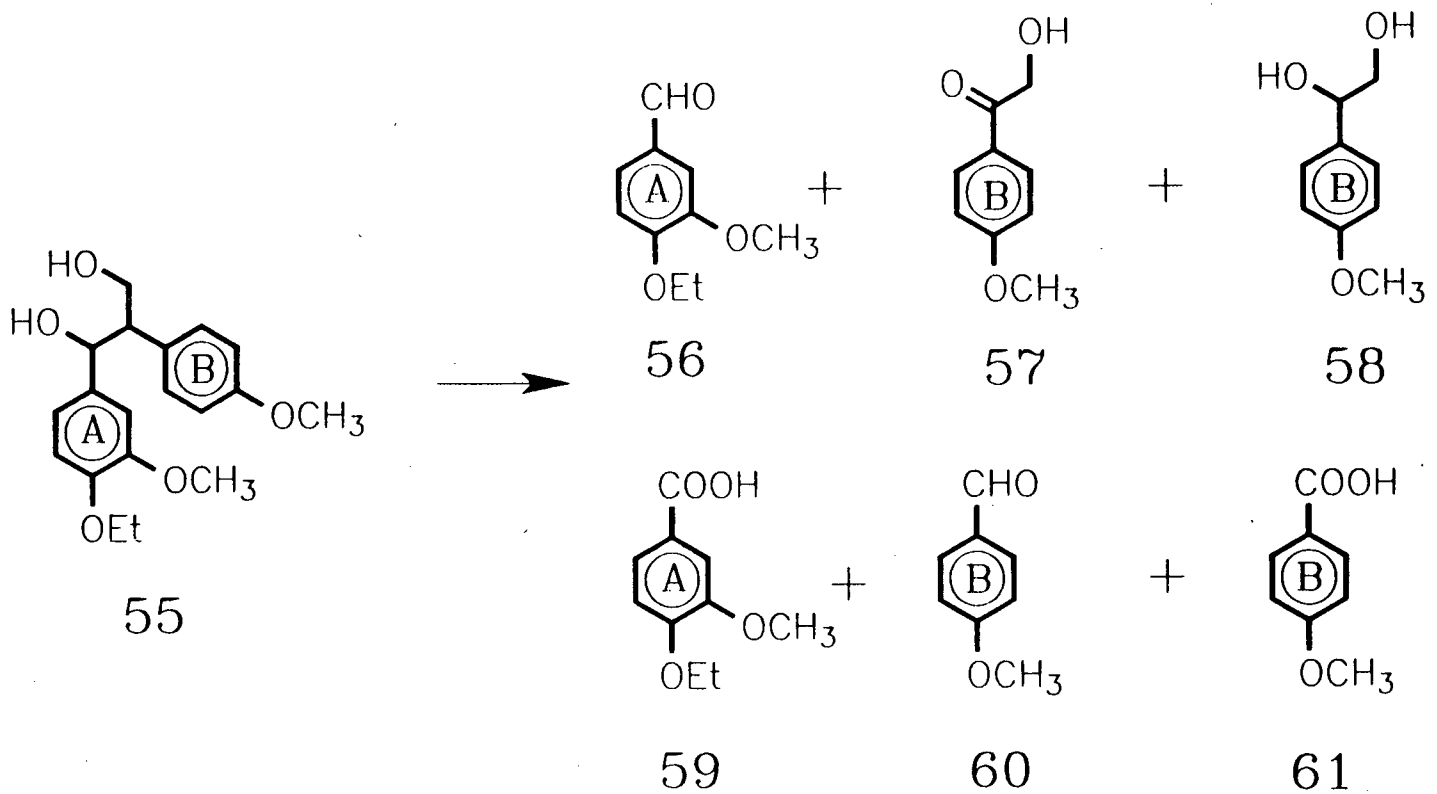

Figure 3.13 The oxidation of 1-(4-ethoxy-3-methoxyphenyl)-2-(4-methoxyphenyl)propane-1,3-diol (**55**) by TDCSPPFeCl and t-BuOOH

Methoxyphenylglycol (**58**), which was a product in the oxidation of **55** by lignin peroxidase,[25,28,33] was not isolated in this study. Careful GC and GCMS analyses of the acetylated products showed the presence of only trace amount of 4-methoxyphenylglycol diacetate. Oxidation of synthetic **58** under the condition used for the oxidation of **55** gave **57**, **60**, and a small amount of **61**. Competitive oxidation of a 1:1 (molar ratio) mixture of **55** and **58** indicated that the ß-1 dimer **55** instead of the glycol **58** was preferentially oxidized under the conditions of this experiment. The glycol **58** was therefore neither a major product nor an important intermediate for the oxidation of **55** by TDCSPPFeCl and t-BuOOH. The ketone **57** was formed directly.

During the oxidation of **55** by lignin peroxidase,[25,28,33] glycol **58** instead of the ketone **57** was the major product of the reaction while under anaerobic condition, the ketone **57** was not found. Oxidation of **55** by TDCSPPFeCl and t-BuOOH under anaerobic conditions also gave **58** as a major product and little ketone **57** was found. This suggests that the differences in the product distribution for the degradation of **55** by lignin peroxidase and by TDCSPPFeCl under aerobic condition was not the result of mechanistic differences. Experimental conditions were most probably responsible. It was noticed that when ß-1 model compounds were oxidized by TPPFeCl[37] or protohemin,[38] the glycol, analogous to **58**, was produced in smaller amounts than the corresponding ketone, suggesting that common differences exist between the reaction catalyzed by lignin peroxidase and those catalyzed by various biomimetic catalysts.

3.1.5. Oxidation of arylglycerol-ß-aryl ether (ß-O-4) model compounds

The arylglycerol-ß-aryl ether (ß-O-4) substructure (**4**) is the most abundant substructure in lignin and in spruce lignin about 48% of the linkages connecting the

phenylpropanoid units are of the ß-O-4 type. ß-O-4 model compounds are one of the most frequently used model compounds in lignin biodegradation studies.

Oxidation of 4-ethoxy-3-methoxyphenylglycerol-ß-guaiacyl ether (**62**) by TDCSPPFeCl and t-BuOOH in aqueous acetonitrile (pH 3) gave 4-ethoxy-3-methoxybenzaldehyde (35% yield) and guaiacol (**63**, 30% yield) as the major products

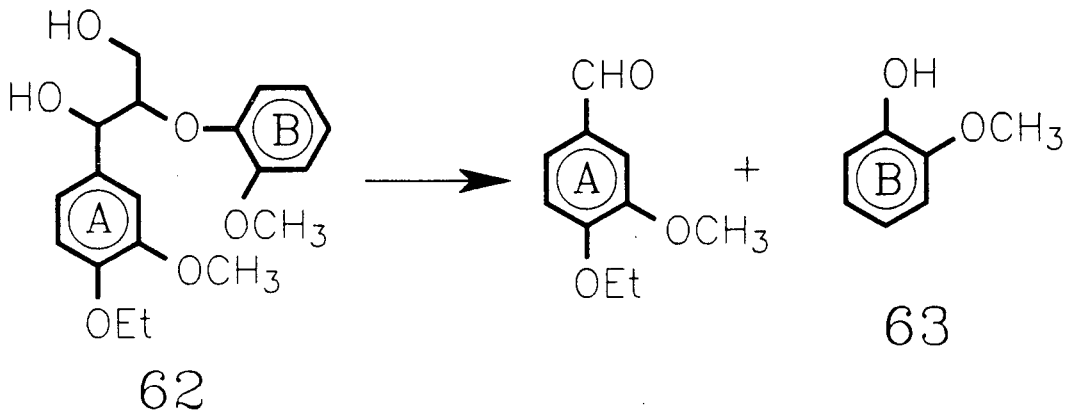

Figure 3.14 The oxidation of 4-ethoxy-3-methoxyphenylglycerol-ß-guaiacyl ether by TDCSPPFeCl and t-BuOOH

(Figure 3.14). Other products were detected in very small amounts and have not been identified. In the degradation of ß-O-4 model compounds by lignin peroxidase,[27,40] C_α-C_β cleavage was also the major reaction.

3.1.6. Oxidation of phenylcoumaran (ß-5) model compounds

The phenylcoumaran substructure (ß-5, **8**) constitutes about 9-12% of the substructures in spruce lignin.[39] The degradation of ß-5 model compounds by lignin peroxidase has not been reported. In order to investigate the ability of TDCSPPFeCl in degrading the various substructures of lignin, we studied the oxidation of an easily

available ß-5 dimer, 4-O-ethyldehydrodiisoeugenol (**64**) by TDCSPPFeCl and t-BuOOH.

Oxidation of **64** by TDCSPPFeCl and t-BuOOH in aqueous acetonitrile (pH 3) gave the side chain cleavage product **65** (~70% isolated yield) as the first product (Figure 3.15), further oxidation of which gave C_α-C_β cleavage products 4-ethoxy-3-methoxybenzaldehyde and **70**, acid **66**, and aromatic ring cleavage products **67**, **68**, and **69**. It was not clear if the ring opened acid **67** was a product of aromatic ring cleavage of acid **66** or was from the oxidation of the ring-cleaved aldehyde **68**. The configuration of the double bonds in the ring cleaved products was elucidated by examining the coupling constants and by using NOE (nuclear overhauser effect) difference spectra as described in the experimental section.

Degradation of ß-5 model compounds by the ligninolytic culture of *P. chrysosporium* has been studied.[41,42] In the oxidation of methyl dehydrodiconiferyl alcohol,[41] the double bond of the side chain was first hydroxylated to give the glycol, which was further cleaved to give an aldehyde. In the oxidation of **64** by TDCSPPFeCl and t-BuOOH, the glycol was not isolated, probably because of its rapid oxidation. Aldehyde **65** was isolated as the first product. As described above, we showed by using 1-(4-ethoxy-3-methoxyphenyl)-1-propene (**52**, Figure 3.11) that TDCSPPFeCl was able to catalyze the diol formation.

Aromatic ring cleavage of veratryl alcohol and ß-O-4 model compounds[43-47] has been reported. It is interesting to note that in the case of ß-O-4 dimers, all the ring cleavage products resulted from B-ring cleavage while cleavage of the A-ring has not been found. In addition, ring cleavage of ß-1 model compounds has never been reported. It is possible that the C_α-C_β cleavage reaction of ß-1 and ß-O-4 model compounds occurs so quickly that the A-ring cation radical is not sufficiently long lived for aromatic ring cleavage to occur. The cation radicals of methoxybenzenes[48] and of

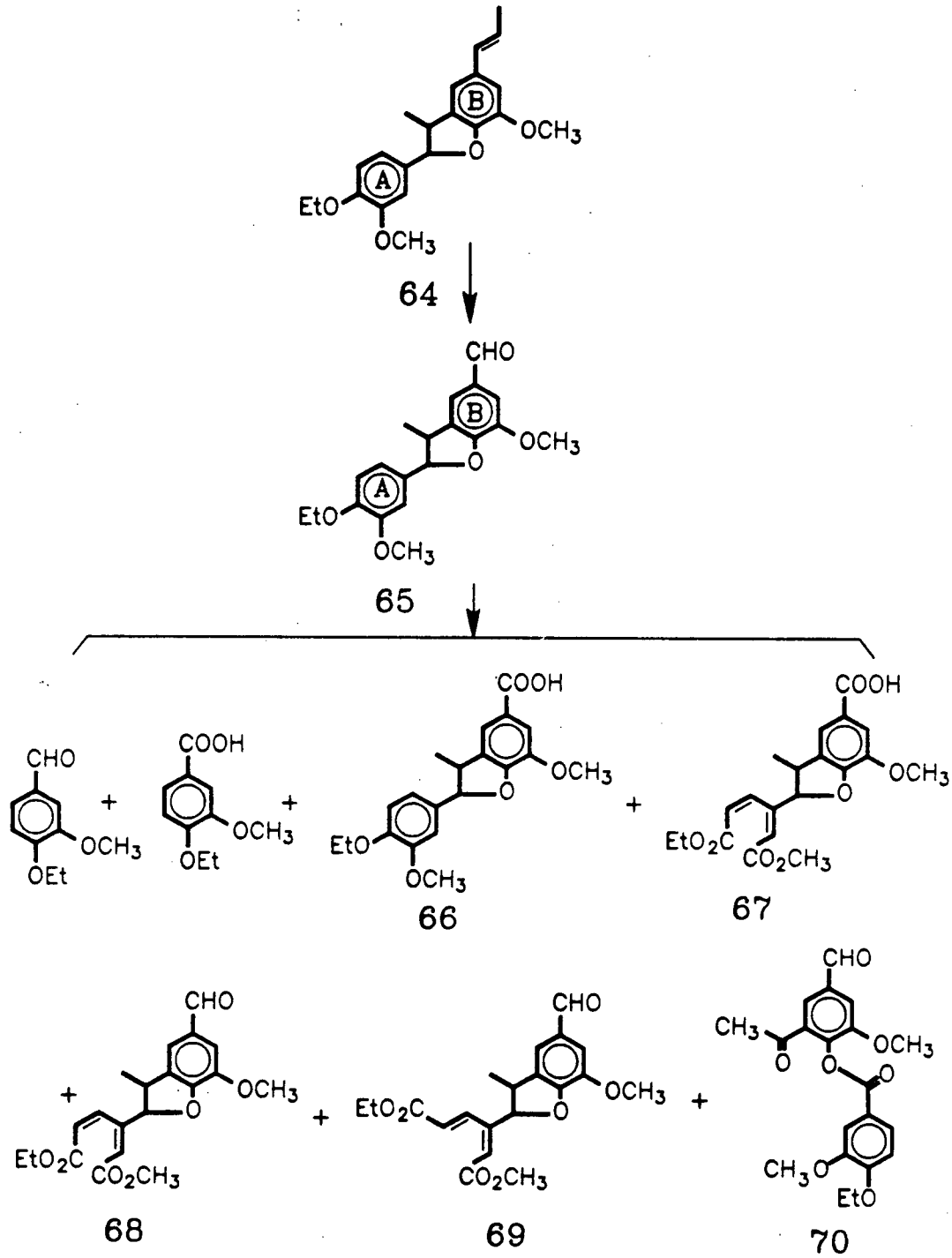

Figure 3.15 The oxidation of 4-O-ethyldehydrodiisoeugenol (64) by TDCSPPFeCl and t-BuOOH

the B-ring of a α-oxo ß-O-4 model compound[18] have been detected by ESR. Spectral observation of the A-ring cation radical of ß-1 and ß-O-4 model compounds has not been reported.

The isolation of A-ring cleavage products from **64** suggested that the C_α-C_β cleavage of this ß-5 model compound is not the preferred route compared to that of ß-1 and ß-O-4 model compounds. The B-ring of **65** is less readily oxidized than the A-ring due to the deactivation by the aldehyde group on the B-ring.

3.1.7. Oxidation of 5-5′ biphenyl model compound

The 5-5′ biphenyl structure (**6**) is another main substructure of lignin and 9.5-11% of the linkages connecting the phenylpropanoid units of spruce lignin are of the biphenyl type.[39] The guaiacyl moieties (**71**) of lignin are easily condensed by the

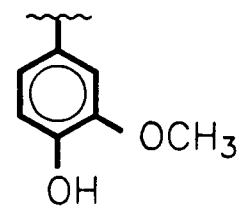

71

phenol oxidizing enzymes of white-rot fungi to give the 5-5′ biphenyl structure,[49,50] which is resistant to microbial attack.[51] The ability of an enzyme or a biomimetic catalyst to degrade this substructure is therefore very important to lignin biodegradation.

The metabolism of dehydrodivanillic acid (**72**) by bacteria[52] and by *P. chrysosporium*[53] has been studied and 5-carboxyvanillic acid **73** was found as a product in both cases (Scheme 3.2). The mechanism and enzyme(s) responsible for the formation of **73** is still not clear. The degradation of tetrameric model compounds

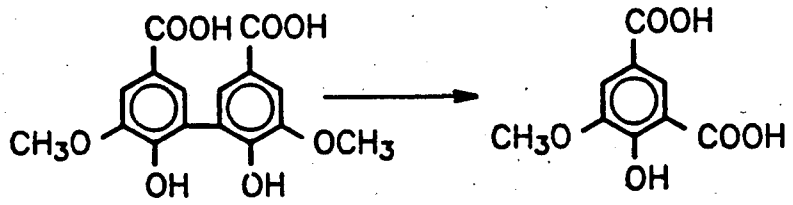

72 73

Scheme 3.2

containing the biphenyl structure by bacteria[54,55] and by *P. chrysosporium*[56] has also been studied. The major reactions were side chain cleavage, no aromatic ring cleavage or biphenyl bond cleavage was found.

We selected 4,4′-diethyldehydrodivanillin (**74**) as a biphenyl model compound to avoid complex side chain reactions. Oxidation of **74** by TDCSPPFeCl and t-BuOOH in aqueous acetonitrile (pH 3) gave acids **75** and **76** from side chain oxidation and aromatic ring cleavage products **77** and **78** from aromatic ring oxidation (Figure 3.16).

It has been proposed[57,58] that the aromatic aldehyde moiety of lignin cannot be metabolized directly by lignin degrading enzymes. It is reduced to an alcohol[12,57] or oxidized to a acid[57,58] before undergoing further metabolism. The fact that ring cleavage occurred only on the ring bearing a carboxyl group certainly supports the second pathway of aromatic aldehyde metabolism.

Direct aromatic ring cleavage products similar to **77** and **78** have been found in this study and reported in the literature[17]. The similarities of these reactions suggest that they follow the same mechanism, that is, initiation by an one-electron oxidation process. The degradation of biphenyl model compounds by lignin peroxidase has not been reported. The formation of aromatic ring cleavage products **77** and **78**, probably

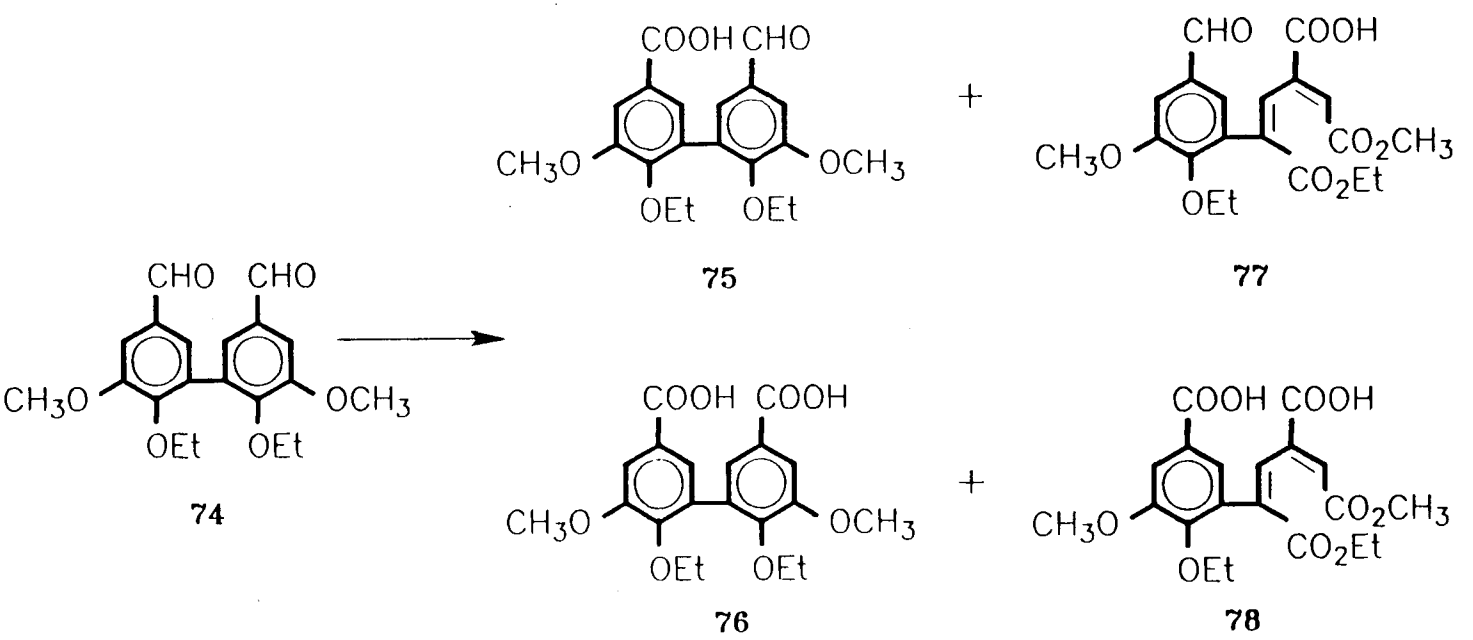

Figure 3.16 The oxidation of 4,4'-diethyldehydrodivanillin (74) by TDCSPPFeCl and t-BuOOH

through an one-electron oxidation pathway, suggests that lignin peroxidase might also oxidize the biphenyl substructure of lignin.

Veratryl alcohol is metabolized to carbon dioxide by *P. chrysosporium* via quinone and ring cleavage product intermediates.[12] No demethoxylation products of the biphenyl model compound **74** were found in this study. Aromatic ring cleavage is probably the first and most critical step for the biodegradation of biphenyl substructures of lignin.

3.1.8. Oxidation of pyrene

In addition to a wide variety of lignin model compounds and polychlorinated phenols, lignin peroxidase can also catalyze the oxidation of polycyclic aromatics. Pyrene (**79**) was oxidized to give pyrene-1,6-dione (**80**) and pyrene-1,8-dione (**81**) through a one-electron oxidation mechanism.[59] Benzo[*a*]pyrene[59,60] was also oxidized by lignin peroxidase to give benzo[*a*]pyrene 1,6-, 3,6-, and 6,12- quinones. The ability of TDCSPPFeCl to catalyze the oxidation of polycyclic aromatics was studied using pyrene as a substrate.

Pyrene was oxidized rapidly by TDCSPPFeCl/*m*CPBA at pH 3 to give pyrene-1,6-dione and pyrene-1,8-dione as major products (Figure 3.17). Further oxidation of

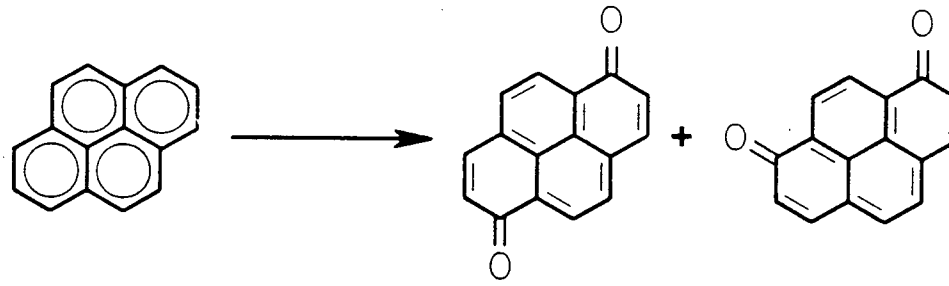

80 81

Figure 3.17 The oxidation of pyrene by TDCSPPFeCl and *m*CPBA

the quinones by TDCSPPFeCl/*m*CPBA was not successful as the quinones were not readily oxidized and TDCSPPFeCl was not stable towards *m*CPBA at pH 3. The oxidation of pyrene-1,8-dione by *m*CPBA and Cl_{16}TSPPMnCl, which is a more stable catalyst than TDCSPPFeCl, gave mainly black tars which was insoluble in either water or organic solvents.

3.1.9 Oxidation of 2,4,6-trichlorophenol

It has been reported[61] that lignin peroxidase could also catalyze the oxidation of chlorinated phenols. Pentachlorophenol and 2,4,6-trichlorophenol was oxidized[61] to give tetrachloro-*p*-benzoquinone and 2,6-dichloro-*p*-benzoquinone, respectively. We have shown that TDCSPPFeCl is able to oxidize 2,4,6-trichlorophenol (**82**) to give 2,6-dichloro-*p*-benzoquinone (**83**) as a major product along with an unidentified product (Figure 3.18).

3.2 Conclusion

It has been shown that TDCSPPFeCl as a biomimetic catalyst can mimic the function of lignin peroxidase in the oxidation of a variety of lignin model compounds

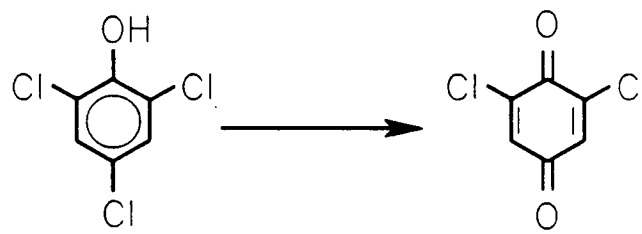

82 **83**

Figure 3.18 The oxidation of 2,4,6-trichlorophenol by TDCSPPFeCl and *m*CPBA.

and related substrates, including veratryl alcohol, veratryl acetate, phenylpropane and phenylpropene model compounds (**44** and **52**), ß-1 (**55**), ß-O-4 (**62**), ß-5 (**64**), and 5,5′-biphenyl (**74**) model compounds. Pyrene and 2,4,6-trichlorophenol can also be oxidized by the iron porphyrin catalyst, suggesting that other environmental pollutants might also be degraded by this catalyst.

The isolation of direct ring cleavage products from the oxidation of veratryl acetate, 1-(4-ethoxy-3-methoxyphenyl)propane (**44**), 4-O-ethyldehydrodiisoeugenol (**64**), and 4,4′-diethyldehydrodivanillin (**74**) supports the mechanism for aromatic ring cleavage of lignin model compounds as shown in Figure 3.3.

The fact that methanol was incorporated only into the C_3-position of veratryl alcohol to give methanol incorporated products **37** and **38** provides evidence that the cation radical of veratryl alcohol is preferentially attacked by solvent at its C_3-position. As shown in Figure 3.3, attack of water onto the cation radical is the first step for both the aromatic ring cleavage and the demethoxylation reactions.

The formation of the acetonitrile incorporated product **54** in the oxidation of the phenylpropene model compound **52** requires the involvement of a carbon centred radical, suggesting a cation radical mechanism for the oxidation of this type of substructure.

The oxidation of the phenylcoumaran (ß-5) model compound **64** to give C_α-C_β cleavage and aromatic ring cleavage products suggests that the ß-5 substructure can be degraded in a manner similar to other substructures of lignin, probably through the same cation radical mechanism. For the first time aromatic ring cleavage products derived from the A-ring of a dimeric model compound have been isolated.

A 5,5′-biphenyl model compound (**74**) which represents the lignin substructure most resistant to microbial degradation can be oxidized by TDCSPPFeCl, suggesting

that the iron porphyrin is powerful enough to oxidize all the major substructures of lignin. The oxidation of 5,5′-biphenyl model compounds by purified lignin peroxidase has not been reported. The formation of aromatic carboxylic acids from TDCSPPFeCl catalyzed oxidation of the biphenyl model compound **74** and the ß-1 model compound **55** suggests that the iron porphyrin is probably a more powerful catalyst than lignin peroxidase.

3.3 Experimental

3.3.1 General

Equipment. ^{1}H NMR spectra were recorded on Varian XL 300 or Bruker WH 400 spectrometers using tetramethylsilane as internal standard. ^{13}C NMR spectra were recorded on Varian XL 300 spectrometer. Low resolution and high resolution mass spectra were recorded on an AE1 MS9 and a Cratos MS50 spectrometer, respectively. A HP 5890A Gas Chromatograph equipped with a 25 meter HP17 capillary column was used for all the GC analyses. A Delsi Nermag R10-10C/Kratos MS80RFA combination was used for the Gas Chromatography-Mass Spectroscopy (GCMS) analyses. Infrared spectra were obtained on a Perkin-Elmer 1710 Fourier Transform spectrometer. Preparative thin layer chromatography (TLC) were carried out on a Model 7924T Chromatotron (Harrison Research) using silica gel PF_{254} as absorbent. The melting points (uncorrected) were determined on a Bristoline 6548-J17 Microscope equipped with a Thomas Model 40 Micro Hot Stage.

Materials. Merck silica gel 60 (70-230 mesh) was used for column chromatography. Merck precoated silica gel PF_{254} TLC plate (0.2 mm) was used for

analytical TLC analyses. Veratryl alcohol, eugenol, isoeugenol, t-BuOOH, 4′-methoxyacetophenone, and pyrene were from Aldrich. Vanillin and *m*CPBA was purchased from Fisher Scientific Company and 2,4,6-trichlorophenol was from Eastman Organic Chemicals. TDCSPPFeCl and Cl_{16}TSPPMnCl were synthesized as described in Chapter 2.

3.3.2 Syntheses of lignin model compounds

Veratryl acetate was prepared by acetylation of veratryl alcohol (0.84 grams, 5 mmole) with excess 1:1 acetic anhydride/pyridine at room temperature for 24 hours. Saturated sodium bicarbonate (5 mL) was then added to the mixture and stirred for 20 minutes, extracted (2×15 mL) with ethyl acetate. The ethyl acetate was combined, washed in sequence with saturated sodium bicarbonate (5 mL), water (5 mL), and 10% HCl (2×5 mL). The ethyl acetate layer was dried over sodium sulphate, evaporated, and purified by column chromatography (silica gel, 7:3 hexanes/ethyl acetate as eluent). The veratryl acetate obtained was characterized by ^{1}H NMR and MS.

4-Ethoxy-3-methoxybenzyl alcohol was prepared as reported.[29]

1-(4-ethoxy-3-methoxyphenyl)propane (**44**) was synthesized by hydrogenation of eugenol in ethanol by hydrogen/Pd (on charcoal, 1%) followed by ethylation with ethyl iodide and sodium hydride in N,N-dimethylformamide (DMF). Eugenol (3.28 grams, 0.01 moles) and Pd (1% on charcoal, 0.03 g) were added to ethanol (20 mL) and stirred at room temperature for overnight under hydrogen (1 atm.). The mixture was filtered, and evaporated to give 2-methoxy-4-propylphenol in quantitative yield. The crude 2-methoxy-4-propylphenol was subjected to ethylation without purification. Sodium hydride (2.8 g, 50%) and ethyl iodide (4 g, 0.026 moles) were added to DMF

(10 mL) containing 3 g of 2-methoxy-4-propylphenol and stirred for 60 minutes. Water (10 mL) was added to the solution to decompose remaining sodium hydride and the solution was then extracted twice with ethyl acetate (20 mL). The ethyl acetate was evaporated and the residue purified by column chromatography using 80:20 petroleum ether (high boiling):ethyl acetate as eluent. 1-(4-Ethoxy-3-methoxyphenyl)propane (**44**) was obtained as colourless flakes in 85% yield after recrystallization from diethyl ether/hexane.

1-(4-Ethoxy-3-methoxyphenyl)-1-propene (**52**) was synthesized by ethylation of isoeugenol with ethyl iodide and sodium hydride in DMF following the same procedures as described above. The product was obtained in 80% yield.

4-Ethoxy-3-methoxyphenylglycerol-ß-guaiacyl ether[62] (**62**), *1-(4-ethoxy-3-methoxyphenyl)-2-(4-methoxyphenyl)propane-1,3-diol*[63] (**55**), *ethyl dehydrodiisoeugenol*[64] (**64**), and *4,4′-diethyldehydrodivanillin*[65] (**74**) were synthesized following reported procedures.

4-Methoxyphenylglycol (**58**) was synthesized following a reported procedure[66]. 4′-Methoxyacetophenone (3.0 g) was reacted with cupric bromide (80 mesh, 9.0 g) in 1:1 ethyl acetate/chloroform mixture (40 mL) at reflux temperature for 3 hours to give 4′-methoxy-α-bromoacetophenone in 90% yield. The product was purified by column chromatography using 1:99 (volume) methanol:methylene chloride as eluent to give a light yellow crystaline product, reaction of which with sodium acetate (3.7 g) in acetic anhydride (10 mL) at reflux temperature for 2 hours gave 4′-methoxy-α-hydroxyacetophenone acetate in 80% yield. Reduction of the resulting 4′-methoxy-α-hydroxyacetophenone acetate by sodium borohydride (2.0 g) in methanol (20 mL) at 0°C for 3 hours gave 4-methoxyphenylglycol (**58**) in 90% yield.

3.3.3 The oxidation of the lignin model and related compounds

The TLC separation of reaction mixtures. The products were separated on a Chromatotron using either methanol/methylene chloride (0-1% methanol, volume) or ethyl acetate/hexane (10-30% ethyl acetate, volume) as eluent. The purity of each components was checked by GC and analytical TLC. Impure components were further separated on the Chromatotron. The yields of the products were based on substrate and estimated from GC integration area.

All the reactions were carried out in air at room temperature unless otherwise indicated. No products were detected by TLC in control experiments without the iron porphyrin catalyst.

The oxidation of veratryl alcohol and veratryl acetate. The substrate (0.3 mmole) and TDCSPPFeCl (0.5 μmole in 0.5 mL water) were dissolved in either pH 3 phosphate buffer (0.1 M) or methanol (20 mL) and *m*CPBA (0.6 mmole) was added as a powder and the solution was stirred at room temperature for 2 hours. The solution was partitioned between saturated sodium bicarbonate (20 mL) and ethyl acetate (20 mL). The aqueous layer was further extracted twice with ethyl acetate (10 mL) and the organic extracts were combined, dried over anhydrous sodium sulphate, and evaporated. When veratryl acetate was the substrate, the products were analyzed by GC and separated on a Chromatotron. When veratryl alcohol was the substrate, the products could be separated on a Chromatotron with or without acetylation with 1:1 acetic anhydride/pyridine. The sample for GC analysis had to be acetylated since veratryl alcohol was found to be oxidized on the GC column.

The oxidation of veratryl alcohol in ethanol was carried out under similar conditions as that for the oxidation of veratryl alcohol in methanol except a mixture of 5 mL DMF (to increase the solubility of TDCSPPFeCl) and 20 mL ethanol was used as

the solvent.

The condition for *the oxidation of 4-ethoxy-3-methoxybenzyl alcohol* was the same as that for veratryl alcohol.

The hydrolysis of 2-hydroxymethyl-4,4,5-trimethoxy-2,5-cyclohexadiene-1-one (**37**). 0.25 grams of **37** was dissolved in 10 mL of 1:1 THF/water, shaken with 2 mL concentrated HCl, and extracted with ethyl acetate. The ethyl acetate was washed with water (5 mL), dried and evaporated. The product was shown to be pure **30** as characterized by ^{1}H NMR and MS.

The oxidation of 1-(4-ethoxy-3-methoxyphenyl)propane (**44**). 0.25 mmole of **44** was oxidized by t-BuOOH (1.25 mmole) and TDCSPPFeCl (0.5 μmole) in 20 mL of 1:1 acetonitrile/pH 3 phosphate buffer at room temperature in air for 3 hours. Unreacted t-BuOOH was decomposed by adding solid potassium iodide. The solution was then extracted with ethyl acetate (3×10 mL) and the iodine in the extract was removed by washing with aqueous sodium thiosulphate. The products were acetylated with 1:1 acetic anhydride/pyridine before being subjected to GC, GCMS analyses and separation on a Chromatotron. The yield (estimated from GC) of the products **45**, **46**, **47**, and **48** was 15%, 23%, 20%, and 20%, respectively.

The oxidation of 1-(4-ethoxy-3-methoxyphenyl)-1-propene (**52**) was carried out under the same conditions as that for **44** except the reaction time was 2 hours.

The oxidation of 4-ethoxy-3-methoxyphenylglycerol-ß-guaiacyl ether (**62**). 0.5 mmole of **62** was oxidized by 1 μmole of TDCSPPFeCl and either 1.5 mmole of *m*CPBA or 2.5 mmole of t-BuOOH in 50 mL of 1:1 acetonitrile/pH 3 buffer for 3 hours at room temperature. The workup and analysis procedure was the same as that for **44**.

The conditions for *the oxidation of 1-(4-ethoxy-3-methoxyphenyl)-2-(4-*

methoxyphenyl)propane-1,3-diol (**55**) were the same as those for **62** except the reaction time was 6 hours. The products were separated into neutral and acidic fractions by extracting the ethyl acetate layer with saturated sodium bicarbonate. The acidic part was methylated with diazomethane which was generated by using *p*-toluenesulfonylmethylnitrosamide as reported.[67] The neutral part was acetylated and both the methylated products and the acetylated products were analyzed as described above.

The oxidation of 55 under anaerobic condition. A 25 mL solution (1:1 acetonitrile/pH 3 buffer) containing **55** (0.25 mmole) and TDCSPPFeCl (0.5 μmole) in a 50 mL Schlenk tube was degassed by means of freeze-thaw (3 cycles). The oxidant (*m*CPBA, 0.75 mmole) was put into another small Schlenk tube (10 mL) connected with the one containing the solution and similarly degassed. The contents of the two Schlenk tubes were mixed and stirred for 6 hours after being warmed up to room temperature. The products were acetylated by excess 1:1 acetic anhydride/pyridine and analyzed by GC and GCMS.

The oxidation of ethyldehydrodiisoeugenol (**64**) (0.5 mmole) by TDCSPPFeCl (0.5 μmole) and t-BuOOH (2.5 mmole) in 2:1 acetonitrile/pH 3 buffer (60 mL) for 2 hours in air gave **65** as the major product along with small amount of 4-ethoxy-3-methoxybenzaldehyde. Compound **65** was separated using a Chromatotron and further oxidized under the same conditions for 3 hours. The oxidation of **65** was found to give both neutral and acidic products but the separation of the two groups of compounds by sodium bicarbonate extraction was not successful due to the large molecular sizes of the products. The products were thus methylated with diazomethane before separation. The products were very difficult to separate on a Chromatotron and each component from first separation was further purified on the Chromatotron. Two

parallel experiments were carried out to obtain enough material for NMR and MS characterization of the products.

The oxidation of 4,4'-diethyldehydrodivanillin (**74**). 0.5 mmole of **74** was oxidized by TDCSPPFeCl (1 μmole) and t-BuOOH (0.25 mmole) in 1:1 acetonitrile/pH 3 buffer (60 mL) for 8 hours. The products were separated into neutral and acidic parts. The neutral part (~ 60% of the starting material) contained only the starting material and the acidic part was methylated with diazomethane before separation on the Chromatotron.

The oxidation of pyrene (0.5 mmole) by TDCSPPFeCl (0.1 μmole) and *m*CPBA was carried out in 3:1 acetonitrile/pH 3 buffer (40 mL) at room temperature. The reaction completed in 30 minutes, as followed by UV-vis spectroscopy. Saturated sodium bicarbonate (30 mL) was added to the reaction mixture followed by extracting with ethyl acetate (3 × 50 mL). The products were separated by column chromatography (a large column, 4×30 cm, had to be used due to the low solubility of the compounds in the solvent) using 80:20 toluene/ethyl acetate as eluent. The further oxidation of one of the oxidation products of pyrene, pyrene-1,8-dione (10 mg), by Cl_{16}TSPPMnCl (0.2 μmole) and *m*CPBA (0.2 g) was carried out for 12 hours in 2:1 acetonitrile/pH 3 buffer (30 mL). The reaction mixture was partitioned between saturated sodium bicarbonate (20 mL) and ethyl acetate (20 mL). Black tars which were insoluble in either water or organic solvents were found. The small amounts of compounds in the ethyl acetate extract was not identified.

The oxidation of 2,4,6-trichlorophenol. 2,4,6-Trichlorophenol (2 mmole) was oxidized by TDCSPPFeCl (0.5 μmole) and *m*CPBA (4 mmole) in 2:1 acetonitrile/pH 3 buffer (30 mL) for 12 hours. The reaction mixture was extracted three times with ethyl acetate (3 × 30 mL). TLC analysis using methanol/methylene chloride (0.5:99.5) as

eluent showed the presence of only small amount of starting material. The products were separated on silica gel column using methanol/methylene chloride (0.5:99.5) as eluent to give a mixture of two yellow compounds, which was further separated on column using ethyl acetate/hexane (5:95) as solvent.

3.3.4 Characterization of compounds

All compounds were characterized by ^{1}NMR and MS unless otherwise specified. Elemental analyses and ^{13}C NMR were performed when enough product was available.

Methyl (z)-furan-5(2H)-one-3-butenoate (**26**) (^{1}H NMR and MS the same as those reported[11])

^{1}H NMR ($CDCl_3$) δ: 3.78 (3H, S), 5.25 (2H, m), 6.13 (1H, d, J=12Hz), 6.30 (1H, m), 6.77 (1H, dd, J_1=12Hz, J_2=1-2 Hz).

MS m/z(%): 168 (12.6, M), 137 (19.4), 136(48.2), 124(35.2), 111(26.0), 109(33.4), 108(21.6), 81(49.2), 80(28.6), 79(60.5), 59(22.5), 53(94.8), 52(45.5), 51(100.0), 50(46.6).

Methyl (Z)-6-oxo-2H-pyran-3(6H)-ylideneacetate (**28**) (^{1}NMR and MS similar to those reported[17])

^{1}H NMR ($CDCl_3$) δ: 3.80(3H, S), 5.03(2H, d, J=2Hz), 5.94(1H, m), 6.21(1H, dd, J_1=10Hz, J_2=2Hz), 8.35(1H, dd, J_1=1Hz, J_2=10Hz).

MS m/z(%): 168(13.0), 136(17.9), 124(14.8), 112(10.7), 109(33.0), 108(14.0),

81(36.5), 80(10.7), 79(10.9), 59(12.6), 53(100.0), 52(23.3), 51(37.0), 50(19.0)

M.P.: 87-90°C (reported[17]: 87-90°C).

Methyl (E)-6-oxo-2H-pyran-3(6H)-ylideneacetate (**29**)(^{1}H NMR and MS similar to those reported[17])

^{1}H NMR ($CDCl_3$) δ: 3.78(S, 3H), 5.69(2H, d, J=3Hz), 5.99(1H, m) 6.19(1H, d, J=10Hz) 7.01(1H, dd, J_1=1Hz, J_2=10Hz).

MS m/z(%): 168(14.0), 137(16.7) 136(100), 111(13.5), 109(25.2), 108(37.3), 97(11.2), 83(10.5), 81(42.3), 80(31.8), 79(29.1), 53(61.0), 52(20.1), 51(37.2).

M.P.: 147-150°C (reported[17]: 147-150 °C).

2-Hydroxymethyl-5-methoxy-2,5-cyclohexadiene-1,4-dione (**30**)(^{1}H NMR and MS similar to those reported[68])

^{1}H NMR ($CDCl_3$) δ: 3.85 (3H, S), 4.57(2H, J=1 Hz), 5.92(1H, S), 6.72(1H, t, J=1 Hz).

^{13}C NMR (CD_3OD) δ: 188.798, 183.500, 160.461, 150.891, 129.456, 108.426, 58.959, 56.959.

MS m/z(%): 170(M, 1.2), 169(16.5), 168(100.0), 167(64.9), 153(16.9), 150(12.2),

140(10.2), 139(55.4), 122(15.6), 111(31.9), 83(14.4).

Exact mass calcd. for $C_8H_{10}O_4$: 170.0579; found (HRMS): 170.0588.

M.P.: 142-143°C (reported[68]: 144-145°C).

4,5-Dimethoxy-3,5-cyclohexadiene-1,2-dione (**32**)(^{1}H NMR and MS similar to those reported[17])

^{1}H NMR ($CDCl_3$) δ: 3.90(6H, S), 5.78(2H, S).

MS m/z(%): 170(5.74), 168(3.38), 167(7.28), 155(4.12), 149(24.44), 140(100.0), 125(27.94), 69(18.34).

Exact mass calcd. for $C_8H_8O_4$: 168.0420; found (HRMS): 168.0403.

2-Acetoxymethyl-5-methoxy-2,5-cyclohexadiene-1,4-dione (**34**)

^{1}H NMR ($CDCl_3$) δ: 2.17(3H, S), 3.85(3H, S), 5.02(2H, d, J=1-2Hz), 5.95(1H, S), 6.62(1H, t, J=1-2Hz).

^{13}C NMR ($CDCl_3$) δ: 185.947, 181.402, 169.860, 158.628, 143.815, 129.264, 107.495, 59.642, 56.468, 20.774.

MS m/z(%): 210(2.41), 168(100.0), 167(25.23), 153(10.16), 139(13.23), 69(22.9),

43(78.0).

Exact mass calcd. for $C_{10}H_{10}O_5$: 210.0528, found (HRMS): 210.0535

M.P.: 158-160°C.

3,4-Dimethoxyphenol (**35**)

^1H NMR ($CDCl_3$) δ: 3.84(3H, S), 3.86(3H, S), 4.56(1H, broad), 6.36(1H, dd, J_1=9Hz, J_2=2Hz), 6.50(1H, d, J=2Hz), 6.75(1H, d, J=9Hz)

MS m/z(%): 154(100.0), 139(94.8), 111(62.7), 96(10.6), 93(40.8), 81(11.0), 69(21.5), 68(11.1), 65(25.4), 55(12.7).

Dimethyl 3-acetoxymethyl-2,4-hexadienedioate (**36**)

^1H NMR ($CDCl_3$) δ: 2.12(3H, S), 3.705(3H, S), 3.710(3H, S), 4.85(2H, m), 6.00(1H, d, J=12Hz), 6.00(1H, d, J=1-2Hz), 7.06(1H, dd, J_1=12Hz, J_2=1-2Hz).

MS m/z(%): 242(0.1), 184(9.8), 183(100.0), 169(28.4), 141(22.7), 136(10.5), 109(43.8), 43(55.5).

Exact mass calcd. for $C_{11}H_{14}O_6$: 242.0786; found (HRMS): 242.0782.

2-Hydroxymethyl-4,4,5-trimethoxy-2,5-cyclohexadiene-1-one (**37**) (identified as its acetate)

^{1}H NMR ($CDCl_3$) δ: 2.14(3H, S), 3.34(6H, S), 3.84(3H, S), 4.92(2H, d, J=1-2Hz), 5.67(1H, S), 6.53(1H, t, J=1-2Hz).

^{13}C NMR ($CDCl_3$) δ: 184.449, 170.076, 169.097, 136.119, 136.057, 103.832, 94.349, 60.314, 56.252, 51.534, 20.898.

MS m/z(%): 256(2.2), 241(25.9), 199(33.2), 183(100.0), 182(25.9), 167(29.0), 155(50.8), 139(29.7), 124(23.4), 123(61.5), 95(28.4), 69(32.9), 43(85.9).

Anal. calcd. for $C_{12}H_{16}O_6$, C: 56.25; H: 6.29. found: C: 56.37; H: 6.37.

Exact mass calcd. for $C_{12}H_{16}O_6$: 256.0948, found (HRMS) 256.0948.

M.P.: 79-81°C.

2-Dimethoxymethyl-4,4,5-trimethoxy-2,5-cyclohexadiene-1-one (**38**)

^{1}H NMR ($CDCl_3$) δ: 3.35(6H, S), 3.39(6H, S), 3.82(3H, S), 5.34(1H, S), 5.65(1H, S), 6.81(1H, S).

^{13}C NMR ($CDCl_3$) δ: 184.744, 168.959, 137.144, 104.092, 97.798, 94.454, 56.222, 54.032, 51.540, 29.679.

MS (EI) m/z(%): 243(0.3), 227(100.0), 212(19.8), 180(37.3), 153(10.8), 75(31.5), 69(12.1).

MS (DCI+NH_3) m/z(%): 259(29.6, M+1), 227(58.4), 213(13.6), 212(100.0).

4-Ethoxy-2-hydroxymethyl-4,5-dimethoxy-2,5-cyclohexadiene-1-one (**40**) (isolated as its acetate)

^{1}H NMR ($CDCl_3$) δ: 1.23(3H, t, J=7Hz), 2.13(3H, S), 3.31(3H, S), 3.40-3.60(2H, m, when decoupled at 1.23 , pattern close to a AB quartet), 4.91(2H, d, J=1Hz), 5.66(1H, S), 6.52(1H, t, J=1Hz).

MS m/z(%): 270(1.5), 241(29.7), 199(35.8), 197(87.2), 183(100.0), 182(26.1), 169(45.2), 167(43.8), 155(32.4), 153(26.7), 141(31.0), 139(25.6), 123(51.3), 109(57.4), 95(24.2), 69(28.6), 43(88.5).

5-Ethoxy-2-hydroxymethyl-4,4-dimethoxy-2,5-cyclohexadiene-1-one (**41**) (identified as its acetate)

^{1}H NMR ($CDCl_3$) δ: 1.47(3H, t, J=8Hz), 2.13(3H, S), 3.33(6H, S), 4.05(2H, q, J=8Hz), 4.92(2H, d, J=1Hz), 5.63(1H, S), 6.51(1H, t, J=1Hz).

MS m/z(%): 270(1.8), 199(23.8), 197(100.0), 182(32.9), 169(37.2), 153(24.6), 141(35.7), 139(34.3), 123(14.8), 109(43.9), 69(27.1), 43(76.0).

2-Dimethoxymethyl-5-ethoxy-3,4-dimethoxy-2,5-cyclohexadiene-1-one (**42**)

^{1}H NMR ($CDCl_3$) δ: 1.46(3H, t, J=8Hz), 3.35(6H, S), 3.39(6H, S), 4.03(2H, q,

J=8Hz), 5.34(1H, S), 5.61(1H, S), 6.79(1H, S).

MS m/z(%): 242(13.3), 241(100.0), 226(28.4), 194(44.9), 181(17.4), 167(10.8), 153(16.2), 75(24.1), 69(13.6).

1-(4-Ethoxy-3-methoxyphenyl)propane (**44**)

^{1}H NMR ($CDCl_3$) δ: 0.94(3H, t, J=8Hz), 1.44(3H, t, J=7Hz), 1.57-1.67(2H, m), 2.53(2H, t, J=9Hz), 3.86(3H, s), 4.07(3H, q, J=7Hz), 6.67-6.81(3H, m).

MS m/z(%): 194(35.2), 166(10.9), 165(35.2), 138(10.6), 137(100.0), 122(6.5).

M.P.: 33-34°C.

(6)-Ethyl (1)-methyl 3-propyl-2,4-hexadienedioate (**45**)

^{1}H NMR ($CDCl_3$) δ: 0.93(3H, t, J=7Hz), 1.26(3H, t, J=7Hz), 1.44-1.57(2H, m), 2.39(2H, t, J=7Hz), 3.67(3H, s), 4.34(2H, q, J=7Hz), 5.76(1H, s, broad), 5.88(1H, d, J=12Hz), 7.05(1H, dd, J_1=12Hz, J_2=1-2Hz).

MS m/z(%): 226(2.74), 211(1.10), 195(4.73), 194(2.27), 181(9.78), 167(71.67), 153(100.0), 149(10.12), 139(75.41).

Exact mass calcd. for $C_{12}H_{18}O_4$: 226.1200; found (HRMS): 226.1204.

2-Ethoxy-5-propyl-2,5-cyclohexadiene-1,4-dione (**46**)

^{1}H NMR ($CDCl_3$) δ: 0.97(3H, t, J=8Hz), 1.47(3H, t, J=7Hz), 1.51-1.57(2H, m), 2.41(2H, m), 4.01(2H, q, J= 7Hz), 5.90(1H, s), 6.49(1H, s, broad).

MS m/z(%): 194(4.0), 179(3.7), 167(4.1), 166(5.1), 165(8.4), 151(34.8), 150(23.7), 149(32.6), 69(100.0), 67(22.3), 57(25.6), 55(23.4), 53(28.0), 44(20.6), 43(34.4), 41(30.0).

1-(4-Ethoxy-3-methoxyphenyl)propanol (**47**) (identified as its acetate, its GC retention time was the same as that of the synthesized standard and its MS was similar to that of the standard.

MS m/z(%) 252(30.1), 193(22.8), 192(28.0), 181(100.0), 165(15.5), 164(27.4), 163(14.7), 149(14.9), 133(12.1), 125(15.4), 107(14.9), 105(12.4), 103(10.9), 93(17.5), 91(15.7), 77(15.5), 65(13.1), 57(18.7), 43(54.3).

4-Hydroxy-2-methoxy-4-propyl-2,5-cyclohexadiene-1-one (**48**)

^{1}H NMR ($CDCl_3$) δ: 0.94(3H, t, J=8Hz), 1.26-1.36(2H, m), 1.76-1.81(2H, m), 1.92(1H, s, exchangeable), 3.69(3H, s), 5.72(1H, d, J=2-3Hz), 6.20(1H, d, J=10Hz), 6.83(1H, dd, J_1=2-3Hz, J_2=10Hz).

MS m/z(%): 182(13.9), 166(21.8), 140(22.8), 139(100.0), 111(39.3), 94(29.41), 93(33.3), 81(26.7), 79(32.0), 77(46.0), 69(88.0), 68(29.3), 67(25.5), 66(28.9), 65(68.4),

55(85.5), 53(53.4), 52(26.6), 51(47.6).

Exact mass calcd. for $C_{10}H_{14}O_3$: 182.0939; found (HRMS): 182.0942.

FTIR (KBr pellet) (cm^{-1}): 3436, 1672, 1645, 1214.

1-(4-Ethoxy-3-methoxyphenyl)-1-propene (**52**)

^1H NMR ($CDCl_3$) δ: 1.45(3H, t, J=7Hz), 1.86(3H, dd, J_1=7Hz, J_2=1-2Hz), 3.88(3H, s), 4.09(2H, q, J=7Hz), 6.06-6.15(1H, m), 6.32-6.37(1H, m), 6.79-6.91(3H, m).

MS M/z(%): 192(100.0, M), 165(6.8), 164(63.1), 163(35.8), 149(31.0), 133(14.7), 131(17.2), 121(11.5), 107(34.6), 103(30.0).

M.P.: 58-59°C (reported[69]: 64°C).

1-(4-Ethoxy-3-methoxyphenyl)propane-1,2-diol (**53**) (isolated as its diacetate)

^1H NMR ($CDCl_3$) δ:1.08(3H, d, J=7Hz), 1.45(3H, t, J=7Hz), 2.05(3H, s), 2.07(3H, s), 3.89(3H, s), 4.10(2H, q, J=7Hz), 5.23-5.29(1H, m), 5.71(1H, d, J=8Hz), 6.82-6.91(3H, m).

MS m/z(%): 310(8.0), 266(3.0), 250(9.0), 223(7.5), 208(15.4), 182(11.3), 181(100.0), 151(19.6), 125(10.1), 43(41.6).

Exact mass calcd. for $C_{16}H_{22}O_6$: 310.1414; found (HRMS): 310.1416.

4-Hydroxy-4-(4-ethoxy-3-methoxyphenyl)-3-methylbutyronitrile **(54)** (identified as its acetate)

^{1}H NMR ($CDCl_3$) δ: 1.00(3H, d, J=7Hz), 1.45(3H, t, J=8Hz), 2.10(3H, s), 2.30-2.40(2H, m), 2.46-2.53(1H, m), 3.89(3H, s), 4.10(2H, q, J=8Hz), 5.51 and 5.60 (1H, two doublets in a ratio of 7:2, J=8Hz), 6.80-6.84(3H, m).

MS m/z(%): 291(10.1), 232(3.4), 223(3.6), 204(1.4), 203(1.8), 182(10.6), 181(100.0), 164(3.7), 153(14.5), 86(17.3), 84(27.4), 43(35.3).

Exact mass calcd. for $C_{16}H_{21}O_4N$: 291.1465; found (HRMS): 291.1471.

1-(4-Ethoxy-3-methoxyphenyl)-2-(4-methoxyphenyl)propane-1,3-diol **(55)** (characterized as its diacetate, mixture of stereo isomers).

^{1}H NMR ($CDCl_3$) δ: 1.38-1.47(3H, two triplets centred at 1.40 and 1.44, respectively), 1.94-2.10(6H, four singlets at 1.94, 1.96, 2.01, and 2.09, respectively), 3.32-3.45(1H, m), 3.70-3.79(6H, four singlets at 3.71, 3.75, 3.76, and 3.79, respectively), 4.00-4.13(2H, m), 4.25-4.51(2H, m), 5.94-6.05(1H, two doublets centred at 5.96 and 6.04, respectively), 6.49-7.11(7H, m).

MS m/z(%): 416(2.9, M), 356(2.3), 297(1.9), 223(23.2), 182(11.1), 181(100.0), 134(12.7), 43(23.0).

4-Ethoxy-3-methoxybenzaldehyde (**56**)

^{1}H NMR ($CDCl_3$) δ: 1.51(3H, t, J=7Hz), 3.94(3H, s), 4.20(2H, q, J=7Hz), 6.98(1H, d, J=8Hz), 7.42-7.48(2H, m), 9.86(1H, s).

MS m/z(%): 181(6.6, M+1), 180(62.0, M), 152(55.1), 151(100.0), 109(11.2).

M.P.: 59-60°C (reported[70]: 64-65°C)

4′-Methoxy-α-hydroxyacetophenone (**57**)

^{1}H NMR ($CDCl_3$) δ: 3.58(1H, t, J=5Hz, exchangeable), 3.90(3H, s), 4.83(2H, d, J=5Hz), 6.98(2H, d, J=9Hz), 7.90(2H, d, J=9Hz).

MS m/z(%): 166(10.0), 136(30.7), 135(100.0), 107(35.5), 92(46.2), 77(64.4), 64(21.0).

M.P.: 101-103°C (reported[71]: 100°C, 104°C).

4′-Methoxyphenylglycol (**58**)

^{1}H NMR ($CDCl_3$) δ: 2.17(1H, broad, exchangeable), 2.55(1H, broad, exchangeable), 3.60-3.79(2H, m), 3.81(3H, s), 4.78(1H, m), 6.90(2H, d, J=8Hz), 7.31(2H, d, J=8Hz).

MS m/z(%): 168(1.1, M), 150(14.5), 137(14.4), 136(14.9), 135(29.5), 122(10.6), 121(100.0), 91(13.7), 78(20.7), 77(43.7).

M.P.: 79-80°C (reported[72]: 82°C)

4-Ethoxy-3-methoxybenzoic acid (**59**) (isolated as its methyl ester)

^{1}H NMR ($CDCl_3$) δ: 1.52(3H, t, J=7Hz), 3.90(3H, s), 3.93(3H, s), 4.16(2H, q, J=7Hz), 6.88(1H, d, J=8Hz), 7.54(1H, d, J=2Hz), 7.66(1H, dd, J_1=8Hz, J_2=2Hz).

MS m/z(%): 211(5.8, M+1), 210(4.2, M), 182(40.4), 179(10.6), 152(11.3), 151(100.0), 149(19.3), 123(15.0), 79(19.6), 77(11.1), 65(14.0).

4-Methoxybenzaldehyde (**60**)

^{1}H NMR ($CDCl_3$) δ: 3.93(3H, s), 7.05(2H, d, J=8Hz), 7.88(2H, d, J=8Hz), 9.62(1H, s).

MS m/z(%): 137(6.1, M+1), 136(73.2, M), 107(15.0), 92(12.7), 77(28.3).

4-Methoxybenzoic acid (**61**) (isolated as its methyl ester)

^{1}H NMR ($CDCl_3$) δ: 3.88(3H, s), 3.90(3H, s), 6.93(2H, d, J=8Hz), 8.00(2H, d, J=8Hz).

MS m/z(%): 167(3.5, M+1), 166(8.9, M), 135(46.0), 107(10.1), 85(27.7), 83(40.2), 77(10.6), 67(24.3), 64(11.4), 55(10.3), 50(11.0), 44(100.0).

4-Ethoxy-3-methoxyphenylglycerol-ß-guaiacyl ether (**62**)

^{1}H NMR ($CDCl_3$) δ: 1.48(3H, t, J=7Hz), 3.88(6H, two close singlets), 3.91(3H, s), 4.02-4.20(3H, m), 4.99(2H, m), 6.80-7.15(7H, m).

MS m/z(%): 348(3.4, M), 300(6.6), 208(10.0), 206(6.6), 195(5.4), 182(16.0), 181(30.8), 180(33.2), 165(15.2), 164(10.3), 153(15.3), 152(21.1), 151(39.2), 150(93.0), 138(35.0), 137(33.7), 125(30.2), 124(78.1), 123(22.3), 122(13.9), 121(20.2), 110(10.0), 109(68.3), 97(10.7), 95(17.5), 93(22.4), 91(13.2), 83(13.3), 81(31.0).

4-O-ethyldehydrodiisoeugenol (**64**)

^{1}H NMR ($CDCl_3$) δ: 1.39(3H, d, J=7Hz), 1.46(3H, t, J=8Hz), 2.07(3H, dd, J_1=7Hz, J_2-0-1Hz), 3.43-3.52(1H, m), 3.87(3H, s), 3.90(3H, s), 4.10(2H, q, J=8Hz), 5.12(1H, d, J=9Hz), 6.07-6.17(1H, m), 6.34-6.42(1H, m), 6.77-7.01(5H, m).

MS m/z(%): 355(24.1, M+1), 354(100.0, M), 137(14.1), 91(16.7), 77(21.0), 65(14.6), 55(19.2).

M.P.: 121-122°C.

2,3-Dihydro-5-formyl-7-methoxy-3-methyl-2-(4-ethoxy-3-methoxypheny)benzofuran (**65**)

^{1}H NMR ($CDCl_3$) δ: 1.44-1.49(6H, overlap of a doublet and a triplet), 3.53-3.62(1H, m), 3.87(3H, s), 3.96(3H, s), 4.12(2H, q, J=8Hz), 5.27(1H, d, J=9Hz), 6.85-6.98(3H, m, aromatic), 7.35-7.42(2H, aromatic), 9.86(1H, s).

MS m/z(%): 343(21.9, M+1), 342(100.0, M), 314(11.9), 313(21.3), 157(11.4), 149(12.7), 137(33.7), 103(10.3), 95(19.1), 91(29.9), 89(16.0), 79(18.2), 78(17.6), 77(58.2), 76(18.0), 65(33.2), 64(12.5), 63(19.5), 55(31.6), 53(16.1), 52(10.6), 51(28.6), 44(22.0), 43(15.0), 41(12.9), 40(24.3).

M.P.: 93-95°C.

5-Carboxy-2,3-dihydro-7-methoxy-3-methyl-2-(4-ethoxy-3-methoxyphenyl)benzofuran (**66**) (isolated as its methyl ester)

^{1}H NMR ($CDCl_3$) δ: 1.42(3H, d, J=7Hz), 1.46(3H, t, J=8Hz), 3.49-3.58(1H, m), 3.87(3H, s), 3.91(3H, s), 3.94(3H, s), 4.11(2H, q, J=8Hz), 5.22(1H, d, J=9Hz), 6.84-6.97(3H, aromatic), 7.51(2H, broad s, aromatic).

MS m/z(%): 372(18.3, M), 167(21.0), 149(58.5), 111(10.4), 83(11.9), 77(10.7), 76(10.9), 71(49.4), 70(50.5), 69(18.8), 65(10.9), 59(16.6), 57(100.0), 56(24.7), 55(47.7), 44(32.1), 43(69.4), 42(13.3), 41(61.0), 40(61.2).

M.P.: 143-145°C.

5-Carboxy-2,3-dihydro-2-[(6)-ethyl (1)-methyl 2-(E)-4-(Z)-2,4-hexadienedioate-3-yl]-

7-methoxy-3-methylbenzofuran (67) (isolated as its methyl ester)

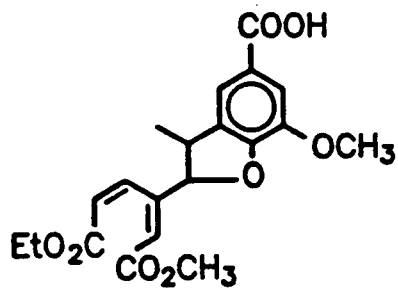

^{1}H NMR ($CDCl_3$) δ: 1.27(3H, t, J=8Hz), 1.39(3H, d, J=7Hz), 3.42-3.47(1H, m), 3.69(3H, s), 3.90(3H, s), 3.95(3H, s), 4.17(2H, q, J=8Hz), 5.18(1H, d, J=8Hz), 6.07(1H, d, J=12-13Hz), 6.14(1H, d, J=0-1Hz), 6.94(1H, dd, J_1=12-13Hz, J_2=0-1Hz), 7.49-7.54(2H, aromatic).

NOE difference spectrum: When irradiated at 5.18 ppm, positive signals appeared at 6.14 and 6.94 ppm.

MS m/z(%): 404(23.8), 373(18.3), 358(35.3), 345(17.3), 344(37.7), 331(27.9), 330(27.7), 315(15.3), 314(17.2), 299(40.0), 298(19.6), 285(20.0), 271(27.7), 269(17.1), 267(22.6), 179(100.0), 167(15.5), 151(23.4), 150(22.3), 149(33.3), 123(26.0), 59(17.1), 57(28.5), 41(20.5).

Exact mass calcd. for $C_{21}H_{24}O_8$: 404.1472; found (HRMS): 404.1479.

2,3-Dihydro-5-formyl-2-[(6)-ethyl (1)-methyl 2-(E)-4-(Z)-2,4-hexadienedioate-3-yl)-7-methoxy-3-methylbenzofuran (68)

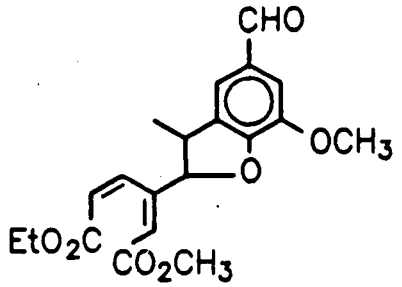

68

^{1}H NMR ($CDCl_3$) δ: 1.26(3H, t, J=8Hz), 1.41(3H, d, J=8Hz), 3.45-3.54 (1H, m), 3.69(3H, s), 3.96(3H, s), 4.18(2H, q, J=8Hz), 5.23(1H, d, J=8Hz), 6.09 (1H, d, J=12Hz), 6.13(1H, m), 6.91-6.97(1H, m), 7.30(1H, broad s), 7.35(1H, broad s), 9.83(1H, s).

NOE difference spectrum: When irradiated at 5.23 ppm, positive signal appeared at 6.13 ppm and 6.1-6.97 ppm.

MS m/z(%): 374(31.0), 342(25.9), 329(24.8), 328(72.2), 315(29.1), 314(42.0), 301(72.7), 300(44.1), 296(29.3), 270(23.2), 269(100.0), 241(61.3), 240(21.3), 213(54.3), 209(21.1), 181(20.9), 155(40.0), 150(35.9), 149(23.3), 135(20.2), 123(67.4), 115(24.2), 111(26.6), 91(28.8), 79(27.0), 77(37.5), 69(26.8), 65(24.1), 59(69.1), 57(25.8), 55(32.6), 53(21.5), 51(25.1), 44(37.8), 43(51.1), 41(33.9).

Exact mass calcd. for $C_{20}H_{22}O_7$: 374.1366; found (HRMS): 374.1369.

2,3-Dihydro-5-formyl-2-[(6)-ethyl (1)-methyl 2-(E)-4-(E)-2,4-hexadienedioate-3-yl]-7-methoxy-3-methylbenzofuran (**69**)

^{1}H NMR ($CDCl_3$) δ: 1.33(3H, t, J=8Hz), 1.49(3H, d, J=8Hz), 3.40-3.46(1H, m),

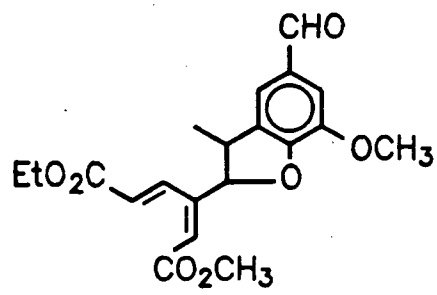

69

3.76(3H, s), 3.98(3H, s), 4.16(2H, q, J=8Hz), 5.25(1H, d, J=7Hz), 6.16(1H, d, J=16Hz), 6.16(1H, s, broad), 7.33(1H, s, broad), 7.40(1H, s, broad), 8.50(1H, d, broad, J=16Hz), 9.85(1H, s).

NOE difference spectrum: When irradiated at 5.25 ppm, positive signal appeared at 6.16 ppm (both the singlet and the doublet).

MS m/z(%): 374(28.7), 342(11.8), 328(37.2), 314(22.8), 301(100.0), 300(23.4), 269(61.9), 268(29.9), 241(38.6), 213(26.1), 150(25.3), 123(25.1), 111(27.8), 77(20.2), 59(25.4), 57(20.9), 55(24.1), 44(33.3), 43(33.9), 41(22.0).

Exact mass calcd. for $C_{20}H_{22}O_7$: 374.1366; found (HRMS): 374.1371.

2-Acetyl-4-formyl-6-methoxyphenyl 4-ethoxy-3-methoxybenzoate (**70**)

^{1}H NMR ($CDCl_3$) δ: 1.53(3H, t, J=8Hz), 2.59(3H, s), 3.92(3H, s), 3.97(3H, s), 4.22(2H, q, J=8Hz), 6.99(1H, d, J=8Hz), 7.68-7.72(2H, m), 7.90(1H, dd, J_1=8Hz, J_2=2Hz), 7.96(1H, d, J=2Hz), 10.03(1H, s).

MS m/z(%): 372(2.4), 180(36.8), 179(100.0), 123(37.3), 65(20.7), 59(31.5),

57(26.4), 55(22.6), 51(20.1), 43(55.9), 41(36.9), 31(20.7).

4,4′-Diethyldehydrodivanillin (**74**)

^{1}H NMR ($CDCl_3$) δ: 1.12(6H, t, J=8Hz), 3.98(6H, s), 4.02(4H, q, J=8Hz), 7.46(2H, d, J=1-2Hz), 7.51(2H, d, J=1-2Hz), 9.91(2H, s).

MS m/z(%): 359(10.4, M+1), 358(52.2, M), 302(20.8), 241(10.7), 91(16.2), 32(16.9), 28(100.0).

M.P.: 142-144°C.

4,4′-Diethoxy-3,3′-dimethoxy-5-carboxy-5′-formylbiphenyl (**75**) (isolated as its methyl ester)

^{1}H NMR ($CDCl_3$) δ: 1.09(3H, t, J=7 Hz), 1.12(3H, t, J=7 Hz), 3.91(3H, s), 3.96(3H, s), 3.97(3H, s), 3.94-4.04(4H, m), 7.43(1H, d, J=1-2 Hz), 7.49(1H, d, J=1-2 Hz), 7.65(2H, s, broad), 9.90(1H, s).

MS m/z (%): 389(M+1, 22.5), 388(M, 100.0), 360(20.7), 332(18.6), 301(15.1), 300(56.9), 272(15.5), 271(15.8).

Exact mass calcd. for $C_{21}H_{24}O_7$: 388.1523; found (HRMS): 388.1529.

M.P.: 110-112°C.

4,4′-Diethyldehydrodivanillic acid (**76**) (isolated as its dimethyl ester)

^{1}H NMR ($CDCl_3$) δ: 1.10(6H, t, J=7 Hz), 3.90(6H, s), 3.95(6H, s), 3.96(4H, q, J=7Hz), 7.62(4H, s).

MS m/z (%): 419(M+1, 22.8), 418(M, 100.0), 390(22.6), 358(21.2), 330(82.6), 313(26.8), 299(20.5), 284(21.6), 242(29.3), 209(21.3), 59(25.3), 57(20.7), 43(21.5), 41(22.9).

Exact mass calcd. for $C_{22}H_{26}O_8$: 418.1628 ; found(HRMS): 418.1632.

M.P.: 102-104°C.

(1)-Ethyl (6)-methyl 2-(2-ethoxy-3-methoxy-5-formylphenyl)-4-carboxy-2,4-hexadienedioate (**77**) (isolated as its methyl ester)

^{1}H NMR ($CDCl_3$) δ: 1.21(3H, t, J=7 Hz), 1.27(3H, t, J=7 Hz) 3.76(3H, s), 3.82(3H, s), 3.94(3H, s), 4.10(2H, q, J=7 Hz), 4.16(2H, q, J=7 Hz), 6.80(1H, d, J=1-2 Hz), 7.26(1H, d, J=1-2 Hz), 7.50(1H, d, J=1-2 Hz), 7.54(1H, d, J=1-2 Hz), 9.93(1H, s).

MS m/z (%): 420(M, 4.6), 361(5.6), 347(14.8), 315(7.1), 287(27.7), 259(13.5), 149(12.7), 115(18.1), 91(14.2), 77(20.8), 69(13.6), 63(13.9), 57(17.3), 55(20.1), 51(18.7), 50(15.0), 45(19.), 44(100.0).

Exact mass calcd. for $C_{21}H_{24}O_9$: 420.1421; found(HRMS): 420.1429.

(1)-Ethyl (6)-methyl 2-(2-ethoxy-3-methoxy-5-carboxyphenyl)-4-carboxy-2,4-hexadienedioate (**78**) (isolated as its dimethyl ester)

^{1}H NMR ($CDCl_3$) δ: 1.21(3H, t, J=7Hz), 1.25(3H, t, J=7Hz), 3.76(3H, s), 3.80(3H, s), 3.92(6H, s), 4.05(2H, q, J=7Hz), 4.14(2H, q, J=7Hz), 6.77(1H, d, J=1-2Hz), 7.24(1H, d, J=1-2Hz), 7.63(1H, d, J=1-2Hz), 7.73(1H, d, J=1-2Hz).

MS m/z (%): 450(M, 18.2), 391(46.3), 377(58.5), 359(21.2), 345(48.1), 331(40.8), 318(23.7), 317(100.0), 303(39.2), 287(23.0), 285(34.9), 273(24.7), 262(42.6), 259(26.8), 258(31.9), 257(22.0), 234(33.3), 233(22.9), 203(67.2), 175(20.5), 149(42.0), 115(25.6), 91(31.5), 77(32.4), 71(20.9), 69(25.2).

Exact mass calcd. for $C_{22}H_{26}O_{10}$: 450.1526; found(HRMS): 450.1524.

Pyrene-1,6-dione (**80**)

^{1}H NMR (DMSO-d_6, δ): 6.72 (2H, d, J=10 Hz), 8.02(2H, d, J=10Hz), 8.14(2H, d, J=8Hz), 8.42(2H, d, J=8Hz).

MS m/z (%): 234(M+2, 14.3), 233(M+1, 19.3), 232(M, 100.0), 204(42.8), 176(89.0), 92(30.9), 91(62.4), 88(79.5), 87(23.0), 75(34.6).

Exact. mass calcd. for $C_{16}H_8O_2$: 232.0540; found (HRMS): 232.0523.

M.P.: sublimes at around 240°C.

Pyrene-1,8-dione (**81**)

^{1}H NMR (DMSO-d_6, δ): 6.69(2H, d, J=9Hz), 7.99-8.03(4H, overlap of a doublet with a singlet at 8.02), 8.54(2H, s).

MS m/z (%): 234(M+2, 27.0), 233(M+1, 20.5), 232(M, 100.0), 205(21.9), 204(44.5), 176(95.9), 175(20.0), 150(20.4), 92(26.7), 91(52.1), 88(82.5), 87(24.2), 75(38.7).

Exact mass calcd. for $C_{16}H_8O_2$: 232.0540; found (HRMS): 232.0519.

M.P.: sublimes at around 190°C.

2,6-Dichloro-*p*-benzoquinone (**83**)

^{1}H NMR ($CDCl_3$) δ: 7.05 (s)

MS m/z (%): 180(10.9), 178(51.8), 176(68.1), 150(13.4), 148(21.8), 141(16.8), 122(36.7), 120(56.8), 116(13.0), 115(15.6), 113(49.1), 90(26.8), 88(77.7), 87(23.0), 85(31.5), 62(47.8), 61(23.0), 60(100.0), 53(94.3), 52(12.1), 50(47.9), 49(38.9).

Exact mass calcd. for $C_6H_2O_2Cl_2$ (Cl^{35} isotope): 175.9432; found (HRMS): 175.9428.

References for chapter 3

1. K. Lundquist, and T.K. Kirk, Phytochem. **17**, 1676, 1978.
2. M. Shimada, F. Nakatsubo, T.K. Kirk, and T. Higuchi, Arch. Microbiol. **129**, 321, 1981.
3. T.K. Kirk, and R.L. Farrell, Annu. Rev. Microbiol. **41**, 465, 1987.
4. M.S.A. Leisola, D.C. Ulmer, R. Waldner, and A. Fiechter, J. Biotechnol. **1**, 331, 1984.
5. D.C. Ulmer, M.S.A. Leisola, and A. Fiechter, J. Biotechnol. **1**, 13, 1984.
6. S.D. Haemmerli, M.S.A. Leisola, D. Sanglard, and A. Fiechter, J. Biol. Chem. **261**, 6900, 1986.
7. T. Tonon, and E. Odier, Appl. Environ. Microbiol. **54**, 466, 1988.
8. P.J. Harvey, H.E. Schoemaker, and J.M. Palmer, Collq. INRA **40** (Lignin Enzymic Microb. Degrad.), 145, 1987.
9. H. Wariishi, and M.H. Gold, FEBS Letters, **243**, 165, 1989.
10. B.D. Faison, T.K. Kirk, and R.L. Farrell, Appl. Environ. Microbiol. **52**, 251, 1986.
11. M.S.A. Leisola, B. Schmidt, U. Thaner-Wyss, and A. Fiechter, FEBS Letters, **189**, 267, 1987.
12. M.S.A. Leisola, S.D. Haemmerli, R. Waldner, H.E. Schoemaker, H.W.H. Schmidt, and A. Fiechter, Cellulose Chem. Technol. **22**, 267, 1988.
13. M. Shimada, T. Hattori, T. Umezawa, T. Higuchi, and T. Okamoto, Collq. INRA **40** (Lignin Enzymic Microb. Degrad.), 151, 1987.

14. M. Shimada, T. Hattori, T. Umezawa, T. Higuchi, and K. Uzura, FEBS Letters, **221**, 327, 1987.

15. M.S.A. Leisola, S.D. Haemmerli, J.D.G. Smit, J. Troller, R. Waldner, H.E. Schoemaker, and H. Schmidt, Collq. INRA **40** (Lignin Enzymic Microb. Degrad.), 81, 1987.

16. T. Hattori, M. Shimada, T. Umezawa, T. Higuchi, M.S.A. Leisola, and A. Fiechter, Agric. Biol. Chem. **52**, 879, 1988.

17. H.W.H. Schmidt, S.D. Haemmerli, H.E. Schoemaker, and M.S.A. Leisola, Biochem. **28**, 1776, 1989.

18. T.K. Kirk, M. Tien, P.J. Kersten, M.D. Mozuch, and B. Kalyanaraman, Biochem. J. **236**, 279, 1986.

19. J.S. Dordick, M.A. Marletta, and A.M. Klibanov, Proc. Natl. Acad. Sci. USA, **83**, 6555, 1986.

20. N.G. Lewis, R.A. Razal, and E. Yamamoto, Proc. Natl. Acad. Sci. USA, **84**, 7925, 1987.

21. F. Cui, and D. Dolphin, in Plant Cell Wall Polymers: Biogenesis and Biodegradation. Ed. N.G. Lewis, and M.G. Paice, Am. Chem. Soc. Washington DC, 1989, chp. 37.

22. A. Sakakibara, in Recent Advances in Lignin Biodegradation Research, Ed. T. Higuchi, H.-M. Chang, and T.K. Kirk, Uni. Publishers, Tokyo, 1983, p12.

23. M. Tien, and T.K. Kirk, Proc. Natl. Acad. Sci. USA, **81**, 2280, 1984.

24. V. Renganathan, K, Mike, and M.H. Gold, Arch. Biochem. Biophys. **241**, 304, 1985.

25. V. Renganathan, K. Mike, and M.H. Gold, Arch. Biochem. Biophys. **246**, 155, 1986.

26. H. Numba, F. Nakatsubo, and T. Higuchi, Wood Res. **69**, 52, 1986.

27. J.K. Glenn, M.A. Morgan, M.B. Mayfield, M. Kuwahara, and M.H. Gold, Biochem. Biophys. Res. Commun. **114**, 1077, 1983.

28. M.H. Gold, M. Kuwahara, A.A. Chiu, and J.K. Glenn, Arch. Biochem. Biophys. **234**, 353, 1984.

29. T. Umezawa, F. Nakatsubo, and T. Higuchi, Agric. Biol. Chem. **47**, 2677, 1983.

30. T. Higuchi, Wood Res. **67**, 47, 1987.

31. T. Katagama, and T. Higuchi, Abst. 25th Symp. Lignin Chem. Fukuoko, Japan, 1980, p5.

32. F. Nakatsubo, T.K. Kirk, M. Shimada, and T. Higuchi, Arch. Microbiol. **128**, 416, 1981.

33. L.A. Anderson, V. Renganathan, A.A. Chiu, T.M. Lohr, and M.H. Gold, J. Biol. Chem. **260**, 6080, 1985.

34. B.W. Griffin, J.A. Peterson, and R.W. Estabrook, in The Porphyrins, Ed. D. Dolphin, Academic Press, New York, 1979, Vol. VII, p333.

35. V. Renganathan, K. Miki, and M.H. Gold, Biochem. **26**, 5127, 1987.

36. J.A. Bumpus, M. Tien, D. Wright, and S.D. Aust, Science, **228**, 434, 1985.

37. M. Shimada, T. Habe, T. Umezawa, T. Higuchi, and T. Okamoto, Biochem. Biophys. Res. Commun. **122**, 1247, 1984.

38. T. Habe, M. Shimada, and T. Higuchi, Mokuzai Gakkaishi, **31**, 54, 1985.

39. E. Adler, Wood Sci. Technol. **11**, 169, 1977.

40. K. Miki, V. Renganathan, and M.H. Gold, Biochem. **25**, 4790, 1986.

41. T. Umezawa, F. Nakatsubo, and T. Higuchi, Arch. Microbiol. **131**, 124, 1982.

42. F. Nakatsubo, T.K. Kirk, M. Shimada, and T. Higuchi, Arch. Microbiol. **126**, 416, 1981.

43. T. Umezawa, M. Shimada, T. Higuchi, and K. Kusai, FEBS Letters, **205**, 287, 1986.

44. T. Umezawa, and T. Higuchi, FEBS Letters, **205**, 293, 1986.

45. K. Miki, V. Renganathan, M.B. Mayfield, and M.H. Gold, FEBS Letters, **210**, 199, 1987.

46. T. Umezawa, and T. Higuchi, Collq. INRA **40** (Lignin Enzymic Microb. Degrad.), 63, 1987.

47. K. Miki, V. Renganathan, M.B. Mayfield, and M.H. Gold, Collq. INRA **40** (Lignin Enzymic Microb. Degrad.), 69, 1987.

48. P.J. Kersten, M. Tien, B. Kalayanaraman, and T.K. Kirk, J. Biol. Chem. **260**, 2609, 1985.

49. T.K. Kirk, J.M. Harkin, and E.B. Cowling, Biochim. Biophys. Acta, **165**, 134, 1968.

50. Y. Kamaya, and T. Higuchi, Mokuzai Gakkaishi, **29**, 789, 1983.

51. K. Krisnangkura, and M.H. Gold, Holzforschung, **33**, 174, 1979.

52. T. Fukuzumi, in Lignin Biodegradation: Microbiology, Chemistry, and Potential Applications. Ed. by T.K. Kirk, T. Higuchi, and H.-M. Chang, CRC Press, 1980, p73.

53. T. Umezawa, and T. Higuchi, Abst. of papers, 27th symposium on lignin chemistry, Nagoya, Japan, 1982, p101.

54. J. Jokela, J. Pellinen, and M. Salkinoja-salonen, Appl. Environ. Microbiol. **53**, 2642, 1987.

55. J. Jokela, J. Pellinen, M. Salkinaja, and G. Brunnow, Appl. Microbiol. Biotechnol. **23**, 38, 1985.

56. Y. Kamaya, and T. Higuchi, Wood Res. **70**, 25, 1984.

57. H.E. Schoemaker, E.M. Meijer, M.S.A. Leisola, S.D. Haemmerli, R. Waldner, D. Sanglard, and H.W.H. Schmidt, in Plant Cell Wall Polymers: Biogenesis and Biodegradation. Ed. by N.G. Lewis, and M.G. Paice, Am. Chem. Soc. Washington DC, 1989, chp. 33.

58. T. Umezawa, S. Kawai, S. Yokota, and T. Higuchi, Wood Res. **73**, 8, 1986.

59. K.E. Hammel, B. Kalyanaraman, and T.K. Kirk, J. Biol. Chem. **261**, 16948, 1986.

60. D. Sanglard, M.S.A. Leisola, and A. Fiechter, Enzyme Microb. Technol. **8**, 209, 1986.

61. K.E. Hammel, B. Kalyanaraman, and T.K. Kirk, Collq. INRA **40** (Lignin Enzyme Microb. Degrad.), 45, 1987.

62. T. Katayama, F. Nakatsubo, and T. Higuchi, Mokuzai Gakkaishi, **27**, 223, 1981.

63. F. Nakatsubo, and T. Higuchi, Holzforschung, **29**, 193, 1975.

64. B. Leopold, Acta Chem. Scand. **4**, 1523, 1950.

65. K. Elbs, and H. Lerch, J. Prakt. Chemie. **93**, 1, 1916.

66. T. Umezawa, T. Higuchi, and F. Nakatsubo, Agric. Biol. Chem. **47**, 2945, 1983.

67. L.F. Fieser, and M. Fieser in Reagents for Organic Synthesis, John Wiley and Sons, 1967, p191.

68. S.D. Haemmerli, H.E. Schoemaker, H.W.H. Schmidt, and M.S.A. Leisola, FEBS Letters, **220**, 149, 1987.

69. Beilsteins Handbuch der Organischen Chemie, Springer-Verlag, Berlin, **6**, 964b.

70. Beilsteins Handbuch der Organischen Chemie, Springer-Verlag, Berlin, **8**, 256b.

71. Beilsteins Handbuch der Organischen Chemie, Springer-Verlag, Berlin, **8** I, 618h.

72. Beilsteins Handbuch der Organischen Chemie, Springer-Verlag, Berlin, **6** III, 6333e.

Chapter 4

Redox mediation in lignin biodegradation

Lignin is a three-dimensional, water-insoluble high molecular weight polymer and the exact pathway by which it is metabolised by fungi is still unknown. Although lignin degrading enzymes, lignin peroxidase (LiP) and manganese-dependent peroxidase (MnP) have been isolated[1,2] and partially characterized by spectroscopic and other physical methods,[3-11] the enzymes are successful only in cleaving the C-C and C-O bonds of low molecular weight lignin model compounds. Effective depolymerization or degradation of isolated lignin polymers by purified enzyme or enzyme combination has not been achieved. It is evident, however, that lignin peroxidase alone can at least modify (oxidize) lignin[12,13] and in some cases release low molecular weight fragments.[1,2] It is interesting and also important to understand how an enzyme (with a molecular weight over 40,000) interacts with an irregular, cross-linked, water-insoluble lignin polymer. Due to the physical properties and complex chemical structure of lignin, it is unlikely that all the substructures of lignin can approach and fit into the active site of lignin degrading enzymes. Both LiP and MnP oxidize lignin model compounds by single electron oxidation.[14] Redox mediators which function as electron carriers between the enzyme and the lignin substrate have been suggested to be involved in lignin biodegradation.

4.1 Manganese complexes as mediators in lignin biodegradation

The manganese dependent peroxidase (MnP) is another enzyme isolated from the ligninolytic culture of *P. chrysosporium*. The reactions catalyzed by this enzyme[7-11] have not been extensively studied and its role in lignin degradation is still not clear. MnP was first found to be dependent on Mn(II) and α-hydroxycarboxylic acids for its activity.[7] All the enzyme activity was lost after dialysis but could be rapidly restored upon addition of Mn(II), suggesting Mn(II) was loosely bound to the enzyme.[8] It was found later[15] that MnP could oxidize Mn(II) to give Mn(III) in the presence of hydrogen peroxide and several α-hydroxycarboxylic acids, and the Mn(III)-α-hydroxycarboxylic acid complex could in turn oxidize the LiP substrates while being reduced to the Mn(II) complex. The function of the α-hydroxycarboxylic acids was to stabilize Mn(III). The manganese complexes, therefore, are the mediators for MnP catalyzed oxidation of lignin model compounds.

LiP and MnP oxidize lignin model compounds by single-electron oxidations. Electrochemical methods, which can initiate one-electron oxidation processes at the anode, have been used to study the oxidation of lignin model compounds.[16,17] Electrochemical oxidation of Mn(II) to give Mn(III) has also been reported.[18,19] In this study, the mediating ability of the manganese complexes was studied in an enzyme free system in which electrochemical and biomimetic methods were used to generate Mn(III) complexes. *Meso*-tetra(2,6-dichloro-3-sulfonatophenyl)porphyrin iron chloride (TDCSPPFeCl) was used as a biomimetic catalyst to mimic the function of MnP. A polymer dye, Poly B-411 (**84**), was used as an oxidizable lignin model compound. It has been shown that Poly B-411 is a convenient water-soluble lignin model and its

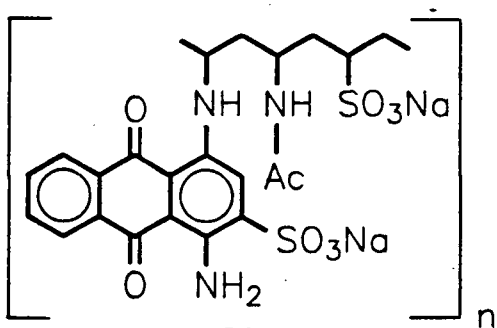

84

decolorization has been correlated with lignin degradation.[8,20] The decolorization of Poly B-411 can be easily quantified by following its absorption at 596 nm. The reason that the mediating ability of manganese complexes is studied in an enzyme free system is that separate evidence would be provided to support its function. Secondly, any mediating power of the manganese complexes in the model system would indicate that the oxidized complexes could function without association with the enzyme.

4.1.1 Results

4.1.1.1 Cyclic voltammetry (CV) of manganese complexes

Cyclic voltammograms (CV) of several manganese(II) species were obtained at pH 4.5 in the presence of several ligands. CV of manganese sulfate (10 mM) containing 50 mM lactic acid exhibited two oxidation peaks at 0.82 V and 1.37 V, respectively. The oxidation peak at 1.37 V disappeared when the CV was carried out in the presence of a large excess of lactic acid. The CV of manganese sulfate alone also showed a peak at 1.37 V. The oxidation peak at 0.82 V was therefore due to the Mn-lactate complex and that at 1.37 V to "uncomplexed" manganese ions. The CV of manganese sulfate in the presence of various carboxylic acids and inorganic ligands was

Table 4.1 Cyclic voltammetry of manganese sulfate (10 mM solution, pH 4.5) in the presence of various ligands[a)]

Ligand	F^-	SO_4^{2-}	ClO_4^-	$CH_3CO_2^-$	L-Lactate	DL-Malate	Malonate	Pyruvate	Citrate	D-tartrate	H_2O
concentration (mM)	>100	100	100	200	70	60	10	50	10	10	-
oxidation potential (V)	0.56[b)]	0.95[b)]	0.93[b)]	0.85[b)]	0.82[b)]	0.91[b)]	0.81[b)]	0.92[c)]	0.83[c)]	0.86[c)]	1.37[c)]

[a)] sweep rate 50 mv/second, [b)] pseudo-reversible, [c)] irreversible

similarly studied and the results are summarized in Table 4.1. Manganese formed complexes with DL-malate, malonate, pyruvate, citrate, L-lactate, and D-tartarate. Manganese seemed even to be complexed by inorganic ligands since oxidation peaks at lower potentials than 1.37 V were observed in the presence of these ligands.

Manganese dioxide, however, was formed on the surface of the working electrode after several runs when the inorganic anions were used as ligands, indicating the relative instability of the complexes having these inorganic ligands. Manganese dioxide was also formed on the electrode when the carboxylic acids were present at lower concentrations than those listed in Table 4.1.

To confirm that the manganese(II)-complexes was oxidized to Mn(III) during the electrochemical oxidation, the manganese-malonate complex in its higher oxidation state was prepared by controlled potential oxidation. The Mn(III)-malonate generated by controlled potential oxidation and that made chemically by mixing manganese(III) acetate and malonic acid gave the same UV-vis spectra (λ_{max} 270 nm). Addition of sodium pyrophosphate to a solution of electrochemically generated Mn(III)-malonate gave Mn(III)-pyrophosphate, which has a characteristic absorption at 296 nm.

Mixing manganese(III) acetate and malic acid in glacial acetic acid gave a light brown gelatinous precipitate. The precipitate was soluble in pH 4.5 buffer (containing malic acid) and the aqueous solution showed a similar UV-vis spectrum as that of manganese(III)-malate prepared by mixing manganese(III) acetate and malic acid in pH 4.5 acetate buffer, suggesting that the precipitate was Mn(III)-malate. Addition of the Mn(III)-malate powder to a solution containing Poly B-411 caused instant decolorization of the dye. Efforts to recrystallize the Mn(III)-malate precipitate failed. Elemental analysis of the Mn(III)-malate supports a formula of $Mn_2(C_4H_4O_5)_3 \cdot 3H_2O$.

4.1.1.2 Manganese mediated decolorization of Poly B-411

The CV of 0.02% Poly B-411 in pH 4.5 acetate buffer showed an oxidation peak at 0.75 V. The controlled potential oxidation (decolorization) of Poly B-411 was, however, very slow, probably because of its polymeric nature. When manganese sulfate (added to a final concentration of 0.1 mM which was the optimum concentration for MnP[8]) and α-hydroxycarboxylic acids or related compounds were added to the solution, the electrochemical decolorization of Poly B-411 was accelerated. Figure 4.1 shows the change of the absorbance of the dye at 596 nm with oxidation time in the presence of different amounts of lactic acid at a constant concentration of manganese sulfate (0.1 mM). Maximum acceleration was achieved when the concentration of lactic acid was

Table 4.2 Comparison of the optimum concentrations of carboxylic acids in the electrochemical decolorization of Poly B-411 and those in the MnP enzyme system.

Ligand	Optimum concentration (mM)		Concentration with highest current efficiency (mM)
	Electrochemical system	Enzyme system[8]	
(L)-lactic acid	50-60	50	70
malic acid	10	10	10
malonic acid	50	-	60
citric acid	10	-	a)
(D)-tartaric acid	20	-	25

a) The current efficiency is higher when the concentration is either 5 or 20 mM but the rate is slower.

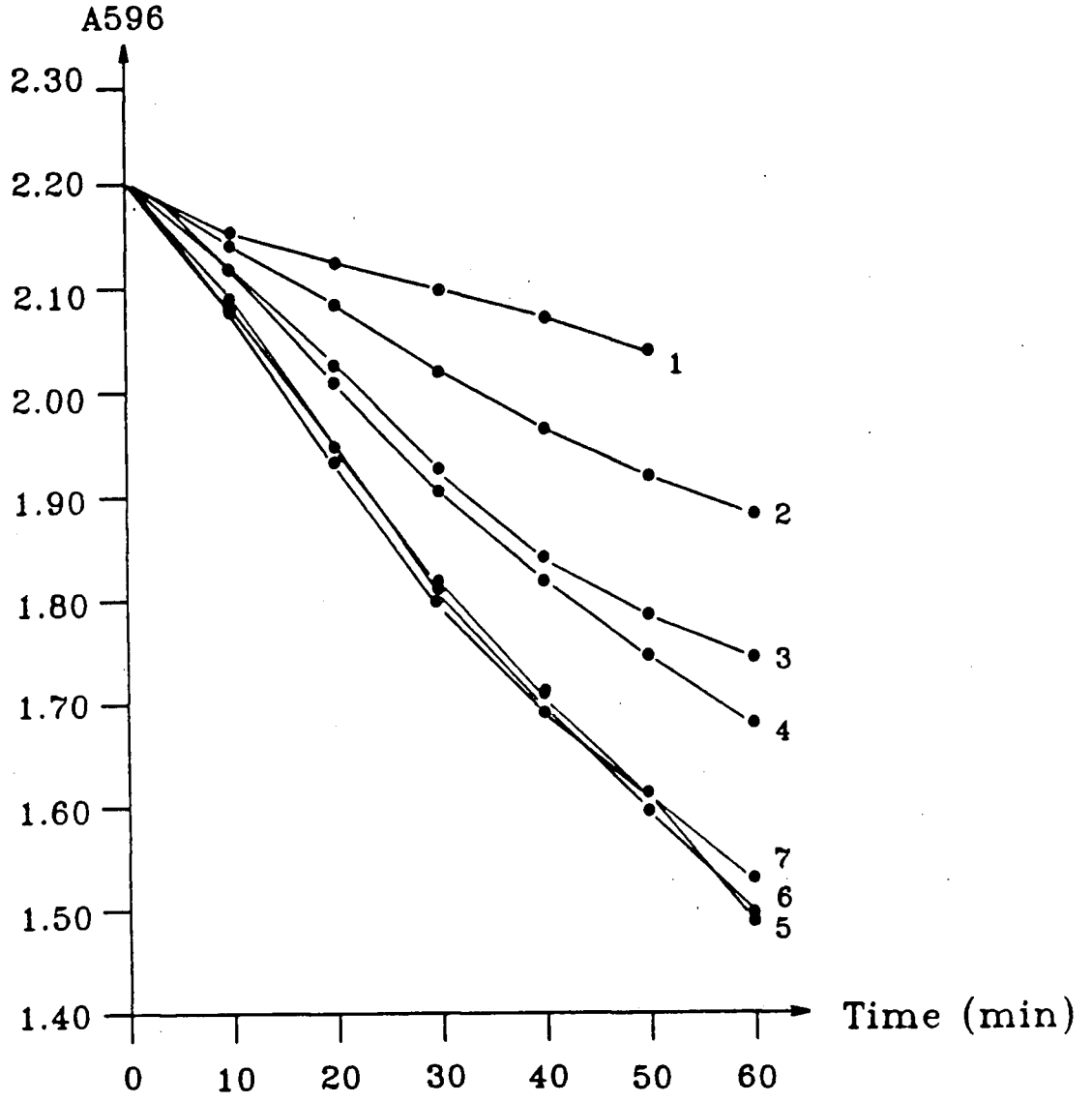

Figure 4.1 The electrochemical decolorization of Poly B-411 in 0.1 M acetate buffer at room temperature in the presence of manganese sulfate (0.1 mM) and lactic acid at various concentrations (mM), 1, 0; 2, 10; 3, 20; 4, 30; 5, 50; 6, 60; 7, 70;

50 or 60 mM (Figure 4.1). The decolorization of Poly B-411 in the presence of manganese sulfate and various amounts of D-tartaric acid, citric acid, malic acid, and malonic acid are shown in Figures 4.2-4.5. The rate of decolorization of Poly B-411 depended on the concentration of the carboxylic acids and the optimum concentrations for maximum decolorization are summarized in Table 4.2. The decolorization of Poly B-411 in the presence of manganese sulfate and various carboxylic acids at their optimum concentration is shown in Figure 4.6

As manganese sulfate gave a pseudo-reversible cyclic voltamogram in the presence of 0.1 M sodium perchlorate, the effect of manganese and perchlorate on the decolorization of Poly B-411 was studied. Dye decolorization was accelerated by addition of 0.1 mM manganese sulfate and 0.1 M sodium perchlorate, but the current efficiency was lower than with the carboxylic acid ligands and manganese dioxide was found on the working electrode surface. Very small acceleration and low current efficiency were observed with pyruvic acid.

To confirm that Mn(III) complexes were the actual oxidant of Poly B-411, a dye solution was added to the anode compartment of a electrochemical cell and the glassy carbon anode was placed in a dialysis bag. Manganese sulfate (0.1 mM) and lactic acid were added to both sides of the dialysis bag. Decolorization of the dye solution was observed after 2 hours oxidation at 0.8 V. No dye decolorization was observed after 5 hours oxidation in a control experiment lacking manganese sulfate and lactic acid.

The decolorization of Poly B-411 by TDCSPPFeCl and *m*CPBA in the presence or absence of manganese-lactate is shown in Figure 4.7. The decolorization was more extensive and faster in the presence of manganese-lactate.

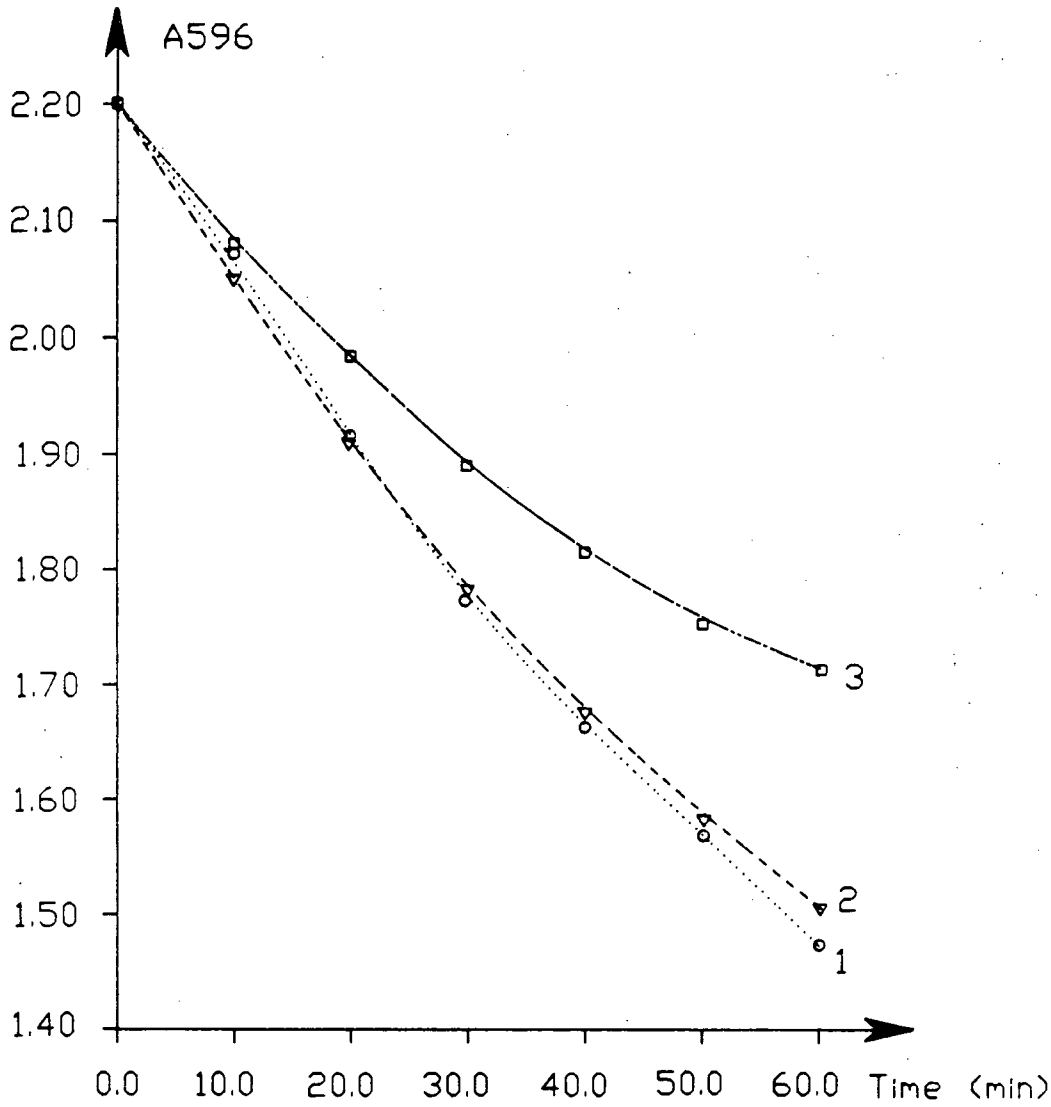

Figure 4.2 The electrochemical decolorization of Poly B-411 (0.02%) in 0.1 M pH 4.5 acetate buffer at room temperature in the presence of manganese sulfate (0.1 mM) and various concentrations of malic acid (mM), 1, 10; 2, 15; 3, 5;

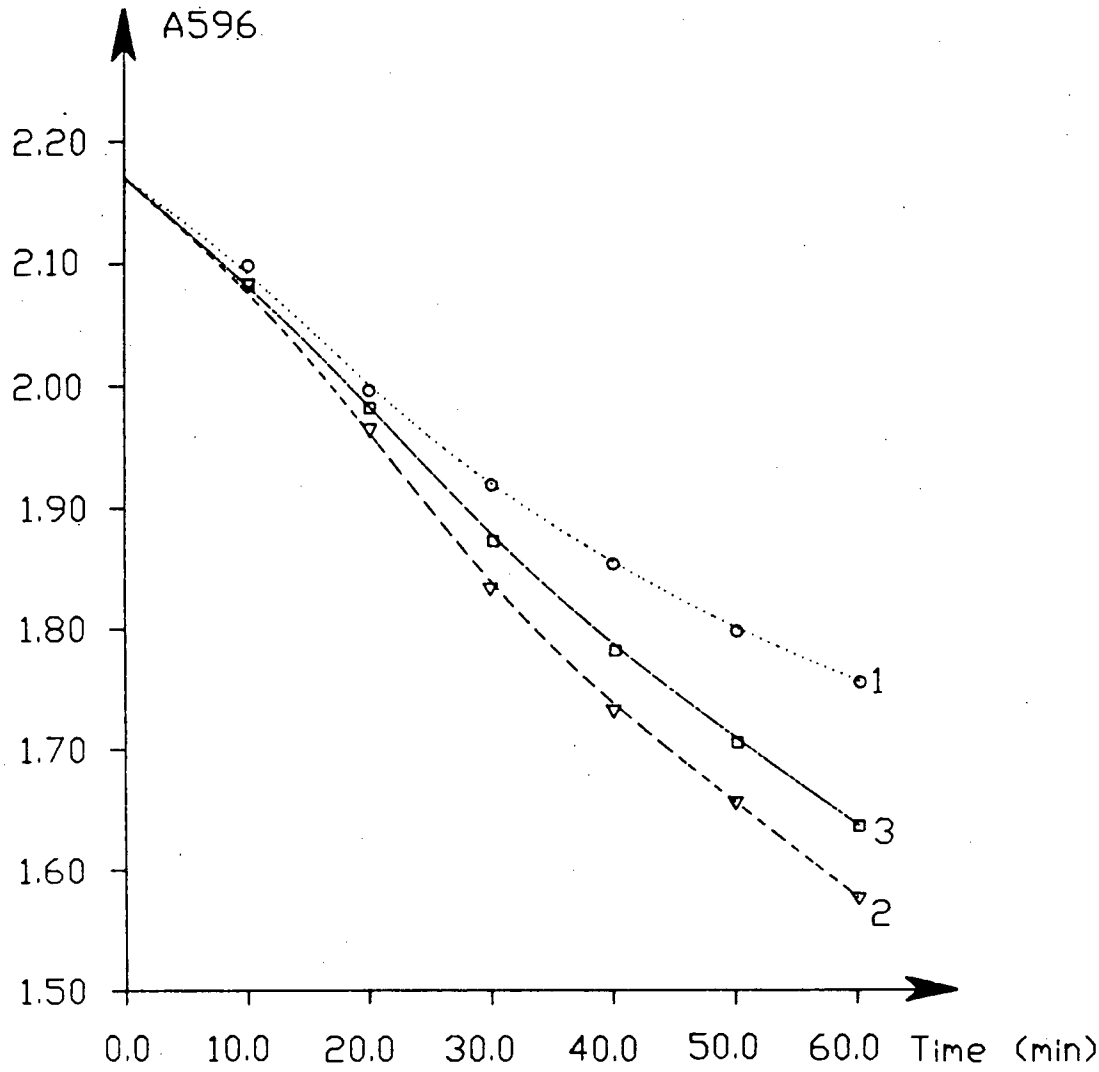

Figure 4.3 The electrochemical decolorization of Poly B-411 (0.02%) in 0.1 M pH 4.5 acetate buffer at room temperature in the presence of manganese sulfate (0.1 mM) and various concentrations of (D)-tartaric acid (mM), 1, 10; 2, 20; 3, 25;

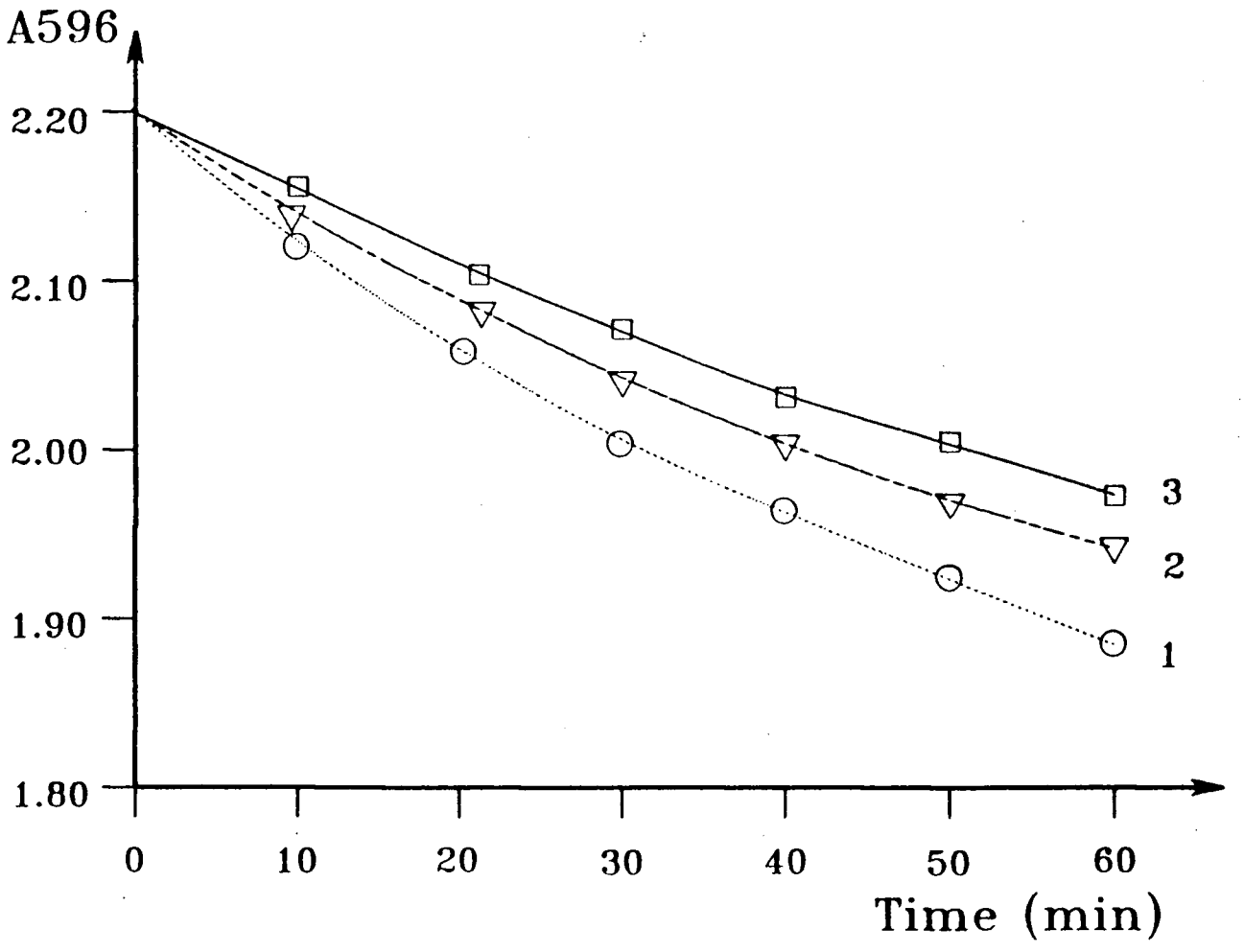

Figure 4.4 The electrochemical decolorization of Poly B-411 (0.02%) in 0.1 M pH 4.5 acetate buffer at room temperature in the presence of manganese sulfate (0.1 mM) and various concentrations of citric acid (mM), 1, 10; 2, 20; 3, 5;

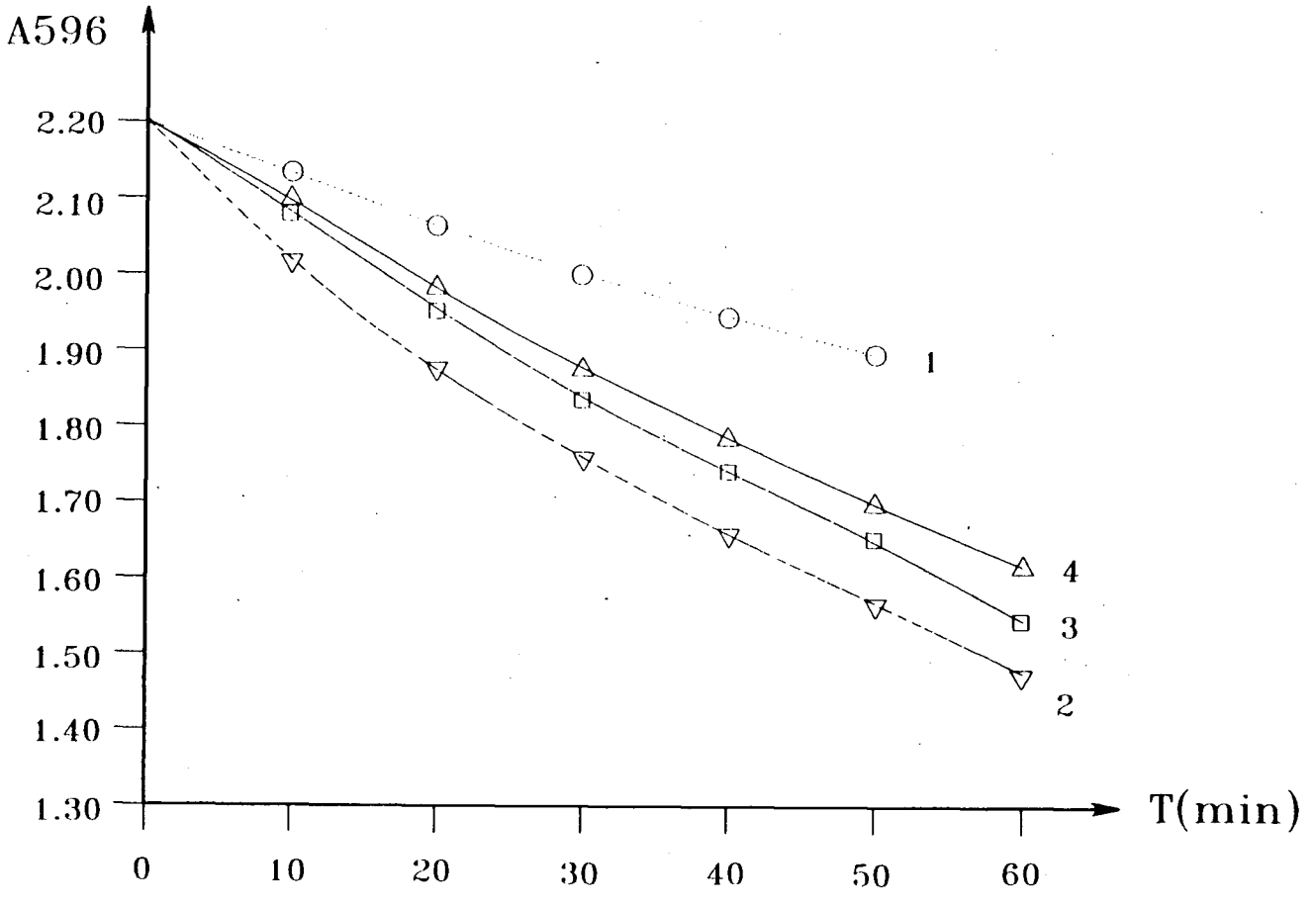

Figure 4.5 The electrochemical decolorization of Poly B-411 (0.02%) in 0.1 M acetate buffer at room temperature in the presence of manganese sulfate (0.1 mM) and various concentrations of malonic acid (mM), 1, 10; 2, 50; 3, 60; 4, 40;

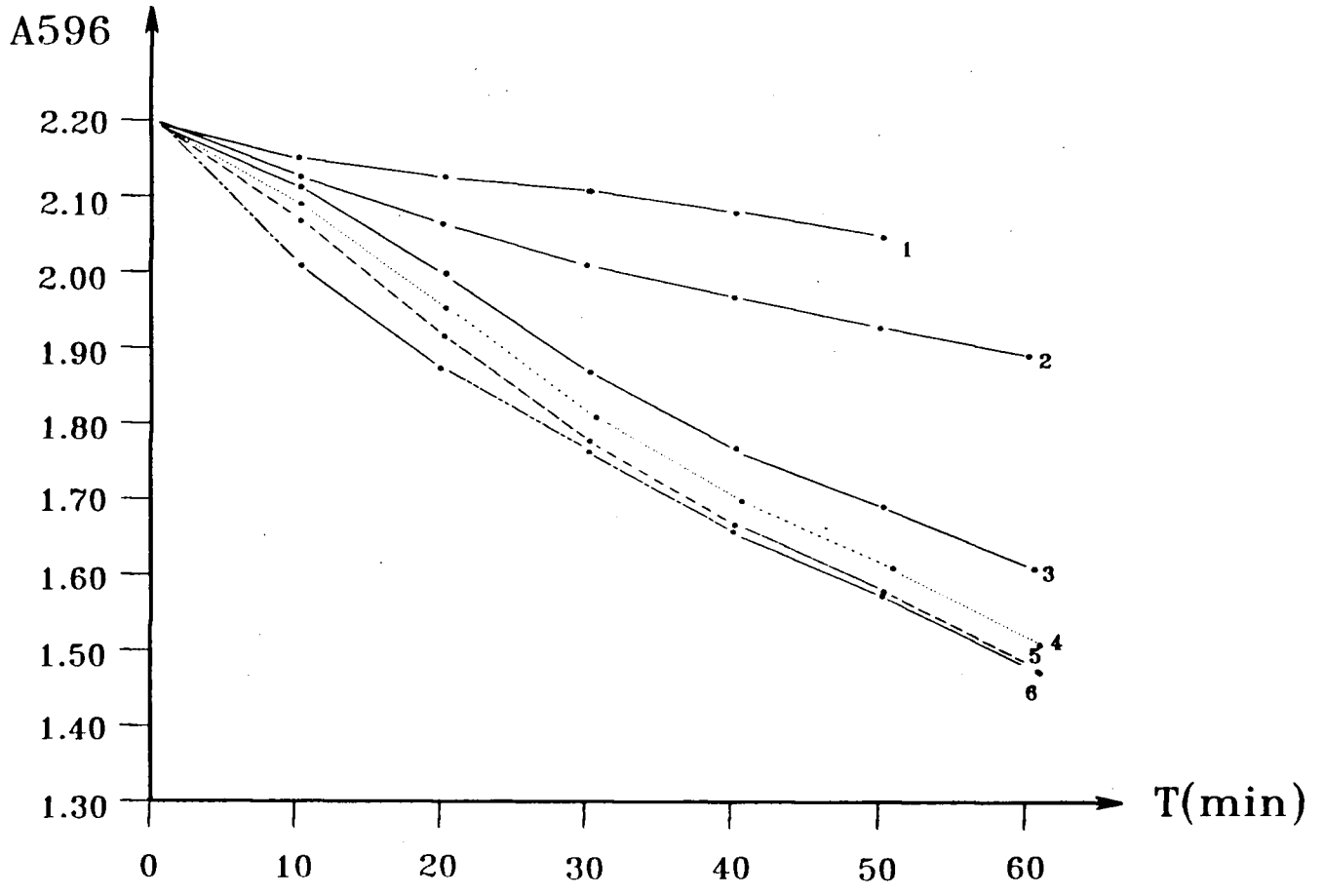

Figure 4.6 The electrochemical decolorization of Poly B-411 (0.02%) in 0.1 M pH 4.5 acetate buffer at room temperature in the presence of manganese sulfate (0.1 mM) and various carboxylic acids at their optimum concentrations, 1, no ligand; 2, 5 mM citric acid; 3, 20 mM (D)-tartaric acid; 4, 60 mM (L)-lactic acid; 5, 10 mM malic acid; 6, 50 mM malonic acid;

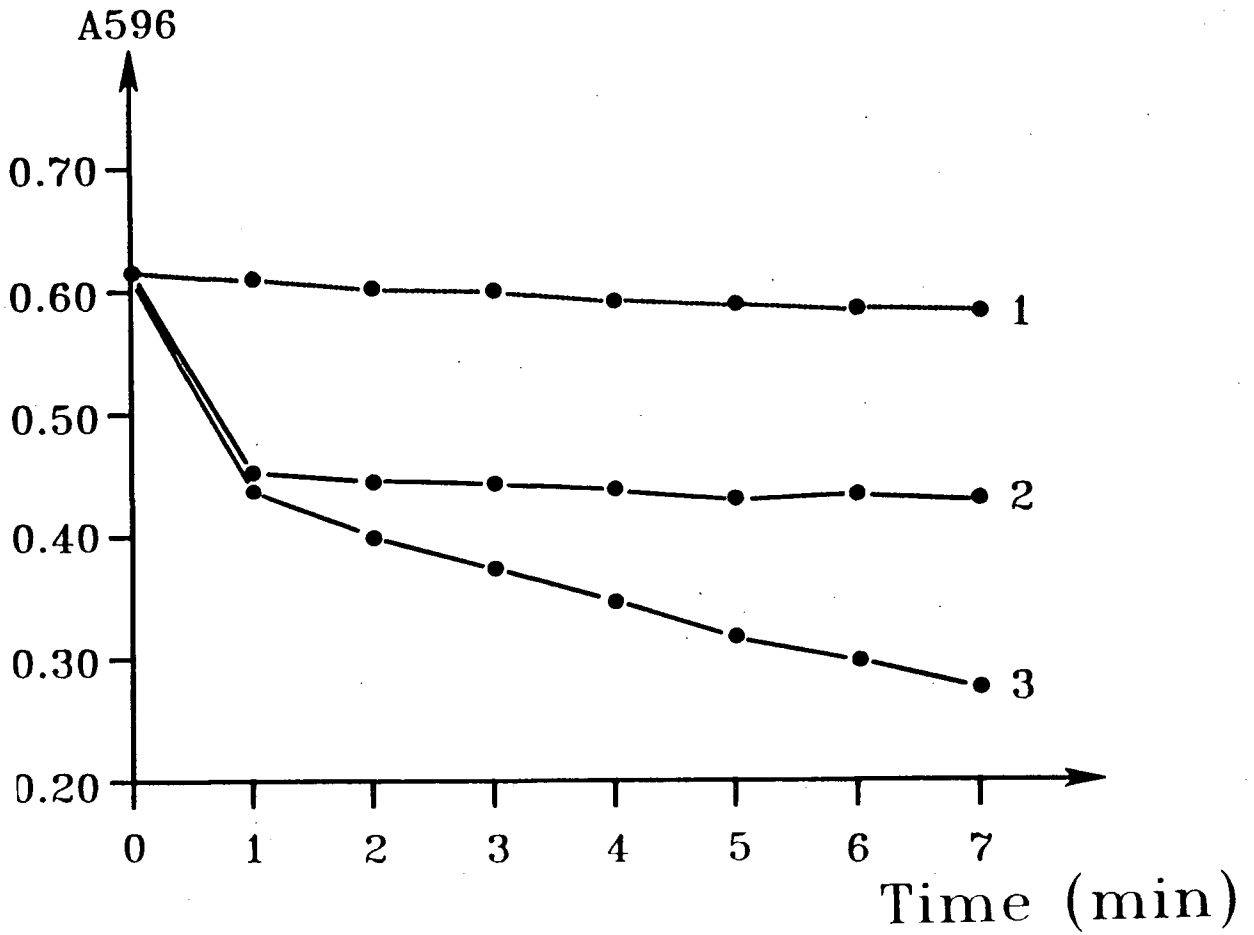

Figure 4.7 The decolorization of Poly B-411 (0.005% in 25 mL 0.1 M pH 4.5 acetate buffer) by TDCSPPFeCl (1×10^{-8} mole) and *m*CPBA (2.5×10^{-5} mole) in the presence of manganese sulfate (2.5×10^{-5} mole) and lactic acid (1.5×10^{-4} mole), 1, without TDCSPPFeCl; 2, without manganese sulfate; 3, complete reaction;

4.1.2 Discussion

Mn(III) has a standard reduction potential of 1.51 V and is stabilized in aqueous solution at very low pH or by formation of coordination complexes. The carboxylic acids used in this work form relatively weak Mn(III) complexes of reasonable oxidizing power, unlike some other strong complexing agents[21] which dramatically decrease the oxidizing power of Mn(III).

Numerous complexes between Mn(III) and α-hydroxycarboxylic acids have been reported.[22-24] The complexes of Mn(III) with simple α-hydroxycarboxylic acids, on the other hand, are not well known. Hydroxyhexafluoroisobutyric acid [H_2(HHIB)] gives a stable Mn(III) complex [Mn(HHIB)$_3$]$^{3-}$ which may be crystallized as its caesium complex. H_2(HHIB), however, is a non-oxidizable ligand and other simple non-oxidizable carboxylic acids such as acetic acid also form stable Mn(III) compounds. Our inability to characterize the complex between malate and Mn(III) probably results from the redox chemistry of the ligand together with the probability of oligomer formation due to the bidentate nature of the ligand. Nevertheless, α-hydroxycarboxylic acids and related acids clearly stabilize Mn(III) and inhibit its disproportionation which otherwise results in the precipitation of manganese dioxide.

We have shown the mediating power of a readily diffusible Mn(III)-α-hydroxycarboxylic acid complex by generating the Mn(III) electrochemically in the presence of lactate and the subsequent oxidation of Poly B-411 separated from the electrode by a semipermeable membrane.

Table 4.1 and Figure 4.6 show that the efficiency of the manganese complexes as redox mediators are not directly related to their redox potentials. Rather, the stability of the manganese(III) complexes and their rates of electron transfer, which are related

to their structures, will be key factors in their roles as effective mediators.

The optimum concentration of lactic acid and malic acid (Table 4.2) in the experiments described above are about the same as that of the enzyme system,[8] suggesting that the electrochemical system used does indeed mimic and describe the enzymic system. Additional evidence is provided that manganese complexes work as diffusible redox mediators for lignin model compound oxidation. The mediating power of manganese complexes are not just restricted to within the MnP enzyme system. The biomimetic oxidation of Poly B-411, a lignin model compound, by electrochemical and metalloporphyrin/oxidant systems are also accelerated by the presence of manganese complexes.

While malonic acid was found to be one of the most effective ligand for the formation of manganese complexes which exhibit maximal mediating power, it was not clear that nature made use of this important cellular metabolite during wood degradation by *P. chrysosporium.* However, after completing this work, we learned that Gold *et al*[25] have recently found malonic acid could significantly stimulate MnP activity.

The effective decolorization of Poly B-411 by TDCSPPFeCl and *mCPBA* in the presence of manganese-lactate indicates that TDCSPPFeCl is also able to mimic the function of MnP. *m*CPBA, a two-electron oxidant, cannot initiate the one-electron oxidation of Poly B-411 (curve 1, Figure 4.7). Addition of TDCSPPFeCl as a biomimetic catalyst causes a rapid but inefficient decolorization (curve 2, Figure 4.7). The TDCSPPFeCl catalyst is rapidly destroyed since it cannot rapidly transfer its oxidizing equivalents readily to the polymeric dye molecule. With the help of manganese-lactate as a mediator, TDCSPPFeCl is able to oxidize Poly B-411 rapidly and more extensively (curve 3, Figure 4.7). TDCSPPFeCl is also more stable in the presence of manganese-lactate since the oxidizing equivalents of oxidized TDCSPPFeCl

are rapidly transferred to the substrate by the manganese mediator.

4.2 Veratryl alcohol as a possible mediator in lignin biodegradation

Veratryl alcohol is a secondary metabolite of lignin degradation by *P. chrysosporium*[26,27] and plays an important role in lignin biodegradation.[3] It can induce the biosynthesis of lignin peroxidase by *P. chrysosporium*.[28] It can also stimulate lignin degradation[29,30] and benzo(*a*)pyrene[31] oxidation with LiP by protecting the enzyme from inactivation.[32-34]

Harvey *et al*[35] found that the presence of a catalytic amount of veratryl alcohol could stimulate the oxidation of anisyl alcohol by LiP and therefore proposed that veratryl alcohol could work as a mediator in lignin biodegradation. Direct evidence for the mediation, however, has not been obtained and more importantly the cation radical of veratryl alcohol, a necessary intermediate in redox mediation, has not been observed spectrally.

Enzymic reactions are the most efficient and also the most complex of chemical reactions. In the experiment of Harvey *et al*[35], veratryl alcohol might stimulate the reaction in conjunction with the enzyme rather than working as a diffusible redox mediator. It is believed that if lignin or its model compounds could be oxidized by a biomimetic system, free of the enzyme, and the reaction could be stimulated by the presence of veratryl alcohol, the mediation role of veratryl alcohol could be established more conclusively in the biomimetic system than in the enzymatic system. In this work, the effect of veratryl alcohol on the oxidation of anisyl alcohol by TDCSPPFeCl and *m*CPBA and on the electrochemical oxidation of Poly B-411 are studied. The mediation roles of veratryl alcohol are clarified.

4.2.1 Results and discussion

Harvey *et al*[35] reported that the presence of catalytic amounts of veratryl alcohol or 1,4-dimethoxybenzene could stimulate the oxidation of anisyl alcohol and 4-methoxymandelic acid by lignin peroxidase. The oxidation of anisyl alcohol by TDCSPPFeCl and *m*CPBA in the presence of varying amounts of veratryl alcohol is shown in Figure 4.8. Instead of stimulating the oxidation, the presence of veratryl

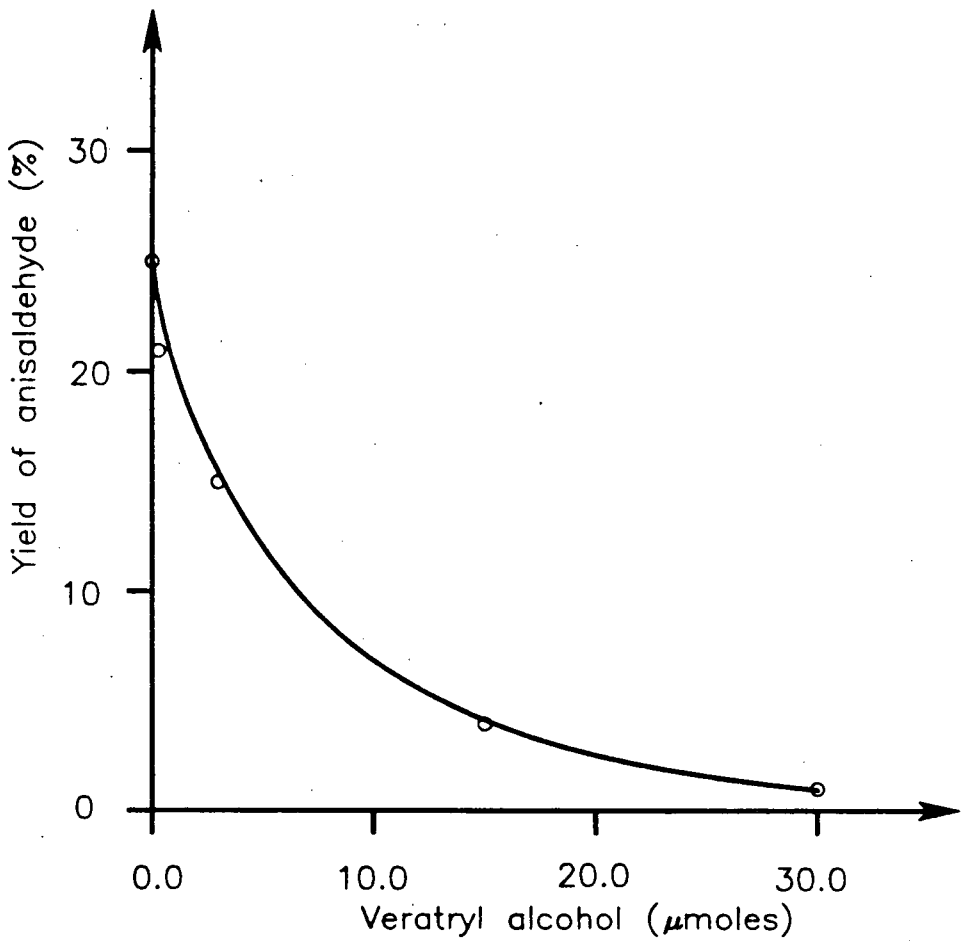

Figure 4.8 The oxidation of anisyl alcohol (3×10^{-5} mole in 6 mL pH 3 0.1 M phosphate buffer) by TDCSPPFeCl (5×10^{-8} mole) and *m*CPBA (3×10^{-5} mole) in the presence of veratryl alcohol

alcohol inhibited the reaction and the yield of anisaldehyde was the highest in the absence of veratryl alcohol. This observation was not surprising since veratryl alcohol, which had a lower redox potential, could be oxidized more readily than anisyl alcohol. Veratryl alcohol inhibited the reaction by competing with anisyl alcohol for oxidant. Similar results were obtained for the oxidation of anisyl alcohol in the presence of 1,4-dimethoxybenzene as shown in Figure 4.9.

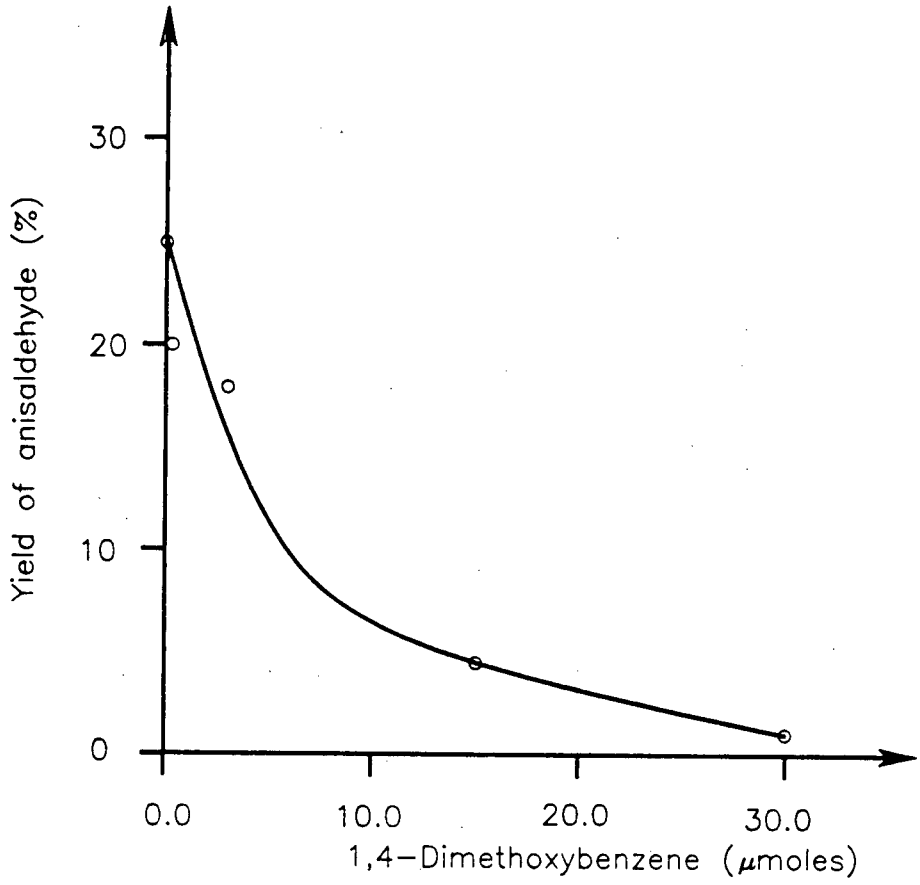

Figure 4.9 The oxidation of anisyl alcohol (3×10^{-5} mole in 6 mL 0.1 M pH 3 phosphate buffer) by TDCSPPFeCl (5×10^{-8} mole) and *m*CPBA (3×10^{-5} mole) in the presence of 1,4-dimethoxybenzene

In the above experiments, the biomimetic catalyst, TDCSPPFeCl, must have a reaction centre more exposed than the enzyme active site. Moreover, both veratryl

alcohol and the substrate anisyl alcohol are small molecules. The mediating ability of veratryl alcohol, if any, could not be easily observed in these model systems. The possibility that veratryl alcohol works as a mediator cannot be excluded based on the above results. As the steric interaction of lignin with lignin peroxidase may be quite difficult, a small mediating effect of veratryl alcohol might be quite important for *in vivo* lignin degradation.

Electrochemical methods, which can initiate one-electron oxidation at the electrode, have been used to oxidize lignin model compounds.[16,17] Unlike other biomimetic systems such as iron porphyrins (hemins) or inorganic one-electron oxidants, the electrode can be considered as 'macromolecular' since the electrode has a limited surface area and its interaction with polymeric molecules, somewhat like the interaction of lignin and lignin peroxidase, is sterically difficult. This property can be utilized to study the mediating function of small molecules having mediating potentials. Being polymeric, Poly B-411 is an excellent lignin model for this study.

The electrochemical decolorization of Poly B-411 at 0.9 V in the presence of varying amounts of veratryl alcohol is shown in Figure 4.10. Veratryl alcohol was able to stimulate the decolorization significantly in all cases. When the concentration of veratryl alcohol was 0.1 mM, the rate of decolorization remained approximately unchanged over a period of 60 minutes. At higher veratryl alcohol concentrations, 1 and 10 mM, an 'induction period' was needed for maximal decolorization to occur. The higher the concentration, the longer the induction period. During the 'induction period', the absorbance of veratraldehyde at 310 nm rapidly reached a limit but very little Poly B-411 decolorization was observed. The steady decolorization rate after the 'induction period' was slightly higher when the original concentration of veratryl alcohol was higher. One possible explanation is that some oxidation or oxidative

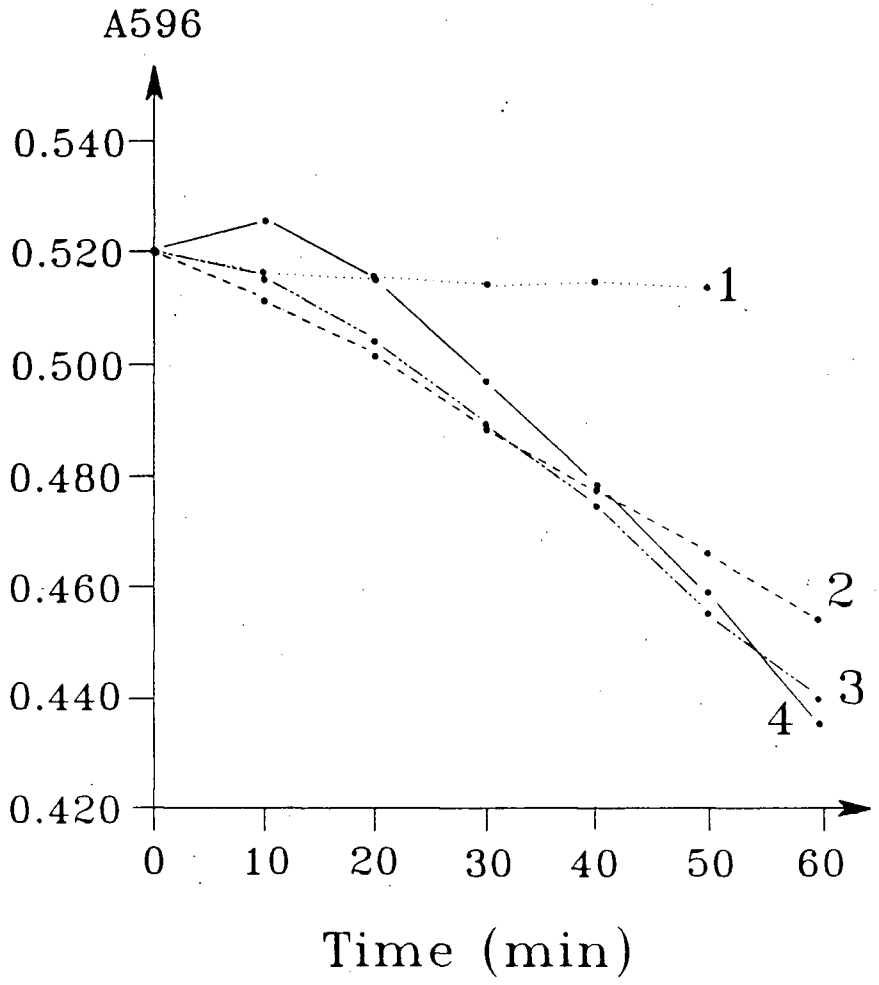

Figure 4.10 The electrochemical decolorization of Poly B-411 (0.005%) in 0.1 M pH 3 phosphate buffer at room temperature in the presence of various amounts of veratryl alcohol (mM). 1, 0; 2, 0.1; 3, 1; 4, 10.

polymerization products of veratryl alcohol might be able to mediate the dye decolorization. A small amount of dimerized product was obtained in the electrochemical oxidation of 4-methoxybenzyl alcohol in acetonitrile.[36] The electrochemical decolorization of Poly B-411 was also carried out in the presence of 1 mM veratraldehyde instead of veratryl alcohol. No mediation effect was observed, suggesting that veratryl alcohol rather than veratraldehyde was the mediator.

In the above experiments in aqueous solution, Poly B-411 molecules can still approach the electrode and thus be oxidized directly. It is assumed that if the polymeric dye were separated from the electrode but were still oxidized in the presence of veratryl alcohol, the decolorization then must be mediated by veratryl alcohol.

Poly B-411 was deposited onto a piece of filter paper which was attached directly to the glassy carbon anode. Methylene chloride, in which Poly B-411 is insoluble, was used as the solvent. After six hours controlled potential oxidation at 1.2 V, the side of the filter paper which directly face the anode was decolorized. The color of the anolyte changed to yellow after the oxidation, suggesting veratryl alcohol was also oxidized. The filter paper with Poly B-411 was not decolorized in a control experiment with no veratryl alcohol in the anolyte solution.

It can be concluded from these experiments that veratryl alcohol can indeed work as a diffusible redox mediator for Poly B-411 oxidation. It, however, cannot mediate the oxidation of anisyl alcohol by TDCSPPFeCl and *m*CPBA. The stimulation effect of veratryl alcohol for the oxidation of anisyl alcohol and 4-methoxymandelic acid reported by Harvey *et al*[35] may be due to other roles of veratryl alcohol, such as preventing enzyme deactivation. Another possibility is that the cation radical of veratryl alcohol is stabilized at the enzyme active site, making veratryl alcohol a much more efficient mediator in the enzyme system than in model systems.

After initially proposing the mediating role of veratryl alcohol, Harvey *et al*[37] further studied its function and showed that it accelerated the oxidation of anisyl alcohol and 4-methoxymandelic acid by preventing the formation of lignin peroxidase Compound III. Compound III of LiP is an inactive form of the enzyme and is formed in the presence of a large excess of oxidant in absence of readily oxidizable substrates. Compound III can also be formed through the reaction of the native enzyme with

superoxide, since it is formally the ferrous dioxygen adduct. Recent work by Cai and Tien[38] indicated that veratryl alcohol could inhibit the accumulation of Compound III of LiP. In the presence of veratryl alcohol and oxidant, Compound III can be reconverted to the native enzyme.

As described earlier in Chapter 2, Cl_{16}TSPPFeCl also forms a stable iron(II)-dioxygen complex (corresponding to Compound III of peroxidases) at high pH. At pH 3, under which condition most enzymic and biomimetic studies are carried out, the Compound III complex of Cl_{16}TSPPFeCl is not observed. The results in Table 4.3 suggest the involvement of the Compound III form of TDCSPPFeCl at high pH. The

Table 4.3 The oxidation of veratryl alcohol by TDCSPPFeCl and *m*CPBA at various pH values (yield based on substrate).

pH	% yield of veratraldehyde	TDCSPPFeCl remaining after reaction
2	50	98 %
4	11	98 %
6	6	97 %
8	4	96 %
10	10	96 %

hemin catalyst was stable but veratraldehyde was produced in very low yield at pH 10. The oxidants was probably consumed by generating Compound III from the oxoiron(IV) porphyrin and by converting the Compound III form back to the iron(III) porphyrin. The Compound III form of TDCSPPFeCl seems to be not involved in the oxidation of anisyl alcohol at pH 3. Veratryl alcohol, therefore, was not able to stimulate the oxidation of anisyl alcohol.

From the results of Harvey et al[35,37], of Cai and Tien,[38] and those described above, it seems certain that veratryl alcohol can indeed function as a redox mediator under certain conditions. It is, however, not an efficient mediator and it can itself be irreversibly oxidized at the same time. Inhibiting the accumulation of Compound III and thus preventing the deactivation of lignin peroxidase is certainly another very important role of veratryl alcohol.

4.3 Experimental

Cyclic voltammetry (CV) was performed in a microcell using a glassy carbon working electrode, a platinum auxiliary electrode and a silver reference electrode. The electrochemical apparatus was a PAR Model 173 Potentiostat/Galvanostat, a PAR Model 175 Universal Programmer and a Tektronix 564B Oscilloscope. The controlled potential oxidation of Poly B-411 was carried out in a two compartment cell, using glassy carbon as the working electrode, a platinum plate as auxiliary electrode, and silver wire as reference electrode (all potentials are quoted according to this standard). The potentials for the oxidation of Poly B-411 in the presence of manganese complexes was controlled at 0.80 V. The formation of manganese dioxide was confirmed by the formation of a blue color upon reaction with 0.1% benzidine in 1% acetic acid.

Poly B-411 was obtained from Sigma. Veratryl alcohol and anisyl alcohol were purified by vacuum distillation. *m*-Chloroperbenzoic acid (*m*CPBA) (Fisher Scientific Company, purified grade) was used without further purification. Sigma cellulose membrane, which retains 90-99% of a cytochrome c (M.W. 12,400) over a 10 hour period, was used as the dialysis bag. It was treated in boiling water for 1 hour before use. All other chemicals were of reagent grade.

The preparation of manganese(III) malonate. The electrochemical generation of Mn(III) malonate was carried out using the same apparatus as for the controlled potential oxidation of Poly B-411. A solution containing $MnSO_4$ (1×10^{-5} mole) and malonate (5×10^{-3} mole) in pH 4.5 acetate buffer (10 mL) was oxidized at a potential of 0.8 V. Solid manganese(III) acetate (1×10^{-5} mole) was added to a 0.5 M malonate solution (pH 4.5, 10 mL) to a final concentration of 1 mM.

The preparation of manganese(III) malate. Enough glacial acetic acid was added separately to manganese(III) acetate (2 mmole) and malic acid (3 mmole) to make them dissolve. The malic acid solution was then added slowly to the manganese(III) acetate solution to give a light brown gelatinous precipitate. The precipitate was filtrated, washed with glacial acetic acid and dried under vacuum at room temperature to give a light brown powder. Elemental analysis of the compound: C: 25.82%; H: 3.05%, calculated for $Mn_2(C_4H_4O_5)_3\cdot H_2O$: C: 25.71%; H:3.21%.

The oxidation of veratryl alcohol by TDCSPPFeCl and mCPBA. The reaction mixture (6 mL 0.1 M phosphate buffer) containing veratryl alcohol (30 μmole), TDCSPPFeCl (0.05 μmole), *m*CPBA (30 μmole), and 4′-methoxyacetophenone (30 μmole) was stirred in air at room temperature for 2 hours. The reaction was stopped by extraction with methylene chloride (3×10 mL). The percentage of TDCSPPFeCl remaining after reaction was estimated from UV-vis spectrum of the aqueous layer based on the Soret band absorption of TDCSPPFeCl at 424 nm. The methylene chloride extract was washed with saturated sodium bicarbonate (10 mL), dried, and the residue acetylated with excess 1:1 acetic anhydride/pyridine for 24 hours. Saturated sodium bicarbonate (10 mL) was then added and the mixture stirred for 20 minutes. Ethyl acetate (20 mL) was used to extract the organic compounds. The ethyl acetate layer was then washed in sequence with saturated sodium bicarbonate (10 mL), water

(10 mL), and 10% HCl (2×10 mL). The ethyl acetate layer was then dried over sodium sulphate, evaporated, and analyzed by gas chromatography.

The oxidation of anisyl alcohol in the presence of varying amounts of veratryl alcohol or 1,4-dimethoxybenzene. Anisyl alcohol (30 μmole) was oxidized by TDCSPPFeCl (0.05 μmole), and *m*CPBA (30 μmole) in 6 mL of pH 3 phosphate buffer in the presence of various amounts of veratryl alcohol or 1,4-dimethoxybenzene as specified in Figure 4.8 and Figure 4.9. The reaction was stopped after two hours by extraction with methylene chloride. The percentage of the TDCSPPFeCl catalyst remaining after reaction was estimated from UV-vis spectra of the aqueous layer based on the Soret band absorption of TDCSPPFeCl at 424 nm. The extraction, derivatization, and analysis of the products was the same as described above for the oxidation of veratryl alcohol. The yield of anisaldehyde and veratraldehyde was calculated from GC integration using 4′-methoxyacetophenone as an internal standard.

The electrochemically mediated decolorization of Poly B-411 in the presence of veratryl alcohol. Poly B-411 (20 mL 0.005% solution in pH 3 buffer) solution containing various amounts of veratryl alcohol (see Figure 4.10) was oxidized at 0.9 V. The decolorization of Poly B-411 was followed by monitoring the absorbance of the dye at 596 nm. The formation of veratraldehyde was followed at 310 nm by UV-vis spectroscopy.

The electrochemical oxidation of Poly B-411 separated from the electrode. Poly B-411 was deposited onto a piece of filter paper by dipping it into a Poly B-411 aqueous solution (0.1%). The filter paper was then air dried and attached directly to the glassy carbon anode. The anolyte (20 mL) contained 10 mM veratryl alcohol and 0.1 M tetrabutylammonium perchlorate (TBAP) in methylene chloride. To prevent the rapid oxidation and oxidative polymerization of veratryl alcohol, the oxidation potential

was set at 1.2 V (0.3 V lower than the first oxidation peak in CV of veratryl alcohol in methylene chloride) and parts of the anode not covered by the filter paper were covered with Teflon tape.

References for Chapter 4

1. M. Tien, and T.K. Kirk, Science, **221**, 661, 1983.
2. J.K. Glenn, M.A. Morgan, M.B. Mayfield, M. Kuwahara, and M.H. Gold, Biochem. Biophys. Res. Commun. **114**, 1077, 1983.
3. T.K. Kirk, and R.L. Farrell, Ann. Rev. in Microbiol. **41**, 465, 1987.
4. M. Tien, CRC Critical Rev. in Microbiol. **15**, 141, 1987.
5. T.K. Kirk, Phil. Trans. R. Soc. Lond. **A321**, 403, 1987.
6. J.A. Buswell, and E. Odier, CRC Critical Rev. in Biotechnol. **6**, 1, 1987.
7. M. Kuwahara, J.K. Glenn, M.A. Morgan, and M.H. Gold, FEBS Letters, **169**, 247, 1984.
8. J.K. Glenn, and M.H. Gold, Arch. Biochem. Biophys. **242**, 329, 1985.
9. A. Paszczunski, Van-Ba Huynh, and R. Crawford, Arch. Biochem. Biophys. **244**, 750, 1986.
10. M. Wariishi, L. Akileswaran, and M.H. Gold, Biochem. **27**, 5365, 1988.
11. Y. Mino, H. Wariishi, N.J. Blackburn, T.M. Loehr, and M.H. Gold, J. Biol. Chem. **263**, 7029, 1988.
12. S.D. Haemmerli, M.S.A. Leisola, and A. Fiechter, FEMS Microb. Letters, **35**, 33, 1986.
13. H.W. Kern, and T.K. Kirk, Appl. Environ. Microbiol. **53**, 2242, 1987.
14. P.J. Kersten, M. Tien, B. Kalyanaraman, and T.K. Kirk, J. Biol. Chem. **260**, 2609, 1985.

15. J.K. Glenn, L. Akileswaran, and M.H. Gold, Arch. Biochem. Biophys. **251**, 688, 1986.

16. F. Sundholm, and G. Sundholm, Holzforschung, **36**, 71, 1982.

17. D. Limosin, G. Pierre, and G. Cauquis, Holzforschung, **39**, 91, 1985.

18. A.T. Kuhn, J. Chem. Soc. Faraday Trans. **79**, 417, 1983.

19. M.E. Bodini, L.A. Willis, T.L. Riechel, and D.T. Sawyer, Inorg. Chem. **15**, 1538, 1976.

20. J.K. Glenn, and M.H. Gold, Appl. Environ. Microbiol. **45**, 1741, 1983.

21. D.T. Sawyer, and M.E. Bodini, J. Am. Chem. Soc. **97**, 6588, 1975.

22. E. Schlertzer-Rust (Ed.), Gmelin Handbuch der Anorganischen Chemie. Koordinationserbindungenz. Springer-verlag, 1980.

23. K.D. Singh, S.C. Jain, T.D. Sakore, and A.B. Biswas, Zeitschr. Kristallograph. **141**, 473, 1975.

24. T. Lis, Acta Cryst. **B38**, 937, 1982.

25. M.H. Gold *et al*, unpublished observations.

26. K. Lundquist, and T.K. Kirk, Phytochem. **17**, 1676, 1978.

27. M. Shimada, F. Natatsubo, T.K. Kirk, and T. Higuchi, Arch. Microbiol. **129**, 321, 1981.

28. B.D. Faison, T.K. Kirk, and R.L. Farrell, Appl. Environ. Microbiol. **52**, 251, 1986.

29. M.S.A. Leilosa, D.C. Ulmer, R. Waldner, and A. Fiechter, J. Biotechnol. **1**, 331, 1984.

30. D.C. Ulmer, M.S.A. Leisola, and A. Fiechter, J. Biotechnol. **1**, 13, 1984.

31. S.D. Haemmerli, M.S.A. Leisola, D. Sanglard, and A. Fiechter, J. Biol. Chem. **261**, 6900, 1986.

32. T. Tonon, and E. Odier, Appl. Environ. Microbiol. **54**, 466, 1988.

33. P.J. Harvey, H.E. Schoemaker, and J.M. Palmer, Collq. INRA **40** (Lignin Enzymic Microb. Degrad.), 145, 1987.

34. H. Wariishi, and M.H. Gold, FEBS Letters, **243**, 165, 1989.

35. P.J. Harvey, H.E. Schoemaker, and J.M. Palmer, FEBS Letters, **195**, 242, 1986.

36. F. Cui, unpublished results, 1986.

37. P.J. Harvey, H.E. Schoemaker, and J.M. Palmer, Collq. INRA **40** (Lignin enzymic Microb. Degradn.), 145, 1987.

38. D. Cai, and M. Tien, Biochem. Biophys. Res. Commun. **162**, 464, 1989.

Chapter 5

Summary

Both lignin peroxidase and the manganese-dependent peroxidase are heme proteins containing iron protoporphyrin IX as the prosthetic group. Their catalytic cycles (Scheme 5.1) are typical of peroxidases whereby the native enzyme is oxidized

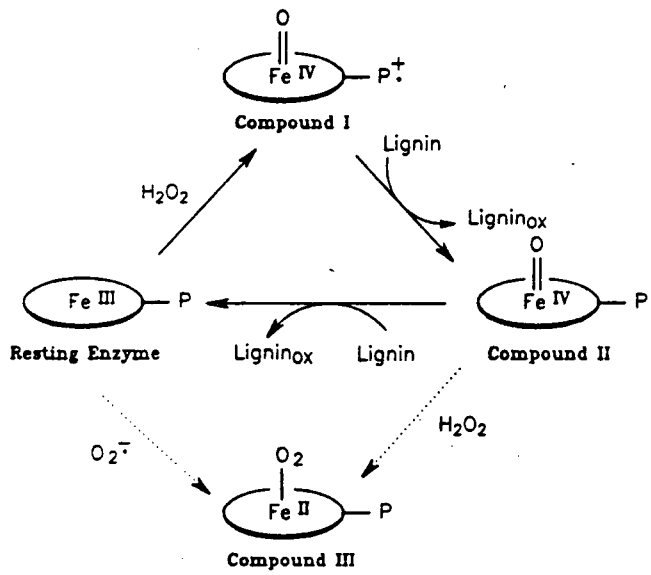

Scheme 5.1 Proposed catalytic cycle of lignin peroxidase

by hydrogen peroxide (a two electron oxidant) to compound I which is two oxidizing equivalents above the resting state and has been characterized as an oxoferryl iron(IV) porphyrin π-cation radical. Like other peroxidases the lignin peroxidase and the manganese-dependent peroxidase can then bring about two subsequent one-electron oxidations arriving back at the resting state through compound II which is an oxoferryl

iron(IV). The complexity of the lignin degrading enzymes and of their final substrate, lignin, has led us to prepare simple biomimetic catalysts (A-D) which have been used to gain an understanding of the more complex natural system.

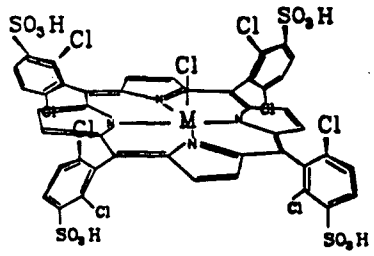

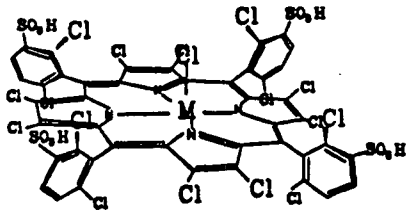

A M=Fe

B M=Mn

C M=Fe

D M=Mn

The oxidation of TDCSPPMnCl (B) gives two oxidized intermediates (Scheme 5.2), possibly oxomanganese(IV) and oxomanganese(V) porphyrins. Veratryl alcohol

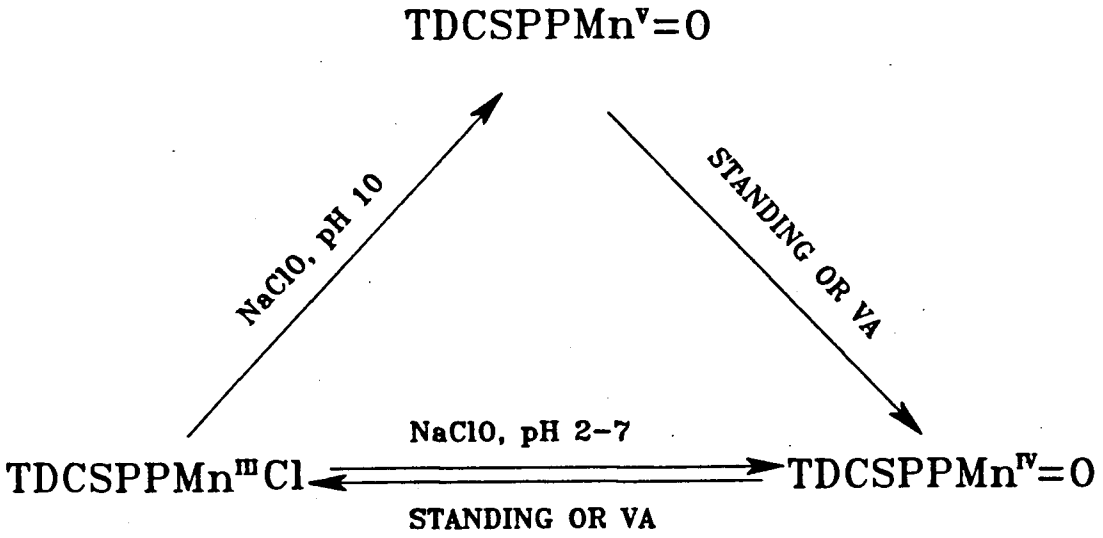

Scheme 5.2 The redox cycle of TDCSPPMnCl (VA: veratryl alcohol)

can reduce the oxomanganese(V) porphyrin rapidly to give the oxomanganese(IV) porphyrin and then the manganese(III) porphyrin, indicating that both oxidized intermediates are responsible for the oxidation of veratryl alcohol. Cl_{16}TSPPMnCl (**D**) has a similar redox cycle. An additional intermediate, Cl_{16}TSPPMn(II), was also observed. It is suggested that the manganese(II) porphyrin is formed by the reaction of the manganese(III) porphyrin with superoxide, which is formed in the oxidation of veratryl alcohol by Cl_{16}TSPPMn(III)Cl and NaClO. Only one oxidized intermediate was observed when TDCSPPFeCl (**A**) or Cl_{16}TSPPFeCl (**C**) was oxidized and the nature of the oxidized intermediate was not clear.

The protein part of these enzymes play at least two critical roles. One is the steric protection of the high oxidation states so that the enzymes do not bring about random oxidations, particularly of the porphyrins themselves and secondly, the protein in peroxidases is known to catalyze the rate of reaction between hydrogen peroxide and the enzyme. In order to achieve steric stabilization of our biomimetic catalysts chlorine atoms have been placed on both the phenyl rings and the ß-positions of the porphyrins. In addition to providing steric stabilization, which we anticipated would make our catalysts more stable, we also expected that the electron withdrawing properties of the electronegative chlorines would increase the redox potential of the metal coordinated at the center of the porphyrin which in turn should be reflected the oxidizing power of the catalysts.

The interaction between the iron and manganese porphyrins and various two-electron oxidants has been studied as a function of pH. The nature of the initial ligands coordinated to the porphyrins, the ionization state of the oxidant which in turn would affect the rate of coordination to the metal center and cleavage of the oxygen-oxygen bond to generate the high oxidation state will all be dependent upon pH. In

addition, some oxidant-consuming side reactions such as:

$$PorM + t\text{-}BuOOH \rightarrow PorM + CH_3COCH_3 + CH_3OH$$

$$(PorM)_{oxidized} + H_2O_2 \rightarrow PorM + H_2O + O_2$$

(where PorM is a metalloporphyrin and $(PorM)_{oxidized}$ is its two-electron oxidized intermediate) are also pH dependent and add to the complexity of the systems. Nevertheless, useful information was obtained to direct further studies for lignin model compound degradation or pulp bleaching.

The stabilities of the metalloporphyrins towards excess oxidants were dramatically increased by introducing chlorines at the phenyl rings. Further chlorination of the porphyrins at their ß-positions, however, did not result in additional stabilization, probably because the ß-substituted porphyrins, which have much higher redox potentials, are more powerful oxidants towards both the substrate and themselves.

The presence of a readily oxidizable substrate, which can rapidly transfer electrons to the highly reactive oxidized porphyrin intermediates, will decrease the rate of self-destruction. The relative stabilities of the metalloporphyrins were measured by observing the decrease in the Soret absorption (characteristic of all porphyrins) in the presence of veratryl alcohol with oxidant present in 100 fold molar excess. It was found that in the presence of veratryl alcohol, the manganese porphyrins were more stable than their iron analogues and the more highly chlorinated porphyrins (with better steric protection) were less stable than the octachlorinated porphyrins and that the metalloporphyrins were more stable at lower pH. In the presence of veratryl alcohol, the stability order of the four metalloporphyrins studied was:

TDCSPPFeCl > Cl_{16}TSPPFeCl > TDCSPPMnCl > Cl_{16}TSPPMnCl

The pH dependency of the catalytic activities of the metalloporphyrins was studied using veratryl alcohol as a substrate. The rate at which substrate is oxidized will also be dependent upon pH in a complex manner. The optimal pH at which a metalloporphyrin/oxidant combination has its maximal catalytic activity is listed in Table 5.1 (A duplication of Table 2.1). In general, the manganese porphyrins have higher optimal pH than their iron porphyrin analogues and the hexadecachloroporphyrins (Cl_{16}TSPPFeCl, Cl_{16}TSPPMnCl) have higher optimal pH than their octachloroporphyrins (TDCSPPFeCl, TDCSPPMnCl). All the metalloporphyrins have low optimal pH when using *m*CPBA as an oxidant. When hydrogen peroxide is the choice of oxidant, TDCSPPMnCl and Cl_{16}TSPPMnCl are better catalysts than their iron analogues and the optimal pH for the reaction is high (pH 10). Overall the best catalytic activity was observed with TDCSPPFeCl using *m*CPBA at low pH.

Oxidation of the oxoiron(IV) (compound II) complex of lignin peroxidase by hydrogen peroxide generates compound III. Compound III is formally the ferric-superoxide complex but is equally well represented by the ferrous dioxygen resonance structure:

$$Fe(III)\text{-}O_2^{\cdot} \leftrightarrow Fe(II)\text{-}O_2$$

Compound III

These complexes can also be formed by reacting the ferrous state with O_2 or the ferric complex with $O_2^{\cdot}$.

Superoxide was formed during the oxidation of veratryl alcohol and deactivated the metalloporphyrin catalysts by formation of Mn(II) or Fe(II)-O_2 species,

Table 5.1 Optimum pH for the oxidation of veratryl alcohol by various metalloporphyrin/oxidant combinations at room temperature

Metalloporphyrin	Oxidant	Optimal pH
Cl_{16}TSPPMnCl	mCPBA	3
Cl_{16}TSPPFeCl	mCPBA	2
TDCSPPMnCl	mCPBA	3
TDCSPPFeCl	mCPBA	2
TDCSPPMnCl	NaClO	6
TDCSPPFeCl	NaClO	7
Cl_{16}TSPPFeCl	t-BuOOH	5
TDCSPPFeCl	t-BuOOH	6
Cl_{16}TSPPMnCl	t-BuOOH	10
TDCSPPMnCl	t-BuOOH	10
Cl_{16}TSPPMnCl	NaClO	10
Cl_{16}TSPPFeCl	NaClO	10
TDCSPPFeCl	H_2O_2	2
TDCSPPMnCl	H_2O_2	10
Cl_{16}TSPPMnCl	H_2O_2	10

corresponding the compound III of the peroxidases. However, addition of a superoxide dismutating agent, manganese(II)-lactate, increased the catalytic activity of the metalloporphyrin catalyst by altering the rate of compound III formation.

Addition of imidazole was also found to increase the catalytic activity of Cl_{16}TSPPMnCl and H_2O_2 for veratryl alcohol oxidation, supporting the suggestion that the ligation of the metalloporphyrin catalysts will change catalytic activity, a phenomenon which is well characterized with heme proteins.

Since the electron transfer between the high molecular weight heme proteins and

the even higher molecular weight lignin can be expected to be very inefficient, it has been suggested that redox mediation must play an important role in the biological degradation of lignin by lignin peroxidase and the manganese-dependent peroxidase. Manganese complexes, which are essential for the activity of the manganese-dependent peroxidase, were found to function as redox mediators between the enzyme and substrates. We have used electrochemical methods to study the mediating ability of manganese complexes. The electrochemical oxidation of Poly B-411, a lignin model compound, was accelerated by addition of manganese(II)-carboxylic acid complexes. The function of the various carboxylic acids was to stabilize the manganese(III) ions and to prevent their disproportion to MnO_2. The optimal concentrations of lactic acid and malic acid in the electrochemical system were similar to those of the enzyme system, indicating the electrochemical system indeed mimics the enzyme system. Malonic acid was found to be the best ligand for maximal acceleration in the electrochemical oxidation of Poly B-411. We learned after finishing this work that M. Gold et al (personal communication) also found that malonic acid could dramatically stimulate the activity of the manganese-dependent peroxidase.

It has been proposed that veratryl alcohol can function as a redox mediator for lignin peroxidase. It has also been proposed that veratryl alcohol can increase the activity of lignin peroxidase by preventing enzyme deactivation. The mediating ability of veratryl alcohol was studied in electrochemical and biomimetic systems, where deactivation of the enzyme is not a problem and the mediating effect can be clearly studied. The electrochemical oxidation of Poly B-411 in aqueous solution was dramatically accelerated by the addition of veratryl alcohol, suggesting that veratryl alcohol was a redox mediator for the reaction. Poly B-411, when deposited on a piece of filter paper and physically separated from the electrode, was also oxidized in the

presence of (but not in the absence) veratryl alcohol, again indicating that veratryl alcohol mediated the electrochemical oxidation of Poly B-411.

Harvey et al suggested that veratryl alcohol facilitated the oxidation of anisyl alcohol and 4-methoxymandelic acid by lignin peroxidase by association of the veratryl alcohol cation radical with the compound II of the enzyme to make it a more powerful oxidant, therefore prevent the formation of compound III. However, in our studies the presence of veratryl alcohol was unable to increase the yield of anisyl alcohol oxidation by TDCSPPFeCl and *m*CPBA.

While lignin peroxidase and the manganese-dependent peroxidase cannot catalyze the depolymerization of lignin polymers, they can catalyze the oxidation of a number of low molecular weight compounds representing the various substructures of lignin. We studied in detail the oxidation of a number of lignin model compounds catalyzed by one of the metalloporphyrins, TDCSPPFeCl.

Veratryl alcohol, one of the simplest lignin model compounds, was oxidized by TDCSPPFeCl and *m*CPBA in aqueous buffer to give products similar to that of lignin peroxidase catalyzed reactions. The oxidation of other lignin model compounds, including ß-1, ß-O-4, phenylpropane and phenylpropene model compounds, were also studied and the reactions were found to be similar to those catalyzed by lignin peroxidase. Almost all the reactions catalyzed by lignin peroxidase, including benzyl alcohol oxidation, benzylic methylene group hydroxylation, carbon-carbon double bond dihydroxylation, side chain carbon-carbon bond cleavage, demethoxylation, and aromatic ring cleavage reactions, were observed in the oxidation of various lignin model compounds by TDCSPPFeCl.

The oxidation of model compounds representing the ß-5 substructure of lignin has not been reported. TDCSPPFeCl was able to catalyze the oxidation of a ß-5 model

compound to give products resulting from side chain carbon-carbon bond cleavage and aromatic ring oxidations. A 5-5' biphenyl model compound, representing a substructure of lignin most resistant to microbial degradation, was also oxidized by TDCSPPFeCl and t-BuOOH to give side chain oxidation and aromatic ring cleavage products. The ß-5 and 5-5' biphenyl model compounds were probably oxidized by TDCSPPFeCl through the same one-electron oxidation mechanism and the formation of the products can be rationalized by this mechanism.

The isolation of novel products from the oxidation of various lignin model compounds also gives insight into the mechanism of the reactions. The formation of direct aromatic ring cleavage products from the oxidation of veratryl acetate, the phenylpropane, ß-5 and 5-5' biphenyl model compounds supports the mechanism of aromatic ring cleavage previous proposed; The formation of a compound (**E**) similar to a proposed intermediate (**F**) for the phenyl-alkyl cleavage supports the proposed mechanism and indicates the necessity of the presence of a hydroxy group on the α-carbon of the side chain; The formation of the methanol incorporated products in the oxidation of veratryl alcohol and veratryl acetate in methanol suggests that the solvent molecule preferentially attacks the C_3-position of the substrate cation radical; The formation of the solvent-incorporated product in the oxidation of the phenylpropene model compound suggests a cation radical mechanism of the reaction.

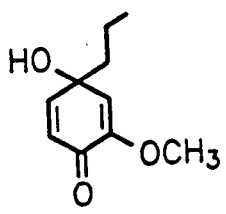

E

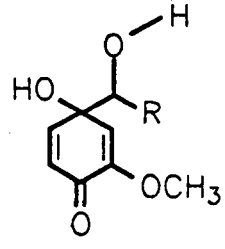

F

Lignin peroxidase can also oxidize environmental pollutants including polycyclic aromatic hydrocarbons and polychlorinated phenols. TDCSPPFeCl was shown able to catalyze the oxidation of pyrene and 2,4,6-trichlorophenol to give products similar to those of the lignin peroxidase catalyzed reactions.

In summary, the metalloporphyrins used in this study have been shown to closely mimic the function of lignin peroxidase in the oxidation of lignin model compounds. Factors affecting the catalytic activities of the metalloporphyrins have been studied. Unlike the enzymes which are very labile, the metalloporphyrins can be used over a wide range of pH and temperature, suggesting that they may have potential industrial applications.

Appendix 1

The oxidation of Lignin Indulin AT

Introduction

Lignin Indulin AT is a commercially available industrial kraft lignin which is insoluble in water and soluble in basic aqueous solution or aqueous DMF. It is not a 'natural' lignin since the lignin structure is modified during the kraft pulping process. Initial studies of possible lignin degradation by metalloporphyrins were carried out using this easily available lignin.

UV-vis spectrometry has been used in the study of lignin chemistry.[1-3] Ionization difference spectra,[2,3] the UV-vis spectra of a lignin sample in basic solution (when the phenolic hydroxyl groups are ionized), subtracted from that of the same sample in neutral or acidic solution, has been used to estimate the hydroxy group content of lignins. The typical difference spectrum of softwood lignosulfonate has peaks at about 250 nm and 300 nm, respectively.[3] This was explained as being due to the presence of unconjugated guaiacyl moieties (**85**) in lignin. The aromatic hydroxy content can be

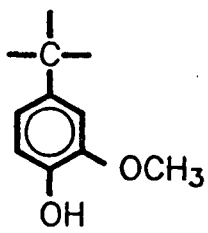

85

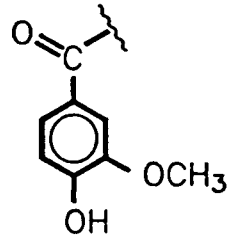

86

estimated based on the intensity of either of these two peaks. When the hydroxyl group was conjugated with a C_α-carbonyl group (**86**), the peak at 300 nm in the difference spectrum will shift to longer wavelength by 50-60 nm accompanied by a large increase in intensity.[3] The estimation of hydroxy content by using the intensity of the long wavelength peak is no longer valid if the lignin sample contains C_α-carbonyl groups. The C_α-carbonyl groups can be reduced by sodium borohydride ($NaBH_4$) to give C_α-alcohols and aromatic hydroxy content of the sample can be determined by this so called reduced-difference spectrum.

Results and discussion

The oxidation of Lignin Indulin AT by $Cl_{16}TSPPMnCl/H_2O_2$ or $Cl_{16}TSPPMnCl$/t-BuOOH was studied. Difference spectra and reduced-difference spectra provide a simple means to roughly predict the chemical changes after oxidation.

The difference spectrum of Lignin Indulin AT has peaks at 252 nm, 300 nm, and 374 nm, respectively. The 374 nm peak was probably due to the presence of conjugated phenolic units. The difference spectra of Lignin Indulin AT treated with $Cl_{16}TSPPMnCl/H_2O_2$ or $Cl_{16}TSPPMnCl$/t-BuOOH at either pH 2 or pH 10 are distinctively different from that of the untreated sample as shown in Figures A-1 to A-4, indicating extensive modification of lignin by $Cl_{16}TSPPMnCl$ catalyzed oxidation. The 374 nm peak in the difference spectra of all the oxidized lignin samples either shifted or disappeared, suggesting that the conjugated structure **86** was converted to other structures. In the case of lignin treated with $Cl_{16}TSPPMnCl$/t-BuOOH at pH 2 (Figure A-1), both the 300 nm and 374 nm peaks disappeared in the difference spectrum and only a negative peak was found in the reduced-difference spectrum,

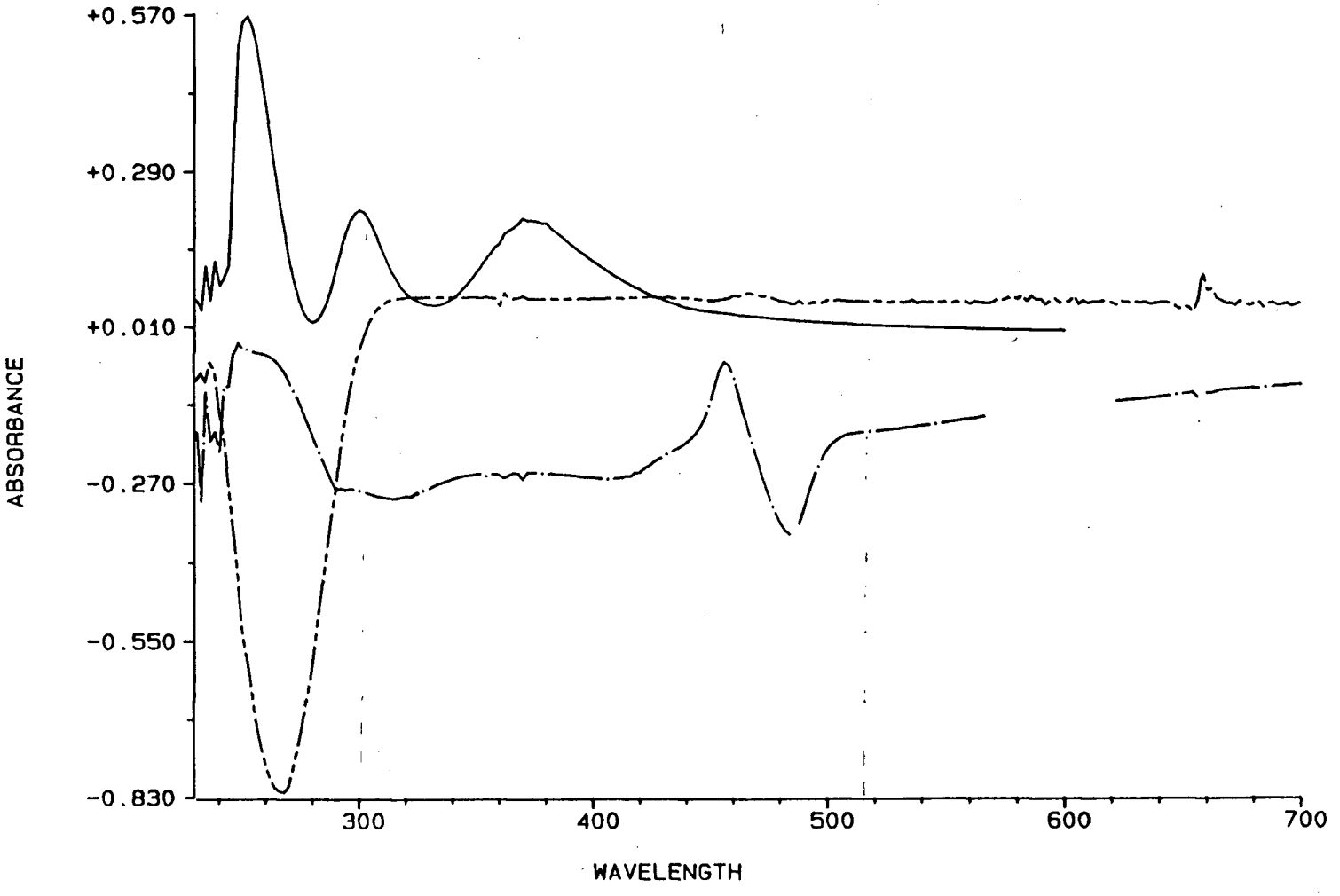

Figure A-1 Difference spectra and reduced-difference spectra of Lignin Indulin AT, — difference spectrum of untreated lignin; -.-.- difference spectrum of lignin treated with Cl_{16}TSPPMnCl and t-BuOOH at pH 2; --- reduced-difference spectrum of lignin treated with Cl_{16}TSPPMnCl and t-BuOOH at pH 2

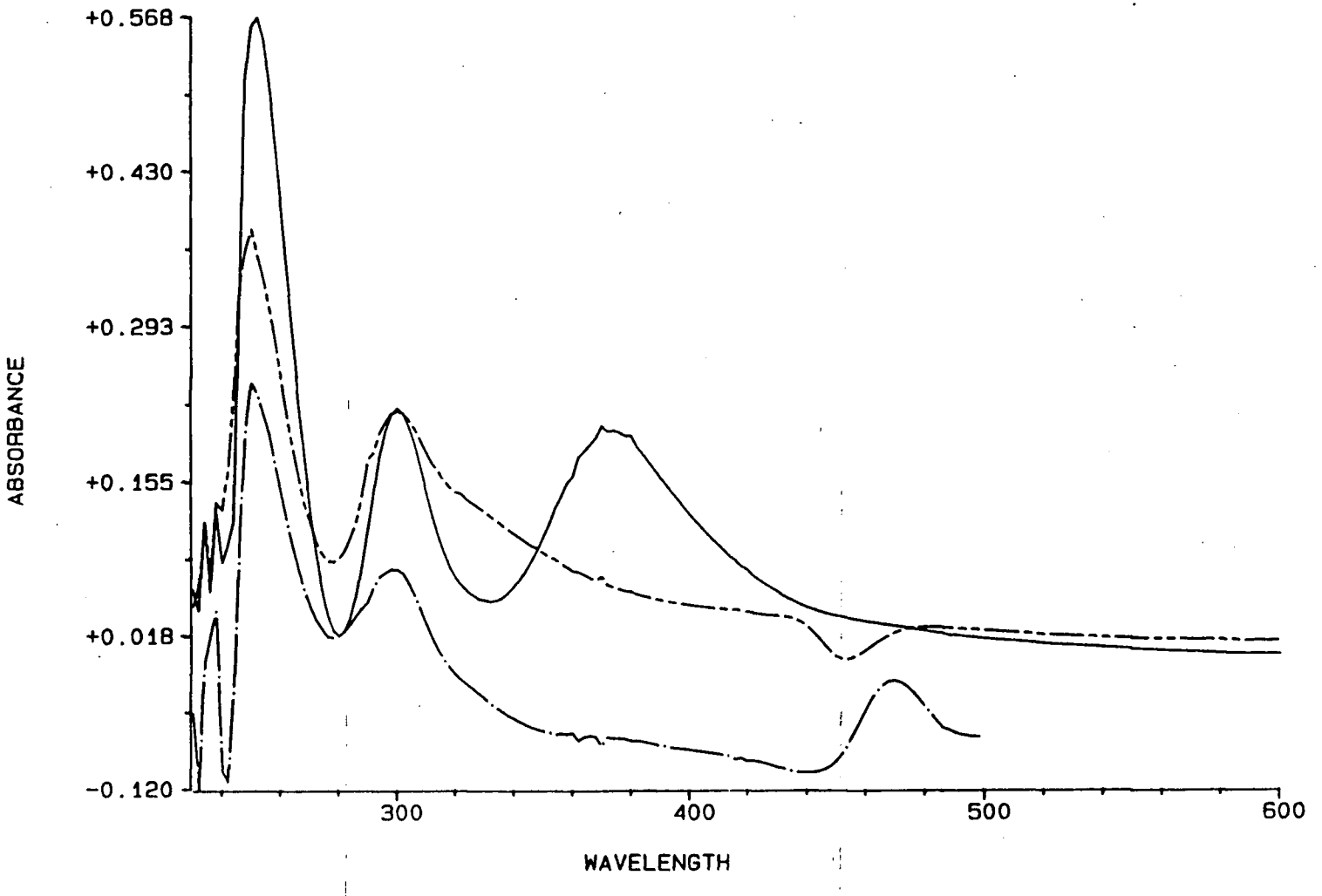

Figure A-2 Difference and reduced-difference spectra of Lignin Indulin AT treated with $Cl_{16}TSPPMnCl$ and H_2O_2 at pH 2, — difference spectrum of untreated lignin; -.-.- difference spectrum of treated lignin; ---- reduced-difference spectrum of treated lignin

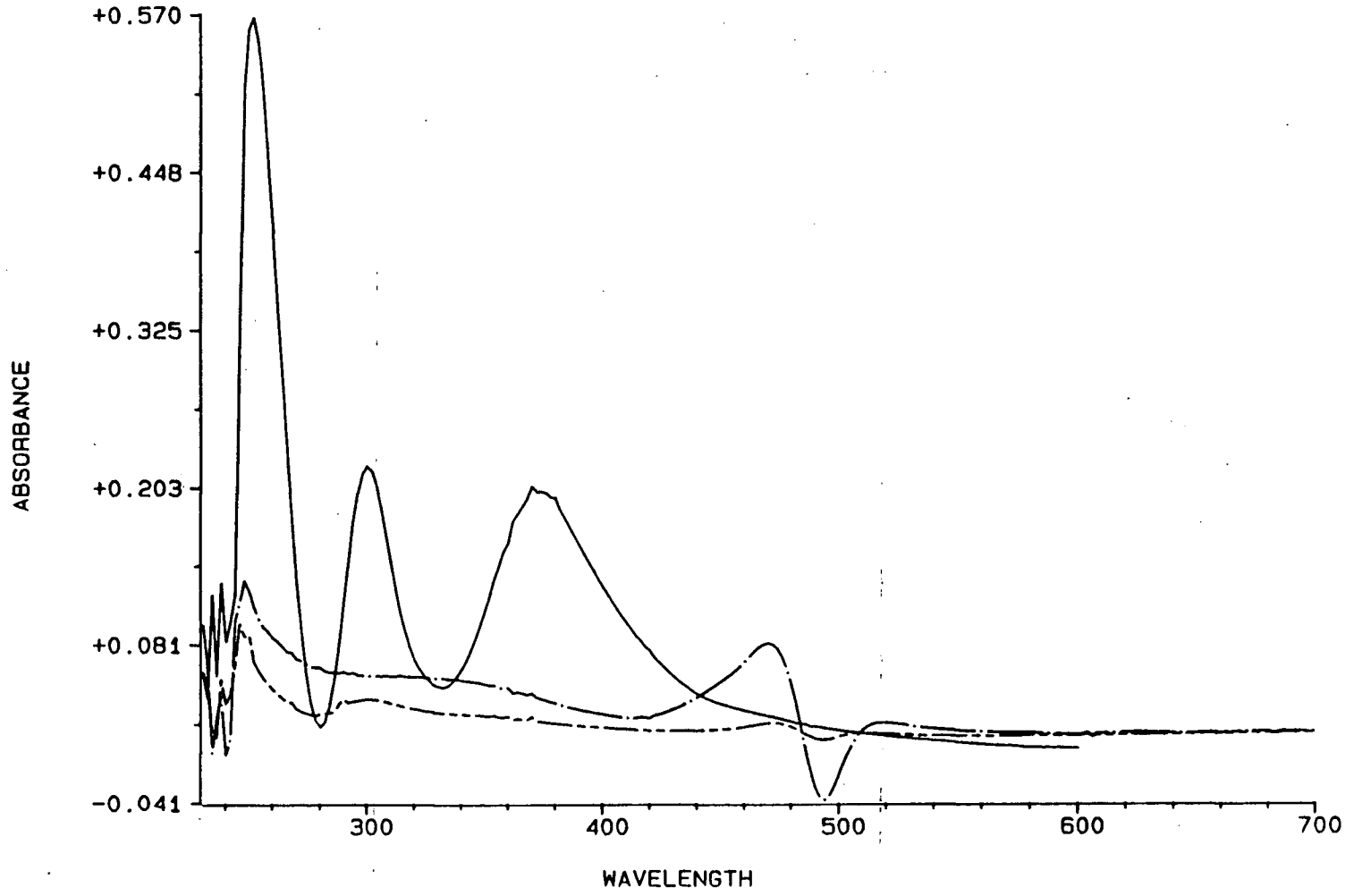

Figure A-3 Difference and reduced-difference spectra of Lignin Indulin AT treated with Cl_{16}TSPPMnCl and t-BuOOH at pH 10, — difference spectrum of untreated lignin; -.-.- difference spectrum of treated lignin; ---- reduced-difference spectrum of treated lignin

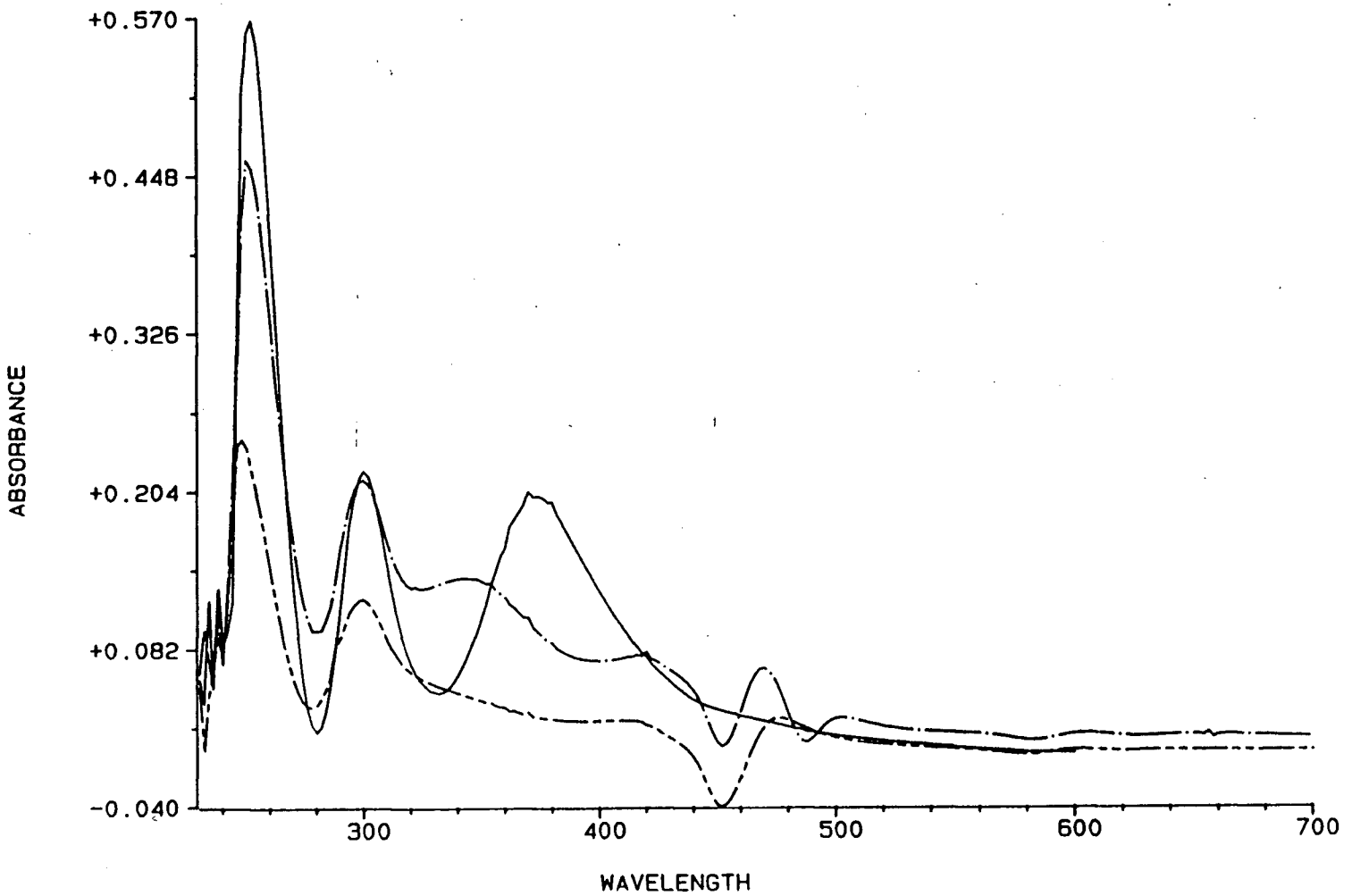

Figure A-4 Difference and reduced-difference spectra of Lignin Indulin AT treated with $Cl_{16}TSPPMnCl$ and H_2O_2 at pH 10, — difference spectrum of untreated lignin; -.-.- difference spectrum of treated lignin; ---- reduced-difference spectrum of treated lignin

indicating both the unconjugated and conjugated guaiacyl structures (**85** and **86**) had disappeared.

Unfortunately, the oxidation of phenolic model compounds by lignin peroxidase and biomimetic catalysts have not been extensively studied. The type of structural changes that have occurred cannot be explained based on our present knowledge of these difference spectra. In addition, reactions occurred on the non-phenolic moiety of the lignin structure, such as side-chain cleavage, demethoxylation, and aromatic ring cleavage reactions cannot be seen from difference spectra or reduced-difference spectra. C^{13} NMR, FT-IR, and molecular weight distribution analyses of the oxidized lignin sample are needed to understand any of the resulting structural changes.

Experimental

Kraft softwood Lignin Indulin AT, obtained from Westraw Corporation, Charleston Heights, S.C., USA, was dried under vacuum at room temperature for 24 hours before use. Lignin Indulin AT (1.0 mg) was dissolved in a mixture of DMF (1 mL) and aqueous buffer (0.1 M phosphate buffer, pH 2 or 10, 2 mL) containing $Cl_{16}TSPPMnCl$ (5×10^{-8} mole). The oxidant (9 μL of 30% H_2O_2 or 90% t-BuOOH) was added in three portions over 60 minutes and the reaction mixture was stirred at room temperature for an additional 24 hours. The resulting solution was diluted with water (7.0 mL) and 1 mL of the diluted solution was mixed with 0.1 M pH 6 buffer (1.0 mL) to serve as the reference for the difference spectral measurements. The sample for the difference spectral measurements was obtained by mixing the diluted solution (1.0 mL) with 0.1 M pH 12 borate buffer (1.0 mL). When the reaction was carried out at pH 2, the solution was first neutralized with 10 drops of 1 M K_2CO_3 before diluting

with water (7.0 mL).

For reduced-difference spectra, the diluted solution (2.0 mL) was mixed with 0.1 M pH 12 borate buffer (2 mL) and reacted with sodium borohydride (2.0 mg) at room temperature for 24 hours. The reference and scanning sample for the reduced-difference spectra was obtained by diluting the reduced solution (1 mL) with pH 6 (1 M phosphate) and pH 12 (1 M borate) buffer (1 mL), respectively.

Appendix 2

Metallophthalocyanines as Possible Lignin Peroxidase Models

Introduction

As described in previous chapters, the chloro-substituted metalloporphyrins (TDCSPPFeCl, TDCSPPMnCl, Cl_{16}TSPPFeCl, and Cl_{16}TSPPMnCl) are very stable and closely mimic the function of lignin peroxidase in the oxidation of lignin model compounds. Cl_{16}TSPPFeCl has also been shown to be an effective catalyst for pulp bleaching and pulp mill effluent decolorization, and therefore has potential industrial applications. The metalloporphyrins are, however, expensive and cheap substitutes need to be found.

The phthalocyanines (**87**) belong to a class of synthetic compounds closely related to the naturally occurring porphyrins[4] (**88**). Metallophthalocyanines are known to have

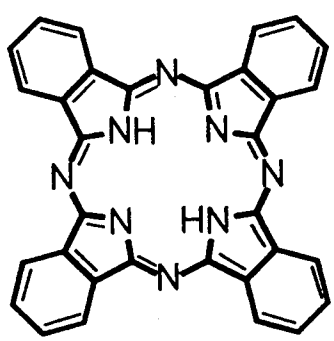

87

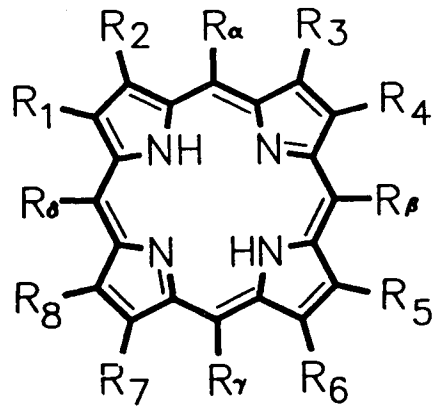

88

catalytic activities for a variety of reactions[5] including hydrocarbon autoxidation,[6,7] olefin epoxidation[8,9] and hydrocarbon hydroxylation.[10] Iron phthalocyanines have also been shown to have catalase- and peroxidase-like activities.[11-13] The use of metallophthalocyanines as lignin peroxidase models, however, have not been previously reported. We studied the oxidation of lignin model compounds by several metallophthalocyanines, including Fe(III)-, Mn(III)-, Ni(II)-, Cu(II)-, and Co(II)-tetrasulfonatophthalocyanine (TSPCFeCl, **89**; TSPCMnCl, **90**; TSPCNi, **91**; TSPCCu, **92**; TSPCCo, **93**; for general structure see **94**). The stability and catalytic activities of these metallophthalocyanines are compared.

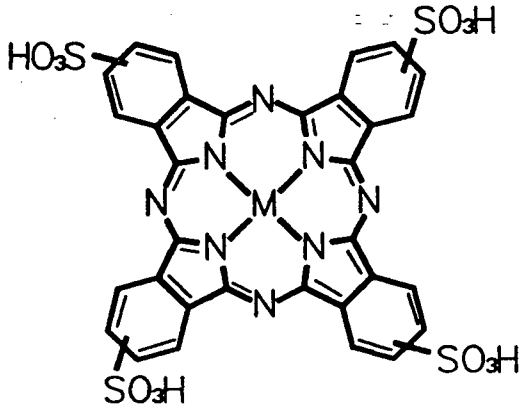

94

Results and Discussion

Veratryl alcohol (3,4-dimethoxybenzyl alcohol) is a secondary metabolite of lignin biodegradation by *P. chrysosporium* and is often used as a lignin model compound. The oxidation of veratryl alcohol to give veratraldehyde (3,4-dimethoxybenzaldehyde) has been used to measure the activity of lignin peroxidases and is used in this study to compare the catalytic activities of the metallophthalocyanines.

With TSPCCo, TSPCCu, and TSPCNi as the catalysts, the oxidation of veratryl alcohol by various oxidants gives only trace amounts of veratraldehyde as seen by thin layer chromatography (TLC). Iron(III) and manganese(III) phthalocyanine are better catalysts for the oxidation of veratryl alcohol and the yields of veratraldehyde under various conditions are listed in Table 1. The yields are still too low for TSPCFeCl and TSPCMnCl to be effective catalysts. In addition, the catalysts are not stable in most cases and are bleached within a few minutes. In the oxidation of veratryl alcohol by TSPCMnCl and mCPBA, for example, TSPCMnCl is bleached within 1 minute. The catalyst can be considered to be effective since it is destroyed within one minute after the addition of oxidant and the yield is still 30% (based on veratryl alcohol), unless the degradation products of TSPCMnCl also have catalytic activity. An experiment was carried out where mCPBA was added to a solution containing TSPCMnCl, and veratryl alcohol was not added to the solution until the deep green color of TSPCMnCl disappeared. Little veratraldehyde was detected after 60 minutes, indicating that TSPCMnCl was the only catalyst and its degradation products had no catalytic activity.

Table A-2. The effect of imidazole on the oxidation of veratryl alcohol by TSPCMnCl and H_2O_2 at pH 7[a)] at room temperature

imidazole/TSPCMnCl (molar ratio)	1	10	50	100
% yield of veratraldehyde (based on veratryl alcohol)	17	20	23	10

a): The reaction mixture contains 5×10^{-7} mole of TSPCMnCl, 1×10^{-4} mole of H_2O_2, and 5×10^{-5} mole of veratryl alcohol.

Peroxidases, including lignin peroxidases, have an iron protoporphyrin IX with a proximal-bound imidazole group of histidine at their active sites.[14,15] Imidazole has been

Table A-1 Yield[a] for the oxidation of veratryl alcohol by TSPCMnCl and TSPCFeCl under various conditions[b]

		*m*CPBA	t-BuOOH	H_2O_2	NaClO	PhIO	$KHSO_5$
	pH 3	32	3	1	3	14	0
	pH 7	27	11	17	4	7	trace
TSPCMnCl	pH 10	29	16	10	6	9	2
	CH_3CN	24	ND[c]	ND	ND	ND	ND
	CH_3OH	27	ND	ND	ND	ND	ND
	pH 3	12	3	trace	3	9	7
TSPCFeCl	pH 7	7	1	1	1	6	trace
	pH 10	16	3	1	1	4	trace

[a]: yield based on veratryl alcohol, reaction carried out at room temperature
[b]: The reaction mixture contains in 5 mL solvent 1×10^{-4} mole of oxidant, 5×10^{-7} mole of metallophthalocyanine and 5×10^{-5} mole of veratryl alcohol.
[c]: not determined

used to facilitate metalloporphyrin catalyzed reactions.[16,17] We have shown that the presence of imidazole could increase the catalytic activity of a manganese porphyrin for the oxidation of veratryl alcohol by hydrogen peroxide. As shown in Table 2, the presence of imidazole at certain concentrations also increased the yield of veratraldehyde.

The yield for the oxidation of veratryl alcohol by metalloporphyrins was dependent on the solvent. The solvent effect for the oxidation of veratryl alcohol by TSPCMnCl and mCPBA was studied. TSPCMnCl was much more stable towards mCPBA in organic solvents such as acetonitrile and methanol (containing 100 μL of water in 5 mL solvent) than in aqueous solution. The yield of veratraldehyde (Table 1), however, does not change much with the solvent.

The oxidation of two dimeric lignin model compounds by TSPCFeCl and TSPCMnCl was also studied. The oxidation of the ß-O-4 dimer, 4-ethoxy-3-methoxyphenylglycerol-ß-guaiacyl ether (**62**), by mCPBA and either TSPCFeCl or TSPCMnCl was not complete and gave only small amounts of 4-ethoxy-3-methoxybenzaldehyde and the α-ketone **95** as shown in Figure A-5. Similar products were found in the oxidation of the ß-O-4 dimer by lignin peroxidases.[18]

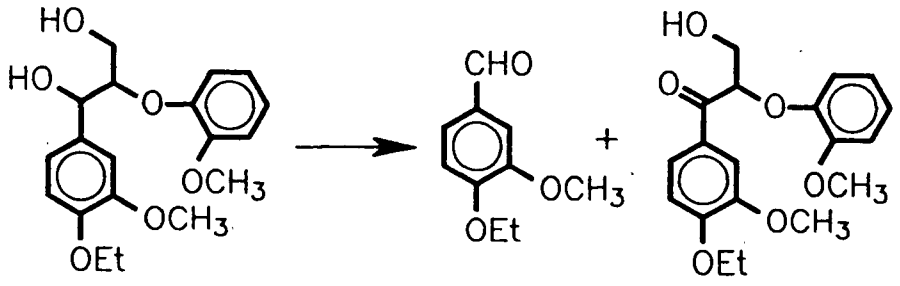

62 95

Figure A-5 The oxidation of **62** by TSPCMnCl (or TSPCFeCl) and *m*CPBA in aqueous acetonitrile (pH 3) at room temperature

The ß-1 dimeric model compound, 1-(4-ethoxy-3-methoxyphenyl)-2-(4-methoxyphenyl)-1,3-propanediol (**55**), was oxidized more readily than the ß-O-4 dimer. No starting material was detected by HPLC when it was oxidized by either TSPCFeCl or TSPCMnCl in the presence of two equivalents of mCPBA. The products were similar to those of the reaction catalyzed by lignin peroxidases and metalloporphyrins[19] (Figure A-6).

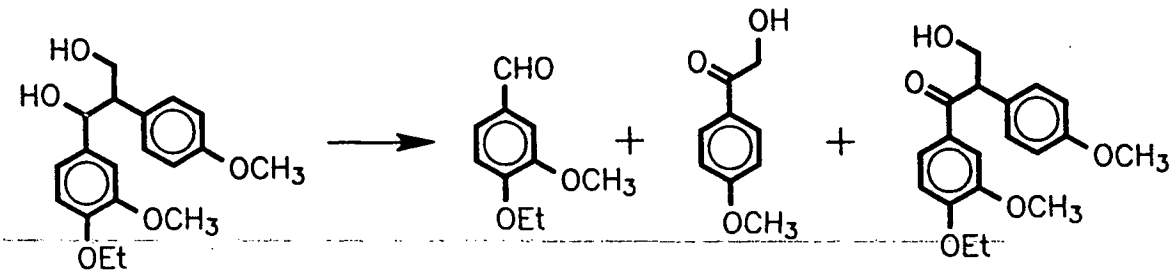

55 96

Figure A-6 The oxidation of **55** by TSPCMnCl (or TSPCFeCl) and *m*CPBA in aqueous acetonitrile at room temperature

Metallophthalocyanines have been used as catalysts for a variety of reactions including epoxidation of olefins,[8,9] hydroxylation of hydrocarbons,[10] and decomposition of hydrogen peroxide.[11,12] The stability of these catalysts in the presence of excess oxidants, which may be a major problem for their industrial applications, have been rarely discussed.[8]

Among the metallophthalocyanines used in this study, TSPCCu, TSPCNi, TSPCCo, TSPCFeCl, and TSPCMnCl, both of the effective catalyst TSPCFeCl and TSPCMnCl were unstable and bleached within a few minutes under the experimental conditions. One exception is that TSPCFeCl is relatively stable in the presence of hydrogen peroxide. TSPCFeCl, however, has very little activity for the oxidation of veratryl alcohol when using hydrogen peroxide as the oxidant. The stability of

TSPCFeCl and TSPCMnCl was dependent on the pH of the solvent as well as the type of oxidant used. As the UV-vis absorption peaks of TSPCFeCl and TSPCMnCl shifts upon addition of oxidants, it is impossible to follow the destruction of TSPCFeCl and TSPCMnCl at a single wavelength and quantitative stability data is not available. Figure A-7 shows UV-vis spectral change of TSPCMnCl and TSPCFeCl upon addition of 1 equivalent of oxidant at pH 3, 7, and 10. In the presence of a large excess of oxidant, *i.e.* 100 fold excess, TSPCFeCl and TSPCMnCl are destroyed very quickly. TSPCFeCl and TSPCMnCl are much less stable compared with the sterically protected metalloporphyrins such as TDCSPPFeCl. They are also less stable than the non-sterically protected metalloporphyrin such as *meso*-tetra(4-sulfonatophenyl)porphyrin iron chloride (TSPPFeCl), which retains about 30% of its activity 10 minutes after adding 100 fold excess of oxidants.

TSPCCu and TSPCNi, on the other hand, are very stable and little spectral change is observed even in the presence of 100 fold excess of oxidants. However, they have little catalytic activity for the oxidation of veratryl alcohol. It can be seen by examining Table A-1 and Figure A-7 that there is no correlation between the catalytic activity and stability of the metallophthalocyanines.

Conclusions

The copper(II), nickel(II), cobalt(II) complexes of tetrasulfonatophthalocyanine were found to have little activity for the oxidation of veratryl alcohol under the conditions used. TSPCFeCl and TSPCMnCl could generally mimic the function of lignin peroxidase in the oxidation of veratryl alcohol, ß-1, and ß-O-4 lignin model compounds. The presence of imidazole slightly increased the yield of the oxidation of

Figure A-7 (A) TSPCMnCl/$KHSO_5$, pH 3

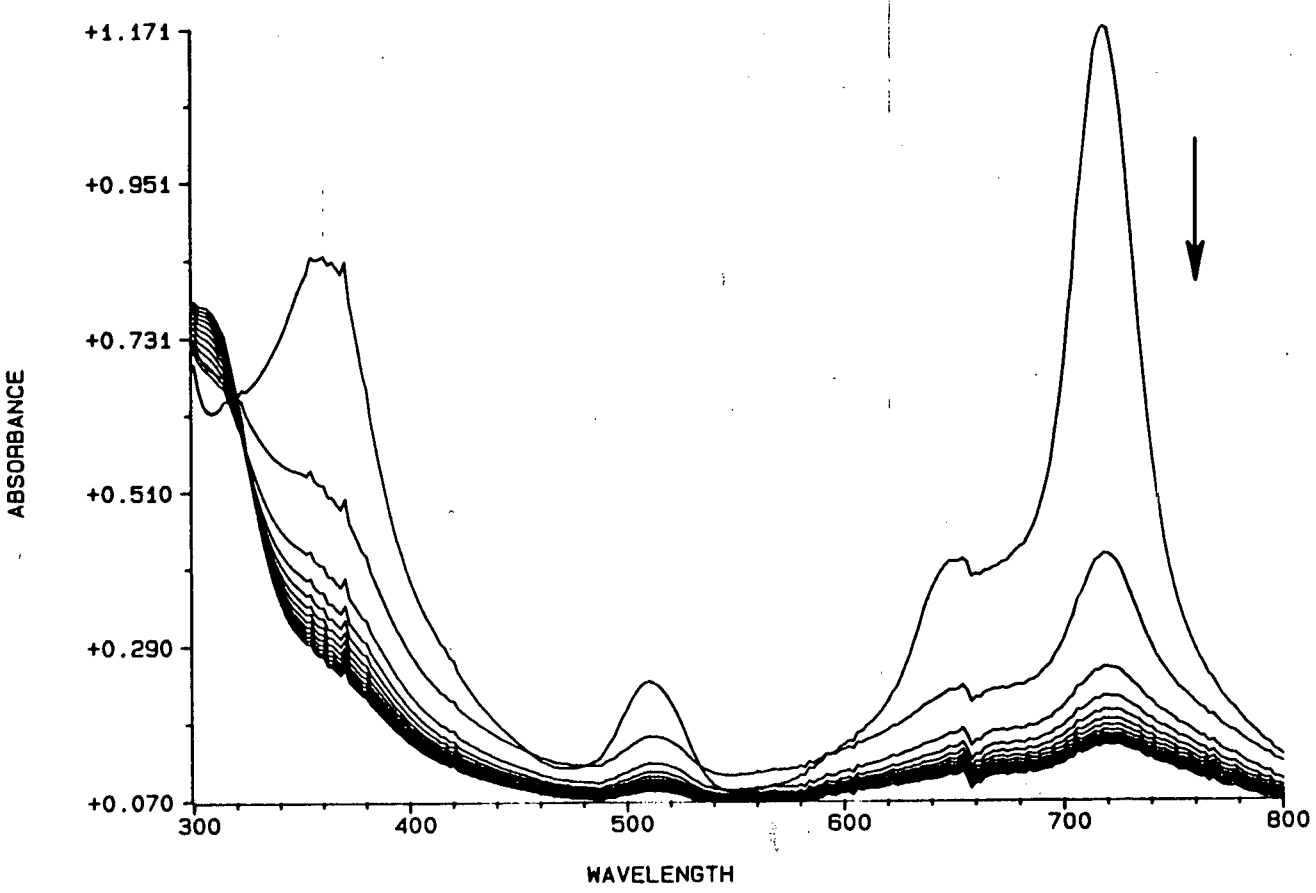

Figure A-7 (B) TSPCMnCl/$KHSO_5$, pH 7

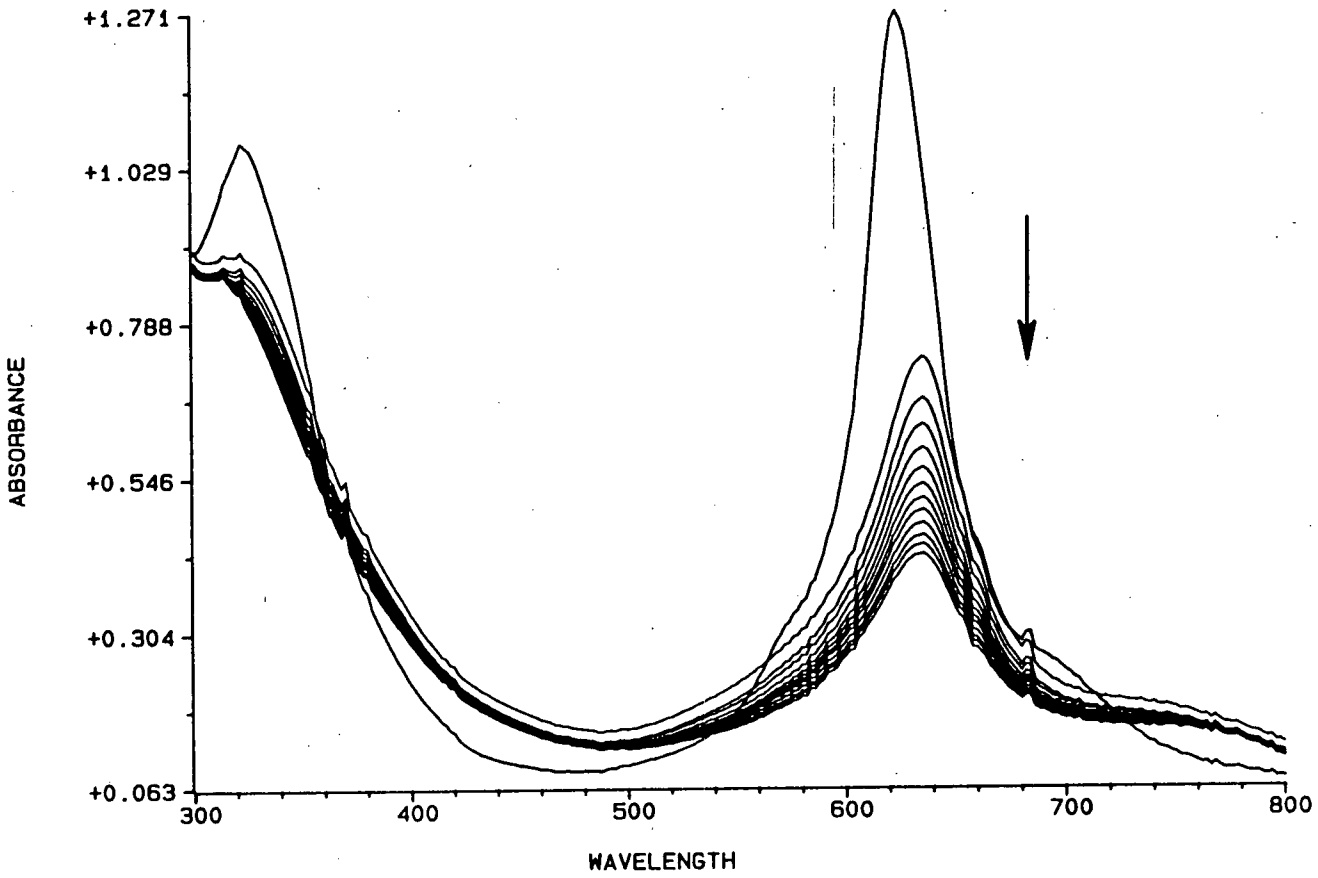

Figure A-7 (C) TSPCMnCl/$KHSO_5$, pH 10

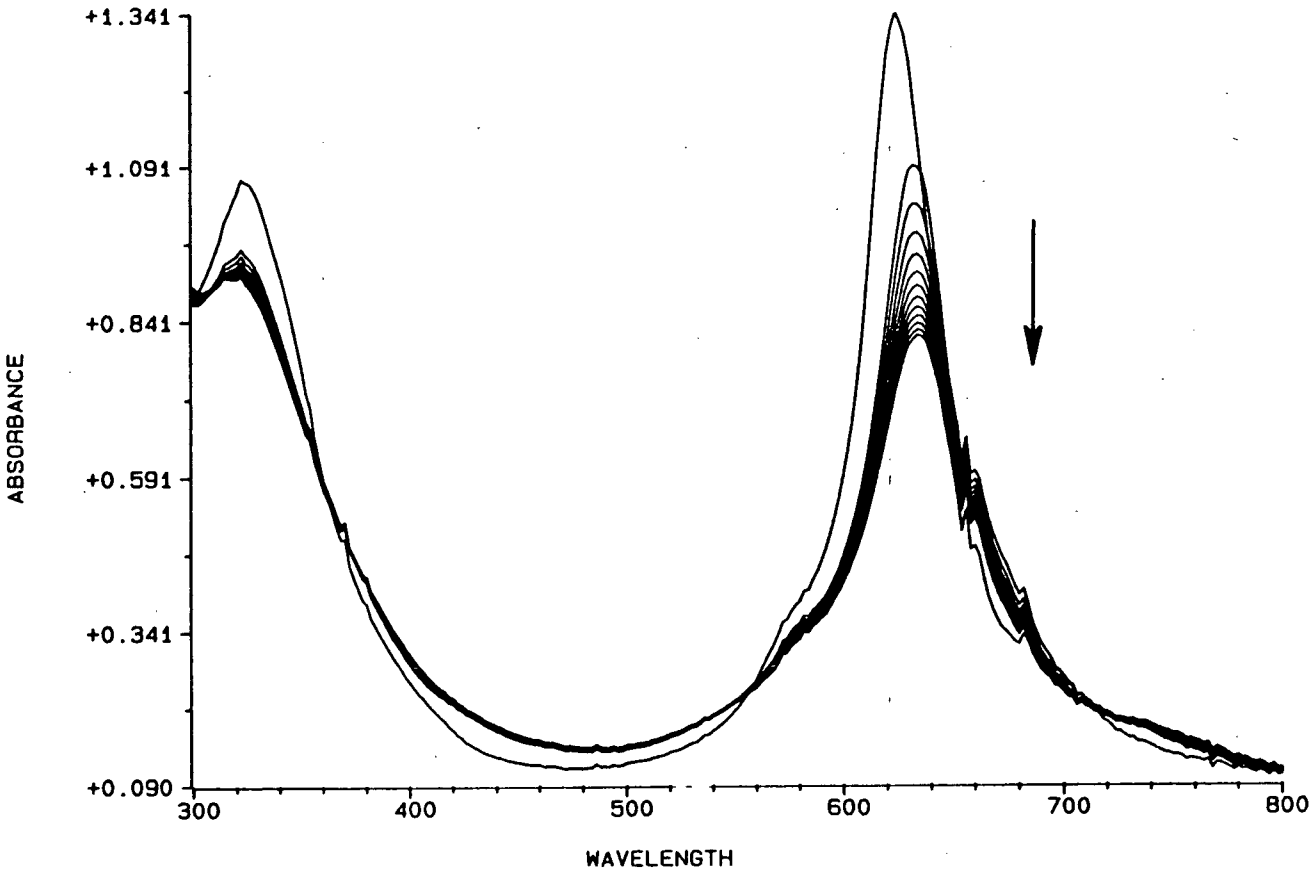

Figure A-7 (D) TSPCMnCl/*m*CPBA, pH 3

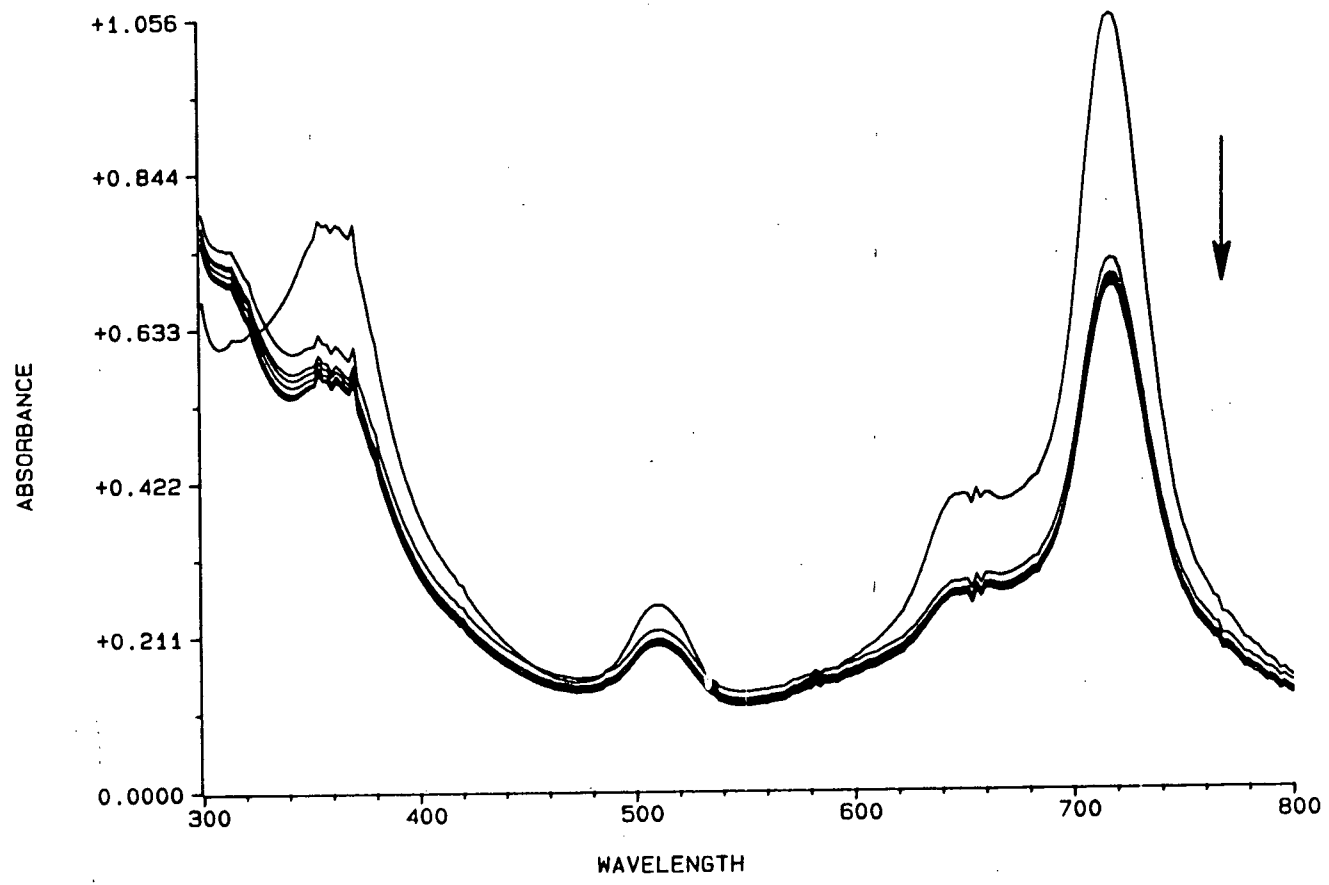

Figure A-7 (E) TSPCMnCl/*m*CPBA, pH 7

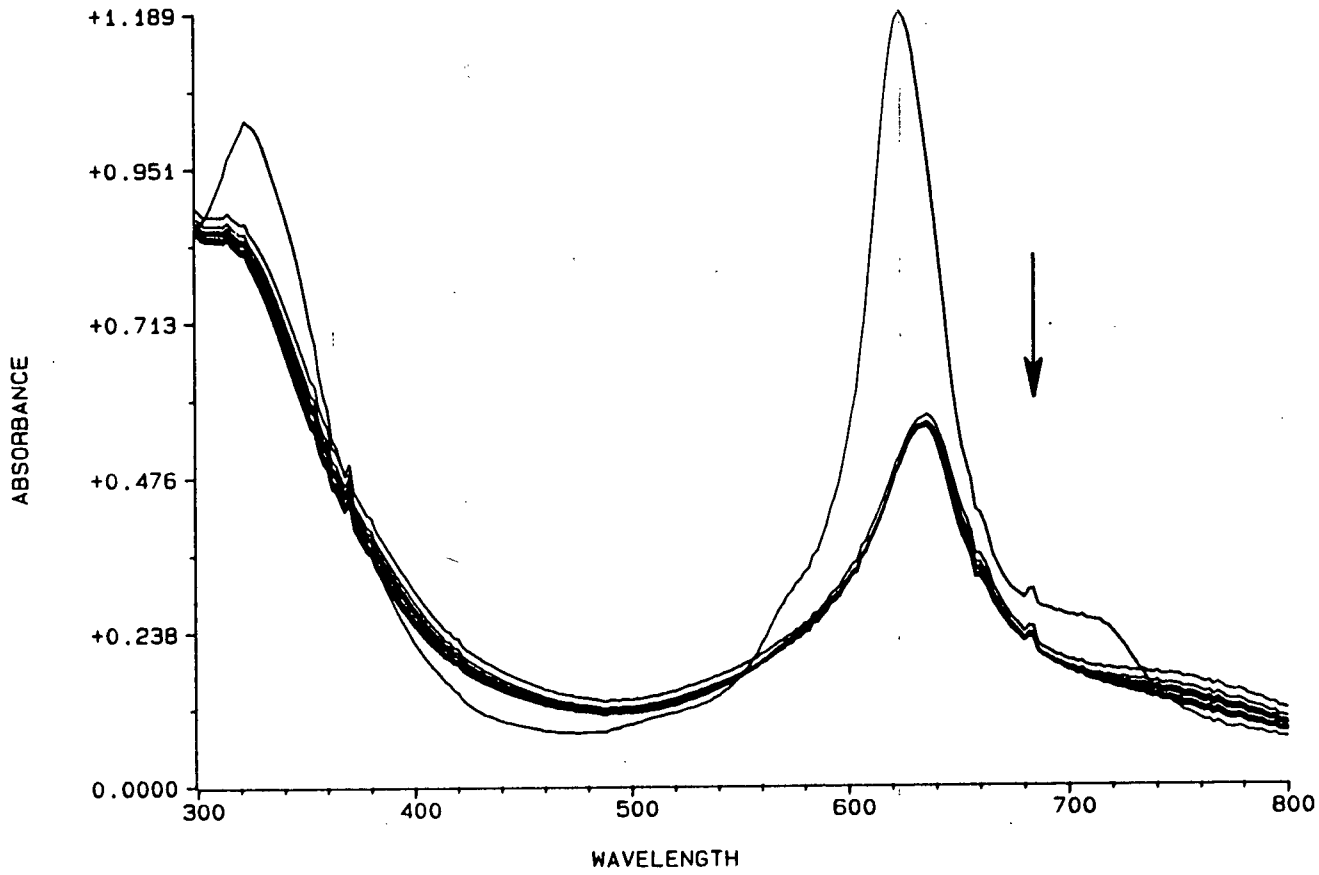

Figure A-7 (F) TSPCMnCl/*m*CPBA, pH 10

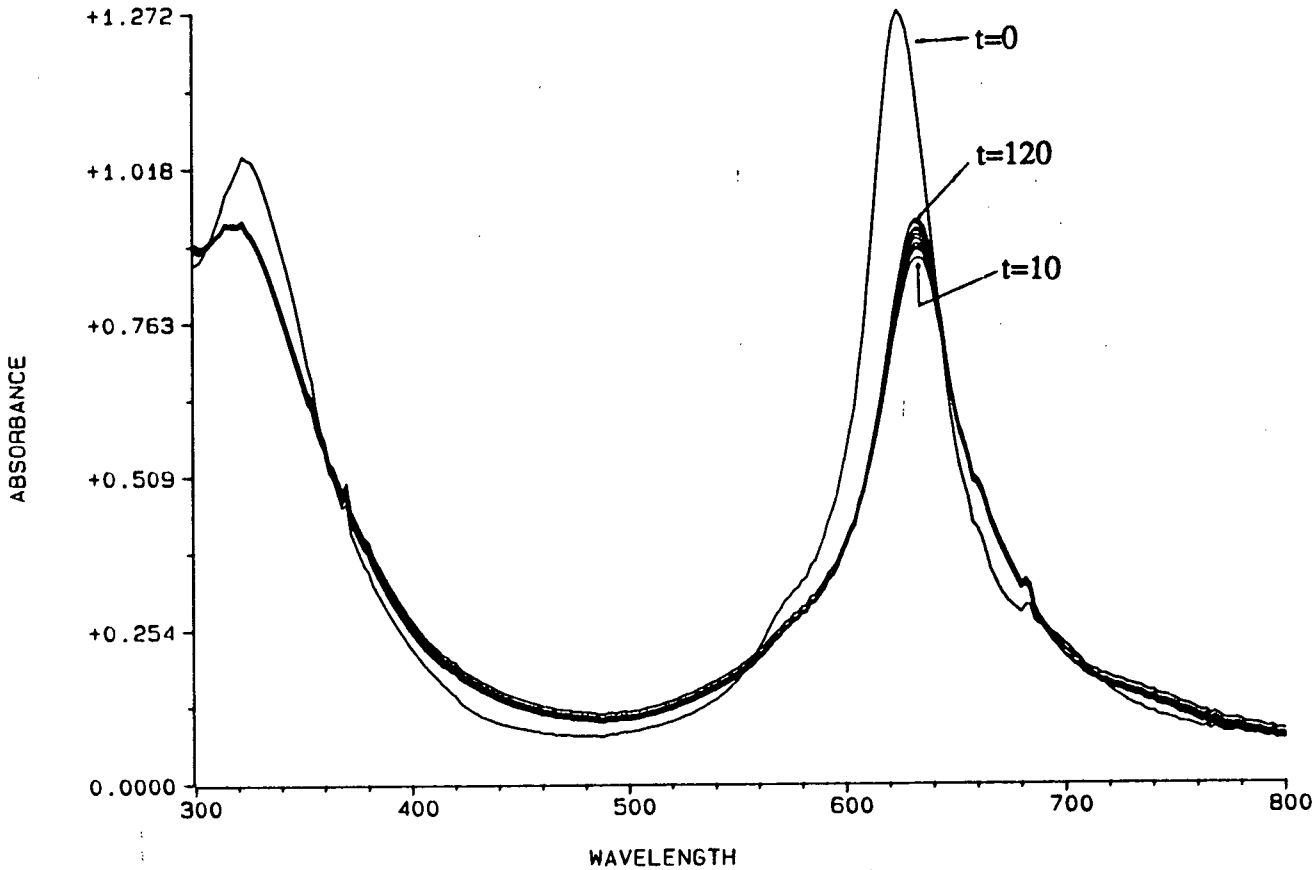

Figure A-7 (G) TSPCMnCl/NaClO, pH 3

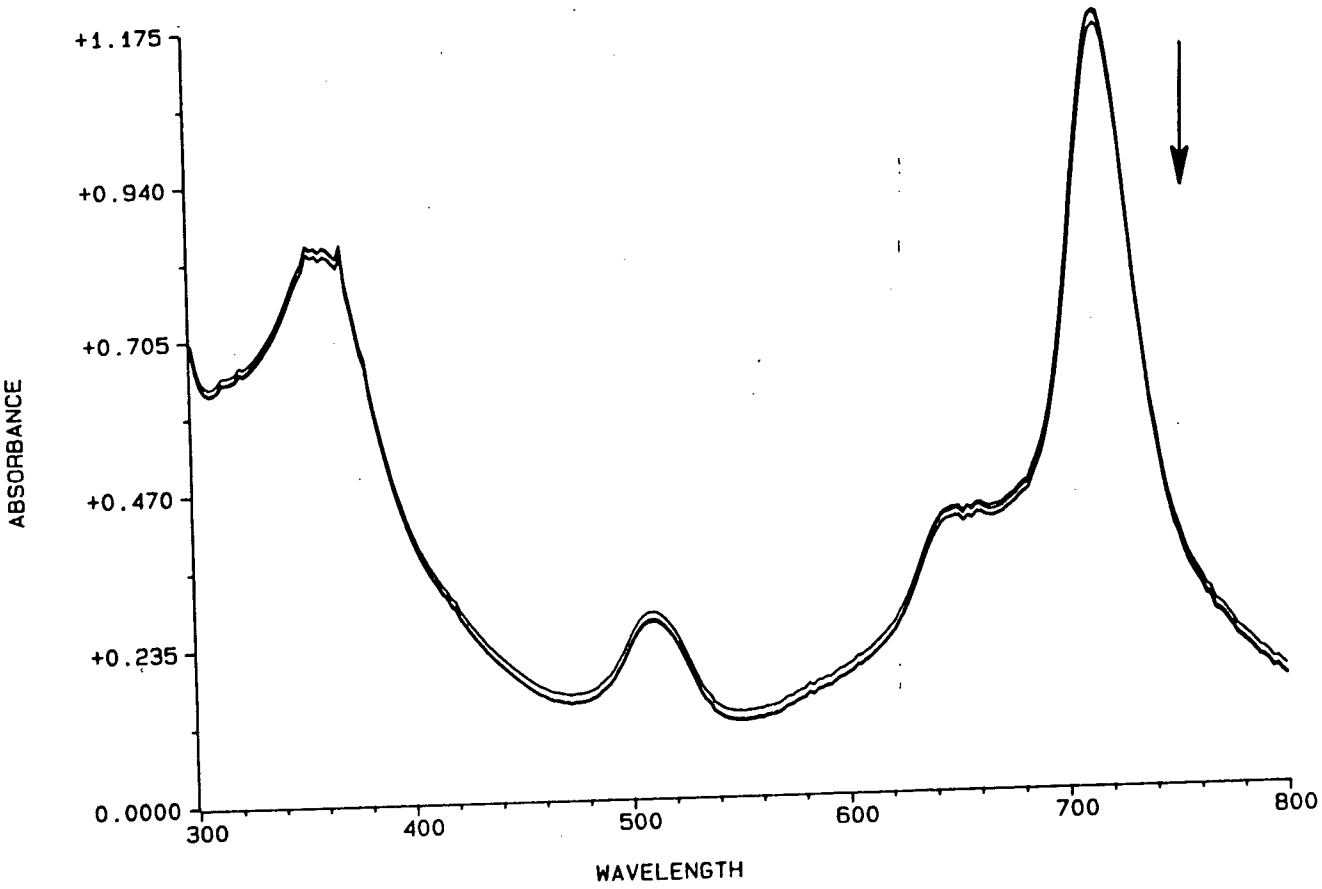

Figure A-7 (H) TSPCMnCl/NaClO, pH 7

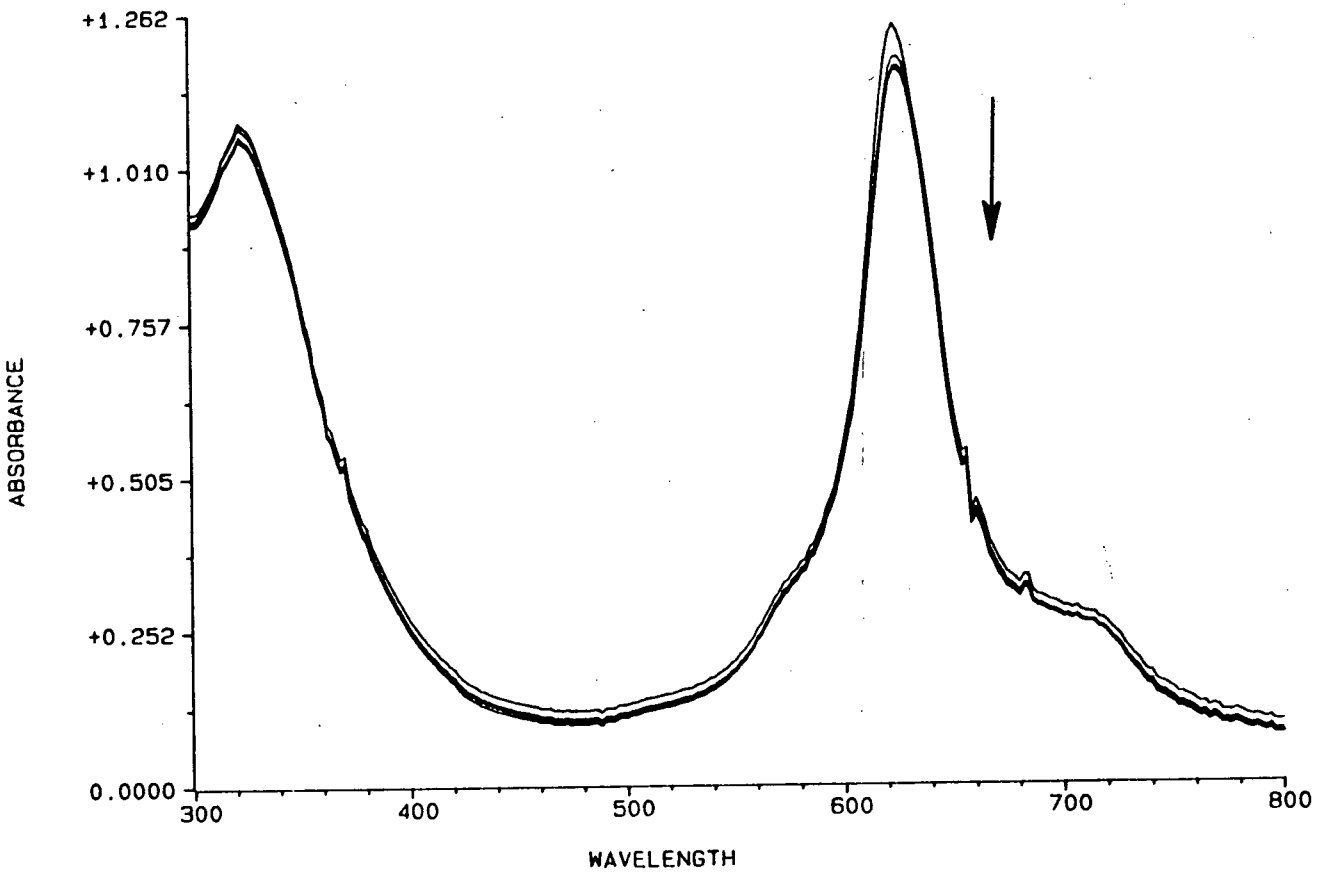

Figure A-7 (I) TSPCMnCl/NaClO, pH 10

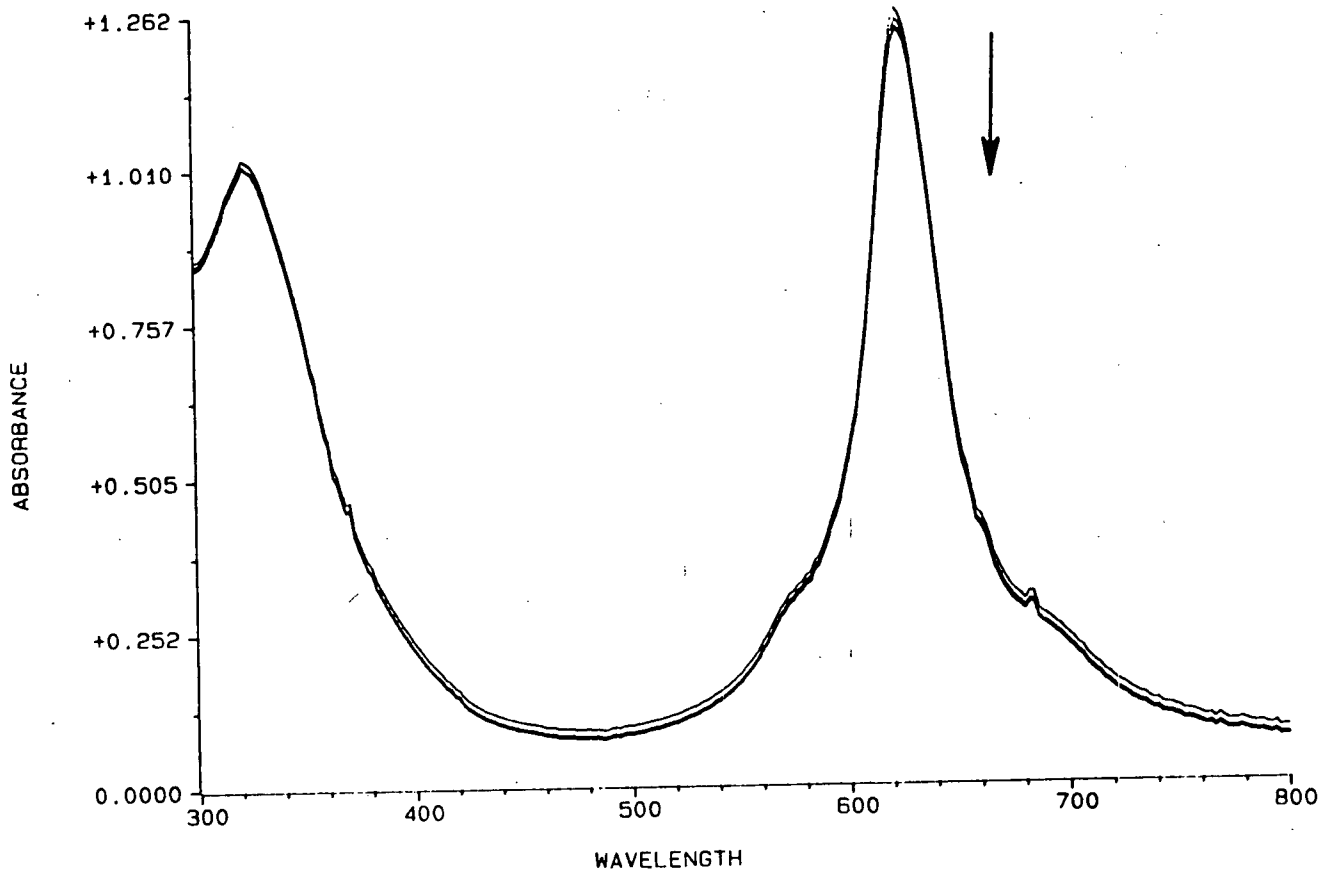

Figure A-7 (J) TSPCMnCl/t-BuOOH, pH 3

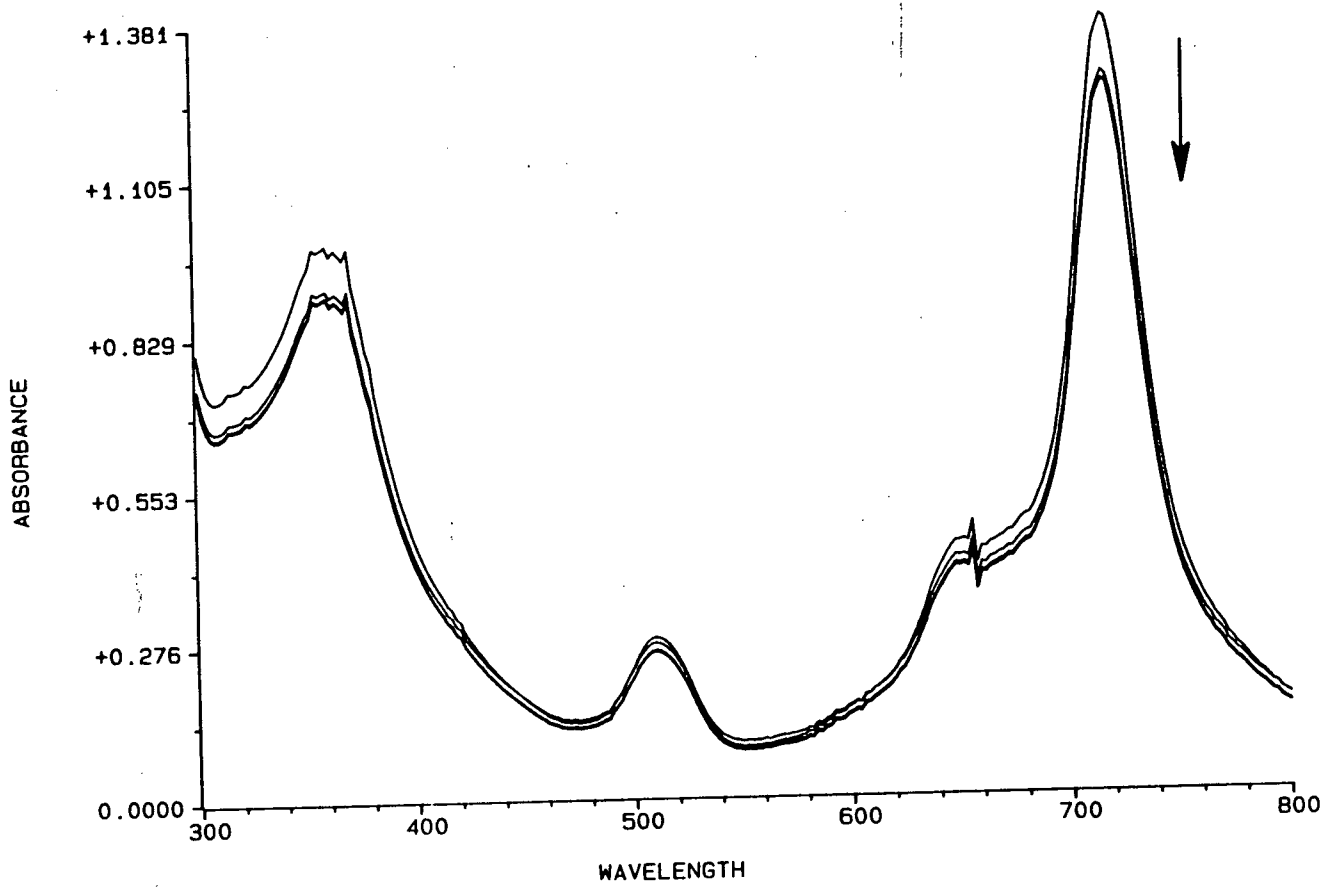

Figure A-7 (K) TSPCMnCl/t-BuOOH, pH 7

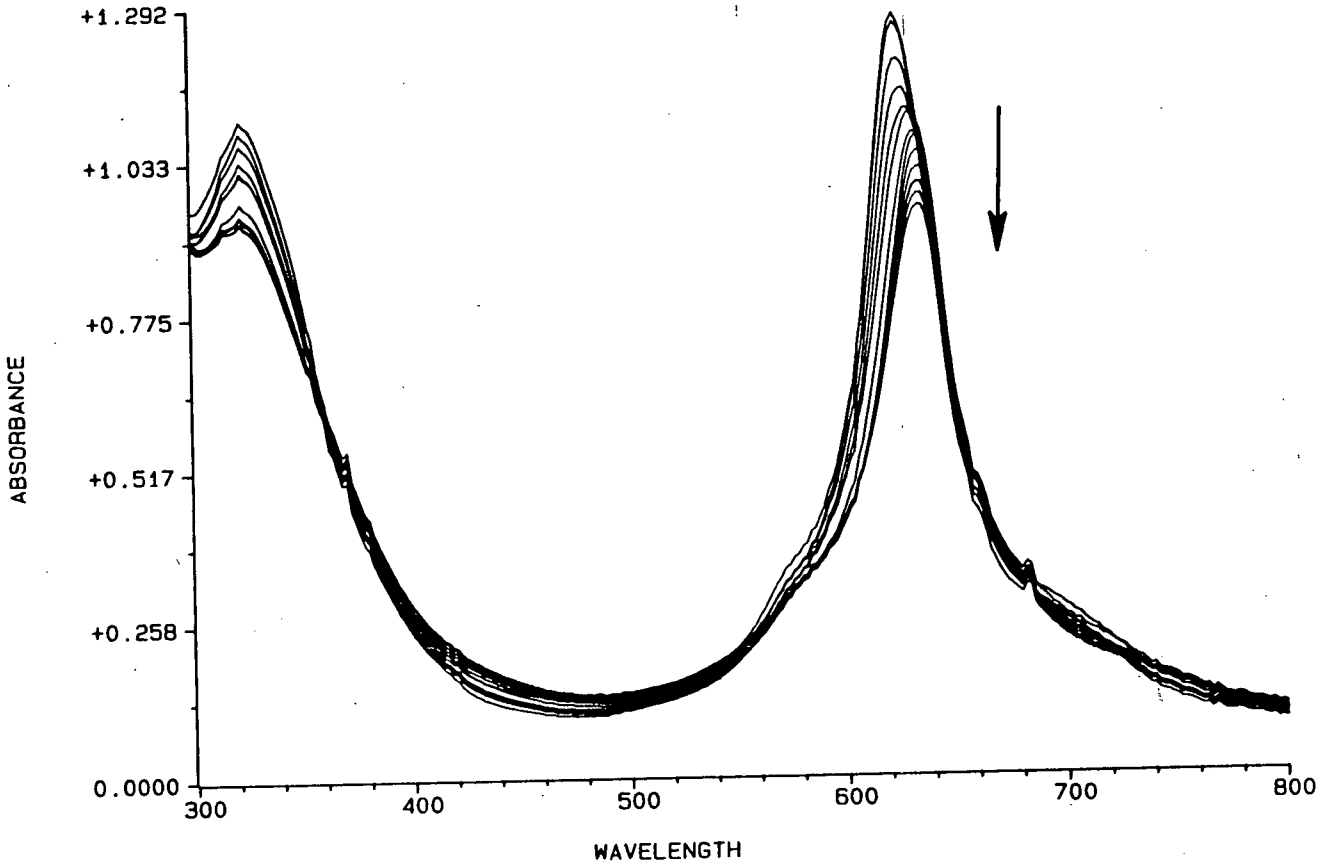

Figure A-7 (L) TSPCMnCl/t-BuOOH, pH 10

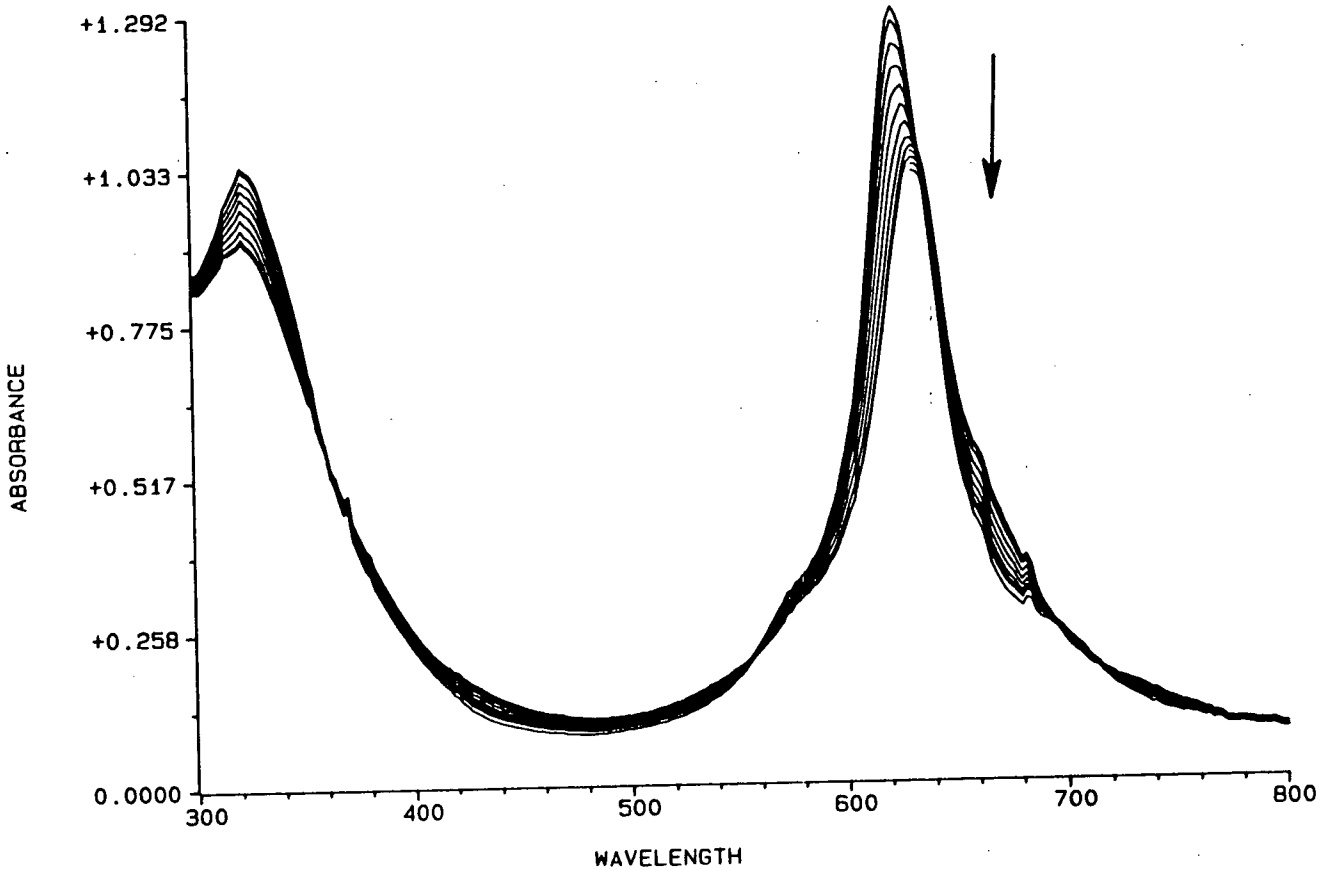

Figure A-7 (M) TSPCMnCl/H_2O_2, pH 3

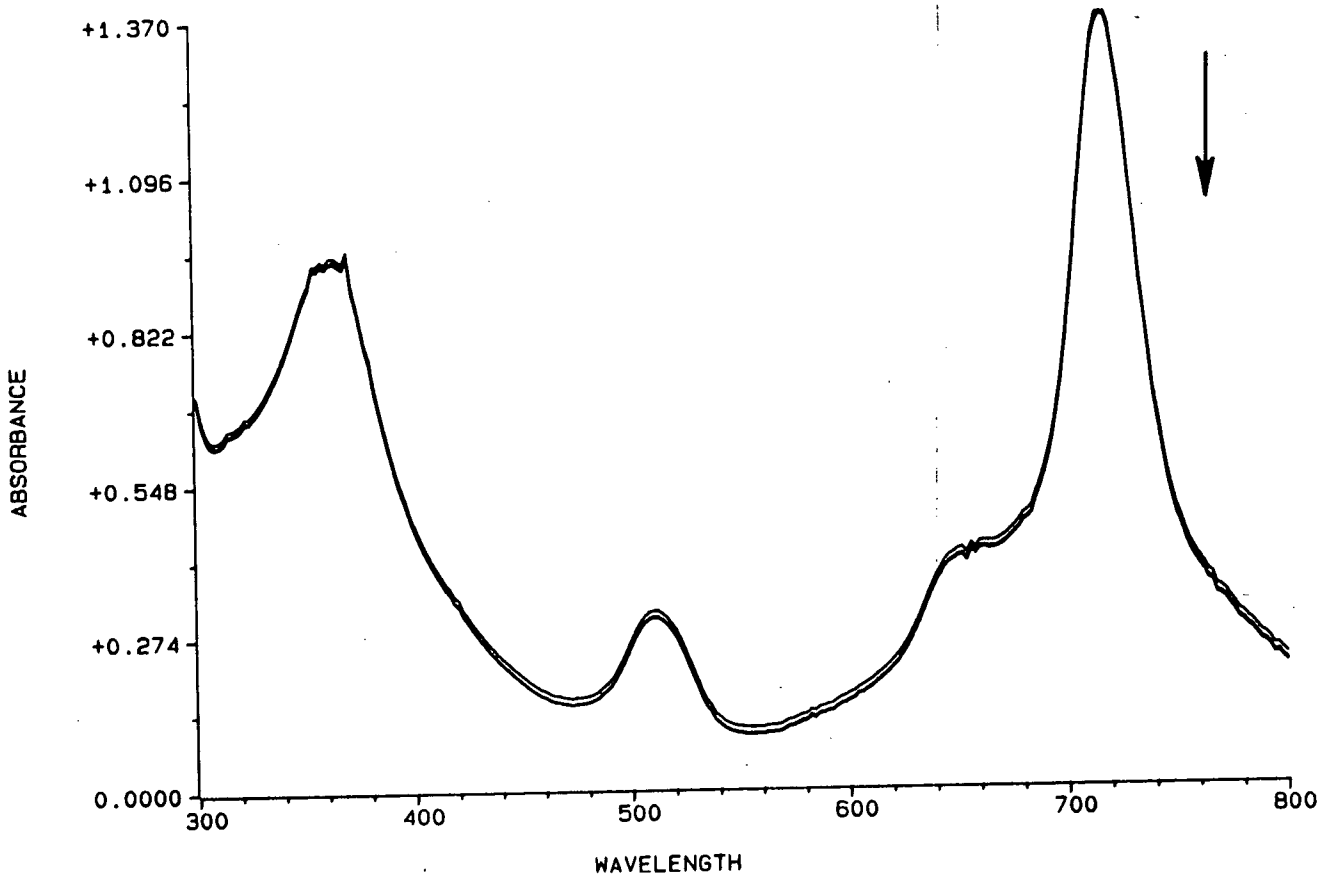

Figure A-7 (N) TSPCMnCl/H_2O_2, pH 7

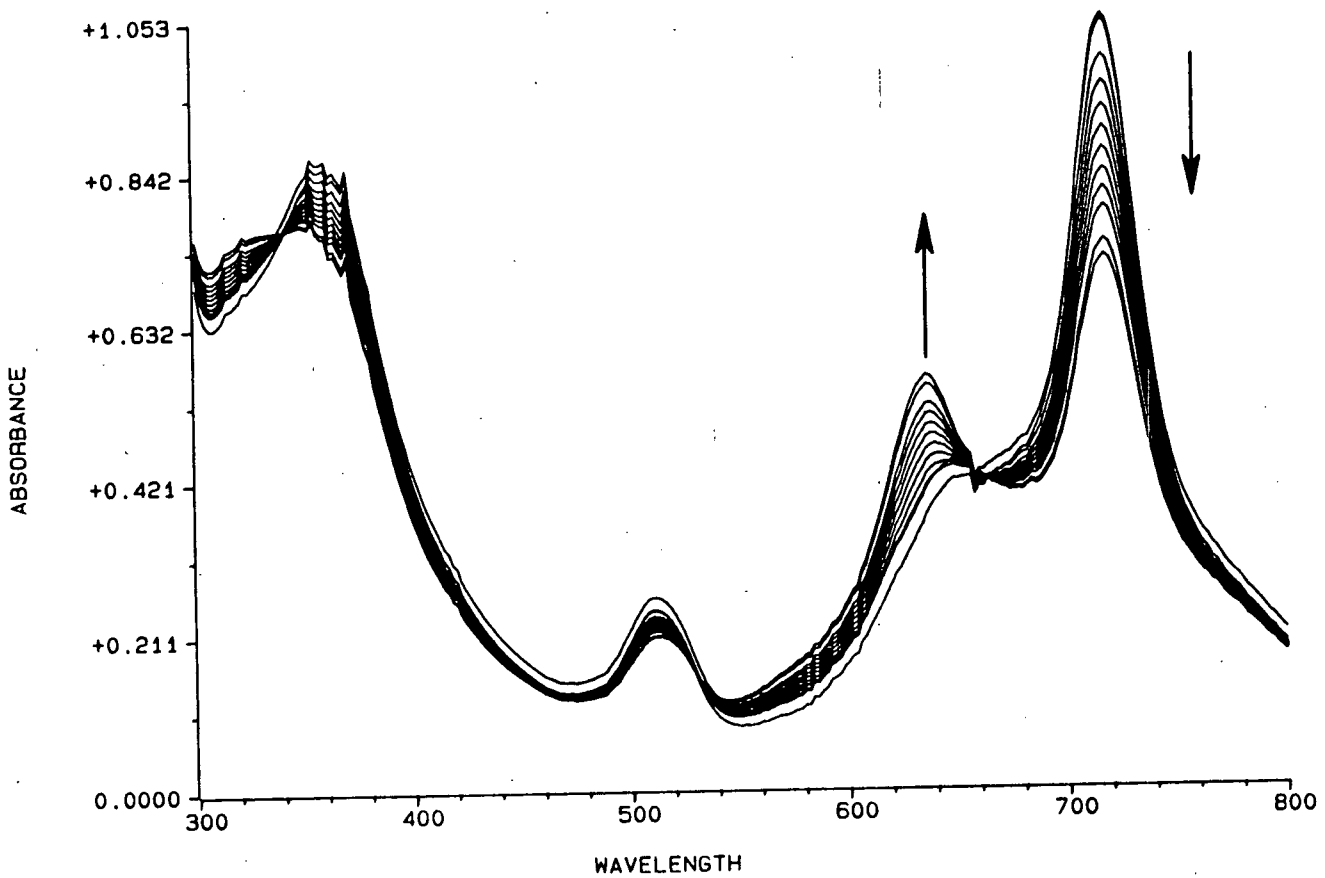

Figure A-7 (O) TSPCMnCl/H_2O_2, pH 10

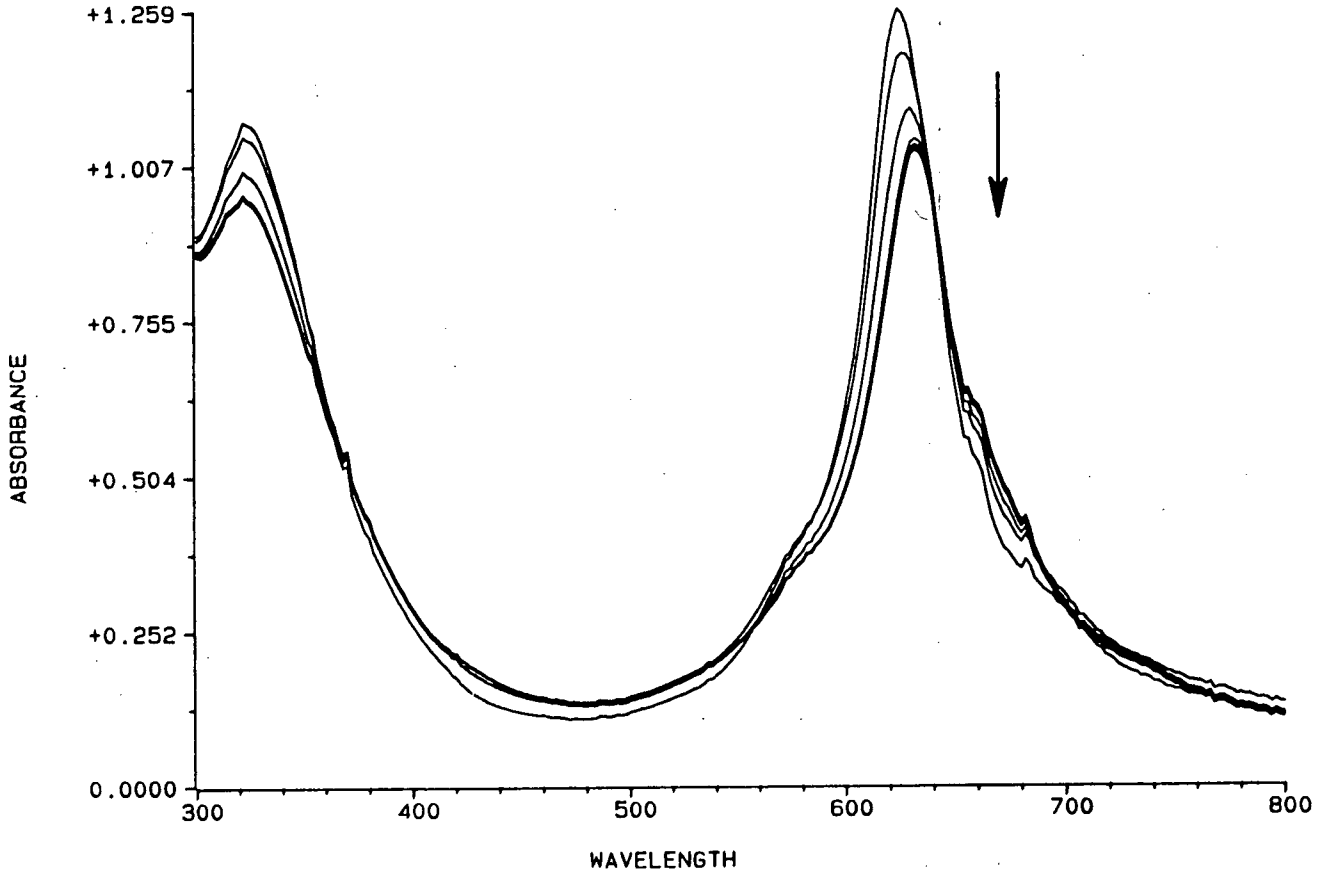

Figure A-7 (P) TSPCFeCl/*m*CPBA, pH 3

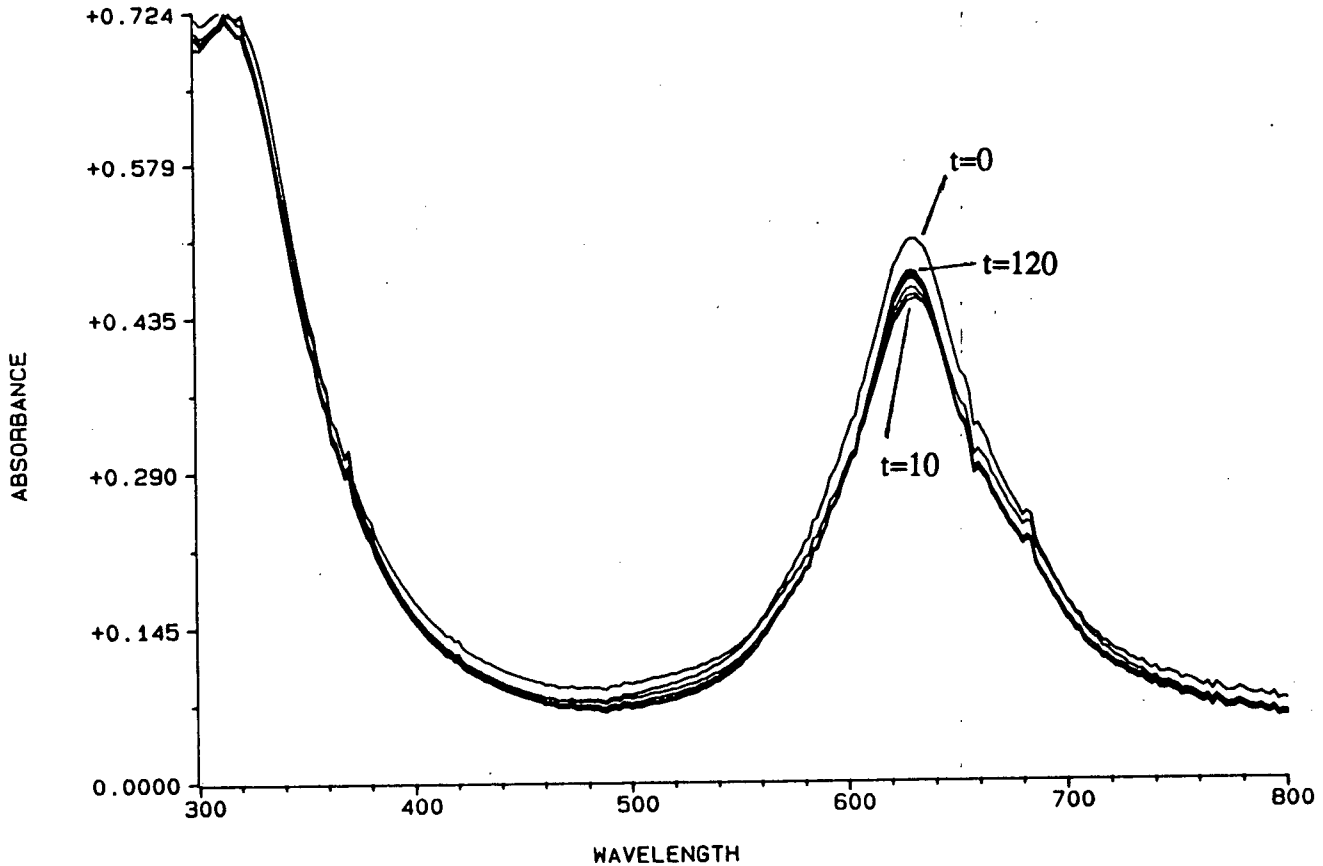

Figure A-7 (Q) TSPCFeCl/*m*CPBA, pH 7

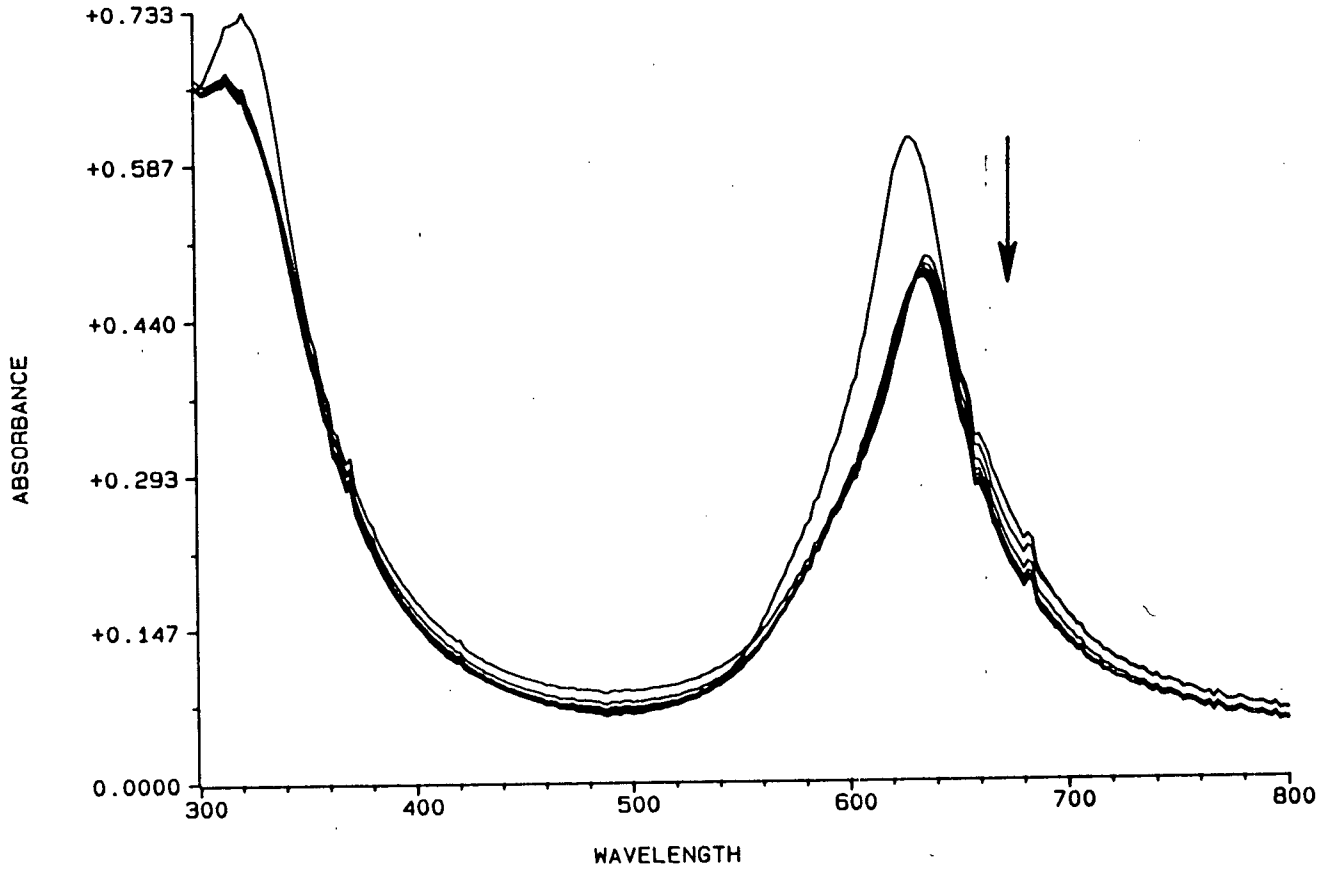

Figure A-7 (R) TSPCFeCl/*m*CPBA, pH 10

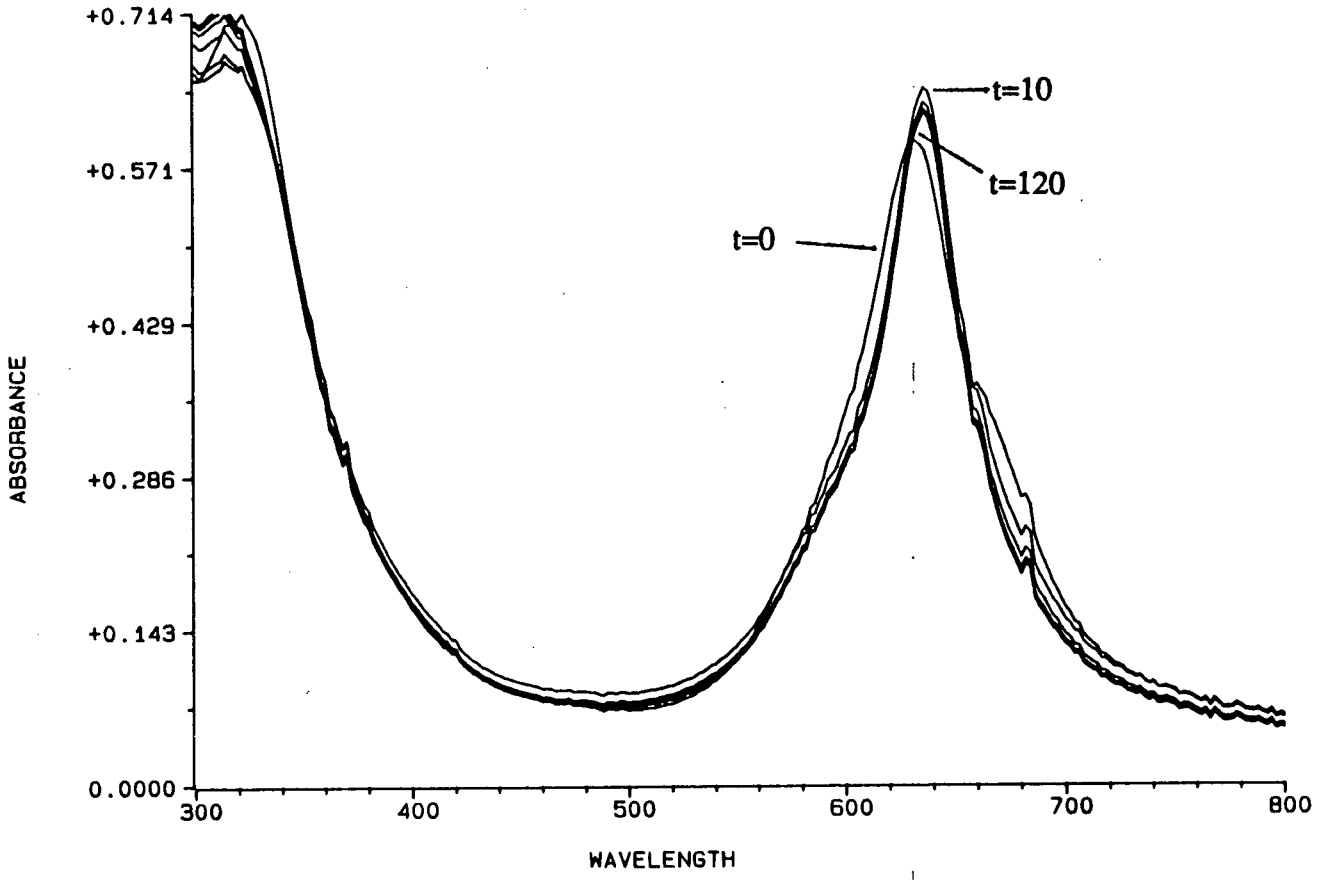

Figure A-7 (S) TSPCFeCl/H_2O_2, pH 3

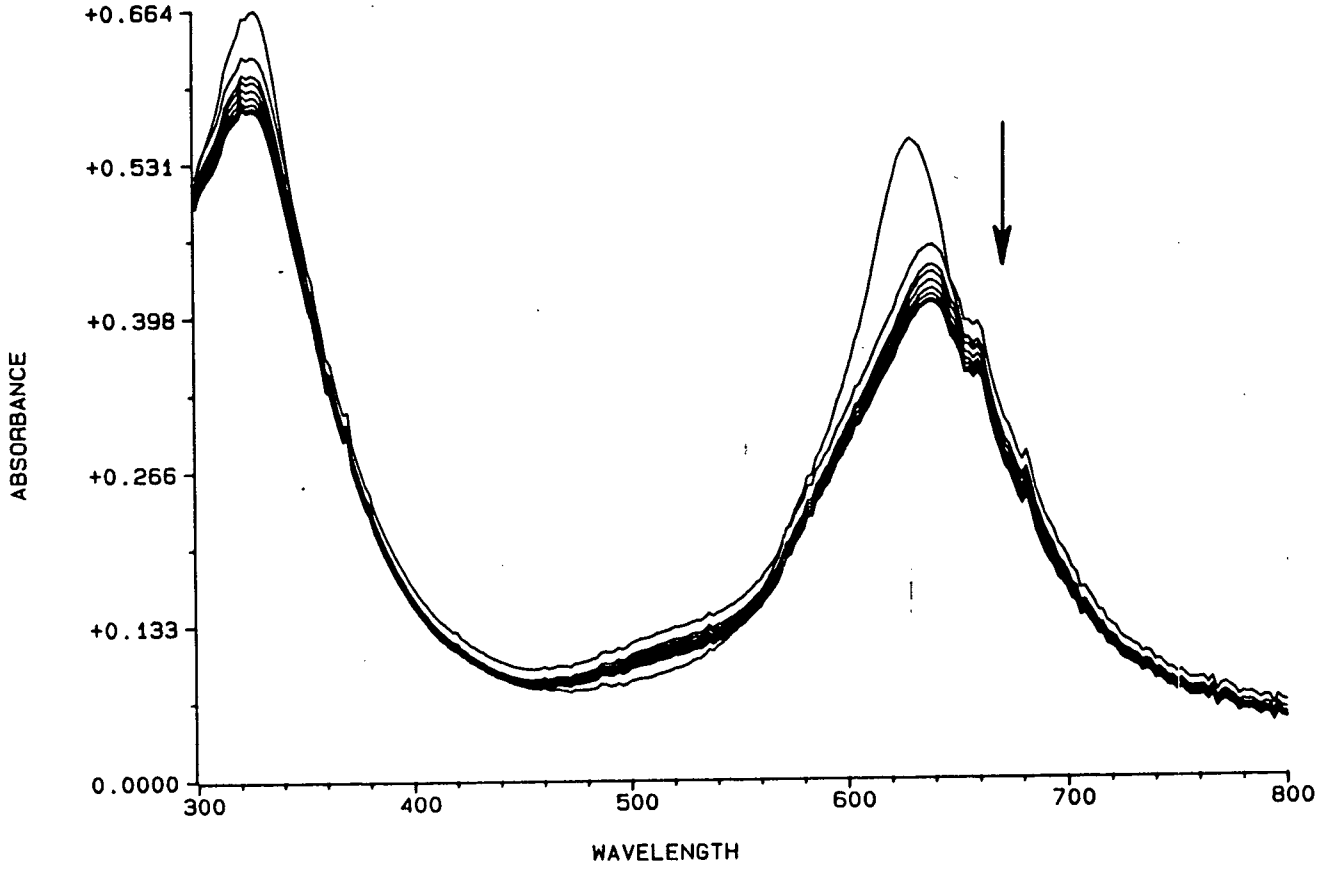

Figure A-7 (T) TSPCFeCl/H_2O_2, pH 7

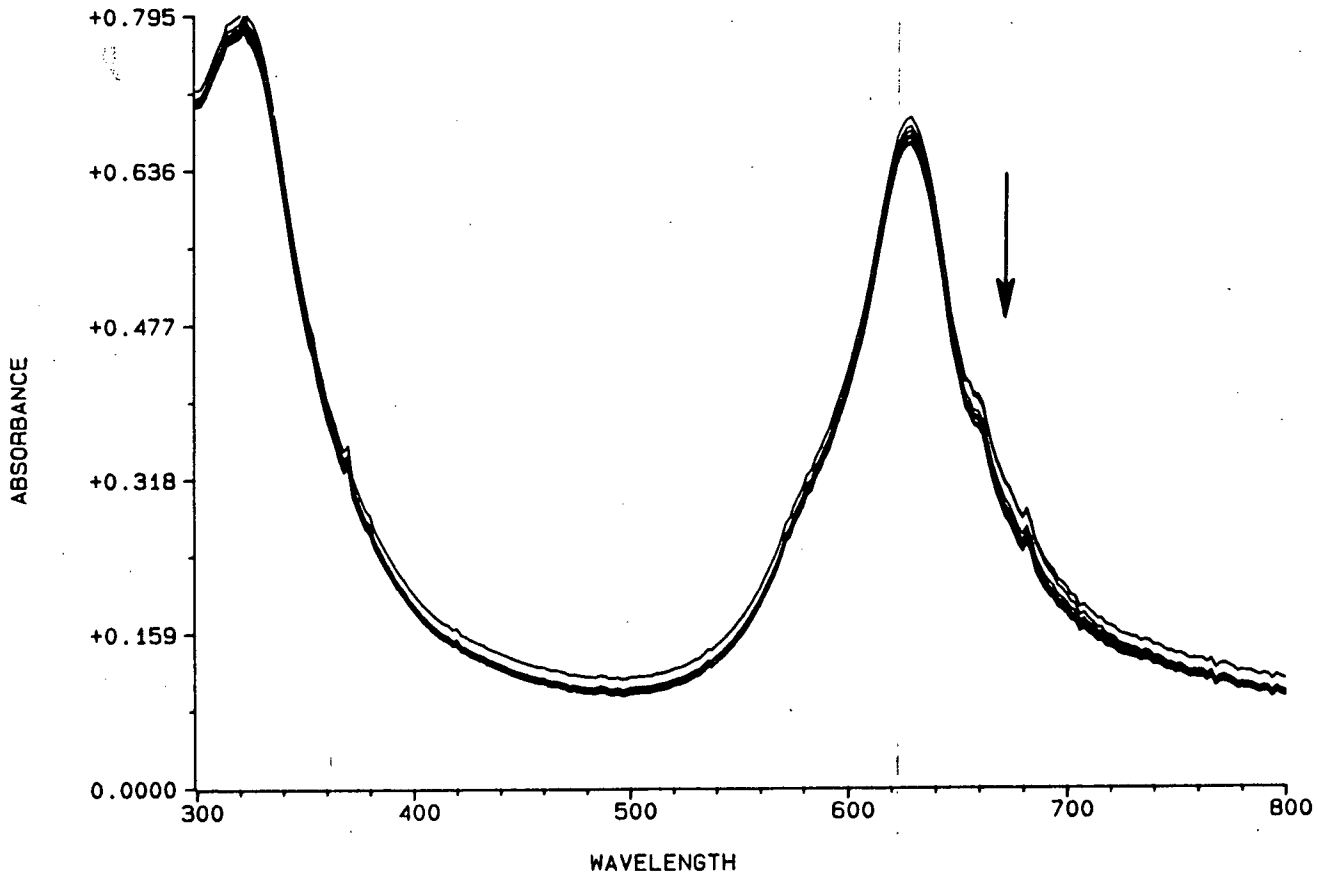

Figure A-7 (U) TSPCFeCl/H_2O_2, pH 10

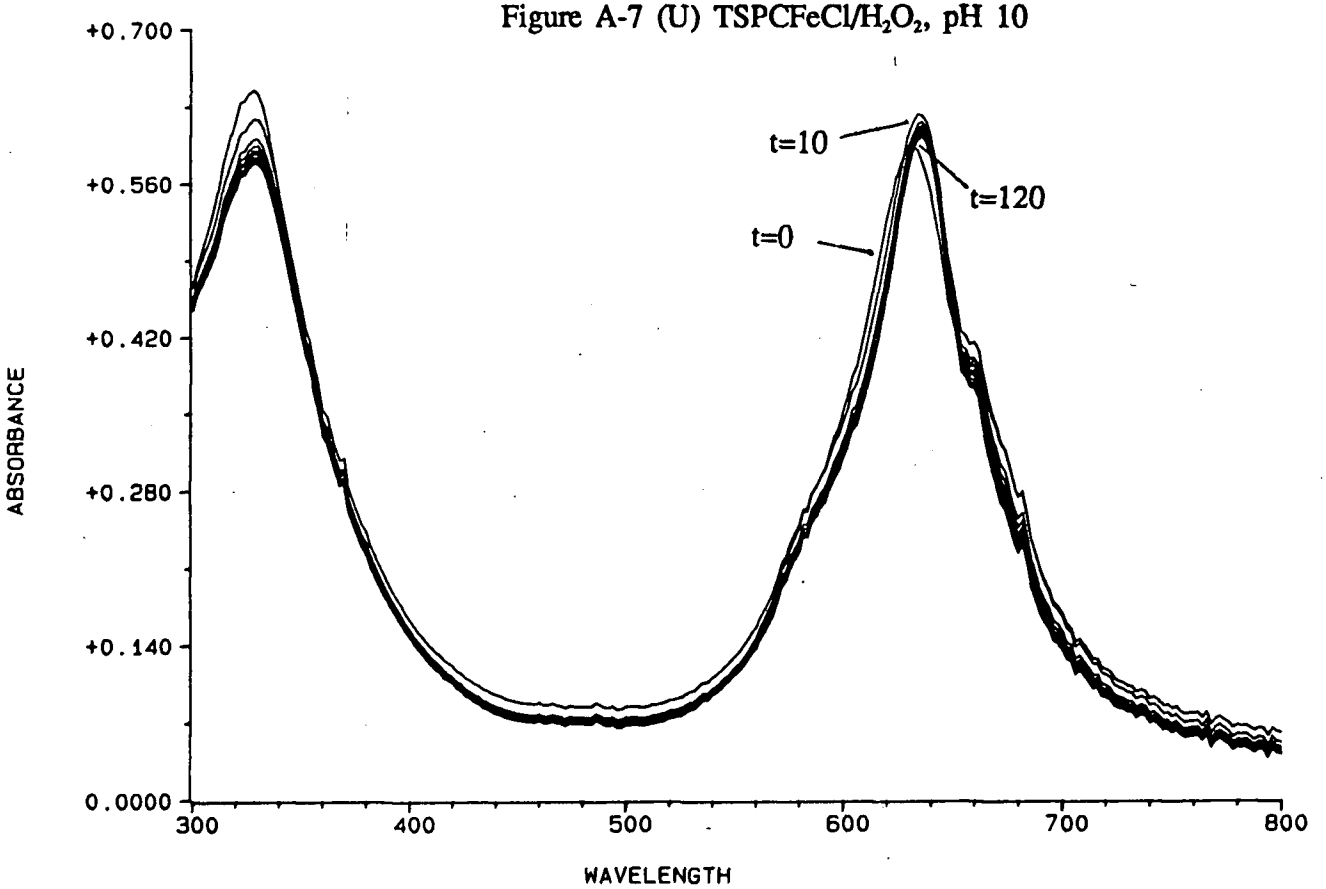

Figure A-7 UV-vis spectral changes of TSPCMnCl and TSPCFeCl (1×10^{-7} mole in 3 mL 0.1 M phosphate buffer) upon addition of one equivalent of oxidant (1×10^{-7} mole) in the presence of veratryl alcohol (5×10^{-6} mole) at room temperature over a time period of 2 minutes, 10 seconds between each scan

veratryl alcohol by TSPCMnCl and hydrogen peroxide. A serious problem with these two catalysts was their low stability, which was dependent on the pH of the solvent and the type of oxidant used. The use of organic solvents instead of aqueous solvents increased their stability but did not change their overall catalytic activity. The structure of the metallophthalocyanines has to be modified to increase their stability before they can be used as effective biomimetic catalysts.

Experimental

Chemicals. Veratryl alcohol, 4′-methoxyacetophenone, hydrogen peroxide, t-butylhydroperoxide, sodium hypochlorite, m-chloroperbenzoic acid (*m*CPBA), and potassium hydrogen monopersulfate (OXONE®) were all of reagent grade. Copper phthalocyanine-3,4′,4″,4‴-tetrasulfonic acid tetrasodium salt (TSPCCu) and nickel phthalocyaninetetrasulfonic acid tetrasodium salt (TSPCNi) were purchased from Aldrich. Phthalocyaninetetrasulfonic acid was purchased from Porphyrin Products. Iodosylbenzene was synthesized as reported.[20] 4-Ethoxy-3-methoxyphenylglycerol-ß-guaiacyl ether (ß-O-4 dimer), and 1-(4-ethoxy-3-methoxy)-2(-4-methoxyphenyl)propane-1,3-diol (ß-1 dimer) were synthesized as described in Chapter 3.

All UV-vis spectra were measured on a HP8452A diode array spectrometer. The HPLC was a Waters 600E pump with a Waters 994 photodiode array detector equipped with a 3.9 mm × 15 cm C-18 column. The mobile phase used for all analyses was 1:1 methanol/water.

The synthesis of cobalt tetrasulfonatophthalocyanine (TSPCCo). Phthalocyaninetetrasulfonic acid (0.5 g) was dissolved in DMF (30 mL). Cobalt(II) chloride (0.5 g) was added to the solution and stirred at 160 °C. The reaction was

complete in 60 minutes as followed by UV-vis spectroscopy. The reaction mixture was then cooled to room temperature and the product precipitated with 200 mL of acetone. The precipitate was collected, washed with acetone, dissolved in water, and filtered. The filtrate was passed through an ion exchange column (3 × 15 cm glass column packed with Amberlite IR-120 ion exchanger, H^+ type) to remove free Co^{2+}. The aqueous solution was dried on rotavapor to give cobalt tetrasulfonatophthalocyanine as black crystalline powder. The UV-vis spectrum (in water) of the TSPCCo so obtained showed that it was a mixture of oxygen free and oxygen-bound cobalt complex.[21,22]

The synthesis of tetrasulfonatophthalocyanine manganese chloride (TSPCMnCl). Phthalocyaninetetrasulfonic acid (0.5) and $Mn(OAC)_2 \cdot 4H_2O$ (1.7 g) were dissolved in water (30 mL) and refluxed for 60 minutes. A black solid was precipitated when the reaction mixture was allowed to cool down. Acetone (200 mL) was added to further precipitate the product. The precipitate was collected and washed with acetone. The manganese tetrasufonatophthalocyanine so obtained was probably a polymer and had very low solubility in water. It was dissolved in dilute sodium hydroxide, filtered, and carefully neutralized to neutral pH with dilute hydrochloric acid. The solution was then passed through ion exchange column and dried as described above. The tetrasufonatophthalocyanine manganese chloride is a black crystalline powder and dissolves in water to give a green solution. Its UV-vis spectrum is similar to that of manganese(III) phthalocyaninetetrasulfonic acid.[21,23]

Tetrasulfonatophthalocyanine iron chloride (TSPCFeCl) was synthesized following the method described above for the synthesis of cobalt tetrasulfonatophthalocyanine except $FeCl_2 \cdot 4H_2O$ (0.25 g) was used. It has the same UV-vis spectrum as that reported for Iron(III) phthalocyaninetetrasulfonic acid.[21,24]

The oxidation of veratryl alcohol. The reaction was started by adding the oxidant

(1×10^{-4} moles) to 5 mL of aqueous phosphate buffer (0.1 M) containing 5×10^{-7} moles of metallophthalocyanine and 5×10^{-5} moles of veratryl alcohol. The mixture was stirred at room temperature for 60 minutes and any remaining oxidant was decomposed by adding solid sodium bisulfite. When the reaction was carried out at pH 3, saturated sodium bicarbonate was added to neutralize the solution before adding sodium bisulfite. Saturated sodium bicarbonate was also added to the solution when *m*CPBA was the oxidant to remove the *m*-chlorobenzoic acid. 5×10^{-5} moles of 4′-methoxyacetophenone was added (as an internal standard for HPLC analysis) and the reaction mixture was then extracted with ethyl acetate (3×3 mL). The extracts were combined and analyzed by HPLC for the formation of veratraldehyde.

The oxidation of ß-O-4 and ß-1 dimers. 5×10^{-6} moles of either ß-O-4 or ß-1 dimer was dissolved in 4 mL 1:1 acetonitrile/pH 3 aqueous buffer containing 5×10^{-7} moles of either iron(III) or manganese(III) tetrasulfonatophthalocyanine, 1×10^{-5} moles of mCPBA was added as a powder and the mixture was stirred at room temperature for 60 minutes. Saturated sodium bicarbonate was added to adjust the pH to neutral and solid sodium bisulfite was added to decompose remaining mCPBA. The solution was extracted with ethyl acetate (3×3 mL), the organic layers were combined, evaporated to 2 mL and subject to HPLC analysis. The products were identified by comparing their retention times on HPLC, their UV-vis spectrum index, and their R_f values on TLC with those of known standards.

*Compounds **95** and **96** were synthesized* by oxidizing compounds **62** and **55**, respectively, by 2,3-dichloro-5,6-dicyano-1,4-benzoquinone in dioxane at room temperature[25].

References for Appendices

1. O. Goldschmid, J. Am. Chem. Soc. **75**, 3780, 1953.
2. O. Goldschmid, Ana. Chem. **26**, 1421, 1954.
3. A.S. Wexler, Ana. Chem. **36**, 213, 1964.
4. B.D. Berezin, Coordination Compounds of Porphyrins and Phthalocyanines, John Wiley & Sons, 1981.
5. F.H. Moser, and A.L. Thomas, The Phthalocyanines, Vol. I, CRC Press, 1983.
6. H. Kropf, Angew. Chem. internat. Edit. **11**, 239, 1972.
7. C.A. Tolman, J.D. Druliner, P.J. Krusic, M.J. Nappa, W.C. Seidel, I.D. Williams, and S.D. Ittel, J. Mol. Cat. **48**, 129, 1988.
8. R. Belal, and B. Meunier, J. Mol. Cat. **44**, 187, 1988.
9. A.L. Stautzenberger, U.S. patent 3,931,249, 1976.
10. S.N. Massie, U.S. patent 3,692,842, 1972.
11. H. Shirai, S. Higaki, K. Hanabusa, and N. Hojo, J. Poly. Sci. Poly. Letters Edit. **21**, 157, 1983.
12. H. Shirai, A. Maruyama, J. Takano, K. Kobayashi, and N. Hojo, Makromol. Chem. **181**, 565, 1980.
13. H. Shirai, A. Maruyama, M. Konishi, and N. Hojo, Makromol. Chem. **181**, 1003, 1980.
14. L.A. Anderson, V. Renganathan, A.A. Chiu, T.M. Lohr, and M.H. Gold, J. Biol. Chem. **260**, 6080, 1985.

15. Y. Mino, H. Wariishi, N.J. Blackburn, T.M. Lohr, and M.H. Gold, J. Biol. Chem. **263**, 7029, 1988.

16. J.-P. Renaud, P. Battioni, J.F. Bartoli, and D. Mansuy, J. Chem. Soc., Chem. Commun. 888, 1985.

17. D. Mansuy, P. Battioni, and J.-P. Renaud, J. Chem. Soc., Chem. Commun. 1255, 1984.

18. T. Umezawa, M. Shimada, T. Higuchi, and K. Kusai, FEBS Letters, **205**, 287, 1986

19. M. Shimada, T. Habe, T. Umezawa, and T. Higuchi, Biochem. Biophys. Res. Commun. **122**, 1247, 1984.

20. Organic Syntheses, Vol. 43, B.C. McKusick Editor, John Wiley & Sons, 1963, p60.

21. J. Veprek-Siska, E. Schwertnerova, and D. M. Wagnerova, Chimia, **26**, 75, 1972.

22. L.C. Gruen, and R.J. Blagrove, Aust. J. Chem. **26**, 319, 1973.

23. K. Fenkart, and C.H. Brubaker, Jr., J. Inorg. Nucl. Chem. **30**, 3245, 1968.

24. H. Sigel, P. Waldmeier, and B. Prijs, Inorg. Nucl. Chem. Letters, **7**, 161, 1971.

25. H. Decker, and E. Adler, Acta Chem. Scand. **15**, 218, 1961.